# Use of *in vitro* and *in vivo* zebrafish infection models to investigate the role of oral microorganisms in cardiovascular disease

**By:**

**Cher Farrugia**

**A thesis submitted in partial fulfilment of the requirement for the degree of Doctor of Philosophy**

**The University of Sheffield**

**Faculty of Medicine, Dentistry and Health**

**School of Clinical Dentistry**

**26/2/2021**

# DEDICATION

This thesis is dedicated to my parents, John and Miriam Farrugia, for their unrelenting and constant support. I am extremely privileged to have been raised by parents who went out of their way to support me in securing opportunities that they themselves did not have when they were growing up.

# ABSTRACT

Increasing evidence links periodontal pathogens with several systemic diseases, including cardiovascular disease, atherosclerosis, diabetes and Alzheimer's disease. A well-established example is the association between periodontal disease that affects over 300 million people worldwide, and cardiovascular disease. Several periodontal pathogens have been detected in atherosclerotic plaques and patient vascular samples. These pathogens can enter the bloodstream through recurrent bleeding, disseminating systemically resulting in transient bacteraemia. However, little is known about how periodontal pathogens interact with the vasculature and which molecular mechanisms and virulence factors are responsible for initiation or potentiation of cardiovascular disease. Most research has focused on the oral pathogen *Porphyromonas gingivalis (Pg)*, at the exclusion of other oral microorganisms identified in the circulation and atherosclerotic plaques, including *Fusobacterium nucleatum (Fn)* and *Tanerella forsythia (Tf)*. *Pg* has been termed a 'keystone pathogen' and produces several virulence factors including cysteine proteases, gingipains and outer membrane vesicles (OMV). This study investigated the role of *Pg* gingipains in whole cell bacteria, as well as from OMV, in mediating endothelial damage assessed through cell adhesion molecule degradation and endothelial permeability *in vitro* and *in vivo* using a zebrafish larvae systemic infection model. In addition, since periodontitis is a polymicrobial infection, effects of *Fn* and *Tf* single species as well as multispecies endothelial infections with *Pg* were also assessed.

The adhesion molecule E-selectin was expressed by Primary human microvascular endothelial cells (HDMEC) but not immortalised human microvascular endothelial cells (HMEC-1) cells, while *Pg* invaded both endothelial cell types equally, contrasting previously published data that E-selectin is essential for *Pg* endothelial invasion. *In vitro* and *in vivo* infection with *Pg* resulted in significantly increased endothelial invasion, permeability, zebrafish embryo mortality and reduced Platelet endothelial cell adhesion molecule-1 (PECAM-1) and Vascular endothelial-cadherin (VE-cadherin) abundance in a gingipain-dependent manner. Similar findings were observed after infection with OMV generated from W83 but not from the gingipain-null mutant ΔK/R-ab. In single species infections, W83 *Pg* and *Fn* but not *Tf* induced a significant decrease in PECAM-1 abundance and increase in endothelium permeability. In multispecies infections, PECAM-1 reduction and increased endothelium permeability was associated with presence of *Fn. In vivo Fn* resulted in a significant increase in the number of diseased zebrafish embryo compared to PBS. Confocal imaging revealed colocalization of *Fn* in the endothelium, while in multispecies *in vivo* imaging some species appeared in close proximity to others suggesting aggregate formation or co-localised infection at the endothelial surface.

The data presented in this thesis show that *Pg* and *Fn,* but not *Tf,* mediate disturbance of endothelium integrity through decreased cell adhesion molecule expression. In *Pg* single species and OMV infection, this is mediated by gingipains. Multispecies data suggests that *Fn* also plays a role in mediating endothelial damage and highlights the need for further research on the role of *Fn* and multispecies interactions in cardiovascular disease*.

# ACKNOWLEDGEMENTS

Special thanks go to my supervisor Prof. Craig Murdoch for his mentorship. I am very grateful for his support, guidance and confidence in me. Without his encouragement and positive attitude this work would not have been possible. I would also like to thank my co-supervisor Prof. Graham Stafford for his advice, for welcoming me into his team and his encouragement throughout the PhD.

I am also very thankful for the technical staff at the Dental School, Brenka and Jason in particular, who always made time in their busy schedule to help me out. Thanks go also to Sue and her team at the flow cytometry facility for providing me with training in flow cytometry, Darren and Nick from the Wolfson Light Microscopy Facility for their technical support, the technical staff, academics and students from the Bateson centre for training and guidance in zebrafish, Chris and Svet from Electron Microscopy Facility and NEUBIAS (network of European bioimage analysists) for funding to attend training in bioimage analysis, especially Laura for helping me out with writing the script for batch analysis.

I would also like to thank fellow PhD students at the School of Clinical Dentistry, particularly Anita, Ash, Beth and Kittie. Couldn't have asked for better colleagues and neighbours with similar appreciation for bad jokes and always ready to make time to help or hear each other out when things don't go to plan. As well as Dr. Magda Widziolek for the times we've shared in the lab whilst we were working together on initial stages of the project.

I am extremely thankful for everyone who has in some way shaped my path to get to this point. Wouldn't have been able to get through the tough times without my Maltese friends' support and my partner Clayton's constant encouragement and blind confidence in me. Lastly, and probably most importantly, I would like to thank my parents for their sacrifices and never-ending strive to help me achieve whatever goal I set my mind on accomplishing.

# ABBREVIATIONS

| | |
|---|---|
| **5(6)-FAM, SE** | 5-(and-6)-carboxyfluorescein, succinimidyl ester |
| **AAP** | American Academy of Periodontology |
| **AGE** | Advanced glycation end products |
| **ApoE** | Apolipoprotein E |
| **B2M** | β-2-microglobulin |
| **BHI** | Brain heart infusion |
| **BSA** | Bovine serum albumin |
| **CA** | Caudal artery |
| **CAL** | Clinical attachment loss |
| **CCL2** | C-C Motif Chemokine Ligand 2 |
| **cDNA** | Complementary DNA |
| **CFU** | Colony forming unit |
| **CHD** | Coronary heart disease |
| **CV** | Caudal vein |
| **CVD** | Cardiovascular disease |
| **CXCL8** | CXC Motif Chemokine Ligand 8 |
| **DA** | Dorsal aorta |
| **DAPI** | 4',6-Diaminidine-2'-phylindole dihydrocholoride |
| **DLAV** | Dorsal longitudinal anastomotic vessel |
| **DNA** | Deoxyribonucleic acid |
| **dpf** | Days post fertilisation |
| **E-cadherin** | Epithelial cadherin |
| **EDTA** | Ethylenediaminetetraacetic acid |
| **EFP** | European Federation of Periodontology |
| **EM** | Electron microscopy |
| **ELISA** | Enzyme-linked immunosorbent assay |
| **eNOS** | Endothelial nitric oxide synthase |
| **FA** | Fastidious anaerobe agar |
| **FACS** | Fluorescence-activated cell sorting/Flow cytometry |
| **FCS** | Foetal calf serum |
| ***Fn*** | *Fusobacterium nucleatum* |

| | |
|---|---|
| **FSC** | Forward scatter |
| **HDMEC** | Primary human microvascular endothelial cells |
| **HMEC-1** | Immortalised human microvascular endothelial cells |
| **HMP** | Human Microbiome Project |
| **HOMD** | Human Oral Microbiome Database |
| **hpf** | Hours post-fertilisation |
| **hpi** | Hours post-infection |
| **HRP** | Horseradish peroxidase |
| **HUVEC** | Human umbilical vein endothelial cells |
| **ICAM-1** | Intercellular adhesion molecule-1 |
| **IL-1** | Interleukin 1 |
| **Kgp** | Lysine-specific gingipain |
| **LPS** | Lipopolysaccharide |
| **MAb 1B5** | Mouse monoclonal antibody 1B5 |
| **MOI** | Multiplicity of infection |
| **NAM** | N-acetylmuramic acid |
| **NC** | Nitrocellulose |
| **NFκB** | Nuclear factor-kappa-B |
| **NLRP3** | NOD-, LRR- and pyrin domain-containing protein 3 |
| **nMFI** | Normalised median fluorescence index |
| **OD$_{600}$** | Optical density at 600 nm |
| **OMV** | Outer membrane vesicles |
| **oxLDL** | Oxidized lipoproteins |
| **PBS** | Phosphate-buffered saline |
| **PCR** | Polymerase chain reaction |
| **PECAM-1** | Platelet endothelial cell adhesion molecule-1 |
| *Pg* | *Porphyromonas gingivalis* |
| **qPCR** | Quantitative polymerase chain reaction |
| **RgpA** | Arginine-specific gingipain |
| **RNA** | Ribonucleic acid |
| **ROS** | Reactive oxygen species |
| **Sch** | Schaedler |
| **SDS** | Sodium dodecyl sulphate |
| **Se** | Intersegmental vessels |

| | |
|---|---|
| **Spp** | Species plural |
| **Ssp** | Subspecies |
| **SSC** | Side scatter |
| **T/E** | Trypsin/EDTA |
| **TF** | Tissue factor |
| ***Tf*** | *Tannerella forsythia* |
| **TLR2** | Toll-like receptor 2 |
| **TMB** | 3,3′,5,5′-Tetramethylbenzidine |
| **TNF-α** | Tumour necrosis factor-alpha |
| **VCAM-1** | Vascular cell adhesion molecule-1 |
| **VE-cadherin** | Vascular endothelial-cadherin |
| **WC** | Whole cell |
| **WGA** | Wheat germ agglutinin |
| **WHF** | World Heart Federation |

# CONTENTS

# TABLES

# FIGURES

# CHAPTER 1: Introduction and literature review

## 1.1    THE ORAL MICROBIOME

In recent years the role of the oral microbiome has been intensely investigated. The scientific community is slowly unravelling its complexity and its role in both health and disease (Kilian et al. 2016).

Humans are far from autonomous organisms, our bodies include several microbial communities living symbiotically (Bordenstein and Theis 2015). Such communities can also be found thriving in our oral cavity that provides several different habitats for microbial colonisation (Zhou, Xu and Shi 2017). Up to 11 microbial habitats have been described and include the hard palate, saliva, dorsum of tongue, pharynx, palatine tonsils, buccal mucosa, supra-gingival plaque, subgingival plaque and vermillion (Jia et al. 2018). These habitats provide distinct and varied environmental conditions for a wide range of microorganisms, making the oral cavity one of the most heavily colonised parts of the human body (Kilian et al. 2016). Developments in culture-independent methods and next generation DNA sequencing are providing a deeper analysis of the oral microbiome composition and its role in the oral cavity and other regions in the body. Nonetheless, further research is required to fully understand host-microbiome interactions and their role in health and disease (Dewhirst et al. 2010). The Human Oral Microbiome Database (HOMD) was developed to provide a much-needed site-specific database for the prokaryotic species present in the oral cavity and aims to coordinate the storage, raw data distribution and sharing of information produced through the Health Human Microbiome Project (HMP) (Chen et al. 2010). It is now recognised that the oral microbiome is an extremely diverse and complex environment, which comprises of a mixture of viruses, protozoa, archea, fungi and over 500 different species of bacteria (Wade 2013, Zhang et al. 2018).

### 1.1.1 Bacteria

Hundreds of bacterial species colonise the oral cavity's diverse environments (Kilian et al. 2016, Holt and Ebersole 2005). The phyla *Firmicutes, Bacteroidetes, Proteobacteria,*

*Actinobacteria, Spirochaetes* and *Fusobacteria* account for 96% of detected species in the oral cavity (Wade 2013). While *Streptococci*, in the *Bacilli* class and phylum *Firmicutes* are the most abundant bacterial species in the oral cavity. The related, but less frequently studied *Abiotrophia, Gemella* and *Granulicatella* species are also very common (Dewhirst et al. 2010).

Understanding and identifying the components of the oral microbiome comes with several challenges. A large portion of the currently known oral cavity colonisers cannot, as yet, be grown in culture (Kilian et al. 2016). In fact, it has been claimed that up to half of the bacteria in the mouth have yet to be cultured (Wade et al. 2016). The advent of culture-independent methods has allowed identification of organisms that were previously unknown (Kilian et al. 2016). 16S ribosomal RNA PCR amplification and amplicon sequencing are currently the most commonly used approaches to characterise microbial communities. Although these methods are useful for providing information regarding community membership and phylogenic relationships, they do not provide much information about the community's functional potential. Alternative methods are therefore being used, such as metagenomics, due to their ability to assess functional potential, even in species other than bacteria (Pride et al. 2012). The oral cavity is in constant contact with the outside environment and therefore identification of transient from endogenous species is important. This cannot be achieved through human sampling studies alone and pairing with environmental studies is necessary (Dewhirst et al. 2010).

The oral microbiome is among the most studied of the human microflora (Chen et al. 2010) and its complexity and gaps in knowledge on its role in human oral and systemic health continue to intrigue the scientific community worldwide.

## 1.1.2 Viruses

Viruses documented in the oral cavity have been generally thought to be disease associated, such as the human papilloma virus and the herpes simplex virus (Wade 2013, Zhang et al. 2018). Very few studies have attempted to characterise oral viral communities, but more recent evidence is unravelling further species, particularly bacteriophages with integrase homologs, suggesting a role in lysogeny (Pride et al. 2012, Edlund et al. 2015). Viruses may

therefore also play a role in both health and disease, such as in chronic periodontitis (Górski and Weber-Dabrowska 2005).

### 1.1.3 Archaea and protozoa

*Archaea* do not normally make up a large component of the healthy oral microbiome and are most prevalent in subjects with periodontitis (Wade 2013). Most studies suggest that *Methanobrevibacter oralis* and other closely related phylotypes are the most predominant archaea in the oral cavity. (Horz et al. 2015) Similar to *archaea*, only a few protozoa have been found in the oral cavity. These include *Entamoeba gingivalis* and *Trichomonas tenax* that are also more prevalent in cases of poor oral hygiene and gingival diseases. These organisms are not currently considered to be pathogens (Wade 2013).

### 1.1.4 Fungi

Fungi have been characterised in detail in the oral cavity and are widely present even in healthy subjects. *Candida* species are the most frequent, but over 100 fungal species have been characterised in healthy subjects. In fact, each individual has up to 23 different fungal species residing commensally in their oral cavities, with *Candida albicans* being the most predominant. Other species frequently present include *Cladosporium, Aureobasidium, Saccharomyces, Aspergillus, Fusarium*, and *Cryptococcus* (Zhang et al. 2018, Ghannoum et al. 2010). The prevalence of Fungi increases with age and they have also been documented to contribute to a wide range of opportunistic acute and chronic oral infections (Wade 2013, Arendorf and Walker 1979).

## 1.2 ORAL MICROBIOME AND ORAL DISEASES

The oral microbiota, similar to other microbial communities, tend to form highly organised multicellular communities known as biofilms (Kilian et al. 2016). In a biofilm multiple species interact and communicate while attached to a surface. (Kilian et al. 2016, Szafranski et al. 2017). Biofilm microbial communities are better equipped at adapting to environmental challenges, partly due to their non-crystalline extracellular matrix made up of polysaccharides and proteins (Bowen et al. 2018). Biofilms are also able to adapt to changes in the

enviornment through genetic changes controlled by quorum-sensing. Quorum-sensing can be described as interbacterial communication or signalling and has been shown to be involved in the pathogenic potential of microorganisms (Szafranski et al. 2017).

Resident species of the human microbiome maintain a healthy relationship with their environment through a complex equilibrium. Loss of this equilibrium, a process also referred to as dysbiosis, results in a disease state. Microbial community diversity and balance can be disrupted by a single or few predominating disease associated species, a process known as the dysbiotic shift (Kilian et al. 2016, Cho and Blaser 2012).

The dysbiosis theory can be applied to explain the pathophysiology of the major oral diseases, which include caries (tooth decay) and periodontitis (gum disease). Dysbiosis can be triggered by several biological changes, as well as modifiable factors. These factors include poor oral hygiene, dietary habits, smoking and salivary gland dysfunction (Kilian et al. 2016, Marsh, Head and Devine 2014, Wu et al. 2016). Oral microbiota adhere to and grow on different surfaces in the oral cavity, forming organised multispecies community biofilms that interact and develop depending on their environment. This organised biofilm is known as dental plaque and is illustrated in Figure 1.1 (Pitts et al. 2017, Kolenbrander 2000).
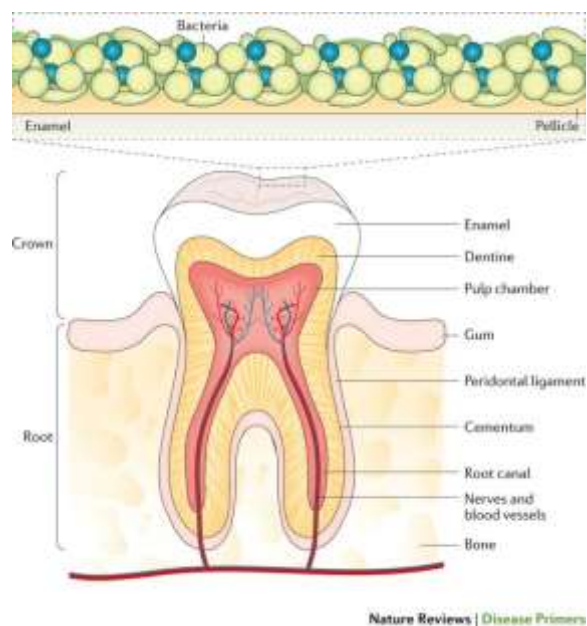


**Figure 1.1: Dental biofilm and tooth anatomy illustration (Pitts et al. 2017) (Licence number 4413090246683)**

## 1.2.1 Dental caries and endodontic disease

Untreated dental caries is the most common human disease worldwide, (Hay et al. 2017) with around 37% global impact increase between 1990 and 2013 (Jepsen et al. 2017). Dental caries involves a process of localised chemical dissolution of enamel and dentine by dental biofilm acid production, which results from sugar exposure (Jepsen et al. 2017). The loss of balance between protective factors such as high salivary flow and pathological factors such as sugar consumption and biofilm formation determines the initiation and progression of this oral disease (Pitts et al. 2017).

The link between caries and oral microorganisms has been established since the 19th century, particularly the role of acid producing streptococci (Tucker 1932). Nowadays, several organisms have been identified in caries lesions and several different species have been associated with dental caries at different stages of the disease (Pitts et al. 2017). Streptococci, particularly *Streptococcus mutans* and *Streptococcus sobrinus* used to be considered the main agents in enamel caries formation. Through the fermentation of sucrose, these bacteria produce organic acids such as lactic acid that soften tooth tissues. These organisms also form insoluble extracellular polysaccharides that provide enhanced adherence and biofilm formation. *Lactobacilli, Streptococcus mitis* and more recently *Bifidobacterium* species (spp), *Actinomyces* spp, *Propionibacterium* spp and *Scardovia wiggsiae* have also been associated with caries (Pitts et al. 2017). The increasing number of associated bacteria as well as the presence of disease in the absence of what were once known as the "key causative bacteria" has led to a shift from the "specific plaque hypothesis".  It is no longer thought that caries is only caused by a limited subset of species as previously described through this hypothesis. Nowadays the ecological plaque hypothesis (such as the "extended caries ecological hypothesis") are accepted as more plausible explanations of the aetiology of dental caries (Bacci et al. 2016, Marsh 1994, Marsh and Zaura 2017, Pitts et al. 2017). This is because the ecological hypothesis reflects the ability of oral microorganisms to adapt to varying ecological factors, such as acid stress and prolonged low pH. These hypotheses further highlight that caries is not a classic infectious disease, but more of a shift in the balance of resident microorganisms as a result of changes in lifestyle and the oral environment (Pitts et al. 2017).
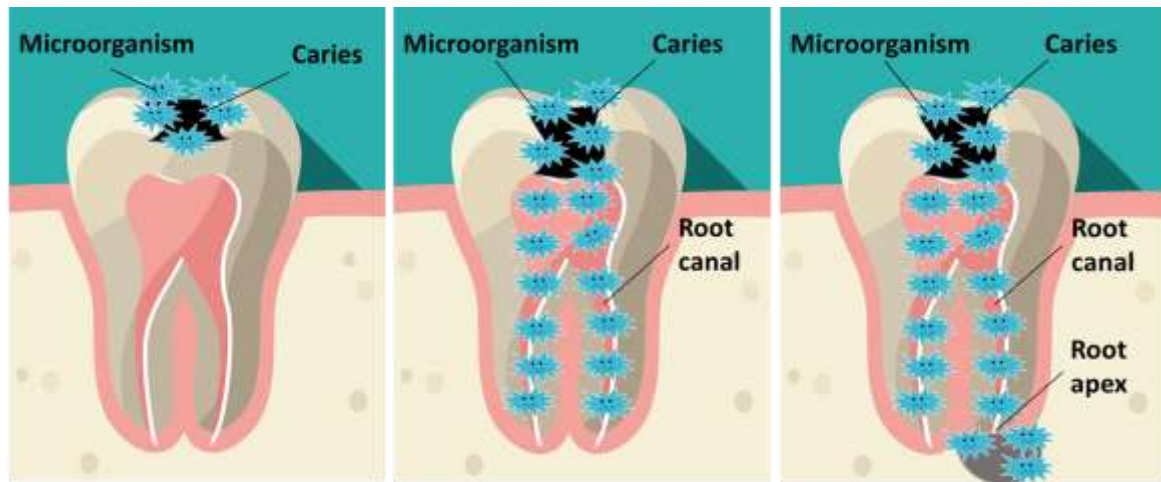
**Figure 1.2: Dental caries, root canal infection and apical periodontitis.**

If left untreated, dental decay may lead to an influx of microorganisms into the root canal. This in turn leads to infection of the root canal, which is referred to as endodontic infection (Figure 1.2). Unlike the oral cavity, in a healthy root canal system, there are no commensal microorganisms. Therefore, any microorganism that manages to survive inside the root canal can be considered as a pathogen. Infection of the root canal can lead to reversible pulpitis, pulp necrosis and eventually apical periodontitis. All of which can only develop in the presence of microorganisms (Persoon and Özok 2017). Apical periodontitis is described as an inflammatory response of the periodontal tissues past the apex of the root to an infected root canal system. Calcified periapical tissues erode, forming a bony lesion. This process is a result of toxic irritation from the infected root canal, the host immune response and through microorganisms that manage to travel past the apex (Persoon and Özok 2017, Siqueira and Roccas 2008, Siqueira and Rocas 2009). Exposure of the root canal through dental decay or dental trauma creates access to a new environment for the commensal microbiota and therefore a wide range of microorganisms have been identified in endodontic infections (Siqueira and Roccas 2008, Siqueira and Rocas 2009, Persoon and Özok 2017, Persoon et al. 2017). It is widely accepted that bacteria are the major contributors to endodontic infections (Persoon and Özok 2017, Persoon et al. 2017). For bacteria to cause infection a population load or density needs to be reached. This in turn leads to tissue damage through the bacteria themselves or due to host response to the infection (Siqueira and Rôças 2007). *Lactobacillus*, *Actinomyces*, and *Streptococcus* are the most abundant bacterial genera identified in apical periodontitis, but recent analytical techniques have been uncovering the diversity of root canal infections (Persoon and Özok 2017, Ozok et al. 2012). Systematic reviews of recent next

generation sequencing studies showed that *Prevotella, Fusobacterium, Parvimonas, Porphyromonas* and *Streptrococcus* were the key genera identified in primary and persistent infected root canals and *Firmicutes, Bacteroidetes, Proteobacteria, Actinobacteria, and Fusobacteria* the most abundant phyla (Shin et al. 2018, Manoil, Al-Manei and Belibasakis 2020, Abusrewil et al. 2020). The microbiota of endodontic infections is much more complex than previously thought and varies between symptomatic and asymptomatic forms (Persoon and Özok 2017), as well as differences between the microbiota in coronal areas when compared to the apical areas (Ozok et al. 2012). Fungi, viruses and archaea have also been detected in infected root canals (Persoon and Özok 2017), and their interaction with bacterial communities within the root canal may contribute to different treatment outcomes (Persoon et al. 2017, Siqueira and Roccas 2008). Endodontic or root canal treatment aims to eliminate microbial populations from within the root canal and seal/obturate the remaining spaces in to cause "entombment" of any remaining microorganisms, therefore preventing their growth (Siqueira and Rôças 2007).

## 1.3    PERIODONTAL DISEASE

Even though dysbiosis and infection are a common denominator in most oral diseases (as highlighted in the previous section), differences in the local and systemic host environment play a major role in disease progression, outcome and complexity. One of the most complex examples of host-pathogen interactions mediated by local and systemic factors is the progression of periodontal disease. In periodontal disease our host immune-recognition system behaves differently in response to a number of opportunistic pathogens, and this response can lead to a cascade effect with tissue destruction as an endpoint. (Ebersole et al. 2017)

Periodontal disease (also known as gum disease) is one of the most common bacterial infections in humans (Chen et al. 2018a). It affects 20-50% of the population and is prevalent in both developed and developing countries. Risk factors for developing periodontal disease include smoking, diabetes, age, genetic predisposition, stress and poor oral hygiene (Nazir 2017). Similarly to dental caries, microbial clusters in dental plaque play a major role in the formation and progression of periodontal disease (Kolenbrander 2000).

Periodontal disease develops through chronic inflammatory mediators, stimulated by microorganisms that cause imbalances in the relative abundance of groups of microorganisms associated with disease and those generally abundant in health (Hajishengallis, Darveau and Curtis 2012, Chen et al. 2018a). The bacteria-induced chronic inflammation (Darveau 2010), initiated by biofilm accumulation on teeth, leads to the initial reversible stage of the disease known as gingivitis (Murakami et al. 2018). Plaque-induced gingivitis can exhibit several patterns of observable signs and symptoms of inflammation. It is generally localized to the gingiva and is characterised by inflamed, red and bleeding gums (Figure 1.3). As the disease and inflammation progresses it results in an irreversible form of the disease known as periodontitis. In periodontitis, chronic inflammation leads to destruction of the periodontium, which consists of the tooth's supporting structures, including the gums and surrounding bone (Darveau 2010, Murakami et al. 2018). The clinical presentations of gingivitis and periodontitis are illustrated in Figure 1.4. Destruction of the periodontium, leads to attachment loss between the teeth and gingivae, resulting in the formation of a periodontal pocket (Wade 2013). This space is ideal for anaerobic bacteria colonisation, which triggers further host inflammatory responses. The host responses produce proteases that lead to further tissues destruction (Wade 2013, Darveau 2010). If destruction of the tooth's supporting structures progresses, affected teeth lose their stability, become mobile in the tooth socket and are eventually lost or extracted (Wade 2013) (Illustrated in Figure 1.3B).
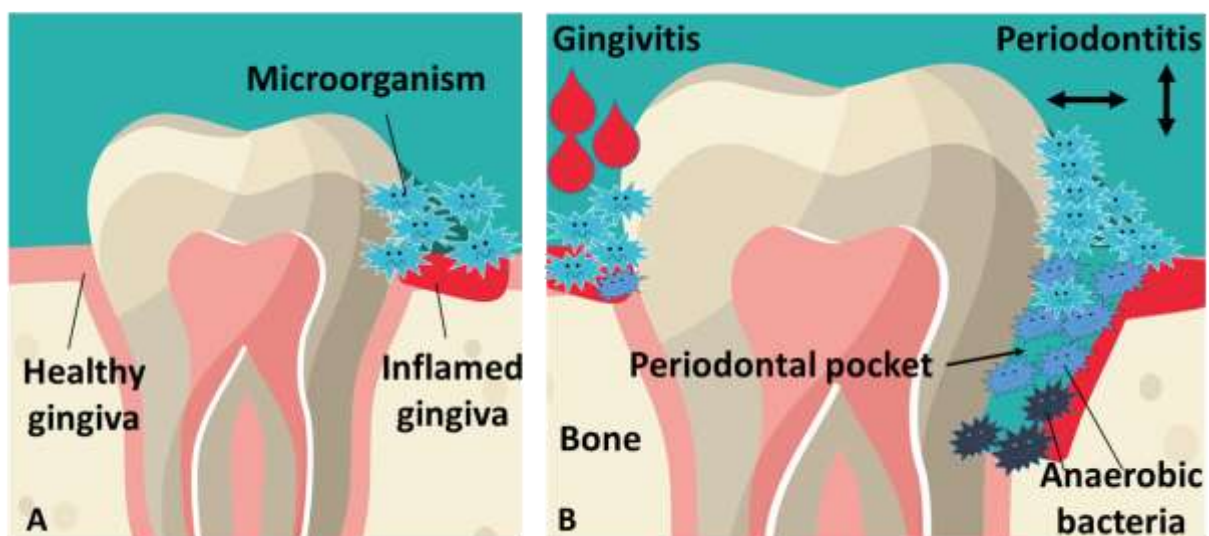


**Figure 1.3: Periodontium in health, gingivitis and periodontitis**
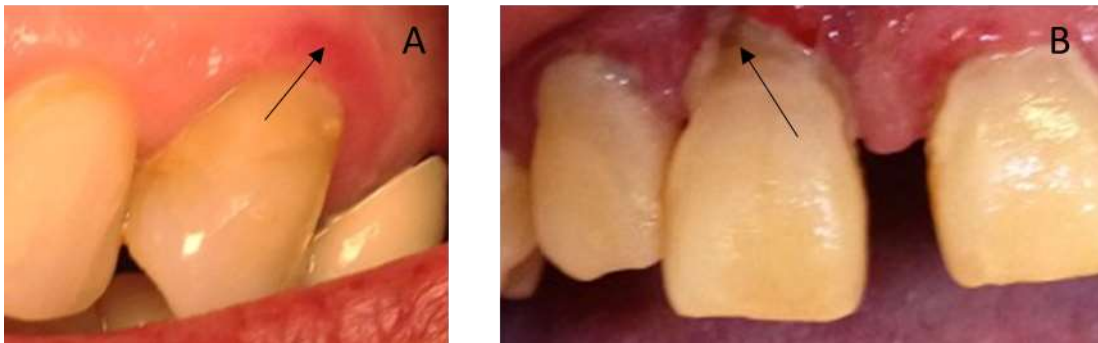
**Figure 1.4: Clinical presentations of gingivitis and periodontitis**. Localised gingivitis (A) typically presents as red, inflamed gingiva as marked by the black arrow. Figure B illustrates bone destruction and exposure of roots typical of periodontitis (highlighted by black arrow). Images adapted from Khan et al. 2015 (Khan et al. 2015).

Periodontal disease classification has been updated in 2018 through collaborative efforts from experts worldwide, the American Academy of Periodontology (AAP) and the European Federation of Periodontology (EFP). The classification was developed to reflect more recent scientific knowledge and understanding of the disease. The classification report also highlights that in some areas, scientific data is still lacking (Caton et al. 2018). Through a series of reports it was concluded that patients affected by gingivitis can revert to a healthy state but patients suffering from periodontitis require life-long supportive care even after successful therapy and remain a periodontitis patient for life (Caton et al. 2018, Chapple et al. 2018). Several changes were made to the previous classification to reflect current scientific knowledge (Caton et al. 2018). The changes from the 1999 classification are a reminder that even common based knowledge must not be taken for granted and that there is much left to be understood on how periodontal diseases affect the host both locally and systemically.

## 1.3.1 The healthy periodontium

The periodontium is made up of the tooth supporting structures. These include the gingiva, cementum, periodontal membrane/ligament and the alveolar bone. The components are illustrated in Figure 1.5 (Goldman 1953).
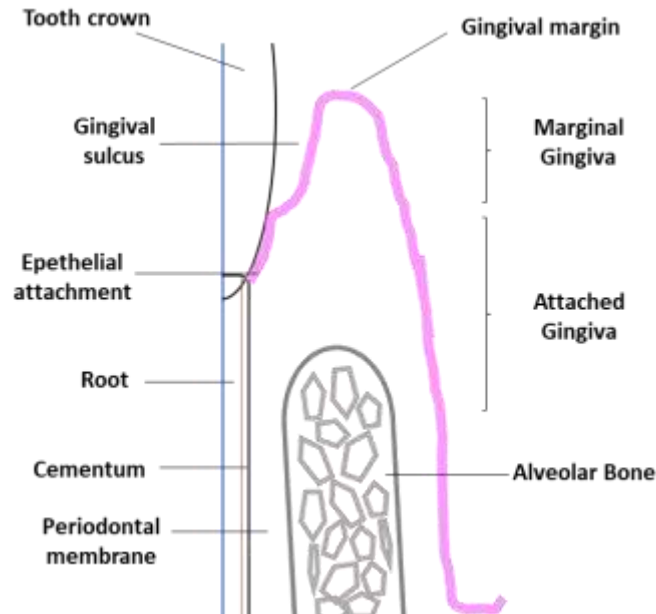
**Figure 1.5: Anatomy of the periodontium**

The gingivae protect underlying tissues and hold the teeth in line and are divided into different sections. The gingival margin is located at the tip of the gingiva and attaches to the tooth surface through epithelial attachments to form the gingival sulcus. The gingival sulcus is lined by sulcular epithelium and is the space between the free or unattached gingiva and the tooth. The attached gingiva is attached firmly to the underlying tooth or bone and has a clinically stippled appearance (Goldman 1953).

The cementum is a specialised mineralised tissue containing collagen fibrils in an organic matrix. It is continuously deposited throughout life on the root portion of the tooth and in small portions of the crown and does not have a lymphatic, blood supply or innervation. It attaches the periodontal ligament to the root and plays a role in root surface repair. In contrast, the periodontal ligament is composed of richly cellular and vascular connective tissue. It surrounds the root surface and joins the cementum to the wall of the alveolar socket. Its function is to allow distribution of masticatory forces and tooth mobility to a certain extent. The alveolar bone that forms and supports the sockets of the teeth is referred to as the alveolar process. In conjunction with the cementum and periodontal ligament it distributes generated forces. The portion of bone facing the periodontal ligament is known as the dense alveolar bone proper. In between the dense portions of the alveolar process stands cancellous bone consisting of mineralised bone and bone marrow. The alveolar portion is remodelled by

osteoclasts and renewed by osteoblasts in response to the functional demands. During this process bone trabeculae and cortical bone mass are resorbed and reformed. This is mediated by proliferating blood vessels, which form lamellae around them in centric layers and refill with new bone (Lang, Lindhe and Lang 2015).

The main source of gingival blood supply originates from vessels situated on the gingival side of the periosteum of the alveolar bone, with lymphatic drainage following a similar course (Goldman 1953). These are known as supraperiostial blood vessels and are terminal branches of several arteries including the sublingual, mental, buccal, facial and greater palatine artery. Specific arteries are considered to supply well-defined regions of the dentition and periodontium, but due to numerous anastomoses along the supplying circulation, it is more adapt to describe the supply from an entire system of blood vessels, rather than individual vessels (Goldman 1953, Lang et al. 2015).

Periodontal health is defined as a "state free from inflammatory periodontal disease" that provides full function, avoiding consequences from current or past episodes of the disease. Assessment of periodontal health must be carried out and defined at both the site and patient level (Chapple et al. 2018). Clinically healthy gingivae are of varying shades of pink (depending on the level of keratinisation), firm and with a shallow sulcus (2 mm). The tooth anatomical crown coincides with the clinical crown (Goldman 1953). The latest classification provides further specifications related to periodontal assessment. Classification is dependent on whether one is assessing gingival health on an intact periodontium or on a reduced periodontium (either due to previous periodontal disease or due other non-related factors such as traumatic recession). This is meant to promote clearer clinical guidelines, as well as increase uniformity in assessment for research purposes. Despite the changes, the main characteristic of periodontal health still remains the absence of bleeding on probing, erythema, oedema and patient symptoms (Chapple et al. 2018).

As previously mentioned, absence of disease does not mean absence of microorganisms. In fact, different genera were found to be associated with subgingival plaque in health. These include *Capnocytophaga, Corynebacterium, Streptococcus, Actinomyces, Veillonella, Exiguobacterium, Paludibacter*, *Opitutus* (Socransky et al. 1998, Chen et al. 2018a), *Atopobium rimae, Atopobium parvulum* species (Kumar et al. 2003)*,* as well as the uncultivated clone W090 from the *Deferribacteres* phylum (Kumar et al. 2003). Some of the mentioned

microorganisms, including *Streptococcus sanguinis, Streptococcus mitis*, *Gemella* spp, *Atopobium* spp, *Fusobacterium nucleatum*, and *Capnocytophaga* spp are referred to as primary or early colonisers. As the name suggests these are organisms that are present during initial colonisation of the tooth surface (Kumar et al. 2003, Socransky and Haffajee 1992). It is still not possible to identify a specific community or "core microbiome" associated with health. For some microorganisms, such as previously uncultivated *Bacteroides* oral clone BU063 (Leys et al. 2002, Kumar et al. 2003), now identified and cultivated as *Tannerella serpentiformis,* it is still unclear whether they are associated with health or not (Ansbro, Wade and Stafford 2020, Beall et al. 2018). This is due to the immense variation between, (Chen et al. 2010) as well as within healthy individuals throughout life as well as the limited amount of data available using newer technologies (Sanz et al. 2017). The shift from health-compatible to disease-inducing microbiome is understood to be due to the proportional increase in pathogenic bacteria and not due to the appearance of pathogenic bacteria in previously healthy sites or individuals (Chen et al. 2018a).

## 1.3.2 Gingivitis

Gingivitis is generally a dental plaque-induced and site-specific inflammatory condition (Trombelli et al. 2018, Theilade et al. 1966). Plaque-induced gingivitis is one of the most common human inflammatory diseases, however other much less frequent forms caused by other factors do exist (Trombelli et al. 2018, Holmstrup, Plemons and Meyle 2018). Clinically, gingivitis is characterised by red and oedematous gingiva (2000, Trombelli et al. 2018), without any periodontal attachment loss (Trombelli et al. 2018, Chapple et al. 2018).

A patient is classified as a gingivitis case if the bleeding on probing score is ≥ 10% following full mouth evaluation. This measurement is obtained by probing the gingival sulcus using specifically designed blunt instruments and recording which sites bleed. The condition is further classified into localised or generalised gingivitis. Gingivitis is described as generalised when over 30% of sites are affected (Trombelli et al. 2018). Bleeding on probing is an important measure since it can be detected clinically before other changes such as redness and oedema, allowing for early detection of the disease (Mühlemann and Son 1971, Trombelli et al. 2018). Histologically, sites exhibiting gingival bleeding have been found to have larger

and denser inflammatory connective tissue than unaffected sites. This feature has been found to reverse once bleeding on probing stops (Trombelli et al. 2018, Brecx et al. 1987).

A number of microorganisms are claimed to be linked to gingivitis. These are mostly Gram-positive species such as *Streptococcus* spp, *Actinomyces viscosus*, and *Parvimonas micra.* Some Gram-negative species have also been associated, including *Campylobacter gracilis*, *F. nucleatum*, *Prevotella intermedia* and *Veillonella* (Kremer et al. 2000, Macuch and Tanner 2000, Theilade et al. 1966). The development of gingival plaque after brushing cessation was documented in detail by Theilade *et al.* 1966 (at a time when it was still ethical to cease brushing for a fixed amount of time in a group with previously good oral hygiene and good periodontal health). Healthy gingivae started developing plaque accumulations, coupled with generalised mild gingivitis after 9 to 21 days of oral hygiene cessation. At the beginning of the experiment, dental plaque flora was almost exclusively comprised of Gram-positive cocci and bacilli. Gram-negative cocci and bacilli started to populate at what was described as the first phase (during the first two days). At 4 days (referred to as the second phase in the study) Fusobacteria and filamentous microorganisms appeared and reached up to 7% of the flora. After 4 to 9 days (third phase) spiral organisms (spirochetes), made up to 2% of the counted microorganisms. Clinical signs of inflammation coincided with formation of the more complex flora, while sub-clinical inflammation was noted even during the early phases of plaque development. The original flora composed of mainly Gram-positive cocci and bacilli was re-established after 1 to 2 days of brushing following the cessation period, which also coincided with disappearance of gingival inflammation (Theilade et al. 1966). Even though this study is rather old and techniques were culture-based rather than today's molecular techniques, it showed very nicely how the microbial communities in dental plaque develop with time and how gingivitis is plaque-induced. Its findings also coincide with today's understanding of gingivitis. Particularly the concept that tissue alterations occurring due to gingival inflammation are completely reversed once the dental biofilm is removed and that this coincides with a change in the microbial communities of dental plaque (Trombelli et al. 2018).

Most gingivitis-affected patients are unaware of the disease, since it rarely leads to spontaneous changes and the associated clinical changes are not very recognisable by patients (Trombelli et al. 2018). Nonetheless, gingivitis is of clinical importance since it is considered to be a precursor to periodontal disease. Longitudinal studies have shown that attachment loss

development and progression were associated with higher levels of gingival inflammation (Trombelli et al. 2018, Schätzle et al. 2003, Ramseier et al. 2017).

## 1.3.3 Periodontitis

Periodontitis is a result of a complex interplay between the host response, microbial challenge and modifying factors (Page, Davies and Allison 1973). Once plaque biofilm develops into one containing proportions of highly specialised community members, subversion and dysregulation of the host immune response occurs (Sanz et al. 2017). This causes release of a wide array of inflammatory mediators, chemokines and cytokines (Holt and Ebersole 2005), which eventually lead to destruction of the periodontium in susceptible individuals (Sanz et al. 2017). Patients are rendered more susceptible through genetic risk factors as well as through environmental and habitual differences such as smoking (Bostanci 2017). In periodontal disease the host immune status can determine whether a virulent organism behaves in a pathogenic manner (Holt and Ebersole 2005).

Periodontitis is characterised by loss of periodontal supporting structures. This is clinically manifested through what is known as clinical attachment loss (CAL), which is described as the distance from the base of the gingival pocket or sulcus and the cemento-enamel junction (where the cementum meets the enamel on the tooth surface). Other characteristics include radiographic alveolar bone loss, periodontal pockets, as well as gingival bleeding. A patient is classified as a "periodontitis case" when either the buccal or oral CAL is equal to or more than 3 mm with pocketing of the same dimensions or when 2 or more non-adjacent teeth experience interdental CAL (Papapanou et al. 2018). Periodontitis is highly prevalent and accounts for a substantial portion of dental extractions (Papapanou et al. 2018), especially in adults aged 40 years or older (Reich and Hiller 1993). Periodontal disease and its effects, impair masticatory function, negatively impact facial aesthetics, impair quality of life and are considered a source of social inequality, so much so that is considered as a major public health problem (Papapanou et al. 2018).

Until recently this disease was classified into chronic periodontitis (slow progressing forms), aggressive periodontitis (highly destructive forms), periodontitis as a manifestation of systemic diseases, necrotizing periodontal diseases (forms that include necrosis of gingival or periodontal tissues) and periodontal abscesses (which also have clinically distinct features and

treatments) (Papapanou et al. 2018, Armitage 1999). In the newly adopted classification "chronic" and "aggressive" are now classified under a single category: "periodontitis", since current evidence suggests that chronic and aggressive periodontitis are not two separate diseases. Instead, the most recent classification "periodontitis" is further characterised using a staging and grading system. The severity of presentation and complexity of periodontitis management translate to the stage of the disease. Grading on the other hand provides supplemental information regarding the biological features. This includes the rate of progression of the disease, possible treatment outcomes and the disease and treatment's possible effects on the patient's general health. Details of the staging and grading systems are provided in Table 1.1 and Table 1.2. Staging and grading aims to take advantage of modern technologies, allowing for enhanced knowledge on diagnosis, pathogenesis, as well as disease management (Papapanou et al. 2018).

**Table 1.1: Periodontitis stage Licence number 4416511255151 (Papapanou et al. 2018)**

| Periodontitis stage | | Stage I | Stage II | Stage III | Stage IV |
|---|---|---|---|---|---|
| **Severity** | **Interdental CAL at site of greatest loss** | 1 to 2 mm | 3 to 4 mm | ≥5 mm | ≥5 mm |
| | **Radiographic bone loss** | Coronal third (<15%) | Coronal third (15% to 33%) | Extending to mid-third of root and beyond | Extending to mid-third of root and beyond |
| | **Tooth loss** | No tooth loss due to periodontitis | | Tooth loss due to periodontitis of ≤4 teeth | Tooth loss due to periodontitis of ≥5 teeth |
| **Complexity** | **Local** | Maximum probing depth ≤4 mm Mostly horizontal bone loss | Maximum probing depth ≤5 mm Mostly horizontal bone loss | In addition to stage II complexity: Probing depth ≥6 mm Vertical bone loss ≥3 mm Furcation involvement Class II or III Moderate ridge defect | In addition to stage III complexity: Need for complex rehabilitation due to: Masticatory dysfunction Secondary occlusal trauma (tooth mobility degree ≥2) Severe ridge defect Bite collapse, drifting, flaring Less than 20 remaining teeth (10 opposing pairs) |
| **Extent and distribution** | **Add to stage as descriptor** | For each stage, describe extent as localized (<30% of teeth involved), generalized, or molar/incisor pattern | | | |

**Table 1.2: Periodontitis grade Licence number 4416511255151 (Papapanou et al. 2018)**

| Periodontitis grade | | | Grade A: Slow rate of progression | Grade B: Moderate rate of progression | Grade C: Rapid rate of progression |
|---|---|---|---|---|---|
| Primary criteria | Direct evidence of progression | Longitudinal data (radiographic bone loss or CAL) | Evidence of no loss over 5 years | <2 mm over 5 years | ≥2 mm over 5 years |
| | Indirect evidence of progression | % bone loss/age | <0.25 | 0.25 to 1.0 | >1.0 |
| | | Case phenotype | Heavy biofilm deposits with low levels of destruction | Destruction commensurate with biofilm deposits | Destruction exceeds expectation given biofilm deposits; specific clinical patterns suggestive of periods of rapid progression and/or early onset disease (e.g., molar/incisor pattern; lack of expected response to standard bacterial control therapies) |
| Grade modifiers | Risk factors | Smoking | Non-smoker | Smoker <10 cigarettes/day | Smoker ≥10 cigarettes/day |
| | | Diabetes | Normoglycemic/ no diagnosis of diabetes | HbA1c <7.0% in patients with diabetes | HbA1c ≥7.0% in patients with diabetes |

## 1.4    SUBGINGIVAL PLAQUE

Subgingival plaque has been deemed to be complex since the first microscopic study of this ecosystem (Socransky et al. 1998). The microbiological characteristics of the progressing periodontal lesion from health to destructive periodontal disease are known to be vast and complicated (Holt and Ebersole 2005). A number of subgingival plaque genera, including *Filifactor, Porphyromonas, Treponema, Tannerella, Eubacterium, Peptostreptococcaceae, Desulfobulbus, Lachnospiraceae, Alloprevotella, Mogibacterium, Hallella, Phocaeicola, Johnsonella, and Mycoplasma* were found to be associated with periodontal disease (Chen et al. 2018a). Due to advancing techniques more organisms are being identified and associated with periodontitis, including viruses, such as Epstein-Barr virus (EBV-1) and human cytomegalovirus (HCMV) (Michalowicz et al. 2000). Even though no single species or group of species have been specifically identified as the cause of periodontitis, species *Tannerella forsythia* (previously also referred to as *Bacteroides forsythus*), *Treponema denticola* and *Porphyromonas gingivalis* in particular are consistently associated with periodontitis, so much so that they are referred to as periodontal pathogens (Leys et al. 2002, Holt and Ebersole 2005, Hajishengallis and Lamont 2012). These three species are part of what is known as the red

bacterial complex and show a strong relationship with clinical parameters or periodontal disease, including increased pocket depth (Socransky et al. 1998, Ali et al. 1997). "Red complex" bacteria appear at the stage of periodontitis progression. They populate and adhere to the sulcular region of teeth, taking advantage of the altered architecture in sulci that have been subjected to attachment loss and/or pocket formation (Holt and Ebersole 2005, Socransky et al. 1998). *P. gingivalis* is rarely detected in the absence of *T. forsythia in vivo* (Socransky et al. 1998) and members of this complex have been found to co-aggregate *in vitro* (Socransky et al. 1998, Yao et al. 1996).

Red complex bacteria are one of the six bacterial clusters in subgingival biofilms described by Socronsky (Socransky et al. 1998). The yellow and purple clusters consist of *Streptococcus* species, *Actinomyces odontolyticus* and *Veillonella parvula* respectively, and are described as "early colonisers". They are characterised by the expression of receptors that mediate firm attachment to the host surface. *Capnocytophaga* spp, *Campylobacter concisus, Eikenella corrodens* and *Aggregatibacter actinomycetemcomitans* (previously known as *Actinobacillus actinomycetemcomitans*) are a group of bacteria that are less associated with other individual bacterial species and make up the green cluster (Socransky et al. 1998, Holt and Ebersole 2005). The orange cluster consists of species that bridge bacteria to others depending on their nutrient use and cell surface structures that allow them to bind to both early colonisers and red complex members. Examples of orange cluster bacteria include *Fusobacterium* ssp., *Prevotella* ssp., *Micormonas micros* (also known as *Peptostreptococcus micrus)*, *Streptococcus constellatus*, *Campylobacter* spp and *Eubacterium* spp (Holt and Ebersole 2005, Kolenbrander et al. 2002).

Amongst the six described clusters, the red cluster is considered the most important in relation to periodontal disease progression. *P. gingivalis* and *T. denticola* are rarely found in solitude. It is understood that *P. gingivalis* benefits from a nutritional interdependence with *T. denticola* and appear to be closely linked topologically in the subgingival biofilm. These organisms have been shown to produce outer membrane-associated proteases that facilitate tissue destruction, including arginine and lysine-specific cysteine proteases. As highlighted earlier *P. gingivalis* is generally found with *T. forsythia*, a nutritionally fastidious anaerobe, which also produces proteases, enzymes with the ability to degrade extracellular matrix and biomolecules related to the host response. The different complexes and bacterial species

highlight the complexity of periodontal disease progression (Holt and Ebersole 2005). In fact, previous studies have identified over 700 organisms that might be involved in periodontal pathogenesis, of which up to 200 can be present in any one individual at any one time, and it is estimated that about 50 can be present at any one oral site (Aas et al. 2005). Much is left to be uncovered on how these organisms as a group and individually contribute to the disease process (Holt and Ebersole 2005).

### 1.4.1 *Porphyromonas gingivalis*

Out of all the red-complex bacteria, *P. gingivalis* has been the most extensively studied. This is due to its strong connection with periodontitis, as well as its ease to be genetically manipulated and to grow when compared to the other members of the red complex bacteria (Hajishengallis and Lamont 2012). *P. gingivalis* is a Gram-negative, small, black-pigmented anaerobe (Holt and Ebersole 2005) and has been identified as a "keystone pathogen" of periodontal disease (Hajishengallis et al. 2012, Nazir 2017). The term "keystone" refers to organisms that exert pathogenic affects that are disproportionately large relative to their population size (Hajishengallis et al. 2012, Power et al. 1996). Several virulence factors contribute to this organism's pathogenicity, including colonisation factors (fimbriae, lipopolysaccharide (LPS), haemagglutinin), outer membrane proteins and vesicles, as well as the proteolytic enzymes known as gingipains (Hajishengallis and Lamont 2012, Lamont and Jenkinson 1998, Imamura 2003, Holt and Ebersole 2005, Naylor et al. 2017). Gingipains HRgpA (95 kDa) and RgpB (50 kDa) are products of the *rgpA* and *rgpB* gene and are specific for Arg-Xaa peptide bonds. Kgp on the other hand is a product of another unrelated gene known as *kgp* and is Lys-Xaa bond-specific. HRgpA and RgpB activate kallikrein/kinin pathways and enhance vascular permeability, while Kgp is associated with bleeding tendency of diseased gingiva. Gingipains are also involved in degradation of macrophage cell surface CD14 which leads to loss of cell activation via this LPS co-receptor, fimbriae maturation, as well as amino acid uptake from the host (Imamura 2003).

These virulence factors allow *P. gingivalis* to play a major role in triggering inflammatory responses through dysbiosis, despite their low-level of colonisation of the periodontium (Hajishengallis et al. 2012). *P. gingivalis* can also activate complement and impair host defence, resulting in an increase in other groups of commensals. This stimulates further

complement-dependent inflammation that provides a nutrient-rich environment (rich in degraded host proteins and haemin) in the gingival exudate. The protein and haemin rich environment is ideal for growth of proteolytic and asaccharolytic bacteria. The bone resorption that follows provides further niches for dysbiotic microorganism colonisation (Hajishengallis et al. 2012). This cascade is led by gingipains, which cleave complement component C5 to produce C5a. As a result, C5a levels increase in the area of infection, which in turn recruits leukocytes that further drives inflammation. Gingipains simultaneously impair leukocyte killing through subversive crosstalk with Toll-like receptor 2 (TLR2) (Hajishengallis et al. 2012, Imamura 2003). This hypothesis of the "self-feeding cycle" was described by Hajishengallis (Figure 1.6).
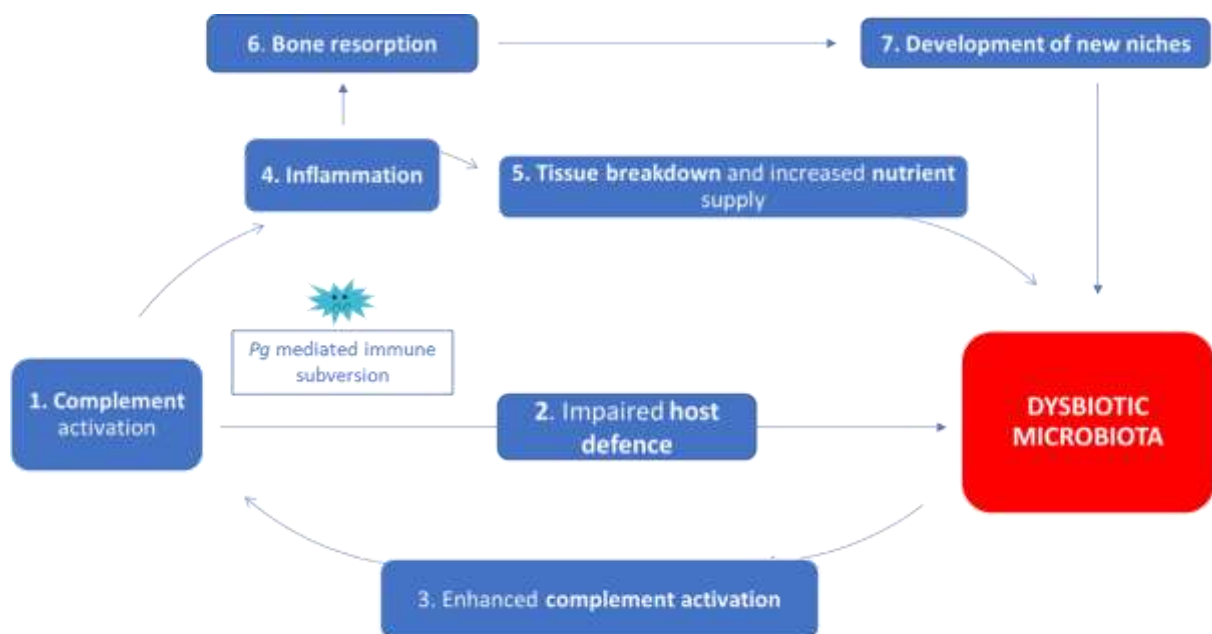


Figure 1.6: *Porphyromonas gingivalis* induced inflammatory cascade (Hajishengallis et al. 2012).

The outer membrane vesicles (OMV) of *P. gingivalis* are also being increasingly recognised as major contributors to this organism's pathogenicity (Gui et al. 2016). OMV are spherical nanostructures typically produced by Gram-negative bacteria made up of an asymmetrical single bilayer membrane (Kulp and Kuehn 2010). An example of *P. gingivalis* OMV production

can be seen in Figure 1.7. OMV can act as a highly complex secretion system capable of delivering a wide range of molecular effectors, which in turn can influence cell–cell interactions, host-immune responses, nutrient acquisition, as well as biofilm formation. Due to their detachment from the parent whole cell, they are able to disseminate further away and increase their influence away from sessile biofilm-associated bacteria (Gui et al. 2016). *P. gingivalis* OMV contain several components of its outer membrane including LPS, fimbriae, capsule components and gingipains (Grenier and Mayrand 1987, Furuta et al. 2009). Virulence factors carried over on OMV such as fimbriae and gingipains are thought to provide adhesive and proteolytic abilities respectively, which allows OMV to penetrate host tissues and cells. This is further enabled by *P. gingivalis* OMV's small size of between 20 to 500 nm (Furuta et al. 2009, Mayrand and Holt 1988). Interestingly, although generally periodontal pathogen outer membrane proteins are passed onto OMV, OMV proteomes can be differentially modulated relative to the outer membrane in response to environmental conditions such as haem availability (Veith et al. 2018).
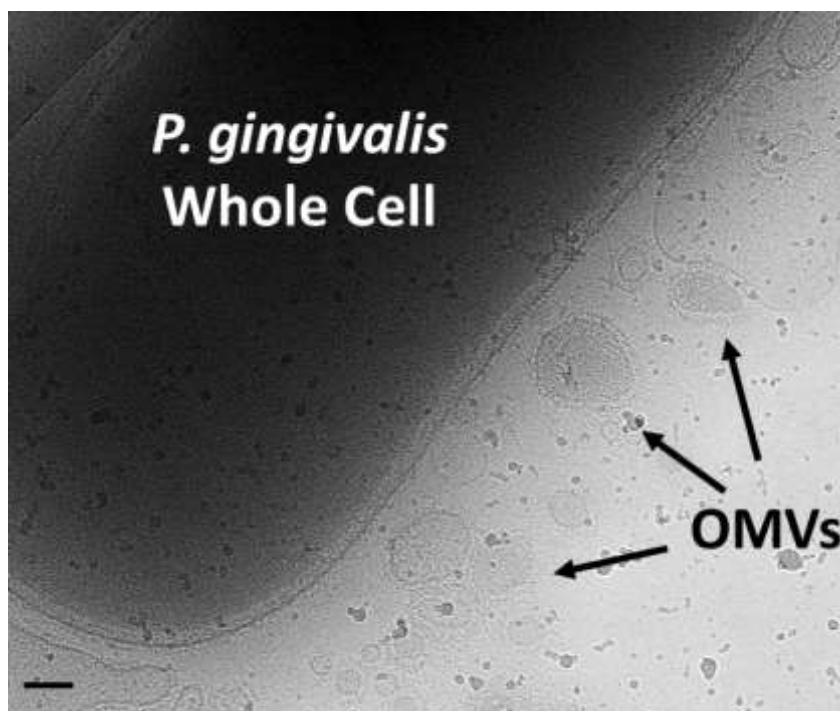


**Figure 1.7: *P. gingivalis* OMV secretion.** Cryo-electron micrograph showing a bacterial cell of *P. gingivalis* W83 secreting OMV (highlighted by black arrows). Scale bar = 100nm. Micrograph taken by Cher Farrugia under guidance of Dr. Svet Tzokov at the Electron Microscopy Facility in the Faculty of Science, University of Sheffield.

*P. gingivalis'* virulence mechanisms provide an insight towards the understanding of the complex host-pathogen interactions that occur in the progression of periodontal disease. However, in the oral cavity *P. gingivalis* is not a lone standing microorganism. *P. gingivalis* is known to aggregate with other red complex bacteria (Holt and Ebersole 2005), as highlighted previously in this section, but also to other microorganisms such as *Streptococcus mitis*, *Actinomyces viscosus*, *Streptococcus gordonii*, and to *F. nucleatum* (Yao et al. 1996).

The importance of microorganisms outside of the red complex in periodontal pathogenesis is highlighted in a more recent model which proposes that periodontitis is initiated by a synergistic and dysbiotic microbial community, rather than exclusively by select keystone periodontal pathogens. In this model different microorganisms fulfil roles that further enhance the microbiota's disease-provoking pathogenicity. While "keystone pathogens" impair immune response and favour a dysbiotic shift, other microorganisms provide other molecules such as adhesins and proinflammatory ligands to nutritionally sustain a microbial community that produces a cycle of continuous inflammation and tissue-destruction. (Hajishengallis and Lamont 2012). Research has in fact shown that *P. gingivalis* expresses different proteins when present in multispecies communities, including *F. nucleatum* (Hendrickson et al. 2014, Kuboniwa et al. 2009, Shokeen et al. 2021). *F. nucleatum* is an orange complex microorganism (Socransky et al. 1998) that is gaining further attention in both medical and research communities (Han 2015). It is one of the most prevalent microorganisms in extra-oral sites in disease conditions (Han and Wang 2013) and intraorally it is capable of adhering and invading epithelial cells (Fardini et al. 2011). *F. nucleatum* is a heterogeneous species with several documented subspecies (ssp), including *ssp animalis*, *ssp fusiforme*, *ssp nucleatum*, *ssp polymorphum*, and *ssp vincentii* (Han 2015, Gharbia and Shah 1992). Similar to *P. gingivalis* it produces several virulence factors including outer membrane proteins, LPS and adhesins (Brennan and Garrett 2019, Vinogradov, St Michael and Cox 2017b, Vinogradov, St Michael and Cox 2017a, Fardini et al. 2011, Kaplan et al. 2010, Kaplan et al. 2009).

Further research using multispecies biofilms is therefore required to grasp a better understanding of periodontitis progression in a clinically translatable manner. Papapanou *et al.* in a recent position paper on periodontitis also claim that there is a need for research that aims to identify methodologies for accurate assessment of longitudinal hard and soft tissue

changes in periodontitis progression and to identify markers differentiating between different types of periodontitis (Papapanou et al. 2018).

## 1.5    ORAL MICROBIOME AND SYSTEMIC DISEASES

Emerging evidence continues to associate the oral microbiome and oral diseases with several systemic diseases. This includes cardiovascular disease, heart disease, stroke, pneumonia, rheumatoid arthritis, pregnancy outcomes, Parkinson's and Alzheimer's disease, as well as some forms of cancer (colorectal, oesophageal and pancreatic) (Hajishengallis et al. 2012, Jia et al. 2018, Pereira et al. 2017, Pritchard et al. 2017, Ganesh et al. 2017, Wu and Nakanishi 2014, Watts, Crimmins and Gatz 2008). These systemic diseases can be grouped into inflammatory diseases, cancers and other diseases and summarised in Figure 1.8 to highlight the wide range of possible systemic links (Jia et al. 2018).



**Figure 1.8: Summary of systemic disease associated with oral diseases or components of the oral microbiome. (Images obtained from Pickitfreeimages ®)**

### 1.5.1  Inflammatory diseases

Oral diseases and oral organisms have been associated with a number of inflammatory diseases beyond the mouth. These include atherosclerosis (Offenbacher et al. 1999, Miyatani et al. 2015, Eberhard et al. 2017, Dietrich et al. 2013), heart disease including coronary artery

disease (Chhibber-Goel et al. 2016, Abranches et al. 2009, Androsz-Kowalska et al. 2013), pneumonia (Scannapieco 2006, Terpenning et al. 2001, Segal et al. 2016) and rheumatoid arthritis (Arvikar et al. 2017, Ayala-Herrera et al. 2018, Ceccarelli et al. 2018). It is hypothesised that this mostly occurs due to systemic dissemination of oral pathogens. Studies show that microbes which colonise the oral cavity frequently enter the bloodstream (Castillo et al. 2011). Sources of bacteraemia from oral bacteria include dental and/or oral tissues manipulation (Barbosa et al. 2015, Araújo et al. 2015, Mang-de la Rosa et al. 2014), periodontal infection sites (Horliana et al. 2014, Tomás et al. 2012) and daily lifestyle habits including brushing and flossing (Wilson et al. 2007, Lockhart et al. 2008). When infections spread systemically they can elicit excessive inflammation and result in tissue or organ specific diseases characterised by tissue destruction (Holt and Ebersole 2005). Bacteraemia is more likely to occur in the presence of oral tissue infection, since during infection tooth-supporting structures become more vascularized and enter into an intimate relationship with the microbial biofilm (Tomás et al. 2012, Vieira Colombo et al. 2016).

Systemic dissemination of oral pathogens has been traditionally associated with infective endocarditis (IE) mostly from bacterial infection of the endocardium or prosthetic replacements (de Souza et al. 2016, Werdan et al. 2014). IE can have fatal consequences and is caused by members of the *Streptococcus viridans* group, *Staphylococcus* and *Enterococcus* species 90% of the time. *Streptococcus mutans* and S*treptococcus sanguinis* being the most common oral microorganisms (Carinci et al. 2018). Organisms that are difficult to culture can also cause IE. Up to 31% of cases of endocarditis are claimed to be culture negative cases, which has led to further studies of IE samples by more advanced molecular techniques (Fournier et al. 2010, Kumar et al. 2013).

In the past two decades several oral microorganisms have been identified in other inflammatory lesions. *S. mutans*, *P. gingivalis*, *Gemella haemolysins and Aggregatibacter actinomycetemcomitans, P. intermedia, T. forsythia, F. nucleatum, S. sanguinis* all been identified in cardiovascular disease and atherosclerotic tissues (Miyatani et al. 2015, Eberhard et al. 2017, Kozarov et al. 2005, Campbell and Rosenfeld 2015), while *Campylobacter rectus*, *P. gingivalis*, *P. endodontalis*, *P. intermedia*, *Prevotella nigrescens* were specifically located in diseased coronary arteries (Chhibber-Goel et al. 2016). The presence of Gram-negative anaerobes in the cardiovascular system has been confirmed by a recent study that identified

*P. gingivalis* as the most frequent organism in femoral and coronary arteries in patients undergoing bypass grafts, followed by *Enterococcus faecalis* and *Finegoldia magna* (Mougeot et al. 2017b). *P. gingivalis and Aggregatibacter actinomycetemcomitans* (Gomes-Filho, Passos and Seixas da Cruz 2010) in addition *to Pseudomonas aeruginosa* have also been identified in pneumonia (Segal et al. 2016).

Studies also show that it is not only the systemic dissemination of oral microorganisms into the bloodstream that can affect distant organs. Oral pathogen virulence factors and inflammatory mediators produced at the local site of infection can also make their way into the bloodstream through degraded gingival tissues. These can then induce their own inflammatory responses systemically, which leads to further pathogenesis in the affected area (Kocgozlu et al. 2009).

## 1.5.2 Cancers

Certain oral bacteria have recently been linked to increased cancer risks (Jia et al. 2018). Oral bacterial dysbiosis has been associated with oral squamous cell carcinoma lesions. Changes in bacterial composition and gene functions were observed in periodontitis-correlated taxa *Fusobacterium, Peptostreptococcus, Dialister, Filifactor, Catonella, Peptococcus and Parvimonas* on oral cancer lesions (Yang et al. 2018, Zhao et al. 2017). In a recent study *P. gingivalis* has also been found in 61% of oesophageal cancer sites and was not detected in the normal oesophageal mucosa (Gao et al. 2016). This link is thought to be due to the increased systemic inflammation that follows periodontal disease, which in turn leads to alteration of gut microbiota that potentially influences carcinogenesis (Momen-Heravi et al. 2017).

Some groups of oral microorganisms were also found to induce additional responses in the gut. *Fusobacteria* encourage excessive immune responses and they have been shown to turn on colorectal cancer growth genes (Idrissi Janati et al. 2016). *Fusobacteria* infection has also been shown to stimulate tumour cells to generate exosomes that promote prometastatic behaviours in uninfected colorectal cancer cells *in vitro* and *in vivo* (Guo et al. 2020). *Fusobacteria* also express surface molecules enabling them to attach to and invade cancer cells. Following invasion, they expand myeloid-derived immune cells, hinder T-cell proliferation and activation, promote T-cell apoptosis (Nosho et al. 2016), and directly protect tumour cells from immune cell killing (Gur et al. 2015). *P. gingivalis* and *Aggregatibacter*

41

*actinomycetemcomitans* (*A. actinomycetemcomitans)* have also been linked to pancreatic cancer (Fan et al. 2016, Huang et al. 2016). Oral pathogens can enter the bloodstream through the epithelium and settle in pancreatic tissues (Huang et al. 2016), promote dysbiosis in the microbial community and in turn drive excessive inflammation potentially promoting pancreatic cancer (Jia et al. 2018). Recently published data also suggests a link between periodontal pathogens and breast cancer (Freudenheim et al. 2016a, Freudenheim, Millen and Wactawski-Wende 2016b, Shi et al. 2018). This evidence has led to further investigation of the use of oral microorganisms as markers or biosensors of cancer diagnosis and progression (Jia et al. 2018).

### 1.5.3  Other systemic diseases

Periodontal pathogens have also been associated with adverse pregnancy outcomes including preclampsia (Chaparro et al. 2013, Cobb et al. 2017, Takii et al. 2018), Alzheimer's disease (Pritchard et al. 2017, Ding et al. 2018, Emery et al. 2017, Ganesh et al. 2017, Harding et al. 2017, Kamer et al. 2008, Noble et al. 2014, Watts et al. 2008), kidney disease (Anand, S C and Alam 2013, Chen et al. 2015, Fisher et al. 2008a, Fisher et al. 2008b, Fisher and Taylor 2009, Kshirsagar et al. 2007, Kshirsagar et al. 2009, Pradeep et al. 2012, Ruokonen et al. 2017, Ruospo et al. 2017), diabetes (Amar and Leeman 2013, Anbalagan et al. 2017, Aoyama et al. 2018, King 2008, Long et al. 2017, Merchant et al. 2016), liver disease (Acharya, Sahingur and Bajaj 2017, Akinkugbe et al. 2017, Ilievski et al. 2016) and new links continue to emerge.

## 1.6    ASSOCIATION    BETWEEN    PERIODONTAL    DISEASE    AND CARDIOVASCULAR DISEASE

Out of all oral diseases, periodontal disease is the most frequently associated with systemic diseases. One of the most widely accepted and supported associations is the association between periodontal disease and different forms of cardiovascular disease. Periodontal disease increases the risk of cardiovascular disease by 19% and up to 44% in the over 65 population group (Nazir 2017) and is considered a risk factor for coronary heart disease (CHD) that is independent of other traditional CHD risk factors or markers (Chhibber-Goel et al.

2016). Such findings highlight the importance of understanding how periodontal disease can affect patients beyond their mouths.

## 1.6.1  Cardiovascular disease

Cardiovascular disease includes all diseases affecting the cardiovascular system. This includes myocardial infarction, coronary heart disease, cerebrovascular accidents or stroke, vascular disease, as well as peripheral arterial diseases (Cole and Kramer 2016, Finegold, Asaria and Francis 2013). Atherosclerotic cardiovascular disease (ACD) includes ischemic heart disease (IHD) and cerebrovascular disease (mainly ischemic stroke) and is the major cause of cardiovascular disease (Barquera et al. 2015). Atherosclerosis, like periodontitis, is a progressive chronic inflammatory disease. Chronic inflammation leads to endothelial dysfunction, increased vessel thickness, increased lipid deposition and potentially total vessel occlusion, which can be fatal (Campbell and Rosenfeld 2015, Atarbashi-Moghadam et al. 2018, Yamaguchi et al. 2015).

In healthy individuals, the endothelium acts as an anatomical barrier between the vessel wall and blood. It is a dynamic organ with several functions, including modulation of vascular tone, vessel permeability, angiogenesis, inflammation and transfer of cells and nutrients (Aird 2005, Kerr, Tam and Plane 2011). The barrier is made up of endothelial cells and proteins including occludins, claudins and VE-cadherin, which allow water and other small molecular weight substances to pass through (Haseloff et al. 2015). Dysregulation of these proteins can have catastrophic effects on the endothelium barrier function and can trigger cardiovascular disease. VE-cadherin is crucial for controlling blood vessel permeability (Zhang and Ge 2017, Corada et al. 2002). To date there is still on-going research on the role of the endothelial barrier and this is partly due to the heterogeneity of its structure. Endothelial features can vary depending on the site, the haemodynamic environment, as well as in response to the current needs of the underlying tissue, reflecting the complex nature of the endothelium's response and role in pathophysiology of vascular diseases (Aird 2005, Aird 2012, Tashiro et al. 1994, Ribatti et al. 2002, Aird 2006, Helmlinger et al. 1991). Current knowledge is mostly derived from the larger parts of the vasculature, known as the conduit vessels (arteries and veins). Less is known about the role of the microvasculature (capillaries), which are

macroscopically invisible and consist of a thin single layered endothelial cell wall surrounded by occasional pericytes and extracellular matrix (Aird 2005).

One of the most important functions of the endothelium is its role in inflammation in response to infection or tissue damage (Kerr et al. 2011). Interleukin-1 (IL-1) has been proposed as a key player in systemically mediated cerebrovascular inflammation (Denes et al. 2012). The actions of inflammatory cytokines such as TNF-α or IL-1 stimulate expression of interleukin-8 (CXCL8) that attracts leukocytes, and increases expression of adhesion molecules such as selectins (Komatsu et al. 2012). This process causes migration of leukocytes towards the infection site and attachment to the extracellular matrix. E-, P- and L- Selectins transiently bind leukocytes to the endothelium surface, facilitating a process known as leukocyte rolling (Komatsu et al. 2012). E- and P-selectin, unlike L-Selectin, are only expressed on the surface of activated endothelial cells. Apart from activating with different stimuli, selectins also act in a time-dependent fashion. E-selectin is stimulated with TNFα and expression peaks after approximately 12 hours then declines by 24 hours of stimulation. Leukocytes progress to firm adhesion by binding to chemokines that are presented on the endothelial cell surface by proteoglycans. This activates β1 and β2 integrins and increases their affinity for intercellular adhesion molecule (ICAM-1) and vascular cell adhesion molecule (VCAM-1) adhesion molecules. ICAM-1 is constantly expressed, although at a higher rate after TNFα stimulation, peaking at 6 hours and continuing for up to 72 hours. VCAM-1 expression is induced by oxidized low-density lipoproteins (LLP), cytokines and reactive oxygen species (ROS). Leukocyte migration occurs through transient disassembly of endothelial cell junctions, which in turn induces clustering of adhesion molecules (ICAM-1 (CD54), VCAM-1 (CD106)). This is followed by remodelling of endothelial cell actin cytoskeleton and cell junctions. Platelet endothelial cell adhesion molecule (PECAM-1, CD31) is a major contributor to the remodelling process. It is present in intercellular junctions and forms homodimers to link two adjacent cells. PECAM-1 also plays a role in leukocyte migration, since they are also expressed on leukocytes (Tapiero et al. 2002, Hordijk 2006, Rahman and Fazal 2009, Wittchen 2009). Inflammatory responses can act as a double-edged sword. While they are necessary for endothelial regeneration and repair, excessive inflammation can lead to endothelial cell dysfunction (Kerr et al. 2011, Gimbrone and García-Cardeña 2016).

Endothelial cell dysfunction is described as a phenotype, occurring locally or systemically, that can represent a net liability to the host (Aird 2006, Gimbrone and García-Cardeña 2016). Diseased endothelial cells start exhibiting focal permeation and sub-endothelial space modifications related to lipoprotein particles, which then triggers a cascade of complex pathological effects especially in the aortic and valvular areas (Gimbrone and García-Cardeña 2016). Several pathogenic processes have been associated with atherosclerosis. These include macrophage foam cell formation and death, extracellular lipid accumulation, changes in the structural intercellular matrix and smooth muscle cells, mineral deposit generation, neovascularization, physical changes to the lesion surface, haematoma and thrombi formation as well as inflammation itself, although this may vary between one lesion and another (Stary 2000, Gimbrone and García-Cardeña 2016).

Inflammation has been well-established as the cause of atherosclerosis (Gimbrone and García-Cardeña 2016), so much so that inflammatory marker CD40 is used as an early indicator of heart attacks (Yamaguchi et al. 2015, Helmlinger et al. 1991, Stary 2000). However, to date little is known about the biological agents that trigger vessel wall inflammation (Yamaguchi et al. 2015). In atherosclerosis-susceptible regions, especially aortic endothelial cells are exposed to altered flow, which can lead to altered cell alignment, increased expression of inflammatory mediators (Passerini et al. 2004, Gimbrone and García-Cardeña 2016) and an increase in VCAM-1 and ICAM-1 expression has been shown in ApoE-deficient mice's aortic arch (Nakashima et al. 1998). E- and P-selectin are expressed on endothelial cell surfaces of atherosclerotic regions indicating their role in formation of atherosclerosis (Kerr et al. 2011). PECAM-1 expression is also increased and was found to trigger endothelial shear stress in atherosclerosis also in ApoE-deficient mice's aortas (Harry et al. 2008). An illustration by Gimbrone *et al.* (Figure 1.9) shows how stimuli such as changes in blood flow or bacterial products can trigger phenotypic changes in endothelial cells including activation of Nuclear factor-kappa-B (NFκB) (a pleiotropic transcription factor). This in turn triggers expression of effector proteins related to the pathogenesis of atherosclerosis including procoagulation molecule Tissue Factor (TF), adhesion molecules (V-CAM-1, E-selectin) and inflammatory chemokines. These changes attract more macrophages and T-cells and therefore further production of cytokines, growth factors and reactive oxygen species (ROS) (Gimbrone and García-Cardeña 2016).
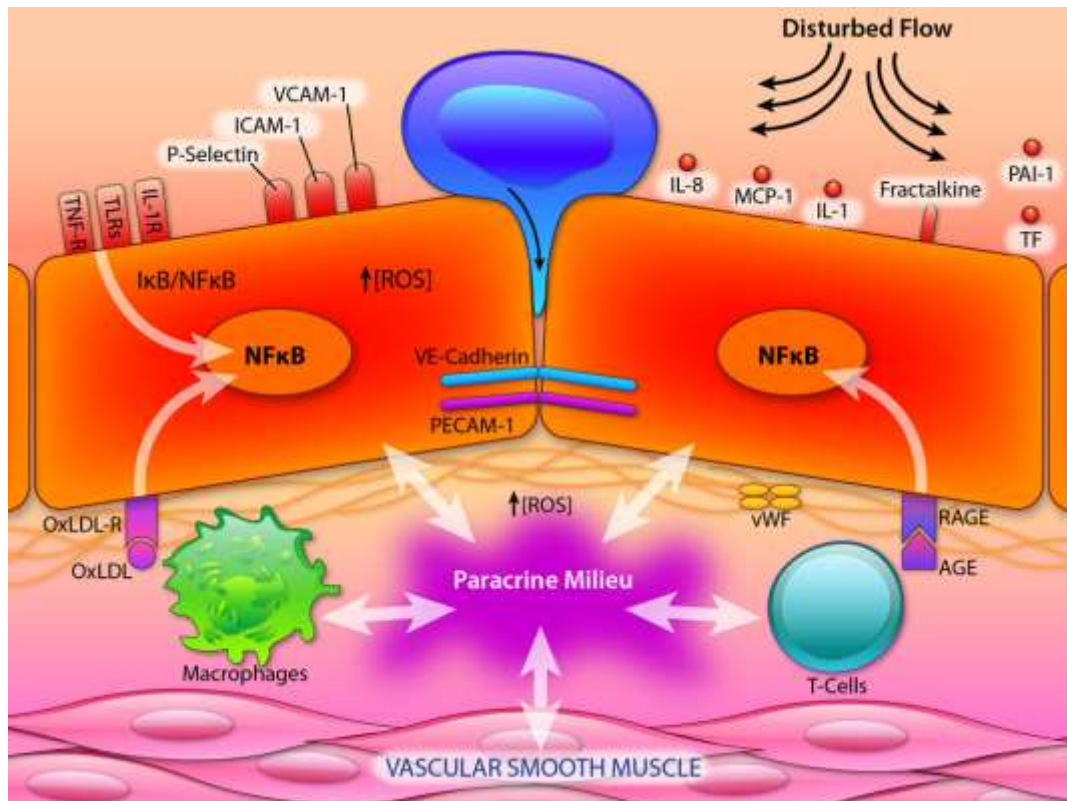
**Figure 1.9: Endothelial cell response to inflammatory mediators.** Stimuli including changes in flow, pro-inflammatory agonists (e.g., IL-1, TNF, endotoxins), oxidized lipoproteins (oxLDL) and advanced glycation end products (AGE) lead to activation of NFκB. This increases expression of cell surface adhesion molecules (e.g., VCAM-1, E-selectin), chemokines secretion (e.g., IL-8 (CXCL8), MCP-1 (CCL2), Fractalkine (CX3CL) and expression of pro-thrombotic mediators (e.g., TF, vWF, PAI-1). This in turn triggers recruitment of macrophages and T-cells, which further increases production of inflammatory cytokines, growth factors and ROS. Resulting in a pro-inflammatory state. (Gimbrone and García-Cardeña 2016)

Several risk factors have been identified for cardiovascular disease. These include genetic factors and family history, hypertension, left ventricular hypertrophy, hypercholesterolemia, diabetes, smoking, microalbuminuria, age, excessive alcohol intake, obesity and lack of physical activity (Atarbashi-Moghadam et al. 2018, Campbell and Rosenfeld 2015, Barquera et al. 2015). Nonetheless cardiovascular disease can also develop in the absence of these factors and infection has been suggested as a possible cause. Inflammation derived from infectious agents can occur either directly or indirectly. Microorganisms can systemically disseminate and directly infect vascular cells. As previously highlighted several oral pathogens have been located in inflamed vasculature and are thought to play a role in inflammatory diseases of the vasculature. Inflammation can be also induced through the indirect effects of cytokines and acute phase reactant proteins from distant sites that are liberated in response to oral

microbial infection (Rosenfeld and Campbell 2011, O'Connor et al. 2001, Campbell and Rosenfeld 2015).

## 1.6.2 Disease mechanisms explaining association

The association between periodontitis and cardiovascular disease has been studied for the last three decades and was confirmed by a landmark "Editorial" by Friedewald *et al.* in 2009 simultaneously published in both the American Journal of Cardiology and the Journal of Periodontology (Friedewald et al. 2009). This was further confirmed more recently by a joint workshop organised by both the European Federation of Periodontology and the American Academy of Periodontology which highlighted the "oral health-systemic connection" (Tonetti, Van Dyke and workshop 2013) and a "Perio & Cardio" campaign which followed a workshop organised by the European Federation of Periodontology (EFP) and the World Heart Federation (WHF) in 2020 (2020). Although this relationship has long been established, there are still several debates related to the underlying mechanism (Atarbashi-Moghadam et al. 2018, Schenkein et al. 2020, Herrera et al. 2020). The main mechanisms currently described can be divided into direct actions of oral microorganisms into the vasculature or indirect effects.

### 1.6.2.1 Direct

Studies have shown that periodontal pathogens can enter the bloodstream, especially in cases of extreme gingivitis or periodontitis (Castillo et al. 2011, Loos 2006, Loos 2005). In these cases the periodontal surfaces are inflamed forming an area coined as the *porte d'entrée*. Ulceration, loss of epithelial lining integrity and bleeding facilitates the movement of bacteria and their products from the periodontal pocket to the bloodstream (Schenkein and Loos 2013, Kremer et al. 2000, Loos et al. 2000, Loos 2005, Loos 2006). Periodontal pathogens, including *P. gingivalis*, *A. actinomycetemcomitans*, *Prevotella intermedia, T. forsythia*, and *F. nucleatum*, are also capable of invading host cells to protect themselves from host defence mechanisms and to take advantage of host cytoplasmic proteins and key nutrients (Reyes et al. 2013a). This behaviour suggests that survival in phagocytic cells might be an additional path for periodontal pathogens to systemically disseminate in a "Trojan Horse" approach (Carrion et al. 2012).

Several periodontal pathogens and/or their DNA have been located from human samples of diseased vasculature (Marcelino et al. 2010, Lindskog Jonsson et al. 2017, Gaetti-Jardim et al. 2009, Szulc et al. 2015, Mougeot et al. 2017b, Chiu 1999). In animal models, oral pathogens accelerate atherosclerotic lesions (Li et al. 2002, Jia et al. 2013, Jia et al. 2015a, Chukkapalli et al. 2014), increased plasma IL-6 levels, increased aortic expression of VCAM-1 and tissue factor (Lalla et al. 2003, Jia et al. 2013), increased plasma CXCL8 (Koizumi et al. 2008, Jia et al. 2013), Th17 cell induction (Jia et al. 2015a) and monocyte invasion (Lucas et al. 2014). These changes have been shown to be not related to gender (Champagne et al. 2009) and to not occur following doxycycline or metronidazole treatment (Madan et al. 2007, Amar, Wu and Madan 2009). In fact, several inflammatory modulators and oral pathogen virulent factors have been claimed to be responsible for the surge in inflammation. These include Nod-like receptor family, pyrin domain containing 3 (NLRP3) (De Nardo and Latz 2011, Li 2015, Latz, Xiao and Stutz 2013, Huck et al. 2015, Yamaguchi et al. 2015), bacterial gingipains (Yamaguchi et al. 2015, Bostanci and Belibasakis 2012, Widziolek et al. 2016), fimbriae (Yamaguchi et al. 2015, Bostanci and Belibasakis 2012), LPS and capsules (Bostanci and Belibasakis 2012). Other theories suggest that oral pathogens are responsible for inducing mitochondrial dysfunction, increased retention of lipids in the vessel wall (Kramer et al. 2014), stimulation and release of soluble P-selectin, activation of platelets (Assinger et al. 2011), and that oral pathogen invasive ability can be mediated by E-selectin (Ho et al. 2016).

Surprisingly, even though *T. forsythia* infection in animal models increases inflammatory modulators, it has not been shown to increase size of atherosclerotic lesions, suggesting that different organisms may contribute to different stages of the disease or that organisms exhibit different virulence potential when present as a single species (Chukkapalli et al. 2015b). This fits well with the recent findings that polymicrobial infection of mice triggered different host responses than single species infection (Chukkapalli et al. 2015c, Chukkapalli et al. 2017b, Nahid et al. 2011). In *in vitro* studies inclusion of *F. nucleatum* was found to enhance the invasion of *P. gingivalis* into aortic endothelial cells (Saito et al. 2008b), further confirming the need to study multispecies infections, since in clinical scenarios species. *P. gingivalis* in particular, is generally found with other pathogens and not as a solitary organism (Yao et al. 1996).

### 1.6.2.2 Indirect

Infectious diseases are characterised by microbial invasion of a susceptible host (Holt and Ebersole 2005), but atherosclerotic changes following *P. gingivalis* infection have been observed even in the absence of periodontal pathogens in the atherosclerotic tissues, suggesting effects through an indirect route (Jain et al. 2003). Indirect routes imply that the organism can instigate an inflammatory cascade without its local presence in the affected vasculature (El Kholy, Genco and Van Dyke 2015).

Some studies suggest that local periodontal infection can increase systemic vascular inflammation and that in turn triggers cardiovascular disease (El Kholy et al. 2015). In animal models, atherosclerotic lesions have been found to decrease following anti-inflammatory treatment (Hasturk et al. 2015), while bacterial antigens (such as LPS) alone can elicit an immune response (Schenkein and Loos 2013). In periodontitis patients, levels of the inflammatory marker C-Reactive protein are consistently elevated and can be reduced by periodontal therapy. C-Reactive protein can in turn induce an inflammatory cascade in the vasculature and increase cardiovascular disease risk (Freitas et al. 2012). As previously highlighted, diabetic patients suffering from periodontal disease have a greater risk of cardiovascular disease (Peng et al. 2017). Although this can be arguably due to the increased invasive ability of *P. gingivalis* in hyperglycaemic environments (Chen et al. 2018b), it can also be related to the increased systemic inflammation in such patients (Mesia et al. 2016).

Studies also suggest a proatherogenic lipid risk profile of elevated low-density lipoprotein (LDL), decreased high-density lipoprotein, increased triglycerides and oxidized low-dentisty lipoproteinin periodontitis patients might be another pathway explaining the link between periodontal disease and cardiovascular disease (Schenkein and Loos 2013). A 2016 study showed a significant correlation between serum LDL levels, fibrinogen levels, white blood cell counts and severity of periodontal disease in myocardial infarction (Górski et al. 2016). The above clinical studies as well as *in vitro* studies confirming the ability of *P. gingivalis* to oxidise HDL, leading to a shift to a proinflammatory lipid, which elicits further production of inflammatory cytokines from monocytic cells, has led to further research in this potential mechanism (Kim et al. 2018, Schenkein et al. 2020).

Other theories stipulate that the association may be due to a prothrombotic state in periodontitis. This is an increased hypercoagulable state and hypofibrinolysis state described

in periodontitis patients, that can facilitate atheroma and thrombus formation (Schenkein and Loos 2013). While more recent studies discovered common genetic factors in periodontitis and cardiovascular disease patients, which may contribute to the association between these two diseases (Aarabi et al. 2017).

The multitude of different theories available in the literature highlights the need for further studies to unravel the molecular basis of this association. Possibly through development of different experimental models to the ones currently used.

## 1.7 MODELS USED TO TEST ASSOCIATION BETWEEN PERIODONTAL DISEASE AND CARDIOVASCULAR DISEASE

Several models have been used to study the association between periodontal disease and cardiovascular disease. All aim to understand and recreate the complexity of the processes involved in oral microorganism induced infection of the cardiovascular system.

### 1.7.1 *In vitro*

The most common *in vitro* model used was that of infection of monolayers of endothelial cells (Huck et al. 2015, Ho et al. 2016, Assinger et al. 2011). For infection to occur microorganisms require adhesion to the vessel walls under shear stress, created through the flow of blood. Most infection studies fail to take flow into account and so may not be representative of what occurs *in vivo*; possibly leading to non-realistic conclusions related to this host-pathogen interaction. To overcome this issue, Claes *et al.* describe a micro-parallel flow chamber model where they studied the effects of *Staphylococcus aureus* under shear stress (Claes et al. 2015). As yet, there are no published articles examining the interaction of oral pathogens with endothelial cells under flow.

### 1.7.2 *In vivo*

Use of animal studies remains essential to study the pathogenesis of diseases (Vandamme 2014). Animal models are frequently used to study the effects of periodontitis and periodontal pathogens on the vasculature. Atherosclerosis-prone animals were used in early studies to

examine periodontitis and/or periodontitis-associated bacteria on the atherogenic process (Schenkein et al. 2020). Approaches used included intravenous injections of periodontal pathogens in apolipoprotein E-deficient mice (Li et al. 2002, Tuomainen et al. 2008) or normo- or hypercholesterolemic pigs (Brodala et al. 2005), as well as *P. gingivalis* applications following ligature-induced periodontal breakdown in rabbits and rats (Jain et al. 2003, Ekuni et al. 2009). Less invasive models were concurrently developed in apolipoprotein E-deficient mice using oral gavage with periodontal pathogens (Lalla et al. 2003, Gibson et al. 2004).

Murine (Li et al. 2002, Lalla et al. 2003, Champagne et al. 2009, Madan et al. 2007, Amar et al. 2009, Koizumi et al. 2008, Lucas et al. 2014, Yamaguchi et al. 2015, Kramer et al. 2014, Jia et al. 2013, Jia et al. 2015a, Chukkapalli et al. 2015c, Chukkapalli et al. 2017b, Nahid et al. 2011, Chukkapalli et al. 2014) and rabbit (Jain et al. 2003, Hasturk et al. 2015) models continue being the most commonly used in this field. These animals allow for different methods of infection including oral infection and can be genetically modified to study different human genetic determinants (Vandamme 2014, Vandamme 2015).

Zebrafish (*Danio rerio)* have recently been proposed as a model for systemic infection of oral pathogens, since murine and mammal models are expensive and may provide limited data on disease molecular mechanisms (Widziolek et al. 2016). The zebrafish has long been identified as a possible infection model despite anatomical differences between zebrafish and humans (Sullivan and Kim 2008). Zebrafish models are showing increasing interest since they allow investigation of infection through injection of a wide range of sites of research interest, including systemic infections to study microorganism-endothelial interactions (Gomes and Mostowy 2020). Zebrafish exhibit a genome with significant homology to that of humans, which can be manipulated relatively easily and due to their transparent nature can be used for real-time imaging *in vivo* (Jim et al. 2016, Sullivan and Kim 2008, Widziolek et al. 2016, Goldsmith and Jobin 2012). The ever growing variety of transgenic lines expressing fluorescent proteins make this model particularly beneficial in the study of molecular mechanisms involved in dynamic host-pathogen interactions (Gomes and Mostowy 2020).

### 1.7.3  Human

Several studies have used human models to study the association between periodontitis and cardiovascular disease. Several studies sampled different human tissues and analysed for

periodontal pathogen DNA to aim to identify a correlation between periodontal pathogen/disease presence and cardiovascular status or risk (Kozarov et al. 2005, Lindskog Jonsson et al. 2017, Gaetti-Jardim et al. 2009, Szulc et al. 2015, Zhang et al. 2008, Marcelino et al. 2010, Mougeot et al. 2017b). Cohort studies (Peng et al. 2017, Androsz-Kowalska et al. 2013, Honda et al. 2005), systemic reviews and meta-analysis of existing human data have also been used to study this association (Humphrey et al. 2008). Human studies are mostly cross-sectional, with few longitudinal studies published. Intervention studies are impractical and expensive and most designs may not be possible or ethical since it would be unethical to stop treatment for identified periodontitis or cardiovascular disease patients (El Kholy et al. 2015).

## 1.7.4  Microroganisms tested

In human experiments several periodontal microorganisms have been identified in the vasculature or vascular tissues samples as highlighted in earlier sections and in Table 1.3. Other studies only specified the taxa they identified, which can also vary greatly between patients (Lindskog Jonsson et al. 2017). Variations can also arise due to different methods of sample collection and varied molecular techniques used to identify such microorganisms and their DNA (Schenkein et al. 2020).  A 2016 review investigated 63 independent studies with a total of 1791 patients that underwent carotid endarterectomies, catheter-based atherectomy and other comparable procedures. In this review 23 oral commensals were confirmed individually or together in atherosclerotic plaques, including *A. actinomycetecomitans*, *P. gingivalis, T. forsythia*, *P. intermedia*, *F. nucleatum*, *Campylobacter rectus*, *T. denticola, Streptococcus gordonii, S. mutans,* and *Streptococcus oralis* as well as other uncultivated species (Chhibber-Goel et al. 2016).

**Table 1.3: Summary of periodontal microorganisms identified in the vasculature**

| Periodontal microorganism | Area identified |
|---|---|
| *Porphyromonas gingivalis* | Atherosclerotic plaque (Kozarov et al. 2005, Gaetti-Jardim et al. 2009, Zhang et al. 2008, Szulc et al. 2015, Marcelino et al. 2010), Non-atherosclerotic arteries (Mougeot et al. 2017) |
| *Agregatibacter actinomycetemcomitans* | Atherosclerotic plaque (Kozarov et al. 2005, Gaetti-Jardim et al. 2009, Marcelino et al. 2010), Blood (Lockhart et al. 2008) |
| *Fusobacterium nucleatum* | Atherosclerotic plaque (Marcelino et al. 2010), Blood (Lockhart et al. 2008) |
| *Prevotella intermedia* | Atherosclerotic plaque (Gaetti-Jardim et al. 2009, Marcelino et al. 2010) |
| *Treponima denticola* | Atherosclerotic plaque (Marcelino et al. 2010), Blood (Lockhart et al. 2008) |
| *Campylobacter rectus* | Atherosclerotic plaque (Marcelino et al. 2010) |
| *Porphyromonas endodontalis* | Atherosclerotic plaque (Marcelino et al. 2010) |
| *Prevotella melaninogenica* | Blood (Lockhart et al. 2008) |
| *Prevotella nigrescens* | Atherosclerotic plaque (Marcelino et al. 2010) |
| *Prevotella oralis* | Blood (Lockhart et al. 2008) |
| *Streptococcus mitis* | Blood (Lockhart et al. 2008) |
| *Streptococcus sanguinis* | Blood (Lockhart et al. 2008) |
| *Tannerella forsythia* | Atherosclerotic plaque (Marcelino et al. 2010) |

Other investigations also suggest presence of herpes simplex virus (HSV) and cytomegalovirus (CMV) in atheromas in periodontitis patients, highlighting the complex nature of atheroma microbiomes. Present evidence indicates this complex environment can harbour organisms of oral, gut, respiratory tract, and skin origin (Armingohar et al. 2014, Schenkein et al. 2020).

This data contrasts with most *in vitro* and *in vivo* studies carried out where infection is most of the time simulated using single species, generally *P. gingivalis.* Polymicrobial investigations

are even more so scarce in *in vivo* models, where only a few studies used polymicrobial infection (Chukkapalli et al. 2015c, Nahid et al. 2011, Rivera et al. 2013, Velsko et al. 2015).

## 1.8    CONCLUSIONS

Periodontal disease and periodontal pathogens are associated with cardiovascular disease, but more research is required to identify the exact mechanism. Several cell adhesion molecules have been shown to play a role in cardiovascular disease progression, and it is hypothesised that they may also be involved in oral pathogen induced cardiovascular disease.

Several *P. gingivalis* virulence factors, including gingipains, can potentially initiate cardiovascular disease, however clearer data is required to identify whether oral microorganisms initiate or else aggravate already existing cardiovascular disease prone vasculature. Although the presence of oral pathogens has been repetitively confirmed in the human vasculature, presence does not provide enough information on the active role of microorganisms in disease processes. 2D cell culture methods are commonly used to study the role of oral pathogens *in vitro* but these models are generally not representative of the clinical scenario, particularly when flow is not incorporated in the model. Murine models are also common and have the advantage of providing several components missing from 2D models. However, mice are different to humans and therefore what is observed in a mouse model may not occur in humans. Not to mention that this model does not allow for real-time molecular investigations and that nowadays models complying with the 3Rs (Replacement, Reduction and Refinement) of animal research are preferred.

This literature review also highlights that periodontal pathogens rarely function as a single unit, but not much research has been done on multispecies infection when studying the association between periodontal disease and cardiovascular disease. Hence, there is a need for investigation of other disease mechanisms from those currently suggested, use of more models to study the role of oral pathogens in the initiation of cardiovascular disease, as well as the need for research using multispecies infections.

## 1.9    HYPOTHESIS, OVERALL AIM AND OBJECTIVES

Hypothesis

Periodontal pathogens mediate detrimental changes to the endothelial cells that line the vasculature leading to alteration in endothelial cell adhesion molecule expression, which in turn increases endothelial permeability and potentially initiates or potentates the development of cardiovascular disease (Figure 1.10).
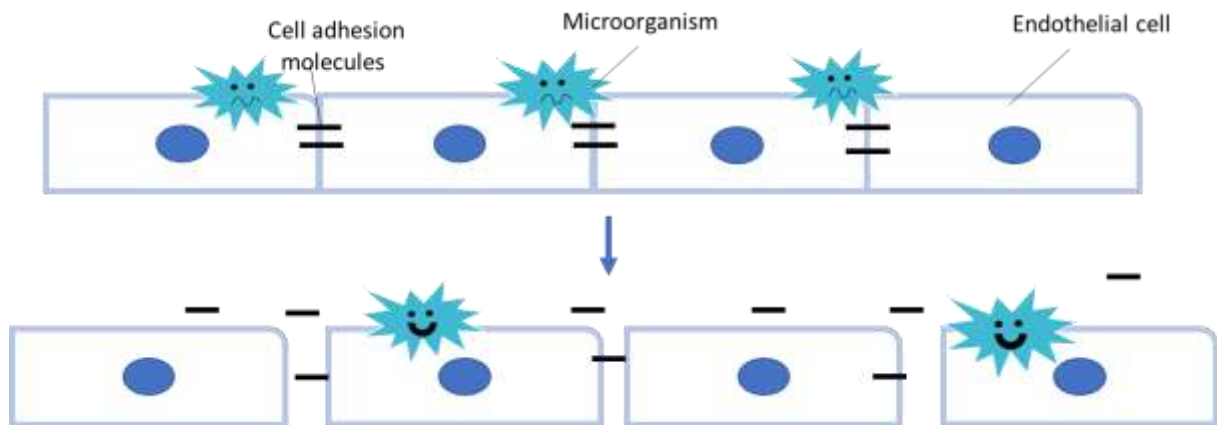


Figure 1.10: Research hypothesis summary

**Aim**

The aim of the project is to use *in vitro* (endothelial cell monolayers) and *in vivo* (zebrafish larvae) models to investigate the molecular mechanism by which periodontal pathogens cause vascular damage and initiate or potentate cardiovascular disease.

**Objectives**

- To develop models to study effects of periodontal pathogen invasion in endothelial cells
- To measure invasion capacity of human endothelial cells using antibiotic protection assays
- To visualise oral microorganism invasion in endothelial cells using confocal microscopy

- To study effects of periodontal pathogens on endothelial cell surface and adhesion molecules abundance using immunostaining and flow cytometry

- To image and quantify effects of periodontal pathogen systemic infection on zebrafish larvae models using confocal microscopy.

- To study the role of specific *P. gingivalis* virulence factors including gingipains and outer membrane vesicles in mediating endothelial damage

- To investigate effects of *F. nucleatum* and *T. forsythia* on endothelial cells

- To assess endothelial multispecies infections involving *P. gingivalis, F. nucleatum* and *T. forsythia* and assess potential differences in pathogenicity to single species infections

# CHAPTER 2: Materials and methods

## 2.1 MATERIALS, MANUFACTURERS AND SUPPLIERS

Reagents used in this study were of analytical grade and were obtained from the following manufacturers and suppliers.

Table 2.1: Supplier and location

| Supplier | Location |
|---|---|
| Abcam | Cambridgeshire, UK |
| Applied Biosystems | Paisley, UK |
| BD Biosciences | Oxfordshire, UK |
| Beckman | Indianapolis, Indiana, USA |
| BioLegend | San Diego, California, USA |
| Bioline | London, UK |
| BTL | Spolka, Poland |
| Cellsignaling | Danvers, Massachusetts, USA |
| eBioscience | Leicestershire, UK |
| Expedeon abcam | Cambridge, Massachusetts, USA |
| Gatan | Pleasanton, California, USA |
| GE Healthcare | Buckinghamshire, UK |
| GeneTex | Alton Pkwy Irvine, California, USA |
| Gibco | Paisley, UK |
| GraphPad | La Jolla, California, USA |
| Imaging Associates Limited | Bicester, UK |
| Invitrogen | Paisley, UK |
| Kodak | Rochester, New York, USA |
| Millicell | Hertfordshire, UK |
| NeoGen | Haywood, UK |
| New England Peptide | Louisville, Kentucky, USA |
| Oxoid | Basingstoke, UK |

| | |
|---|---|
| Particle Metrix | Meerbusch, Germany |
| Peprotech | London, UK |
| Perkin Elmer | Waltham, Massachusetts, USA |
| Promocell | Heidelberg, Germany |
| Quantifoil Micro Tools GmbH | Jena, Germany |
| R&D Systems | Abingdon, UK |
| Sarstedt AG | Nümbrecht, Germany |
| Seracare | Milford, Massachusetts, USA |
| Sigma Aldrich | Dorset, UK |
| Syngene | Cambridge, UK |
| Thermofisher Scientific | Leicestershire, UK |
| Treestar | Ashland, Oregon, USA |
| WILD | Heerbrugg, Switzerland |
| Xograph | Gloucestershire, UK |
| Zeiss | Hertfordshire, UK |
| Zetaview | Meerbusch, Germany |

## 2.2 GENERAL CELL CULTURE METHODS

All cell culture work was carried out in a Class II laminar flow hood and all equipment and armamentarium used was sterilised prior to use with 70 % (v/v) industrial methylated spirits, by filter sterilisation or by autoclaving.

### 2.2.1 Primary human dermal microvascular endothelial cells (HDMEC)

Human dermal microvascular endothelial cells (HDMEC) were purchased from PromoCell. Microvascular endothelial cells isolated from human dermal juvenile foreskin and adult skin were received cryopreserved at passage 2 in serum-free freezing medium (Cryo-SFM, Promocell) containing around $5 \times 10^5$ viable cells per vial. MV Medium containing growth factor supplement (Promocell) was used as the cell culture medium.

## 2.3.2  Immortalised human microvascular endothelial cell line

The immortalised human microvascular endothelial cells, HMEC-1 (Ades et al. 1992) were obtained from Michael Dillon & Paco Candal of the National Center for Infectious Diseases under Materials Transfer Agreement. HMEC-1 were cultured in MCDB 131 (Gibco) supplemented with 10 ng/mL epidermal growth factor (EGF) derived from mouse submaxillary glands (Sigma), 1 μg/mL water soluble hydrocortisone (Sigma), 10% v/v foetal calf serum (FCS; Gibco) and 2mM L-Glutamine (Sigma).

## 2.3.3  Thawing, sub-culture and cryopreservation

Cells were stored in cryovials by cryopreservation in liquid nitrogen. Vials were thawed by rapid agitation in a 37°C water bath, the contents diluted in culture medium to a seeding density of $1 \times 10^4$ viable cells per $cm^2$ in a tissue culture-treated flask and incubated at 37°C in a 5 % $CO_2$ atmosphere.  Culture medium was replaced after 24 hours and further replaced at two-day intervals until 70-90 % confluent. Culture medium was aspirated, the cell monolayer washed twice with phosphate-buffered saline (PBS) (Sigma) and 0.05 % trypsin/0.02 % EDTA v/v (T/E) (Sigma) solution added to detach the cells for 1-2 minutes. The same volume of growth medium containing 10 % v/v FCS was used to stop T/E activity.  Cells were dispersed using a pipette, centrifuged at 200 x g for 5 minutes to pellet and supernatant discarded. Cells were then re-suspended in medium and counted using Trypan Blue, to determine cell viability. Cells were then inoculated into a tissue culture flask and sub-cultured at 37°C in a 5 % $CO_2$ atmosphere.  Cells not immediately required for experiments were cryopreserved in liquid nitrogen in appropriate cryopreservation medium Cryo-SFM (Promocell) and frozen at a concentration of $1 \times 10^6$ cells/mL.

## 2.3  GENERAL MICROBIOLOGY METHODS

## 2.3.1  Culture of microbial strains

*P. gingivalis* (wild-type strains W50 from Prof. Curtis' collection, ATCC33277 from Prof. Stafford's collection, W83 from Prof. Potempas's collection and clinical strain A245Br from

Prof. Murdoch's collection), along with *F. nucleatum* ssp *nucleatum* (ATCC 25586) and *polymorphum* (ATCC 10953) from Prof. Wade's collection were maintained on Fastidious Anaerobe (FA) (NeoGen) agar plates supplemented with 5% v/v oxylated horse blood (Oxoid). The *P. gingivalis* W83 isogenic ΔK/R-ab (*kgpΔ598-1732::Tc$^R$ rgpA-::Cm$^R$ rgpBΔ410-507::Em$^R$*) strain from Prof. Potempa's collection was grown on FA plates supplemented with 1 μg/mL tetracycline while *Tannerella forsythia* (ATCC 43037) from Prof. Sharma's collection was grown on FA plates supplemented with 1 % N-acetylmuramic acid (NAM) in addition to oxylated horse blood. Liquid cultures were maintained in either Schaedler (BTL) or Brain-heart infusion broth (Oxoid) supplemented with 5 mg/mL yeast extract, 250 μg/mL L-cysteine, 1 mg/mL haemin and 1 mg/mL vitamin K. Both liquid and agar cultures were incubated at 37°C in an anaerobic chamber with an atmosphere of 80 % $N_2$, 10 % $CO_2$ and 10 % $H_2$.

For use in experiments, strains were grown in broth overnight in an anaerobic chamber, fresh cultures were set up form the overnight culture to an optical density ($OD_{600}$) equal to 0.1 and cultured until late log phase. Bacteria were then harvested by centrifugation at 8,000 × g for 3 minutes, washed with PBS or appropriate medium and resuspended at the required density.

## 2.3.2  Bacterial growth curves

*P. gingivalis* grown on FA plates were transferred to 3 mL supplemented broth (BHI or Schaedler) and incubated at 37°C overnight under anaerobic conditions. Cultures were then adjusted in 10 mL of broth to an $OD_{600}$ of around 0.1 with broth alone used as blank control. 100 μL broth was taken at different time points, diluted in 900 μL of media and OD measured. An additional culture at 0.1 $OD_{600}$ was set in the evening for additional time points.

## 2.3.3  Colony viability count

Bacteria were prepared as described in section 2.3.1 Culture of microbial and adjusted to $OD_{600}$ 1.0 and 20 μL of this suspension diluted with 180 μL BHI. Serial dilutions of up to 8 concentrations were carried out, after which 10 μL of each dilution was spotted onto an FA-blood agar plate in triplicate. Plates were left to dry for a few minutes then incubated in an anaerobic incubator for 3 days. The number of colonies was counted for each drop and the

number of bacteria per one millilitre in the original culture was calculated by multiplying with the dilution factor counted. Counting was performed where more than 10 CFU but less than 100 CFU could be clearly observed.

### 2.3.4 Metronidazole sensitivity assay

*P. gingivalis* metronidazole sensitivity for strains used was confirmed using a commercial E-Strip Test method. *P. gingivalis* was prepared as described in section 2.3.1. $OD_{600}$ nm was adjusted to 0.1 and 1, and 100 µL of *P. gingivalis* was spread onto a blood agar plate. The plates were left to dry for 3 minutes and the metronidazole E-Strip (M.I.C. Evaluator, Oxoid) was placed on the middle portion of the plate and then incubated in an anaerobic incubator for 3 days. The clear zone of antibacterial activity was assessed and images taken.

## 2.4   GENERAL ZEBRAFISH METHODS

Zebrafish maintenance and experimental work were carried out in accordance with UK Home Office regulations and UK Animals (Scientific Procedures) Act 1986 and under Project Licence P1A4A7A5E (Prof. Steven Renshaw) using zebrafish embryos under 5 days post fertilisation (dpf). London wild-type (LWT), Nacre wild-type, VE-cadherin/Cdh5 transgenic *tg(cdh5$^{ubs8-/-}$;cdh5TS),* PECAM-1 transgenic *tg(fli1a:PECAM1-EGFP)sh524* and kdrl:mCherry transgenic were obtained from The Bateson Centre, University of Sheffield and maintained in E3 medium at 30°C according to standard protocols. Autoclaved 1 x E3 medium diluted in distilled water was prepared from 10 x stock (NaCl 50 mM, KCl 1.7 mM, CaCl2 3.3 mM,MgSO4 3.3 mM) and diluted to a 1 × solution with distilled water and supplemented with methylene blue (0.00005% (w/v)).

## 2.5 INVASION ASSAYS

### 2.5.1 Antibiotic protection invasion assay

Antibiotic protection invasion assays were carried out using a modification of Naylor *et al.* (Naylor et al. 2017). This method uses *P. gingivalis'* sensitivity to metronidazole (as confirmed through the metronidazole sensitivity assay) to measure portion of invaded cells. HMEC-1 and HDMEC cells were seeded at 2 x $10^5$ cells per well in a 24-well plate to confluence. Cell monolayers were washed with PBS then incubated with 2 % w/v bovine serum albumin (BSA) (Sigma) in cell culture medium to block nonspecific binding sites for 1 hour at 37°C, 5 % $CO_2$. A sacrificial well was trypsinised to carry out a cell count and determine the multiplicity of infection (MOI; multiplicity of infection refers to the number of bacteria one human cell). *P. gingivalis* strains were prepared as previously described in section2.3.1. The bacterial suspension was adjusted to an MOI 100 in cell culture medium and incubated with cells for 90 minutes at 37°C. This initial bacterial suspension was serially diluted on blood agar (BA) plates and grown anaerobically for 3 days to determine viable counts through colony forming units (CFUs). Cells were gently washed wit PBS to remove non-adherent bacteria and the infected monolayer then incubated with 200 μg/mL metronidazole for 1 hour at 37°C, 5 % $CO_2$ to kill external cell-adherent bacteria. Following antibiotic incubation cells were washed three times with PBS, lysed with $dH_2O$ for 20 minutes, scraped with a pipette and serially diluted on FA plates and incubated anaerobically for 3 days. CFU were enumerated to determine the total number of invading bacteria, expressed as a percentage of the viable count of the initial inoculum.

### 2.5.2 Intracellular and extracellular *P. gingivalis* visualisation

HMEC-1 (1 x $10^5$) were grown on 4-well glass-bottom culture chambers (Sarstedt AG) overnight. *P. gingivalis* was prepared as described in section2.3.1. Cultures were adjusted to an MOI 2000, washed twice with PBS and fluorescently labelled by re-suspension in 0.4 μg/mL 5-(and-6)-carboxyfluorescein, succinimidyl ester (5(6)-FAM, SE) (excitation 494 nm, emission 518 nm) (Invitrogen) in PBS for 15 minutes with shaking at 4°C. FAM-labelled *P. gingivalis* were diluted in 6-((Biotinoyl)Amino)Hexanoic Acid, Succinimidyl Ester (Biotinamidocaproate, *N*-Hydroxysuccinimidyl Ester; Biotin-X SE, Invitrogen) in PBS to give a final concentration of 0.3

mg/mL and incubated for 30 minutes at 4°C without shaking to biotinylate the surface of *P. gingivalis*. The excess biotin was removed by washing three times with PBS and resuspended in non-supplemented MCDB medium. These FAM-biotinylated *P. gingivalis* were used for invasion (MOI 1000) into HMEC-1 cells for 1 hour. HMEC-1 cells were fixed with 4 % PBS-buffered paraformaldehyde for 20 minutes and culture chambers were washed 3 times with PBS. 10 % v/v FCS in PBS was applied for 5 minutes at room temperature to block non-specific binding sites. Five micrograms of Alexa Fluor 647®-conjugated streptavidin (excitation is 650 nm, emission 655 nm) (ThermoFisher Scientific) in 1 mL of 10 % v/v FCS was added and cells were incubated for 45 minutes at 37°C in a 5 % $CO_2$ incubator. Streptavidin binds to biotin, resulting in extracellular *P. gingivalis* stained by both 5(6)-FAM, SE and Alexa Fluo 647®, leaving the intracellular bacteria stained with 5(6)-FAM, SE alone. After incubation the excess Alexa Fluor 647®-conjugated streptavidin was removed by washing 3 times with PBS. Nuclei were then stained with 7.5 µg/mL Hoechst® (excitation 350 nm, emission 461 nm) (Thermofisher Scientific) for 10 minutes, rinsed in PBS and the endothelial plasma membrane stained with 5 µg/mL Wheat Germ Agglutinin (WGA) (excitation 555 nm, emission 565 nm) (Thermofisher Scientific) for 10 minutes at 37°C. Chamber slides were rinsed again with PBS then mounted using ProLong® Glass (Thermofisher Scientific) antifade and slides kept in the dark overnight, allowing the mounting agent to cure. Chamber slides were analysed using a Zeiss LSM 880 invert Axio Imager and AiryScan detector. Images were generated using a X63 lens and processed using AiryScan® processing (Zeiss). Composites and orthogonal views were created using FIJI®.

## 2.6 E-SELECTIN EXPRESSION AND ROLE IN INVASION

### 2.6.1 E-selectin abundance

#### 2.6.1.1 In-cell enzyme-linked immunosorbent assay (ELISA)

An in-cell ELISA was used to identify cell surface E-selectin expression directly on the cultured HDMEC and HMEC-1 cells. Cells were seeded overnight at $2 \times 10^4$ cells per well until confluent in a 96-well plate. Cells were then stimulated with 25 ng/mL TNFα (Peprotech) for up to 24 hours stimulation and unstimulated cells were used as a control. Wells were then washed twice with PBS and fixed with 2% PBS-buffered paraformaldehyde overnight at 4°C. Fixing

solution was removed and wells washed twice with PBS and the monolayer checked. Wells were then blocked with PBS supplemented with 3 % BSA for 2 hours at room temperature to block non-specific binding sites. 50 µL of 5 µg/mL E-selectin primary antibody (R&D) or IgG isotype-matched control (R&D) diluted in blocking buffer were added and incubated for 1 hour at room temperature. Wells were washed 3 times with PBS and 50 µL HRP-conjugated secondary antibody (Cell Signalling) diluted in blocking buffer (1:1000) added and incubated for 30 minutes at room temperature. Wells were once again washed three times with PBS and 50 µL 3,3′,5,5′-Tetramethylbenzidine (TMB) substrate (SeraCare) added. Stop solution (0.16 M sulphuric acid) was added once the solution developed and optical density read at 450 nm using an Infinite 200 Pro spectrophotometer (TECAN).

### 2.6.1.2　Flow cytometry

HMEC-1 and HDMEC cells were seeded at $4 \times 10^5$ cells per well in 6-well plates and cultured until confluent. Cells were stimulated with 25 ng/mL TNFα for 5 hours (ensuring maximal E-selectin expression) while unstimulated cells were used as a control. Cells were washed with PBS, and 500 µL of 0.02 % EDTA (Sigma) was added for 20 minutes to non-enzymatically detach cells, followed by 500 µl of cold FACS buffer (0.1 % BSA and 0.1 % sodium azide w/v in PBS). The cell suspension was pipetted to create a single cell suspension and centrifuged for 5 minutes at 1100 g. The supernatant was removed and cells resuspended in 100 µL of FACS buffer. 5 µL of phycoerythrin-conjugated E-selectin CD62E (Clone:P2H3; eBioscience) or phycoerythrin-conjugated mouse IgG1 isotype control (Clone P3.6.2.8.1; eBioscience) were added for 45 minutes and incubated on ice in the dark. 500 µL of FACS was added and cells centrifuged for a further 2 minutes to pellet, after which the supernatant was removed, and cells resuspended in 300 µL FACS buffer. Single-colour sample analysis was carried out using a FACS Calibur flow cytometer (BD Biosciences) and the normalised median fluorescence index (nMFI) calculated as previously described by Chan *et al.,* 2013 (Chan, Yim and Choo 2013) by dividing the median fluorescence intensity of the positive samples by that of the negative stained samples (IgG isotype control).

### 2.6.1.3    Immunostaining

Glass coverslips were ethanol sterilised and dried under a flow hood and coated with 300 µl of 10 µg/mL bovine fibronectin (Sigma). HMEC-1 or HDMEC cells were seeded at 1 x 10$^5$ cells per glass slide and incubated overnight at 37$^0$C in 5 % CO$_2$ then stimulated with 25 ng/mL TNFα. Cells were rinsed with non-supplemented medium, fixed with 3.7 % v/v formalin in PBS for 10 minutes and blocked for 30 minutes using blocking buffer composed of 2 % w/v BSA and 5 % v/v goat serum in PBS (Sigma). Immunofluorescence staining was performed using 5 µg/mL of either mouse anti-E-selectin primary antibody clone BBIG-E4 (R&D) or IgG isotype-matched control Clone 11711 (R&D) at 4$^o$C overnight, washed with PBS and incubated with 1 µg/mL Alexa Fluor 488-conjurgated goat anti-mouse IgG (H+L) cross-adsorbed secondary antibody (Abcam) for 1 hour. Cells were rinsed again, mounted in ProLong™ Diamond antifade containing 4',6-Diaminidine-2'-phylindole dihydrocholoride (DAPI) (Thermofisher Scientific) and imaged using a Zeiss Axiovert 200 M inverted fluorescence microscope with an integrated high-resolution digital camera (AxioCam MRm; Zeiss) with AxioVision 4.6 software (Imaging Associates Limited).

## 2.6.2  E-selectin and *P. gingivalis* invasion

### 2.6.2.1    Antibiotic protection assay

HMEC-1 and HDMEC cells were seeded at 2 x 10$^5$ cells per well in a 24-well plate until confluent. Cells were then stimulated with 25 ng/mL TNFα for 5 hours, while unstimulated cells were used as a control. Cells were then treated as previously described in section 3.4.1 and % invasion calculated.

# 2.7 PERMEABILITY OF ENDOTHELIAL CELLS FOLLOWING INFECTION

## 2.7.1  Dextran permeability assay

A fluorescent dextran permeability assay was performed as previously described (Wang and Alexander 2011). Fibronectin-coated (10 µg/mL) 0.4 µm-pore hanging cell culture inserts (Millicell) were seeded with HMEC-1 until confluent. Seeded cell culture inserts were then

infected with increasing bacterial MOI for 1.5 hours at 37°C in serum-free medium. Inserts without cells or HMEC-1 alone were used as controls. Solutions were removed, inserts transferred to a new plate containing 500 µL supplemented MCDB131, and 450 µL supplemented MCDB131 containing 65 µg/mL 70 kDa fluorescent dextran (Molecular probes, Thermofisher) was added to the insert. Dextran leakage through the cell monolayer to the bottom well was monitored hourly for a 5-hour period by aspirating 250 µL medium from the bottom well. Dextran fluorescence was measured at 494 nm excitation, 521 nm emission and the aspirated volume was replaced with supplemented MCDB131 for further readings.

## 2.8  ADHESION MOLECULE ABUNDANCE FOLLOWING INFECTION

### 2.8.1  *In vitro* methods

Monolayers of HDMEC or HMEC-1 cells were infected and then subjected to flow cytometry or immunofluorescence staining to investigate the effects of infection on cell surface levels of E-selectin, VE-cadherin and PECAM-1.  Real-Time quantitative Polymerase Chain Reaction (qPCR) was used to analyse gene expression of the same molecules by endothelial cells.

#### 2.8.1.1    Flow cytometry

HMEC-1 and HDMEC cells were prepared as described in section 2.6.1.2. Cells were rinsed with PBS and infected at varying MOI for up to 1.5 hours, while medium alone was used as a control. Cells were washed with PBS, and 500 µL of 0.02% EDTA (Sigma) added for 20 minutes to remove cells, followed by 500 µL of cold FACS buffer (0.1 % w/v BSA and 0.1 % w/v sodium azide PBS). The cell suspension was pipetted vigorously and centrifuged for 5 minutes at 1100 g. The supernatant was removed and cells resuspended in 100 µL of FACS buffer. For PECAM-1 (CD31) expression, 0.06 µg per test of PE-Cyanine7-conjugated anti-human CD31 (clone MW59, Invitrogen) or its matching conjugated IgG control (IgG2254 Isotype control; Invitrogen) was added for 45 minutes on ice. For VE-cadherin 0.25 µg per reaction anti-VE-cadherin antibody (clone 55-7H1, BD Bioscience), anti-human VE-cadherin antibody (clone 123413, R&D Systems) or IgG Isotype-matched control (clone 11711, R&D Systems) were incubated for 45 minutes on ice then centrifuged for 2 minutes at 2300 g. The supernatant

was removed and Alexa Fluor® 488 goat anti-mouse (Abcam) diluted in 100 μL of FACS buffer (1 μg/ml) was added for 30 minutes on ice. 500 μL of FACS was added and cell suspension centrifuged for a further 2 minutes. The supernatant was removed and cells resuspended in 300 μL of FACS buffer.

Single-colour sample analysis was carried out using a LSRII flow cytometer (BD Biosciences) for PE-CAM1 and FACS Calibur flow cytometer (BD Biosciences) for VE-cadherin analysis. 3 μL per sample of cell viability dye TO-PRO-3® (1 mg/mL, Invitrogen) was added to each sample before analysis to exclude dead cells. Cell populations were gated using forward scatter (FSC) and side scatter (SSC) voltages for size and granularity respectively. TO-PRO-3 positive cells were selected by setting gates using unstained cells treated under the same conditions and excluded from the analysed population. $5 \times 10^3$ viable cells were collected for HDMEC analysis, while $1 \times 10^4$ viable cells were collected for HMEC-1 analysis. Threshold for positively fluorescent cells was set using isotype-matched controls and data was analysed using FlowJo software (TreeStar). The normalised median fluorescence index (nMFI) was calculated as previously described (Chan et al. 2013) by dividing the median fluorescence intensity of the positive samples by that of the negative stained samples (IgG isotype control).

### 2.8.1.2    Immunofluorescence

HDMEC cells were prepared as previously described in section 2.6.1.3 and *P. gingivalis* were prepared as previously described in section 2.3.1. $OD_{600}$ 1.0 *P. gingivalis* was stained with 5 μM Red CMTPX Cell Tracker® (Invitrogen) and diluted to an MOI 1000 in non-supplemented cell culture medium. Cells were infected for 1 hour at $37^0C$ in 5 % $CO_2$ and non-infected cells were used as a control, fixed for 10 minutes using 3.7%  v/v formalin in PBS and blocked in blocking buffer (2% w/v BSA and 5% v/v goat serum PBS) for 30 minutes. Cells were incubated with 5 μg/mL of either anti-E-selectin primary antibody (R&D), anti-VE-cadherin antibody (BD Biosciences), anti-VE-cadherin antibody (R&D Systems) or IgG Isotype control antibody (eBioscience) at 4°C overnight, washed with PBS and incubated with 1 μg/mL Alexa Fluor 488-conjurgated goat anti-mouse IgG (H+L) cross-adsorbed secondary antibody (Abcam) for 1 hour. Cells were rinsed again, mounted in ProLong™ Diamond anti-fade containing 4',6-Diaminidine-2'-phylindole dihydrocholoride (DAPI) (ThermoFisher Scientific) and imaged using a Zeiss Axiovert 200 M inverted fluorescence microscope with an integrated high-

resolution digital camera (AxioCam MRm; Zeiss) with AxioVision 4.6 software (Imaging Associates Limited) as previously described in section 2.6.1.3.

### 2.8.1.3 RNA isolation, Reverse Transcription and Quantitative Polymerase Chain Reaction

HMEC-1 and HDMEC cells were seeded at 4 x $10^5$ cells per well in a 6-well plate until confluent. Cell counting of a sacrificial well was carried out and wells were stimulated with 25 ng/mL TNFα for 5 hours, *P. gingivalis* W83 or ΔK/R-ab mutant were added at an MOI 100 for 4 hours (a non-stimulated well was used as a control) and cells incubated at 37°C at 5 % $CO_2$.

Total RNA extraction was carried out using Isolate II RNA Mini Kit (Bioline) according to the manufacturers instructions and RNA quantified using a Nanodrop spectrophotometer (Thermofisher Scientific). RNA was then adjusted to 500 ng of RNA per sample in 10 µL of RNAse-free water. High-Capacity cDNA reverse transcription kit (ThermoFisher Scientific) was used to produce cDNA. A reaction without the reverse transcription mix was used as a control.

Quantitative polymerase chain reaction (qPCR) was then used to assess gene expression. 5 µl of TaqMan® qPCR BioProbe Blue Mix Master Mix (PCR Biosystems), 3.5 µL of RNAse-free water, 0.5 µl of housekeeping gene human β-2-microglobulin as an endogenous control (VIC/MGB probe, Applied Biosystems), 0.5 µL of target primer and 0.5 µL of cDNA. Target primers used are listed in Table 2.2.

**Table 2.2: Real-time quantitative polymerase chain reaction target primers**

| Target primer | Assay ID | Company |
|---|---|---|
| β-2-microglobulin/B2M | Hs99999907_m1 | ThermoFisher Scientific |
| CXCL8/IL8 | Hs00174103_m1 | ThermoFisher Scientific |
| CCL2/MCP1 | Hs00234140_m1 | ThermoFisher Scientific |
| ICAM-1/CD54 | Hs00164932_m1 | ThermoFisher Scientific |
| Interleukin 1 alpha/IL-1α | Hs00174092_m1 | ThermoFisher Scientific |
| Interleukin 1 receptor, type I/IL1R1 | Hs00991010_m1 | ThermoFisher Scientific |
| VECADHERIN/CD144 | Hs00901465_m1 | ThermoFisher Scientific |

| PECAM-1/CD31 | Hs01065279_m1 | ThermoFisher Scientific |

All samples were run in triplicate for each sample, including control samples without cDNA. All experiments were performed using at least three independent biological repeats and assays performed using a Rotor-Gene qPCR machine (Qiagen). The threshold cycle (Ct) for each test gene was normalized against their respective reference controls. Fold change in expression relative to that of unstimulated cells was calculated with ΔCt values of the sample and reference gene using the formula $2^{-\Delta\Delta Ct}$ (Livak and Schmittgen 2001).

## 2.8.2  *In vivo* zebrafish infection assays

VE-cadherin/Cdh5 transgenic and PECAM-1 transgenic zebrafish were outcrossed with Nacre wild-type zebrafish by pair mating. Dechorionated embryos were sorted for fluorescence using an Axio Zoom.V16 (Zeiss) stereo zoom microscope fitted with an HXP200C Illuminator and Axiocam503 mono camera (Zeiss). Zebrafish embryos 30 hours post fertilisation (hpf) were tricaine anaesthetised, positioned in a solution of 3% (w/v) methylcellulose (Sigma Aldrich) in E3 medium on glass slides and 2 nL of *P. gingivalis* suspension injected systemically via direct inoculation into the Duct of Cuvier (the common cardinal vein); PBS was used as control. Injection was carried out individually using a micro-capillary needle with a known concentration of *P. gingivalis.*

### 2.8.2.1    Confocal imaging and analysis

Transgenic zebrafish embryos were infected systemically with $5 \times 10^4$ CFU of 5 µM Red CMPTX (Cell Tracker™, Invitrogen) stained W83 or ΔK/R-ab *P. gingivalis* as described in section 2.8.2. Anesthetized embryos were transferred into an Eppendorf tube with 1 % low-melting point agarose E3 medium. Embryos in a small volume of agarose containing E3 medium were transferred using a Pasteur pipette into a 5 cm diameter mini glass bottom petri dish and positioned laterally and to the bottom of the petri dish. More agarose containing E3 medium was added after positioning and once the agarose set, the petri dish was topped up with more E3 medium without agarose and tricaine.

Live imaging of anaesthetised fish (5 zebrafish embryos per treatment group) was carried out 24 hours post infection (hpi) using a spinning disc confocal microscope (Perkin Elmer Ultraview VoX) running on an inverted Olympus IX81 motorised microscope. A 20X objective, and 488 nm and 561 nm lasers were used to visualise fluorescent PECAM-1 or CDH5/VE-cadherin (green) and *P. gingivalis* bacteria (red) in zebrafish embryos. Micrographs were captured in two areas of the tail; adjacent to the cloche (closer to the yolk) and 4 vessels further away from the cloche (closer to the tip of the tail) using Velocity® software. GFP-relative fluorescence intensity was then quantified using the below script in ImageJ®.

```
title=getTitle();

run("Split Channels");

selectWindow("C1-" + title);

run("Z Project...", "projection=[Max Intensity]");

rename("green" + title);

run("Green");

run("Duplicate...", " ");

saveAs("Tiff", dirR +File.separator + ori + ".tif");

selectWindow("C2-" + title);

run("Z Project...", "projection=[Max Intensity]");

rename("red" + title);

run("Red");

run("Duplicate...", " ");

saveAs("Tiff", dirR +File.separator + ori + ".tif");

close("C3-" + title);

run("Set Measurements...", "area mean min median area_fraction redirect=None decimal=3");

selectWindow("green" + title);

run("Measure");

saveAs("Results", dirR + File.separator + ori + "_Results.csv");
```

The script was designed for quantification of green channel fluorescence (by pixel value) of a maximum intensity z projection of each micrograph. Fluorescence varied considerably between the 3 biological repeats, therefore median fluorescence values of embryos infected with *P. gingivalis* were normalised to the PBS control average values per experiment.

## 2.9 OUTER MEMBERANE VESICLES AND SECRETED PROTEIN ISOLATION

### 2.9.1 Sample preparation

*P. gingivalis* W83 and ΔK/R-ab were cultured overnight as previously described in section 2.3.1and adjusted to 9 mL of $OD_{600}$ 1. The suspension was then centrifuged for 5 minutes at 8000 g at 4°C and whole cell bacterial pellet was collected.  The remaining supernatant was sterile filtered through a 0.2 μm and centrifuged at 100,000 x g at 4°C for 1 hour in an ultracentrifuge (Beckman). The supernatant was collected, sterile filtered and centrifuged in a 10K MW centrifugal concentrator (GE Healthcare) at 2500 g for 40 min at 10°C and concentrated supernatant collected. The pellet in the polycarbonate ultracentrifuge tube containing the outer membrane vesicles (OMV) was washed with PBS then centrifuged for an additional hour at 100,000 x g at 4°C.

### 2.9.2 Sample characterisation

#### 2.9.2.1    Outer Membrane Vesicle Quantification

Nanoparticle tracking analysis of prepared samples was conducted using the ZetaView (RRID:SCR_016647; Particle Metrix) and its respective software (RRID:SCR_016647; ZetaView 8.03.08.03).  Prior to use, the instrument was calibrated using polystyrene beads (100 nm). Samples were appropriately diluted and nanoparticle tracking analysis measurements were recorded through three cycles of readings at 11 different positions. Concentration and median particle sizes were calculated form Zetaview software.

## 2.9.2.2    Bicinchoninic Acid Protein Assay

Samples were diluted in 1 mL of sterile PBS (Sigma) and a Bicinchoninic acid (BCA) protein assay was performed to quantify and compare the total protein in *P. gingivalis* W83 and ΔK/R-ab samples in each group (Whole Cell, OMV, Concentrated Supernatant). In brief, BCA was prepared as per manufacturer's instructions, serial dilutions carried out where appropriate and absorption (562 nm) was evaluated after 30 minutes at 37 °C using a TECAN Infinite® PRO plate reader to measure the colour changes associated with protein-induced Copper ion (present in the assay) reduction. A standard curve was established and protein concentration of samples calculated.

## 2.9.2.3    SDS-PAGE (sodium dodecyl sulfate–polyacrylamide gel electrophoresis) and Immunoblotting

Samples (8 µL whole cell and 36 µl for OMV) diluted in 5 X loading buffer (Natural Diagnostics), as well as a protein ladder (Prime Step®, BioLegend) were resolved using NuPAGE ® MES sodium dodecyl sulphate (SDS) running buffer and run on 4-12% NuPAGE® gels and apparatus (Invitrogen™) at 200 V for 35 minutes. Gels were then stained using a Coomasie stain (Instant Blue, Expedeon abcam) and imaged using an InGenius® (Syngene) gel documentation system.

Western blots were performed by transferring onto nitrocellulose membrane (NC) (GE Healthcare) using a wet transfer method with NuPAGE reagents. Transfer was achieved by running at 30 V for 60 minutes, or until the protein had fully transferred to the NC sheet (detected by the transfer of the coloured Prime-Step™ protein ladder). 50 mL blocking buffer (5 % w/v milk protein in Tris-buffered saline (TBS)) was added to the NC sheet and incubated with agitation at 4 °C overnight. Following blocking, the NC sheet was washed three times with blocking buffer supplemented 0.1% Tween-20 and incubated for 1 hour with primary antibody, mouse monoclonal antibody 1B5 (MAb 1B5) (Curtis et al. 1999) or rabbit Rb7 antiserum (Aduse-Opoku et al. 2006) raised to the catalytic domain of RgpA/B (gifts from Professor M.A. Curtis, King's College London, London, UK). Following 3 washes in blocking buffer NC were incubated with a secondary antibody (horse anti-mouse horseradish peroxidase (HRP)-conjugated IgG secondary antibody (GeneTex®) for MAb 1B5 or anti-rabbit HRP-conjugated IgG secondary antibody (Thermo Scientific) for 1 hour. The NC sheet was washed for a further 3 times and exposed to the developing solution, Pierce® ECL Western

Blotting Substrate (Thermo Scientific) for 1 minute. Following removal of excess ECL, the NC sheet was placed in cling film in an X-ray cassette folder (Kodak). Sheets of CL-Xposure™ X-ray films (Thermo Scientific) were placed in the cassette in contact with the NC sheet for varying lengths of time, ranging from 1 second to 3 minutes, and the sheets developed using a Compact X4 Xray Film Processor (Xograph).

### 2.9.2.4    Gingipains activity assay

Arg- and Lys-proteinase activity of gingipains was determined using a fluorescent-based substrate gingipains activity assay adapted from Chen *et al*. 2001 and (Naylor et al. 2017). For Arg-proteinase activity, a reaction mixture of 100 µL PBS containing 1 mM L-cysteine, 200 µM αN-benzoyl-L-arginine-7-amido-4-methylcourmarin substrate (Sigma) was added to 50 µL of each sample. After 10 minutes incubation at room temperature the reaction was terminated by the addition of 200 µM N-α-tosyl-L-phenylalanine chloromethyl ketone (TPCK) (Sigma). Lys-proteinase activity was quantified using 100 µl PBS containing 1 mM L-cysteine, 10 µM D-ab-Leu-Lys-7-amido-4-methylcourmain substrate (Sigma) and 50 µL of sample. The mixture was incubated at 37°C for 10 minutes and the reaction terminated using 500 µM N-α-p-tosyl-L-lysine chloromethyl ketone (TLCK) (Sigma). In both assays released 7-amido-4-methylcourmarin was measured using a TECAN Infinite® PRO plate reader with excitation and emission wavelengths of 365 nm and 460 nm, respectively.

### 2.9.2.5    Immunogold labelling and Cryo Electron Microscopy

W83 and ΔK/R-ab were grown to exponential phase and adjusted to $OD_{600}$ 1. 4 mL of the original $OD_{600}$ 1 cell suspension was centrifuged at 6000g for 10 minutes at 10°C, washed with sterile twice-diluted PBS and resuspended in the same buffer (50% v/v). For immunogold labelling, cell suspension was blocked with 3% w/v bovine serum albumin (BSA; Sigma) in twice-diluted PBS at 4°C, then incubated with MAb 1B5 antibody 1/100 diluted in the same buffer with 1% w/v BSA. After three washes, the cells were incubated goat anti-mouse IgG+IgM H&L gold (12nm) conjugated pre-adsorbed antibody (Abcam) (1/20 dilution) for 1 hour. After another wash, cells were resuspended in twice-diluted PBS. For cryoEM 5 µL of sample was applied to a Quantifoil R3.5/1 holey carbon film mounted on a 300 mesh copper grid (Quantifoil Micro Tools GmbH), which was rendered hydrophilic by glow discharge in a

reduced atmosphere of air for 30 s. After 30 s adsorption, the grid was frozen in liquid ethane using a Leica EM GP automated plunging device (Leica). Imaging under cryogenic temperatures was carried out using a Tecnai Artica (FEI, ThermoFisher) operated at 200 kV and equipped with a Falcon 3 Camera (Gatan). Micrographs were recorded under low-dose conditions with underfocus values of 4–10 µm.

## 2.9.3  Systemic infection in zebrafish larvae

London wild-type (LWT) zebrafish were maintained as described in section 2.4 and at 30 hours post-fertilisation (hpf) tricaine-anesthetized, dechorionated zebrafish larvae were injected with either PBS, whole cell W83, W83 OMV or ΔK/R-ab OMV via direct systemic inoculation into the common cardinal vein as described in (Widziolek et al. 2016). Zebrafish embryo viability was assessed every 24 hours up to 72 hours post-infection (hpi) by examining the presence of a heartbeat and blood flow within the circulation. Live imaging was performed using a stereomicroscope (WILD) equipped with a camera.

## 2.9.4  *In vitro* effects

HMEC-1 were grown in MCDB131 as described in section 2.3.2. Effects were analysed by a permeability assay as previously described in section 2.7.1 and for PECAM-1 abundance by flow cytometry as described in section 2.8.1.1.

For flow cytometry, the method was adapted to assess the effects of gingipain inhibition. Confluent HMEC-1 cultured in 6-well plates were infected with W83 or ΔK/R-ab for 1.5 h at 37°C in serum-free medium. For inhibition of gingipain activity, bacterial liquid cultures were pre-treated with 2 µM KYT-1 and KYT-36 (NewEnglandPeptide) for 30 minutes in anaerobic conditions prior to isolation. Medium alone was used as control. HMEC-1 were then analysed for PECAM-1 cell surface abundance as described in section 2.8.1.1.

## 2.10 SINGLE SPECIES AND MULTISPECIES INFECTIONS

### 2.10.1 *In vitro* single species infection

*Porphyromonas gingivalis* W83 and ΔK/R-ab, *Fusobacterium nucleatum* ssp nucleatum ATCC 25586 and polymorphum ATCC 10953 and *Tannerella forsythia* ATCC 43037 were maintained on FA agar plates as described in section2.3.1. Cultures at 3- or 4-days growth (depending on growth of cultures) were then adjusted to $OD_{600}$ 1 in cell culture medium and MOI calculated. Bacteria were added to HMEC-1 cells and PECAM-1 abundance measured by flow cytometry as described in section 2.8.1.1, while endothelial permeability was assessed using dextran permeability assay as described in section 22.7.1.

### 2.10.2 *In vivo F. nucleatum* systemic infection

#### 2.10.2.1 Assessment of zebrafish larvae morbidity and mortality after systemic infection

LWT larvae (minimum of 9 embryos per group) at 30 hpf were systemically injected as previously described (section 2.8.2) using 2nL of *F. nucleatum* ($1 \times 10^2$, $6 \times 10^2$ and $2 \times 10^3$ CFU/mL). PBS was used as control. Zebrafish viability was assessed by and live imaging at 24, 48 and 72 hours post infection (hpi) as described in section 2.9.3.

#### 2.10.2.2 Assessment of zebrafish larvae morbidity and mortality after systemic infection

*F. nucleatum* subsp. polymorphum was prepared as described in section 2.10.1 and labelled in 0.4 µg/mL 5-(and-6)-carboxyfluorescein, succinimidyl ester (5(6)-FAM, SE) (excitation 494 nm, emission 518 nm) (Invitrogen) in PBS for 15 minutes with shaking at 4°C. $2 \times 10^3$ CFU/mL FAM-labelled *F. nucleatum* was injected in the Duct of cauvier (as described in section 2.8.2) of 72 hpf kdrl:mCherry transgenic zebrafish and imaged 2 hpi using Lightsheet microscopy (Zeiss) to visualize *F. nucleatum* vascular interactions similarly to published work with *P. gingivalis* (Widziolek et al. 2016).

### 2.10.3 *In vitro* multispecies infection

Microbial cultures were prepared as described in section 22.10.1 and mixed at either a 1:1 ratio when analysed in pairs or at a 1:1:1 ratio when analysed in groups of three prior to use in experiments.

### 2.10.4 *In vivo* multispecies systemic infection

*P. gingivalis, F. nucleatum* subsp. polymorphum and *T. forsythia* were cultured and prepared as described in section 2.10.1. *P. gingivalis* was labelled with 0.4 µg/mL 5-(and-6)-carboxyfluorescein, succinimidyl ester (5(6)-FAM, SE) (excitation 494 nm, emission 518 nm) (Invitrogen), while *F. nucleatum* and *T. forsythia* were labelled with 5 µM Red CMPTX (577 nm/602 nm) and Deep Red (630 nm/650 nm) (Cell Tracker$^{TM}$, Invitrogen) respectively. Labelled bacteria were rinsed in PBS and mixed at 1:1:1 ratio for a total $2 \times 10^3$ CFU/mL systemic injection. Zebrafish embryos were imaged using Lightsheet (Zeiss) microscopy at 2 hpi.

### 2.10.5 Role of multispecies adhesion on PECAM-1

Multispecies microbial cultures were prepared as described in section 2.3.1 and adjusted to MOI 100 in supplemented BHI. Control (non-adhered) group bacteria were prepared separately in liquid BHI cultures, while the experimental group cultures were allowed to mix. Both groups were then placed in anaerobic chamber for 1 hour, after which liquid cultures were centrifuged at 8,000 × g for 3 minutes, rinsed with and then resuspended in cell culture medium. HMEC-1 cells were incubated with the bacteria for 1.5 hours then PECAM-1 abundance measured by flow cytometry as previously described in section 2.8.1.1.

## 2.11  STATISTICS

All data presented are from at least 3 independent experiments performed in triplicate technical repeats (unless specified). Results are expressed as the mean ± standard deviation (SD) except for flow cytometry data where the nMFI (normalised median fluorescence index) was used. Normality was determined using Kormogorov-Smirnof analysis. Differences

between two groups were assessed using either Students t test (for parametric) or Mann Whitney U Test (for non-parametric), whilst differences between group data was assessed using one-way ANOVA followed by the appropriate post-hoc multiple comparison test (Tukey or Dunn) depending on the nature of the data (parametric or non-parametric). Survival data were evaluated using the Kaplan-Meier method and comparisons between individual curves were made using the log rank test. All tests were carried out using Graphpad Prism v8.4.0 (GraphPad) and statistical significance was assumed at $p < 0.05$.

# CHAPTER 3: *Porphyromonas gingivalis* gingipains and their affects on endothelial cell invasion and adhesion molecule abundance

## 3.1    INTRODUCTION

The effect of periodontal health on systemic disease is currently a highly debated topic with increasing evidence indicating that blood-borne periodontal pathogens can contribute to conditions such as cardiovascular disease (CVD) (Tonetti et al. 2013, Fiehn et al. 2005), rheumatoid arthritis (Mikuls et al. 2014), diabetes (Saremi et al. 2005) and Alzheimer's disease (Olsen, Taubman and Singhrao 2016). The association between periodontitis and cardiovascular disease has been studied for the last three decades and is now generally accepted in the field (Friedewald et al. 2009).

Periodontitis is a chronic multifactorial inflammatory disease caused by a multispecies bacterial infection that is characterized by destruction of tooth supporting structures leading to tooth loss (Darveau 2010). *P. gingivalis*, an oral anaerobic microbe, is considered the keystone pathogen or pathobiont that promotes development of severe periodontitis by favouring oral microbial dysbiosis and dysregulation of the host immune response (Hajishengallis et al. 2012). *P. gingivalis* resides in dental plaque and produces several virulence factors that enable this microbe to colonize the host, evade the immune system and contribute to disease progression and tissue destruction (How, Song and Chan 2016a, Hajishengallis et al. 2012). The predominant virulence factors appear to be gingipains, cysteine proteases with significant proteolytic activity (Potempa et al. 2003).

The presence of oral bacteria has been detected in peripheral blood following dental procedures such as tooth extractions and even regular oral hygiene procedures such as tooth brushing, giving rise to a transient bacteraemia in healthy individuals (Bahrani-Mougeot et al. 2008). However, the likelihood of bacterial entry to the circulation is greatly increased in patients with chronic gingivitis or periodontitis where bacterial-mediated loss of gingival epithelial integrity facilitates bleeding, allowing bacteria in the periodontal pocket facile movement into the bloodstream (Schenkein and Loos 2013, Loos 2005, Castillo et al. 2011). Indeed, oral microbiome profiling performed on patients with atherosclerotic CVD revealed

that *P. gingivalis* was the most abundant species found in these lesions (Mougeot et al. 2017a). Furthermore, *P. gingivalis* DNA was detected in cardiac valves of patients with CVD and deep periodontal pockets (Oliveira et al. 2015).

*P. gingivalis* is able to bind to and invade a wide range of endothelial cells cultured *in vitro* including human coronary artery cells and aortic cells (Dorn, Dunn and Progulske-Fox 1999, Deshpande, Khan and Genco 1998b). This microbial-host interaction mediates increased gene expression of several chemokines (e.g. CXCL8, CCL2), adhesion molecules (CD54, CD62E, PECAM-1) and inflammatory factors by endothelial cells via various mechanisms (Nassar et al. 2002, Takahashi et al. 2006, Walter et al. 2004). Paradoxically, in an attempt by the pathogen to subvert the host immune response, the proteins of these pro-inflammatory genes are degraded by *Pg*-derived gingipains (Nassar et al. 2002, Yun et al. 2005, Sheets et al. 2005). Adhesion molecules are localised at the cellular junctions of adjacent endothelial cells and are involved in selectively regulating vascular permeability (Dejana, Orsenigo and Lampugnani 2008). Dysregulated adhesion molecule expression may initiate vascular pathology due to abnormally elevated vascular permeability leading to oedema, chronic inflammatory and vascular damage (Aghajanian et al. 2008). It was recently shown that *P. gingivalis* can cause vascular damage in an *in vivo* zebrafish larvae model of systemic infection in a gingipain-dependent manner (Widziolek et al. 2016), suggesting that these bacterial proteases may be important drivers of CVD *in vivo*.

In this chapter it was hypothesized that gingipain-dependent cleavage of endothelial cell junction adhesion molecules is important in mediating vascular damage.

## 3.2   AIMS AND OBJECTIVES

Aim:

The aims of this chapter were to use *in vitro* cultured human endothelial cell monolayers, as well as *in vivo* zebrafish embryo experiments to determine the molecular mechanism by which *P. gingivalis* causes vascular damage.

Objectives:

- To develop models to study the effects of *P. gingivalis* invasion in endothelial cells.

- To measure invasion capacity of human endothelial cells using an antibiotic protection assays.

- To visualise oral microorganism invasion in endothelial cells using confocal microscopy.

- To study the effects of *P. gingivalis* on endothelial cell surface and adhesion molecules expression using qPCR, immunostaining and flow cytometry.

- To image and quantify the effects of *P. gingivalis* systemic infection on zebrafish embryo models using confocal microscopy.

- Assess the role of *P. gingivalis* gingipains in endothelial cell damage.


## 3.3  MATERIALS AND METHODS

Methods used in this chapter and their relevant chapter 2 section are listed below:

- 22.2.1 Primary human dermal microvascular endothelial cells (HDMEC)

- 2.3.2 Immortalised human microvascular endothelial cell line (HMEC-1)Fig

- 2.3.1 Culture of microbial strains

- 2.3.3 Colony viability count

- 2.3.4 Metronidazole sensitivity assay

- 2.5.1 Antibiotic protection invasion assay

- 2.5.2 Intracellular and extracellular *P. gingivalis* visualisation

- 2.6.1 E-selectin abundance

- 2.6.1.1 In-cell enzyme-linked immunosorbent assay (ELISA)

- 2.6.1.2 Flow cytometry

- 2.6.1.3 Immunostaining

- 2.7.1 Dextran permeability assay

- 2.8 ADHESION MOLECULE ABUNDANCE FOLLOWING INFECTION

## 3.4  RESULTS

### 3.4.1  *P. gingivalis* strain growth curves in BHI and Schaedler

Knowledge of the specific growth patterns of individual bacterial strains is essential so that the time and $OD_{600}$ values of different phases of microbial growth can be estimated. This allows for greater experimental reproducibility since testing can be carried out using strains at the same growth stage, as well as allowing comparisons to be made with other published work. All strains of *P. gingivalis* examined grew to higher $OD_{600}$ values when cultured in BHI broth compared to Schaedler (Sch). In both media, after an initial lag phase, *P. gingivalis* (reference strain W83; clinical strain A245Br and mutant strain ΔK/R-ab) start growing exponentially (log phase) after approximately 6 hours of anaerobic culture (Figure 3.1A-C). Stationary phase of growth is reached at approximately 15 hours in BHI and 18 hours in Sch, with all strains reaching a minimum $OD_{600}$ of 1.26 for BHI and for Sch (Figure 3.1A-C). The ΔK/R-ab triple gingipain mutant grew less well than its wild-type W83 counterpart, reaching an average $OD_{600}$ of 1.95 for BHI and 0.82 for Sch media at 24 hours. BHI was chosen over Sch for use in future experiments as it  provided nutrients to generate marked and reproducible bacterial growth with a consistent exponential phase growth.
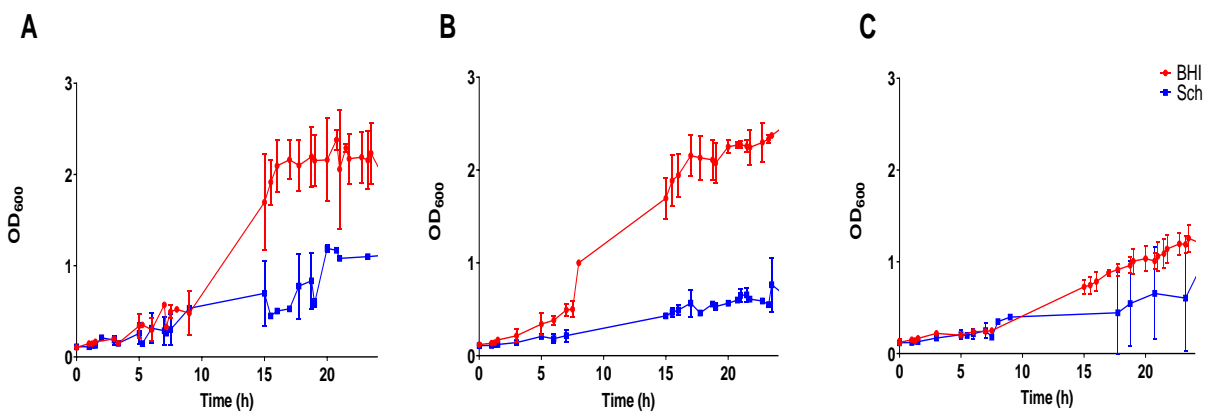


**Figure 3.1: Growth curves of *P. gingivalis* strains.** The graphs show growth of wild-type strain (A) W83, clinical strain (B) A245Br and mutant strain (C) ΔK/R-ab in BHI and Sch over 24 hours from an initial $OD_{600}$ 0.1 showing mean ± SD. Growth in BHI is shown in red whilst growth in Sch is shown in blue. n = 3.

## 3.4.2 Determination of *P. gingivalis* CFU at $OD_{600}$ 1

Optical density at 600 nm ($OD_{600}$) can be used to calculate the number of bacteria used during experiments. On average 1.01 X $10^9$ CFU of *P. gingivalis* were present in 1 mL of $OD_{600}$ 1 broth (mean ± SD values) are summarised in Table 3.1. BHI provided nutrients that generated marked and reproducible bacterial growth with a consistent exponential growth, with mid-log being around 13 hours. No significant differences were observed between CFU/mL values of W83, A245Br and ΔK/R-ab strains when grown in BHI (p = 0.57) (Figure 3.2). Wild-type strains W83 was since this is the parent strain of the ΔK/R-ab null gingipain mutant and therefore can be used to analyse the pathogenic effects of gingipains (Widziolek et al. 2016, Rapala-Kozik et al. 2011).

**Table 3.1: *P. gingivalis* strains (W83, A245Br and ΔK/R-ab) mean CFU/mL in $OD_{600}$ 1**

| Strain | W83 | A245Br | ΔK/R-ab |
|---|---|---|---|
| Mean CFU/mL (SD) | 9.63 X $10^8$ (±4.7 X $10^8$) | 1.07 X $10^9$ (±5 X$10^8$) | 1.24 X $10^9$ (±4.98 X $10^8$) |
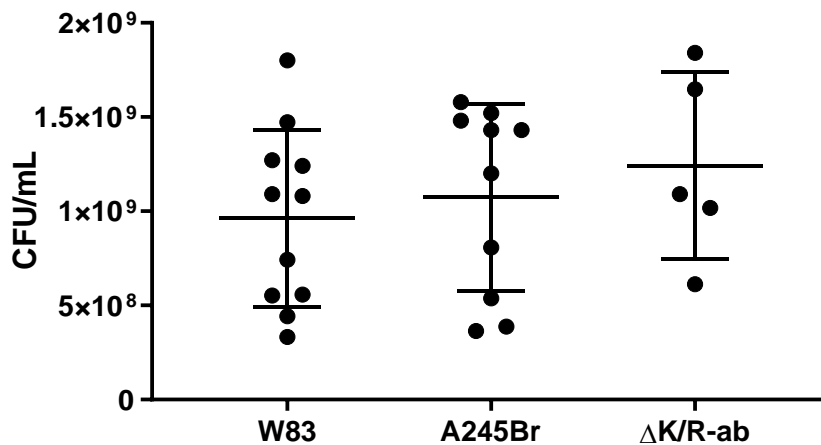


**Figure 3.2: CFU/mL in $OD_{600}$ 1 in bacterial culture medium**. Whisker plot of CFU/mL in $OD_{600}$ 1 bacterial medium showing mean ± SD for *P. gingivalis* W83, A245Br and ΔK/R-ab strains in BHI. n = at least 5 individual experiments. Ordinary One-way Anova revealed no significant differences between CFU/mL of the different *P. gingivalis* strains (p = 0.5685).

## 3.4.3 *P. gingivalis* sensitivity to metronidazole

Knowledge of the sensitivity of *P. gingivalis* strains to metronidazole is important for use in the antibiotic protection invasion assays, since the assay relies on the ability of metronidazole

to kill extracellular bacteria leaving invaded, intracellular bacteria viable (metronidazole can not pass through the host cell plasma membrane). Following E-Test strips analysis the sensitivity of all *P. gingivalis* strains plated at $OD_{600}$ 0.1 on FA plates was 0.015 μg/mL (Figure 3.3). When a bacterial suspension of $OD_{600}$ 1.0 was used the sensitivity decreased to 0.06 μg/mL for all 3 strains tested (data not shown).
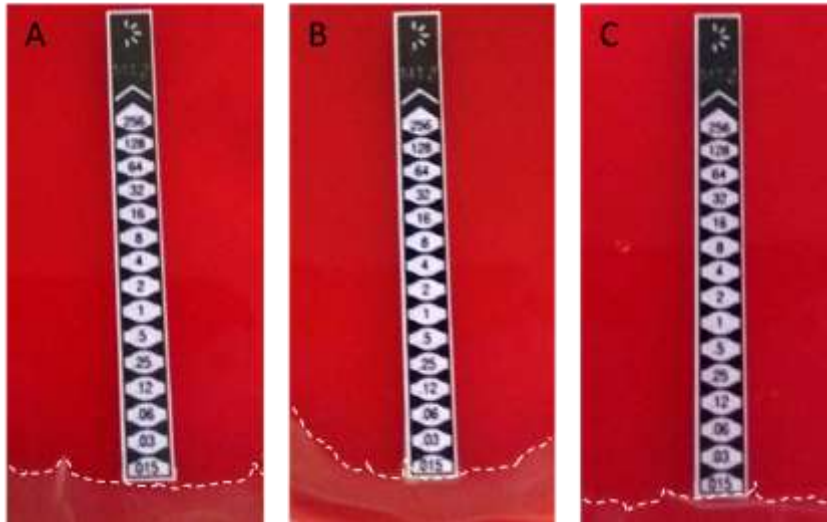


**Figure 3.3: Metronidazole sensitivity of *P. gingivalis* strains.** Images of FA plates with OD0.1$_{600}$ *P. gingivalis* (A) W83, (B) A245Br and (C) ΔK/R-ab strains and E-Test metronidazole sensitivity strips. Zones of bacterial growth inhibition show metronidazole sensitivity in all strains tested. White dotted line highlighting border of bacterial growth.

### 3.4.4 *P. gingivalis* invasion of endothelial cells is influenced by gingipains

*P. gingivalis* invasion of human primary and immortalised microvascular endothelial cells was confirmed using an antibiotic protection assay at MOI 100 for 90 minutes. MOI levels for ATCC33277 and W50 was calculated using previously calculated CFU/mL $OD_{600}$ 1 (data not shown). All wild-type laboratory strains examined (ATCC33277, W83, W50) invaded HDMEC at similar levels but at significantly greater levels than the clinical isolate (A245Br) ($p \leq 0.05$, Figure 3.4A). Wild-type W83 was able to invade both primary (HDMEC) (0.072% ± 0.032; Figure 3.4B) and immortalised (HMEC-1) (0.48% ± 0.2 Figure 3.4C), vascular endothelial cells and at significantly greater levels than the isogenic gingipain-deficient ΔK/R-ab mutant (0.002% ±

0.002 and 0.003% ± 0.003 for HDMEC and HMEC-1 respectively; $p<0.001$), which displayed

an overall 85% reduction in endothelial cell invasion (Figure 3.4B&C).
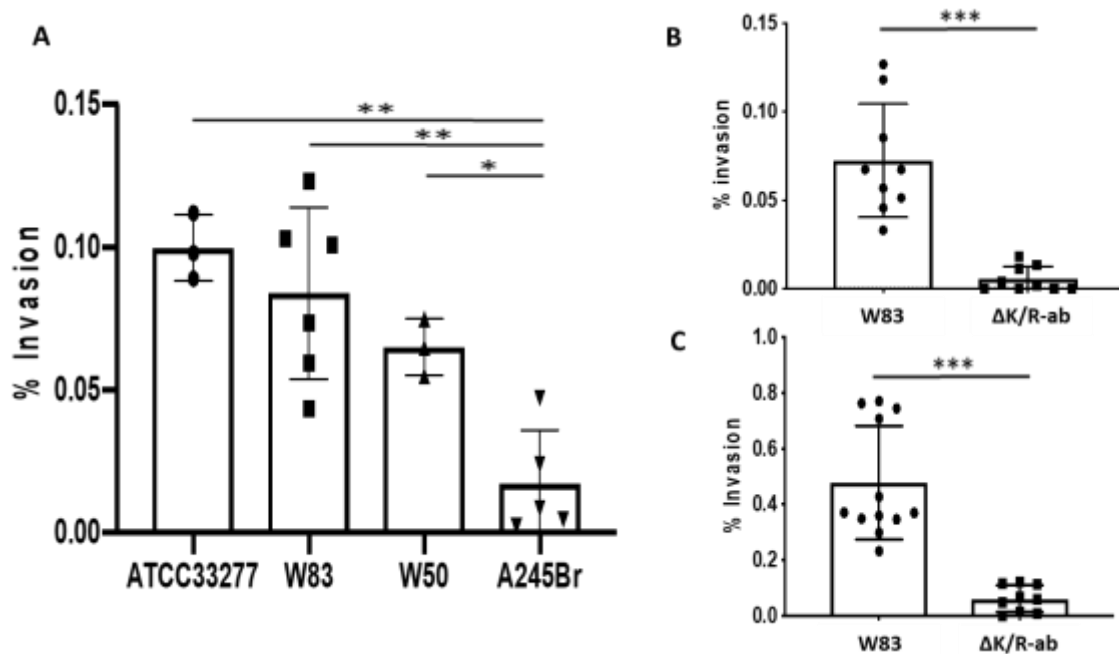


**Figure 3.4: *P. gingivalis* invasion of endothelial cells.** (A) HDMEC were infected with wild-type *P. gingivalis* (ATCC332277, W83, W50 or A245Br) at a MOI 1:100 for 90 minutes and cell invasion determined by antibiotic protection assay. (B) HDMEC and (C) HMEC-1 were infected with wild-type *P. gingivalis* W83 or the ΔK/R-ab mutant at a MOI 1:100 for 90 minutes and cell invasion determined by antibiotic protection assay. Graphs show mean ± SD (n = at least 3 individual experiments). Data were analysed using One-way ANOVA with (A) Tukey's post-hoc comparison test or (B and C) Students t-test *$p<0.05$, **$p<0.01$, ***$p<0.001$.

Invasion of *P. gingivalis* W83 in HMEC-1 was further confirmed using multi-chromatic confocal

microscopy by adapting a method previously used to visualise *P. gingivalis* invasion in

epithelial cells (Wayakanon et al. 2013). Bacteria were labelled green with (5(6)-FAM, SE),

biotinylated and used in an invasion assay. Following infection of HMEC-1 cells, excess bacteria

were removed and bacteria adherent to the cell plasma membrane were labelled using

fluorescently conjugated streptavidin. Wheat germ agglutinin (WGA) was used to stain the

endothelial cell membrane and Hoechst was used to counterstain nuclei. Figure 3.5 shows

intracellular dwelling *P. gingivalis* (orange; green and red co-fluorescence) and extracellular

(cyan) bacteria bound to the cell plasma membrane (red) (Figure 3.5). Imaging revealed that intracellular dwelling *P. gingivalis* were predominantly localised to the perinuclear regions, where they were co-localised with Wheat Germ Agglutinin (WGA)-positive membranes, suggesting residence within membrane-bound intracellular vesicles following internalization (Figure 3.5).
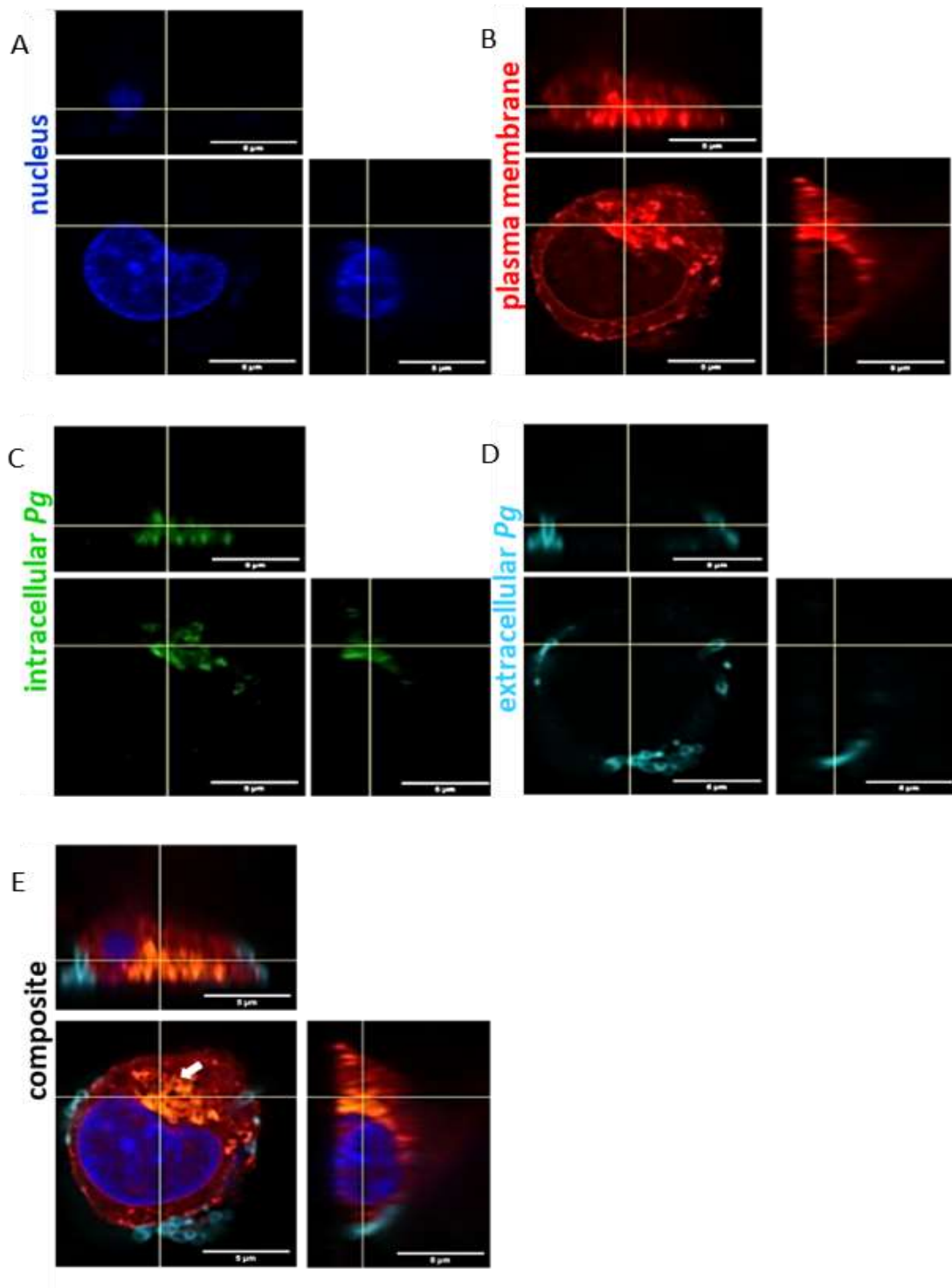
**Figure 3.5: Laser scanning confocal microscopy images of HMEC-1 with intracellular and extracellular *P. gingivalis.*** (A-D) Single channel views show (A) cell nucleus staining (Hoechst, blue), (B) plasma membrane (WGA, red), (C) intracellular *P. gingivalis* (green) and (D) extracellular *P. gingivalis* (cyan). (E) Composite image shows intracellular dwelling *P. gingivalis* (white arrow) as orange (due to green and red co-localisation) and extracellular (cyan) bacteria bound to the cell surface. All images show X-axis, Y-axis and Z-axis planes. Scale bars = 5 μm.

### 3.4.5  *P. gingivalis* invasion is independent of E-selectin

E-selectin has been previously shown to play a role in human umbilical vein endothelial cell invasion by *P. gingivalis* ATCC 33277 (Komatsu et al. 2012). Differences in E-selectin cell surface abundance was studied by analysing primary (HDMEC) and immortalised (HMEC-1) endothelial cells using a cell-based ELISA, immunostaining and flow cytometry. While the invasion potential of *P. gingivalis* in the different endothelial cell types was analysed using an antibiotic protection invasion assay.

In-cell ELISA data shows that HMEC-1 cells do not express cell surface E-selectin, either unstimulated or when stimulated with 25 ng/mL TNFα for up to 24 hours (Figure 3.6A). Similarly, unstimulated HDMEC did not express E-selectin at any time point examined (Figure 3.6B). In contrast, expression of cell surface E-selectin increased on HDMEC after 4 hours stimulation with TNFα and continued to increased to reach maxima expression at 8 hours at which point E-selectin expression was significantly higher than the IgG negative control (p = 0.0247). Thereafter, E-selectin expression decreased to levels similar to the IgG control after 24 hours of TNFα treatment (Figure 3.6B).
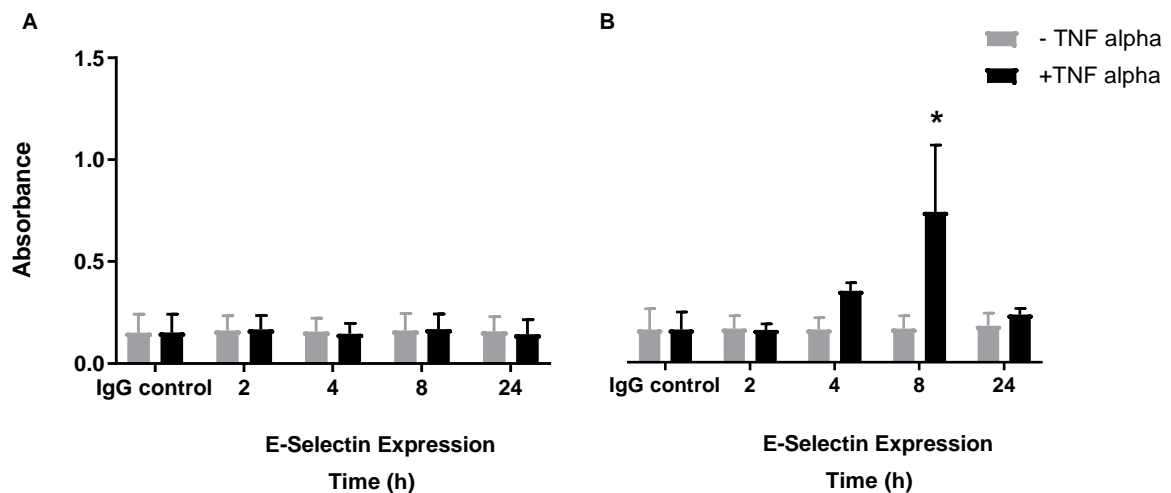


**Figure 3.6: E-selectin Expression in HMEC-1 and HDMEC at different times of TNFα stimulation.** Interleaved bar plot showing E-selectin expression in (A) HMEC-1 and (B) HDMEC. Grey plots represent data from unstimulated cells while black plots are from TNFα stimulated cells, with increased absorbance representing an increased expression of the tested antibody. HMEC-1 cells did not express E-selectin, even when stimulated with TNFα. HDMEC started expressing TNFα after 4 hours. At 8 hours of TNFα stimulation expression is statistically significantly different to the IgG control following a Dunn's multiple comparison test (*p = 0.0247). E-selectin expression was shown to decrease again after 24 hours of TNFα stimulation to levels similar to the IgG control (p> 0.05). Data are mean ± SD (n=3).

Differences in E-selectin expression of TNFα-stimulated HMEC-1 and HDMEC were confirmed by flow cytometry analysis of viable cells (Figure 3.7A-B). HMEC-1 displayed low median fluorescence values for the IgG control (4.45), unstimulated cells (3.68) and TNFα stimulated cells (6.11). While for HDMEC, TNFα stimulation resulted in a higher median fluorescence value for E-selectin (918.00) compared to the IgG control (3.58) and to unstimulated cells (4.58) showing that HDMEC express E-selectin only when stimulated with TNFα (Figure 3.7A-B). These data were further confirmed by immunostaining followed by florescence microscopy of HDMEC and HMEC-1 after 8 h stimulation with TNFα. Here only HDMEC cells displayed cell surface staining for E-selectin (Figure 3.7C-F). Combined these data clearly show that, unlike HDMEC, HMEC-1 do not express cell surface E-selectin.

Once differences in E-selectin abundance were identified antibiotic protection assays were performed to assess whether this would translate to differences in *P. gingivalis* invasion. HDMEC and HMEC-1 were stimulated for 5 hours with TNFα to increase E-selectin expression and subjected to an antibiotic protection invasion assay for 90 minutes. Unstimulated cells were used as a control. There was no significant difference in the per cent invasion of *P. gingivalis* between stimulated and unstimulated HMEC-1 (non-E-selectin expressing) (Figure 3.8A) or HDMEC (E-selectin expressing) (Figure 3.8B) (p > 0.05), suggesting that E-selectin is not involved in the invasion process.
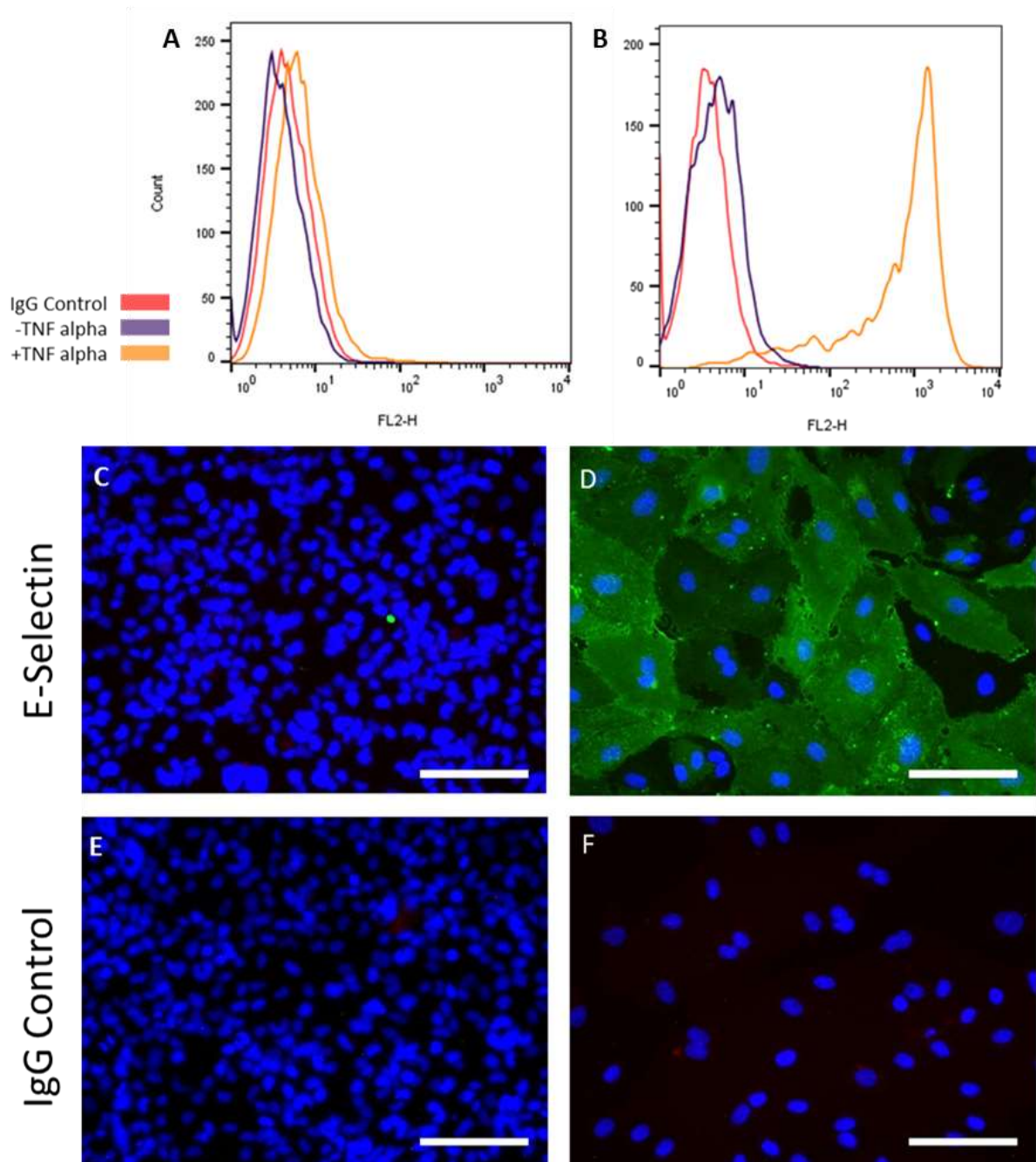
**Figure 3.7: E-selectin Expression in HMEC-1 and HDMEC.** Figures A and B depict histograms of E-selectin expression through fluorescence expressed in the FL2-H channel following flow cytometry. (A) HMEC-1 does not express E-selectin and expression is similar to the IgG control in both stimulated and unstimulated cells. (B) HDMEC stimulated for 5 hours with TNFα express E-Selectin, in contrast to unstimulated cells, which shown E-Selectin expression similar to that of the IgG control. a Representative immunostaining Images C-F show nuclei in blue and E-selectin expression in green. No E-selectin expression was observed in TNFα-stimulated (C) HMEC-1 and IgG controls of HMEC-1 and HDMEC respectively (E,F). (D) Simulated HDMEC showed E-selectin expression. Scale bar = 100 μm.
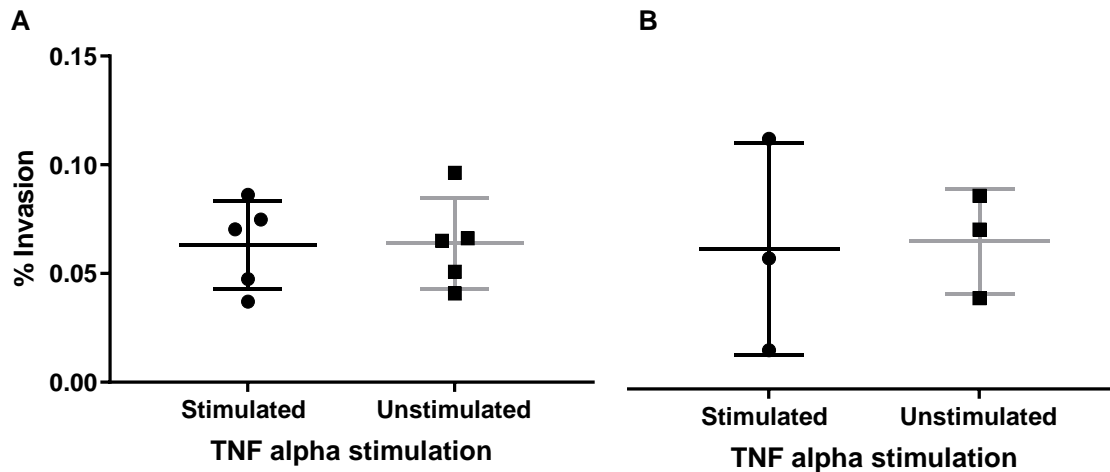
**Figure 3.8: Invasion of *P. gingivalis* in HMEC-1 and HDMEC.** Whisker plots showing % invasion by *P. gingivalis* in (A) HMEC-1 and (B) HDMEC. *P. gingivalis* W83 shows no significant differences in invasion in stimulated cells (black) compared to unstimulated cells (grey) in both the (A) immortalised non-E-selectin expressing HMEC-1 (n=5) and (B) primary E-selectin expressing HDMEC (n=3) suggesting that E-selectin expression is not necessary for *P. gingivalis* W83 endothelial invasion. Data are mean ± SD. A Mann Whitney U test showed no differences between stimulated and unstimulated HMEC-1 and HDMEC (p > 0.05). n = experiments on different days using new different cell flask and new primary bacterial culture

## 3.4.6  Increase in endothelial cell permeability post *P. gingivalis in vitro* infection is gingipain dependent

A previous study on human umbilical vein endothelial cells (HUVECs) showed increased endothelial permeability after *P. gingivalis* infection (Yun et al. 2005). It was therefore assessed whether *P. gingivalis* W83 infection on HMEC-1 would also result in increased endothelial permeability and through the use of the gingipain-null mutant ΔK/R-ab the role of gingipains in this mechanism was assessed. A dextran permeability assay revealed significantly increased permeability of HMEC-1 cells after 90 minutes infection with *P. gingivalis* W83 (p = 0.0049), but not after ΔK/R-ab infection (p = 0.469) when compared to the untreated control. Dextran % release in W83 infected group was 1.65 fold (6.96% ± 4.16) that of the ΔK/R-ab infected group (4.34% ± 2.23), suggesting gingipains' role in endothelial permeability.
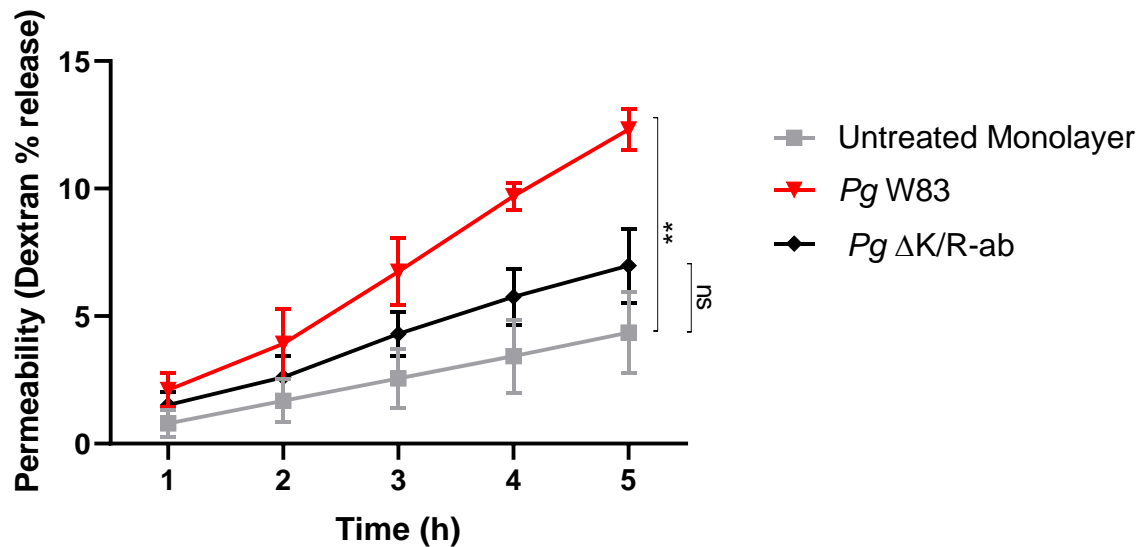
**Figure 3.9: Increased endothelial permeability following *P. gingivalis* W83 infection at MOI100.** Movement of fluorescently labelled 70 kDa dextran from the upper well to the lower well in a Transwell assay increased in a time-dependent manner when HMEC-1 endothelial monolayers were treated with *P. gingivalis* W83 (red) for 1.5 hours and dextran permeability across the endothelium measured for up to after 5 hours. Uninfected controls (grey) and *P. gingivalis* ΔK/R-ab-treated (black) did not result in significant changes in permeability (p > 0.05). Permeability data are presented as mean ± SD of 3 independent experiments. Statistical differences were analysed by one‑way ANOVA with Tukey's multiple comparison test. **p < 0.01, ns = not statistically significant.

### 3.4.7 *P. gingivalis* infection decreases endothelial cell surface adhesion molecule abundance *in vitro*

Data highlighting the increased permeability in endothelial cells following *P. gingivalis* led to an interest in studying the effects of *P. gingivalis* on endothelial cell adhesion molecules PECAM-1 (CD31) and VE-cadherin (CD144).

The endothelial cell surface adhesion proteins PECAM-1 and VE-cadherin are crucial for maintaining cell-cell junction integrity and preserving a restrictive endothelial permeability barrier (Dejana et al. 2008, Privratsky and Newman 2014). Gingipains have been shown to mediate the proteolytic degradation of several human proteins (Yun, Decarlo and Hunter 2006, Nassar et al. 2002), therefore the effects of gingipain proteases on cell surface PECAM-1 and VE-cadherin abundance was examined.

PECAM-1 expression following *P. gingivalis* infection was assessed by flow cytometry. Figure 3.10 shows the flow cytometry strategy, selecting cells firstly by shape and size followed by viable cell selection using the Live/Dead stain, TO-PRO-3. Viable cells do not take up the TO-

PRO-3 stain and so are non-fluorescent, while dead cells take up the stain and are highly fluorescent, allowing non-viable cells to be excluded from the analysis.
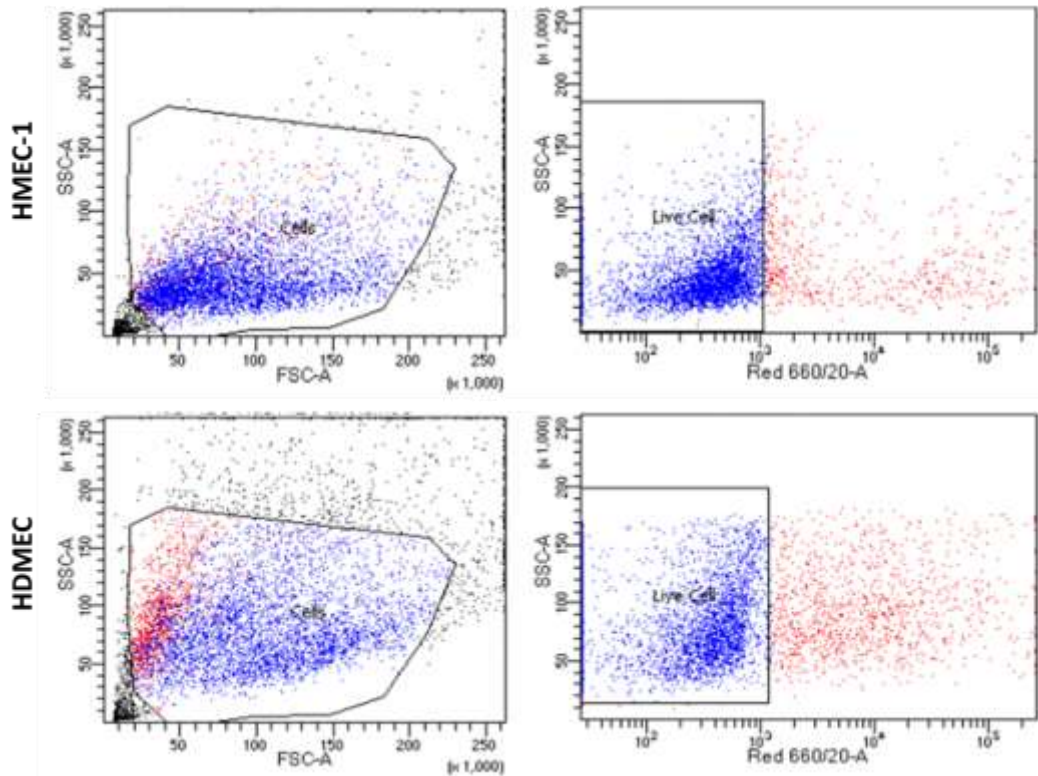


**Figure 3.10: Gating strategy for cell selection following *P. gingivalis* infection.** Representative scatter dot plots show cell selection in a side scatter area (SSC-A) and forward scatter plot, which allowed for cell selection according to shape and size. Live cells were then selected through a SSC-A and Red 66/20-A fluorescence (TO-PRO-3). Non-fluorescent cells were gated as live cells, while dead fluorescent cells were excluded from the analysis.

Viability staining was also used to determine the percentage (%) live cells in the flow cytometry assay in all of the tested conditions (IgG, untreated control and following W83 infections at different MOI and ΔK/R-ab at MOI 1000 *P. gingivalis* infections). The data shows that there was no significant differences in % live cells in the different parameters tested (Figure 3.11).
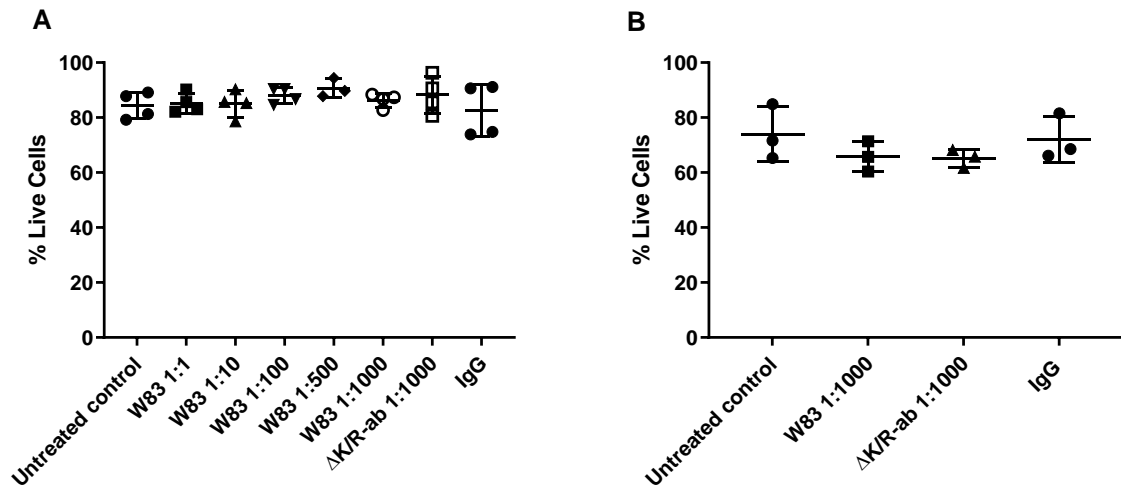
**Figure 3.11: Per cent (%) live cells following flow cytometry infection assay.** Whisker plots with mean and SD showing % live cells assessed by flow cytometry following *P. gingivalis* (W83 or ΔK/R-ab) infection of (A) HMEC-1 and (C) HDMEC. A Kurskal Wallis test showed no statistically significant differences in cell survival following different *P. gingivalis* treatments, with a p = 0.7238 for (A) HMEC-1 and p = 0.4226 for (B) HDMEC. n = 4 for (A) HMEC-1 and n = 3 for (B) HDMEC.

Flow cytometric analysis revealed that cell surface abundance of PECAM-1 on both HMEC-1 and HDMEC was almost completely abolished upon W83 infection compared to uninfected controls (p < 0.05; Figure 3.12A&C). nMFI decreased from 8.124 ± 3.689 to 0.469 ± 0.246 in HMEC-1 and from nMFI 114.6 ± 72.62 to 0.613 ± 0.098 in HDMEC. This was further confirmed by immunofluorescence microscopy (Figure 3.12E&F). In contrast, endothelial cells infected with the gingipain-null mutant, ΔK/R-ab, showed no loss of PECAM-1, displaying levels similar to uninfected controls (Figure 3.12A&C) in both HMEC-1 (nMFI 9.537 ± 3.012) and HDMEC (nMFI 122.2 ± 66.81). Similarly, cell surface abundance of VE-cadherin on both HMEC-1 and HDMEC was reduced by 6-fold upon infection with W83 (p≤0.05; Figure 3.12B&D), while cells infected with ΔK/R-ab displayed VE-cadherin at levels similar to those of uninfected controls (Figure 3.12B&D). Confocal microscopy showed loss of VE-cadherin predominantly at the cell-cell junctions; sites where this protein preferentially accumulates (Figure 3.12F).
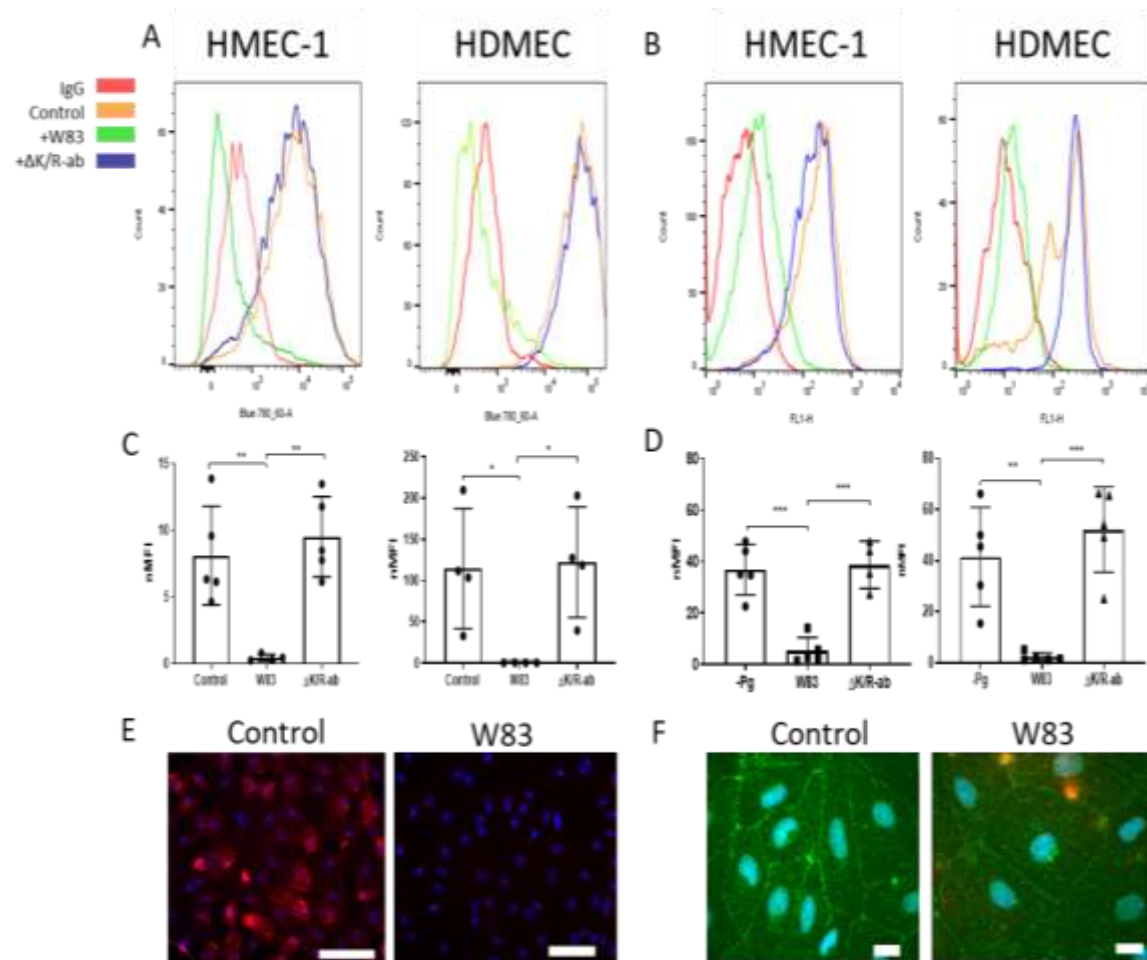
**Figure 3.12: Degradation of endothelial cell surface expressed junctional adhesion molecules *in vitro*.** Representative flow cytometry histograms of cell surface expression of PECAM-1 (A) and VE-cadherin (B) on HMEC-1 and HDMEC following infection with *P. gingivalis* W83 (green) or ΔK/R-ab mutant (blue); IgG control (red) and uninfected control (orange). Normalized median fluorescence intensity (nMFI) histograms of PECAM-1 (C) and VE-cadherin (D) on HMEC-1 and HDMEC following infection with *P. gingivalis* W83, ΔK/R-ab or uninfected control (enclosed circles represent data from each individual experiment, n=4). Statistical differences were analysed by one-Way ANOVA with Tukey's multiple comparison test *p<0.05, **p<0.01, ***p<0.001. Micrograph images show immunofluorescent detection of cell surface expression of PECAM-1 (red, E) and VE-cadherin (green, F) in control or *Pg*-treated HDMEC. Nuclei were counterstained blue with DAPI. Scale bars in E & F= 100 μm.

Interestingly, the levels of *Pg*-induced reduction in VE-cadherin abundance results varied depending on the anti-VE-cadherin antibody clones used. While cell surface abundance of VE-cadherin was significantly reduced from nMFI 36.86 ± 9.781 to 5.257 ± 5.217 in HMEC-1 and from nMFI 41.48 ± 19.37 to 2.273 ± 1.668 in HDMEC when clone 123413 (R&D Systems) was used (Figure 3.12), the decrease in fluorescence was markedly less from nMFI 27.57 ± 11.526 to nMFI 7.31 ± 8.57 when anti-VE-cadherin clone 11711 (BD Biosciences) was used (Figure 3.13B). Moreover, no notable differences in VE-cadherin cell surface abundance were noted when W83 was used to infect these cells followed by immunodetection with the clone 11711

94

antibody (Figure 3.13C-F). Information regarding the antibody binding site revealed that clone 11711 is more optimal for intracellular applications binding to the short intracellular domain, while clone 123413 binds to the extracellular loop of VE-cadherin indicating that differences in fluorescence immunostaining were due to different antibody epitope binding sites, further suggesting that *P. gingivalis* effects are more pronounced on the extracellular portions of protein.
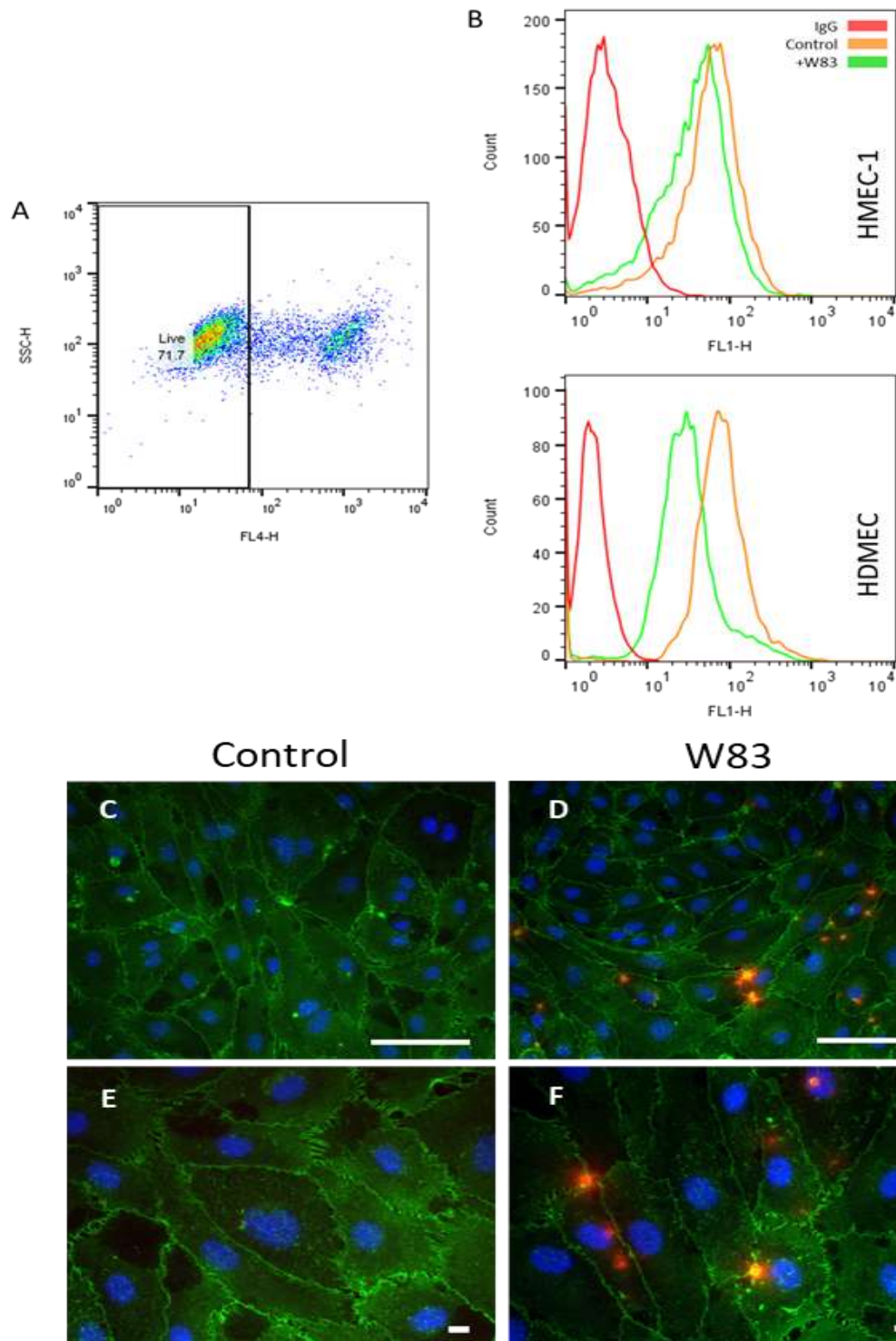
**Figure 3.13: VE-cadherin (BD) clone 11711. abundance following *P. gingivalis* W83 infection.** (A) Live cell gating for flow cytometry using Top-ro-3; live cells were selected during flow cytometry analysis. (B) Histograms showing VE-cadherin (BD) clone 11711 expression in HMEC-1 and HDMEC when subjected to an IgG isotype control (red), *P. gingivalis* infection (green) and no infection (orange). In both cell types, VE-cadherin clone 11711 expression does not seem to drastically decrease following bacterial infection. This is mirrored in the immunostaining micrographs shown in Figures C-F. (C-F) Micrographs shown illustrate VE-cadherin clone 11711 expression (green) in primary endothelial cells (HDMEC) with nuclei stained in blue and bacteria in red (D and F). In both magnifications differences in VE-cadherin expression are not evident. White bars represent 100 μm in Figures C and D and 10 μm in Figures E and F.

Further investigation revealed that loss of PECAM-1 was MOI-dependent, with significantly decreased nMFI at MOI 500 (p < 0.05) and 1000 (p < 0.01) after 1 hour infection with *Porphyromonas gingivalis* W83 (Figure 3.14). As highlighted in Figure 3.11, this was not due to differences in endothelial cell death upon infection as cell viability was similar to controls following infection with either W83 or ΔK/R-ab.
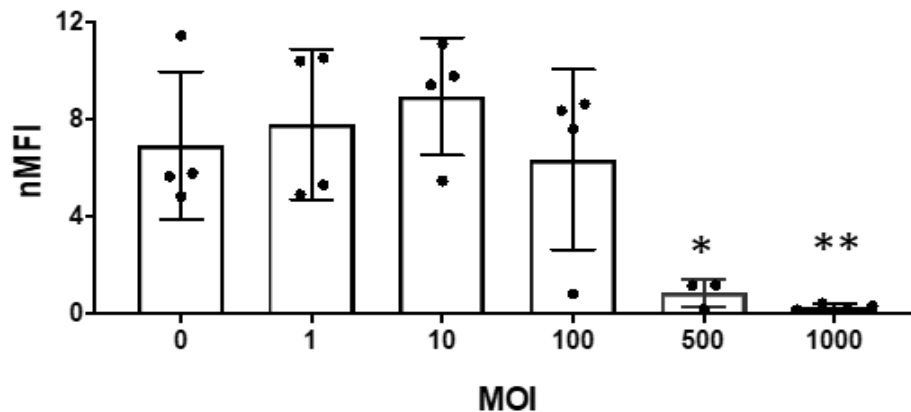


**Figure 3.14: *P. gingivalis*-mediated decrease in PECAM-1 cell surface abundance is MOI-dependent.** PECAM-1 cell surface abundance on HMEC-1 cells following infection with increasing MOI of *P. gingivalis* W83, uninfected cells were controls (enclosed circles represent data from each individual experiment). Data are displayed as normalized median fluorescence intensity (nMFI) mean ± SD. n = 4. Statistical differences were analysed by One-Way ANOVA with Tukey's multiple comparison test *p<0.05, **p<0.01 compared to MOI 0, 1, 10.

An alternative explanation for the loss of endothelial cell surface adhesion molecule expression is that the bacterial infection might reduce gene expression. Differences in endothelial mRNA expression by qRT-PCR following incubation with wild-type W83 and mutant ΔK/R-ab *P. gingivalis* were examined to test for this possibility. Incubation with either of the *P. gingivalis* strains did not significantly alter gene expression of VE-cadherin, PECAM-1 or other tested inflammatory cytokines (IL-1 α, IL-1 R1, CXCL8, CCL2, ICAM-1) in HMEC-1 and HDMEC cultures when compared to treatment with the potent pro-inflammatory cytokine, TNFα (Figure 3. 15A&B).

**A**



**B**
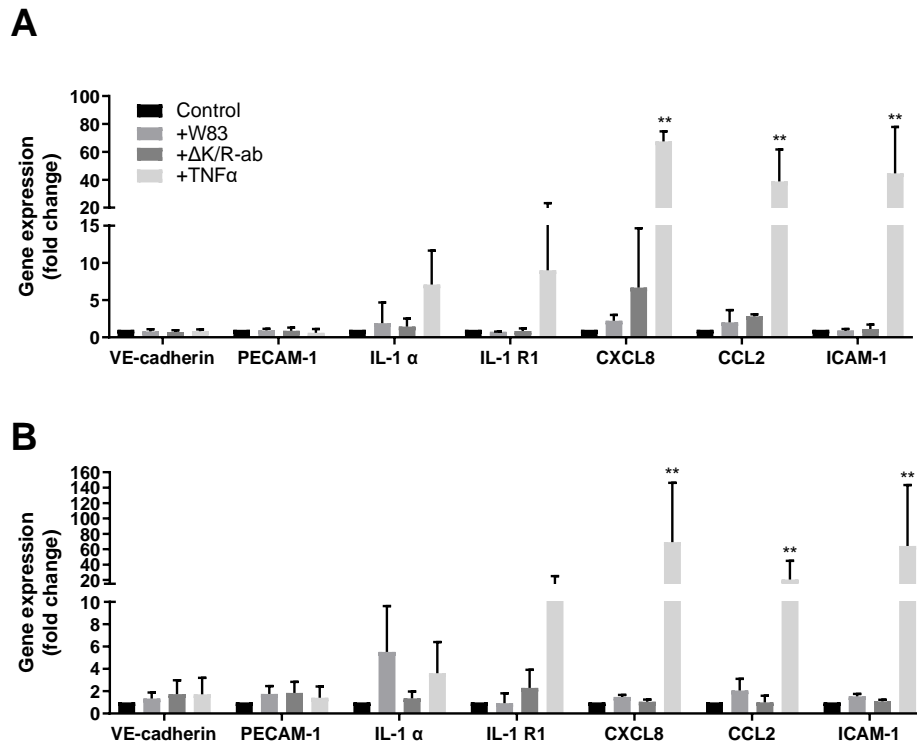


**Figure 3. 15: Infection of endothelial cells with *P. gingvalis* W83 or ΔK/R-ab does not alter mRNA expression of pro-inflammatory genes.** HMEC-1 (A) and HDMEC (B) were infected with either W83 or ΔK/R-ab (MOI 100) for 4 hours, un-stimulated or TNFα-stimulated (25 ng/mL) cells were used as controls. Bars represent means ± SD of relative fold change expression of VE-cadherin, PECAM-1, IL-1α, IL-1 R1, CXCL8, CCL2 and ICAM-1. Data were analysed by Kruskal-Wallis with Dunn's multiple comparison test; **p ≤ 0.01, n = 3 individual biological experiments each performed in triplicate technical repeats.

## 3.4.8 *P. gingivalis* reduces endothelial cell surface adhesion molecule abundance *in vivo*

An established *P. gingivalis* zebrafish embryo infection model (Widziolek et al. 2016) was used to determine if the observed changes in adhesion molecule cell surface abundance seen *in vitro* was replicated *in vivo*. Transgenic zebrafish with endothelial cell-specific PECAM-1-EGFP expression *tg(fli1a:PECAM1-EGFP)sh524* were inoculated systemically with either red labelled wild-type W83 or ΔK/R-ab *P. gingivalis*. Reporter fluorescence was quantified where the endothelium and *P. gingivalis* co-localised in the intersegmental vessels and the caudal vein adjacent to the yolk sac; anatomical sites that are free from any natural pigmentation to avoid

problems with background fluorescence and where individual vessels were easily distinguished. In PBS injected zebrafish embryos, PECAM-1 expression was observed on the endothelial cell surface of the intersegmental vessels as well as the caudal artery and vein (Figure 3.16A&D).  Both W83 and ΔK/R-ab gingipain-null bacteria could be visualised within the vessels at these sites (Figure 3.16B&E and C&F), binding to and in some instances having traversed the vascular barrier into surrounding tissue (Figure 3.16Gii). Importantly, in W83-infected zebrafish embryos, co-localisation of *P. gingivalis* at the endothelial surface was associated with a marked reduction of endothelial PECAM-1 fluorescence at these sites (Figure 3.16Gi and Gii). This is consistent with the *in vitro* experiments, where PECAM-1-EGFP fluorescence loss was gingipain-dependent since infection with the gingipain-null mutant, ΔK/R-ab, was not associated with the loss of PECAM-1-EGFP fluorescence (Figure 3.16Gi). Indeed, fluorescence intensity analysis showed that PECAM-1 fluorescence was significantly reduced in the presence of W83 compared to ΔK/R-ab on both the intersegmental vessels in the tail (Figure 3.16H, $p<0.001$) and caudal vein (Figure 3.16I, $p<0.01$). In the tail W83 relative fluorescence was -71.44 ± 103.4 compared to 53.82 ± 83.96 in the ΔK/R-ab-injected group (Figure 3.16H). In the caudal vein relative fluorescence in larvae injected with W83 was -24.09 ± 113.1 and 85.18 ± 114.1 in the ΔK/R-ab-injected larvae (Figure 3.16I).
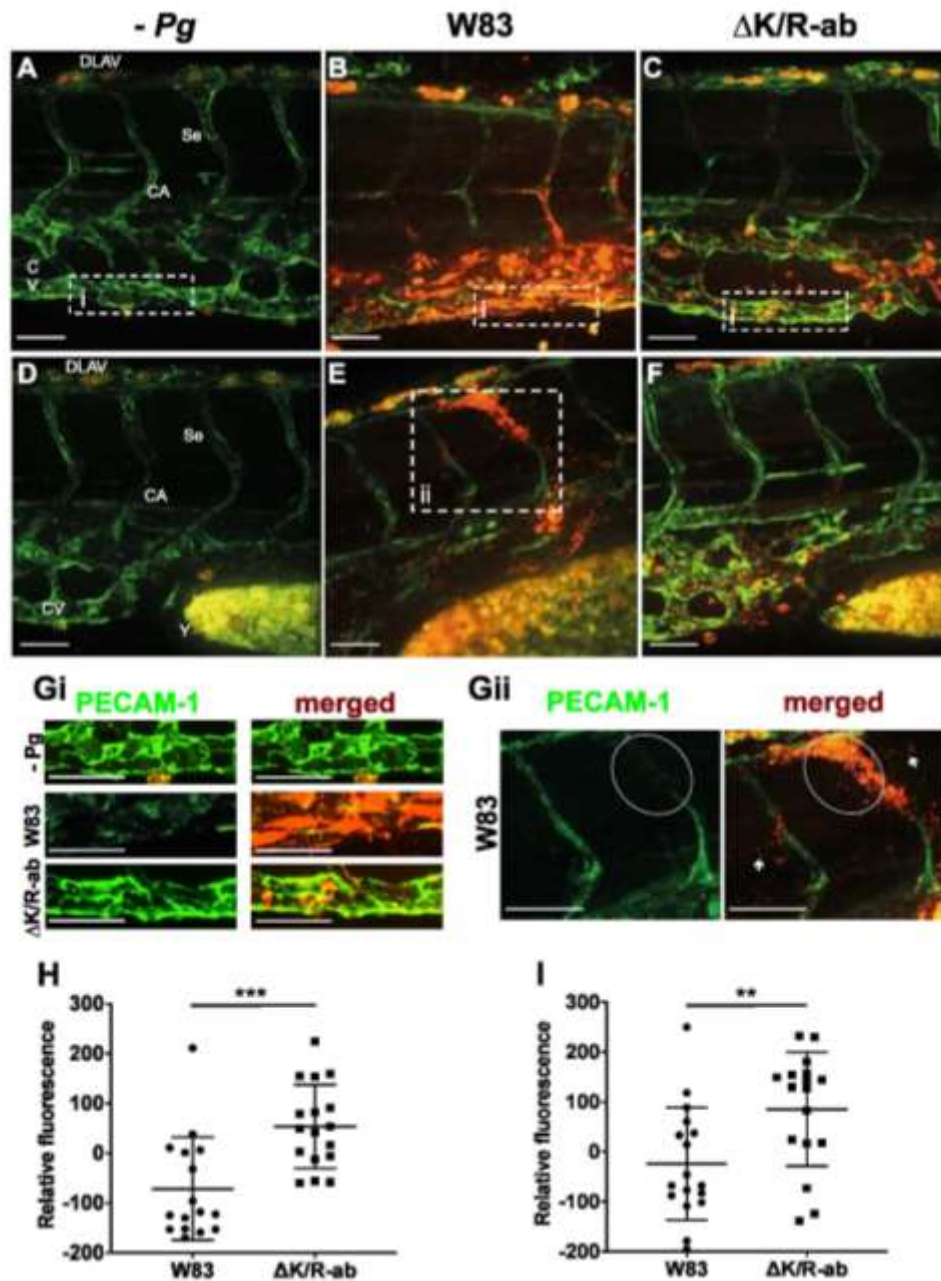
**Figure 3.16: PECAM-1 expression in an *in vivo* zebrafish embryo systemic infection model**. Representative images of spinning disc confocal micrographs showing PECAM-1 expression (green) in the (A-C) tail region and (D-F) yolk region of zebrafish embryos at 24 hpi. Embryos were injected with (A&D) PBS control, (red, B&E) wild-type W83 *Pg* or (red, C&F) ΔK/R-ab mutant. Decreased fluorescence in W83 expression was observed in infected segmental vessels, while loss of definition in W83 infected vessels is clearer the in caudal vein and artery. Loss of PECAM-1 expression is exemplified in high magnification images of the caudal vein showing (Gi, top) PBS controls, (Gi, middle) W83 infected and (Gi, lower) ΔK/R-ab infected embryos and in the intersegmental vessels which show (Gii, white arrows) a marked loss of PECAM-1 fluorescence (green) when co-localised with (Gii, circled areas) red-labelled W83. W83 can also be observed in the tissues having traversed the vasculature. Image analysis showed significantly decreased normalised median fluorescence values and therefore PECAM-1 expression in both the (H) tail and (I) caudal vein between zebrafish embryo infected with W83 and ΔK/R-ab mutant *Pg* (**$< p$ 0.01, ***$p < 0.001$, Student's t-test; n = 3 biological experiments with at least 5 technical repeats per experiment). CA - caudal artery, CV - caudal vein, Se - intersegmental vessels, DLAV - Dorsal longitudinal anastomotic vessel, Y - yolk sac. Scale bar A-G = 40 μm.

PBS, *P. gingivalis* W83 and ΔK/R-ab were also systemically injected in fluorescently tagged VE-cadherin-TS transgenic zebrafish larvae and transgene fluorescence quantified (Figure 3.17A-F). Similar to the effect on PECAM1-EGFP, when co-localised with the vasculature (Figure 3.17B&Gi), wild-type *P. gingivalis* significantly reduced the fluorescence intensity of the VE-cadherin-TS reporter on both the intersegmental (Figure 3.17H, $p<0.01$) and caudal vein (Figure 3.17I, $p<0.05$) vessels when compared to ΔK/R-ab mutants, suggesting reduced fluorescence of this reporter fusion protein was also gingipain-dependent. In the tail intersegmental region VE-cadherin relative fluorescence in W83-injected larvae was $-85.98 \pm 148.1$ and $99.47 \pm 138.1$ in the gingipain-null mutant-injected group (Figure 3.17H). Similarly in the caudal vein region VE-cadherin relative fluorescence was less in W83-injected larvae ($-63.75 \pm 171.5$) compared to ΔK/R-ab-injected larvae ($96.13 \pm 153.2$; Figure 3.17I).
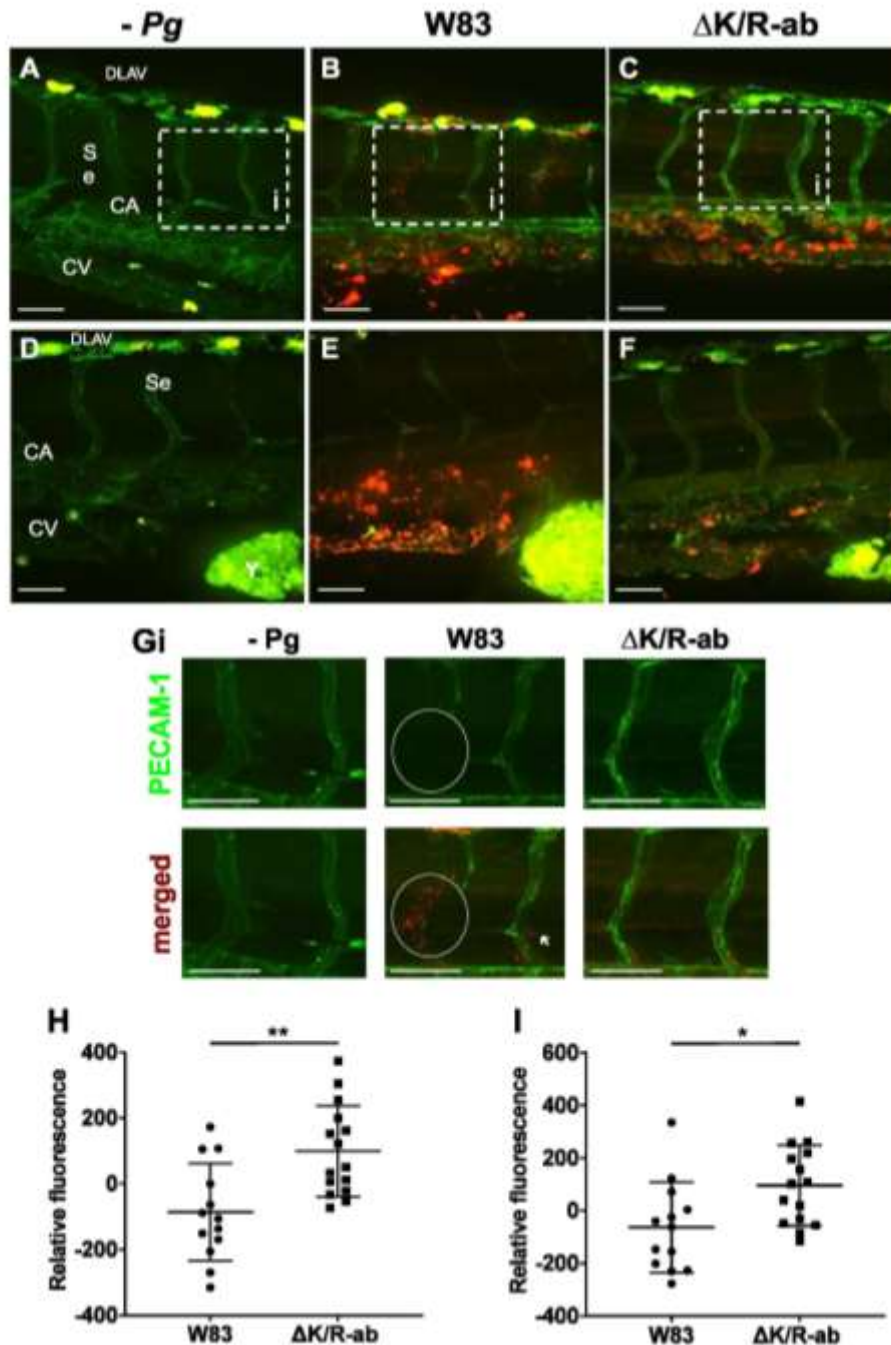
**Figure 3.17: VE-cadherin (CDH5) expression in an in vivo zebrafish embryo systemic infection model.** (A-F) Representative images of spinning disc confocal micrographs showing VE-cadherin expression (green) in the (A-C) tail region and (D-F) yolk region of zebrafish embryos at 24 hpi. Embryos were injected with (A&D) PBS control, (red, B&E) wild-type *P. gingivalis* W83 or (red, C&F) ΔK/R-ab mutant. Decreased VE-cadherin fluorescence when co-localised with W83 was observed in infected segmental vessels, and caudal vein. The loss of VE-cadherin expression is exemplified in high magnification images from A, B and C showing (Gi, left) PBS controls, (Gi, middle) W83-infected and (Gi, right) ΔK/R-ab infected intersegmental vessels. Image analysis showed significantly decreased normalised median fluorescence values and therefore VE-cadherin expression in both the (G) tail and (H) caudal vein between zebrafish embryo infected with W83 and ΔK/R-ab mutant *P. gingivalis* ($*<p$ 0.05, $**p< 0.01$, Student's t-test, data are means ± SD of 3 pooled independent biological experiments. CA - caudal artery, CV - caudal vein, Se - intersegmental vessels, DLAV-Dorsal longitudinal anastomotic vessel, Y - yolk sac. Scale bar = A-G 40 μm.

## 3.5    DISCUSSION

Increasing evidence suggests that periodontal disease is associated with CVD and that this is influenced, in part, by bacteria that enter the circulation via diseased tissues in the oral cavity (Friedewald et al. 2009, Tonetti et al. 2013). Further supporting evidence comes from *in vitro* studies showing that oral microbes, in particular *P. gingivalis*, can invade endothelial cells, and possibly more compelling evidence from human studies where the DNA of several oral bacteria, including *P. gingivalis*, have been found in non-diseased vascular tissue from patients undergoing bypass surgery (Mougeot et al. 2017a) as well as in atherosclerotic plaques (Kozarov et al. 2005, Gaetti-Jardim et al. 2009, Szulc et al. 2015). However, the molecular mechanism driving this association is, as yet, unknown, with several divided theories proposed on how this relationship develops. Therefore, the work described in this chapter used both *in vitro* and *in vivo* approaches to investigate the mechanisms at play, with particular emphasis on the role of gingipains,  potent proteases known to play a key role in *Pg*-mediated disease processes (Fitzpatrick, Wijeyewickrema and Pike 2009).

### 3.5.1  *P. gingivalis* growth

*P. gingivalis* is a Gram-negative anaerobic oral microorganism, with a strong connection with periodontal disease. So much so, that it is referred to as a keystone periodontal pathogen (How, Song and Chan 2016b).

*P. gingivalis* utilises haemin compounds as a source of iron that is essential for growth, which gives *P. gingivalis* a pathogenic advantage in the vasculature. *In vitro* haemin was therefore added to media or blood to fastidious anaerobe agar plates to facilitate growth (Genco, Odusanya and Brown 1994, Genco 1995). Other additives include vitamin K that is considered a stimulant of growth for *P. gingivialis* (Hojo et al. 2007) and cysteine is used as a source and facilitator of amino acid uptake (Dashper et al. 2001).  Growth of *P. gingivalis* in BHI (Brain Heart Infusion) was compared to that in Schaedler (Sch) since these have both been used for culture of different strains of *P. gingivalis* in the literature. BHI was used previously for growth of several wild-type strains such as W50 (Curtis et al. 2002, Stafford et al. 2013), ATCC 33277 (Romero-Lastra et al. 2017) and W83 (Wunsch and Lewis 2015), while Schaedler has been used to culture W83 (Potempa et al. 2008), as well as ΔK/R-ab mutant (Benedyk et al. 2016). Growth

curves showed that all wild-type strains of *P. gingivalis* tested grew faster and to a higher OD$_{600}$ in BHI than Schaedler, except for the ΔK/R-ab gingipain mutant that grew to a lower OD$_{600}$ than the rest of the strains irrespective of medium used. The numbers of CFU/mL in OD$_{600}$ 1 of the strains grown in the same broth were comparable. Growth curves are widely used to study growth of bacteria and allow for consistent calculation of numbers of bacterial isolates (Edberg and Miskin 1980). This allowed for CFU calculations that facilitated Multiplicity of infection (MOI) calculations, since it is faster and more accurate than counting bacteria under a light microscope. W83 was selected from the wild-type strains, since its growth (CFU/mL) was most consistent and that is the parent strain of the ΔK/R-ab gingipain-null mutant, allowing the role of gingipains to be examined. A245Br was chosen as a clinical strain since previous published data in oral epithelial cells showed it to be highly invasive (Wayakanon et al. 2013), which is consistent with other published findings in epithelial cells showing that clinical strains tend to be more invasive than laboratory strains depending on the clinical parameters (Baek et al. 2015). *Δkgp ΔrgpA ΔrgpB* (ΔK/R-ab) is a triple protease mutant that does not produce gingipains, an important virulence factor produced by *P. gingivalis* (Benedyk et al. 2016). Blocking gingipains activity has been shown to inhibit *P. gingivalis* growth (Kariu et al. 2017). The slower growth rates observed for ΔK/R-ab are therefore likely due to the absence of gingipains.

### 3.5.2 *P. gingivalis* invasion of endothelial cells

The antibiotic protection assay allowed for assessment of the invasive ability of the different *P. gingivalis* strains in human endothelial cells. This assay has been used to assess the invasive ability of *P. gingivalis* into oral epithelial cells (Naylor et al. 2017) and relies on the bacterium's sensitivity to metronidazole (Kulik et al. 2008) as evidenced by the E-test data that showed inhibition of growth for all strains tested.

Initial *in vitro* studies using monolayers of endothelial cells from microvascular beds showed that *P. gingivalis* (strains ATCC33277, W83, W50, A245Br) were invasive but at low levels (~0.1%), which is in agreement with previous findings from other groups (Deshpande et al. 1998b, Rodrigues et al. 2012, Olsen and Progulske-Fox 2015, Dorn et al. 1999). Collectively, these data show that endothelial cells are less susceptible to invasion than oral epithelial keratinocytes that can display from 2-10% cell invasion depending on the strain examined

(Lamont et al. 1995, Pinnock et al. 2014). The decreased invasion in endothelial cells might be due to adaptability of strains to their original oral cavity environment (Jandik et al. 2008) or differences in expression of adhesion receptors for *P. gingivalis* between endothelial and epithelial cells. Low levels of invasion in bovine heart endothelial cells, bovine aortic endothelial cells and human umbilical vein endothelial cells (have also been observed by other groups (Deshpande et al. 1998b) and strain variability described by Rodrigues *et al* 2012, where W83 also exhibited higher invasive ability in human coronary artery endothelial cells than other strains (Rodrigues et al. 2012). Moreover, the gingipain-null mutant ΔK/R-ab failed to invade endothelial cells, suggesting that bacterial gingipains are crucial for this process.

Confocal microscopy analysis confirmed the presence of intracellular dwelling *P. gingivalis* enclosed within membrane-bound vesicles at perinuclear sites in endothelial cells. Similar observations were documented for gingival epithelial cells, most likely as a result of endocytosis (Yamatake et al. 2007, Deshpande et al. 1998b, Deshpande, Khan and Genco 1998a). Internalisation into cells is beneficial for the bacteria as it provides protection from the host immune response, resistance to antibiotic therapy (many cannot pass the host cell plasma membrane) as well as increased survival (Yamatake et al. 2007). When infected with wild-type *P. gingivalis*, data shows that HDMEC within confluent monolayers become detached and the endothelium display significant loss of permeability *in vitro* that was prevented by inhibition of gingipain enzyme activity or upon infection with ΔK/R-ab, the gingipain-null strain (Farrugia et al. 2020b). Similar observations were reported by Sheets *et al.* who noted that bovine coronary artery endothelial cells and HDMEC exhibited loss of adhesion to tissue culture plastic upon culture with *Pg*-derived culture extracts (Sheets et al. 2005). These data clearly point to proteolytic degradation function of cell surface molecules as the likely mechanism for loss of cell-cell contacts and adhesion, a hypothesis that was subsequently tested *in vitro* and *in vivo*.

### 3.5.3  Degradation of cell adhesion molecules *in vivo*

*P. gingivalis* infection was found to increase in human umbilical vein endothelial cell permeability and it was concluded that this was due to macrophage migration inhibitory factor (MIF) acting through an E-selectin-mediated mechanism (Xu et al. 2018).

E-selectin mediates leukocyte rolling (Rosen and Bertozzi 1994, Komatsu et al. 2012) and has been previously shown to mediate adherence of *P. gingivalis* to endothelial cells (Komatsu et al. 2012). Contrary to these findings, data from this chapter shows that E-selectin does not play a role in *P. gingivalis* invasion into endothelial cells. Komatsu *et al.* used a different strain of *P. gingivalis* (ATCC33277) and antigen sialyl Lewis X in their experiments (Komatsu et al. 2012), which was later shown to block the interaction of *P. gingivalis* with epithelial cells (Frey et al. 2018), and might explain these differences. Expression of E-selectin was not detected in any of the assays used for HMEC-1, while HDMEC (Zhang et al. 1999) expressed E-selectin after 4-5 hours of TNFα stimulation, similarly to other studies (To et al. 1996, Read et al. 1997, Wyble et al. 1997). Differences in E-selectin expression by HMEC-1 and HDMEC did not result in different invasion of *P. gingivalis,* suggesting that E-selectin does not play a significant role in mediating *P. gingivalis* invasion into endothelial cells. *P. gingivalis* has been shown in other studies to induce expression of E-selectin in human umbilical vein endothelial cells (HUVEC)(Wan et al. 2015, Khlgatian et al. 2002, Hashizume, Kurita-Ochiai and Yamamoto 2011). Gingipain-dependent degradation of other leukocyte adhesion molecules (ICAM-1/CD54, VACM-1/CD106) has been previously described (Yun et al. 2006), suggesting that *P. gingivalis* is able to modulate leukocyte recruitment at the endothelium surface. On the other hand, *P. gingivalis* gingipain-dependent degradation of PECAM-1 and VE-Cadherin was not investigated in the aforementioned studies.

PECAM-1 and VE-cadherin act to form intercellular junctions that are crucial for maintaining a continuous endothelium and so loss of these cell-cell contacts will inevitably lead to loss of tissue integrity, increased permeability and endothelial dysfunction. In this study, loss of PECAM-1 and VE-cadherin cell surface abundance was identified in response to whole bacteria, whereas previous studies have used recombinant gingipains to show cleavage of bovine coronary artery endothelial cell and human microvascular endothelial cell surface proteins including N-cadherin and integrin β1 as well as VE-cadherin (Sheets et al. 2005). Gene expression analysis showed no change in expression levels of PECAM-1 or VE-cadherin as well as other inflammatory cytokines (CCL2, CXCL8 and ICAM-1) in response to infection with either wild-type W83 or ΔK/R-ab *P. gingivalis*, confirming that loss of cell surface protein was due to protein cleavage and not altered gene transcription. Flow cytometry is a commonly used tool to correlate fluorescence intensity to protein expression on the cell surface (Hogg et al. 2015, Hashizume et al. 2011). Fluorescence intensity was quantified by using the normalised median

fluorescence intensity method, which was developed to account for shifts in fluorescence intensity of the entire live population (Chan et al. 2013). Loss of PECAM-1 expression was also confirmed by immunostaining. VE-cadherin expression was also found to decrease significantly by flow cytometry and immunostaining data when anti-VE-Cadherin antibody clone 123413 was used. Similar to PECAM-1 data, VE-Cadherin expression did not decrease following infection with ΔK/R-ab, confirming that loss of protein expression is gingipain dependent. Data using a different anti-VE-cadherin antibody (clone 11711) did not show as sharp a decrease in VE-cadherin expression. This is because the binding site of clone 123413 is to an extracellular loop of VE-cadherin whilst clone 11711 binds to an intracellular domain (BD Biosciences), suggesting that the effects of *P. gingivalis* infection are more severe on the extracellular portions of the proteins tested. The decreased fluorescence signal associated with loss of VE-cadherin expression can therefore be discriminated by different antibody clones that bind to different epitopes on VE-cadherin (Corada et al. 2001). Moreover, the gingipain cleavage site must be associated with the clone 123413 binding epitope since this is lost following infection. Interestingly, the gene expression data presented in this chapter is in contrast to those reported by others who have observed increased gene expression for CCL2 (formally MCP-1) by HUVEC in response to *P. gingivalis* strain 381 (Choi et al. 2005) and ICAM-1 by E.A.hy926 cells (an endothelial/epithelial hybrid cell line) or HUVEC upon infection with *P. gingivalis* strain ATCC33277 or W83 respectively (Mao et al. 2004, Xu et al. 2018), which may be due to bacterial strain differences or to use of cell lines or endothelial cells derived from large compared to microvascular vessels. Variability between *P. gingivalis* endothelial and epithelial cell invasion potential has been previously described (Dorn et al. 2000). Since fimbriae encoded by *fimA* have been previously identified as necessary for *P. gingivalis* cell adhesion and invasion, it was thought that differences in *fimA* between different strains might be a contributor towards differences in invasion (Nakagawa et al. 2002). Despite this Dorn et al. 2000 showed that *P. gingivalis* with the same type of IV class of the *fimA* gene resulted in varying invasion suggesting that fimbrae type cannot solely explain differences adhesion and invasion rates (Dorn et al. 2000).

### 3.5.4 Translation of cell adhesion molecule decreased abundance in an *in vivo* zebrafish larvae model

*In vitro* generated data using monolayer endothelium provide valuable information but these experiments lack conditions such as flow, shear stress and presence of other cells that are important when examining systemic infection. To confirm the *in vitro* data a previously validated zebrafish embryo *P. gingivalis* infection model (Widziolek et al. 2016) was used. Zebrafish have been extensively used for host pathogen interactions as well as for cardiovascular studies (Gut et al. 2017) and have several advantages over murine models such as transparency and availability of fluorescently-tagged proteins that allow for real-time analysis of cell-cell interactions (Widziolek et al. 2016). Imaging of cell-to-cell adhesion in zebrafish models is also frequently used in the literature (Lagendijk, Yap and Hogan 2014, Wiggenhauser and Kroll 2018, Ando et al. 2016, Lagendijk et al. 2017). Moreover, the close homology between numerous zebrafish and human innate immune and cardiovascular-associated molecules means that this *in vivo* model system is also ideally placed to examine pathogen-mediated host responses that may impact on CVD risk. A recent publication has shown that zebrafish embryos present with oedema upon infection with wild-type but not the ΔK/R-ab gingipain-null mutant (Widziolek et al. 2016) and given our *in vitro* data on gingipain-dependent endothelial cell adhesion molecule degradation we hypothesised that gingipains would be responsible for cleavage of these molecules *in vivo* leading to vascular permeability. Using genetically engineered zebrafish whereby PECAM-1 or VE-cadherin were fluorescently labelled it was observed, for the first time, *in vivo Pg*-mediated loss of fluorescence upon infection with wild- type (W83) but not with the gingipain-null mutant strain, indicating gingipain-dependent degradation of these molecules. Loss of PECAM-1 and VE-cadherin on the endothelium was most evident when co-localised with *P. gingivalis* W83 and was apparent in several vascular regions of the zebrafish embryos indicating that infection is widespread and that *P. gingivalis* adhesion and gingipain-mediated protein degradation is not confined to specific vascular beds. *P. gingivalis* infection also appeared to decrease the definition of vessels in the zebrafish embryo caudal plexus, which can be an indication of increased permeability, which was not observed in PBS and ΔK/R-ab infected zebrafish embryos.

Several *in vivo* studies using murine experimental models, in particular the hyperlipidemic ApoE(null) mice, have shown that *P. gingivalis* infection directly influences atherosclerotic

lesion formation or development (Koizumi et al. 2008, Velsko et al. 2014) and several mechanisms have been suggested. However, visualising bacterial-host interactions at a cellular and even protein level are not possible in these models. This is the first time that the effects of systemic *P. gingivalis* infection at the cellular level, *in vivo*, have been reported and this data clearly points to a role for *P. gingivalis* in mediating vascular damage. At present it is unknown if *P. gingivalis* acts as an initiating event, where it could be speculated that *Pg*-mediated endothelial cell damage leads to the exposure of the underlying vascular connective tissue leading to localised platelet activation and leukocyte recruitment. However, it could also be speculated that *P. gingivalis* may exacerbate the disease process by modulating the immune response. Clearly, further studies are warranted to decipher the precise role of *P. gingivalis* in CVD. *P. gingivalis* infection did not significantly alter IL-1α and IL-1 R1 gene expression at the time frames and MOI used. A study on gingival epithelial cells has previously shown that *P. gingivalis* infection results in increased levels of IL-1β (Stathopoulou et al. 2009). Further research on whether such results can be translated to *P. gingivalis* systemic vascular infection would further contribute to knowledge on effects of periodontal pathogen vascular interactions and their role in vascular damage. Especially since studies have shown that IL-1β has several beneficial effects in late-stage murine atherosclerosis (Gomez et al. 2018) and therefore gingipains effects might be reduced by other innate mechanisms.

As with most *in vivo* experimental infection models, animals (mice or zebrafish) are systemically inoculated with high numbers of bacteria, which are very likely much more than would be observed in humans. It therefore could be argued that such studies are therefore not completely physiologically relevant. However, it should be noted that many cardiovascular diseases are long term, chronic conditions where the disease manifests over long periods with repeat exposure to transient levels of one if not several aetiological agents. Replicating this experimentally *in vivo* is extremely challenging and would require repeat low dose inoculation or a longer time frame, giving raise to ethical concerns over animal distress as well as experimental cost. Current, *in vivo* infection strategies aim to provide key information that collectively point to significant risk factors within the full knowledge of their limitations. In this regard, zebrafish provide clear benefits as an *in vivo* model to examine systemic host-pathogen interactions, and the data presented in this chapter significantly adds to others in implicating *P. gingivalis* in vascular pathogenicity.

## 3.6    SUMMARY

These data add significantly to the role of gingipains and their wide array of proteolytic potential in pathogenicity (Giacaman et al. 2009, Baba et al. 2002, Benedyk et al. 2016, Fitzpatrick et al. 2009, Imamura, Travis and Potempa 2003, Imamura 2003, Kadowaki et al. 2003, Lourbakos et al. 2001, Sheets et al. 2005, Totten, Dunn and Progulske-Fox 2006, Widziolek et al. 2016), not only in the periodontium but also systemically. Using *in vitro* and *in vivo* models, data discussed in this chapter provide crucial evidence for the role of *P. gingivalis,* and gingipains in particular, in affecting endothelial function, reaffirming the likely role of oral microbes in influencing systemic disease outcomes. These findings prompted further investigation of the role of gingipains indirect dissemination in the vasculature through *P. gingivalis* Outer membrane Vesicles (OMV), which is the basis of the following chapter.

# CHAPTER 4: Role of *P. gingivalis* Outer Membrane Vesicles (OMV) and secreted proteins in PECAM-1 abundance

## 4.1 INTRODUCTION

As highlighted in previous chapters periodontal disease increases the risk of both cardiovascular disease and coronary heart disease (Gustafsson et al. 2020, Masi, D'Aiuto and Deanfield 2019, Chhibber-Goel et al. 2016), and the association between periodontal disease and cardiovascular disease is nowadays well established (Friedewald et al. 2009, Sanz et al. 2020). Nonetheless, the biological mechanisms through which this occurs are still unknown. Increasing evidence suggests that in cases of extreme gingivitis or periodontitis, the anaerobic periodontal pathobiont, *P. gingivalis* can enter the bloodstream through inflamed and ulcerated periodontal tissue, a process coined as the *porte d'entrée* (Castillo et al. 2011, Loos 2005). Here, loss of tissue integrity and increased bleeding facilitates movement of bacteria from the periodontal pocket into the bloodstream (Schenkein and Loos 2013, Loos 2005), with *P. gingivalis* repetitively detected in disease-free and diseased vascular tissue (Kozarov et al. 2005, Gaetti-Jardim et al. 2009, Szulc et al. 2015, Marcelino et al. 2010, Mougeot et al. 2017b).

As data presented in chapter 3 showed, gingipains (lysine and arginine-specific cysteine proteases) can cause virulence by cleaving host proteins, not only avoiding immune response by degradation of cytokines and pro-inflammatory molecules but also mediating cell surface protein and extracellular matrix disruption facilitating the loss of cellular and tissue integrity (Hočevar, Potempa and Turk 2018), (Tada et al. 2003, Yun et al. 2005)).

Like most Gram-negative organisms, *P. gingivalis* produces outer membrane vesicles (OMV) that appear to retain many of the virulence factors of the parent cell including LPS (Haurat et al. 2011), fimbrae (Mantri et al. 2015) and gingipains (Haurat et al. 2011, Nakao et al. 2014). OMV-derived virulence factors have been shown to drive oral epithelial cell responses (Nakao et al. 2014, Cecil et al. 2016) and influence the differentiation and calcification of smooth muscle cells *in vitro* (Yang et al. 2016), suggesting that OMV may affect cells of the vasculature. Interestingly, the presence of *Pg*-derived OMV has been detected in the peripheral blood and cerebrospinal fluid in animal models with severe bacterial infections (Jia et al. 2015b, Bai et al. 2015), indicating that OMV may be widespread within the circulation and importantly

access areas of tissue not accessible to whole bacteria. However, the effects of *P. gingivalis* OMV and secreted proteins on endothelial cells have not yet been examined.

In this chapter it was hypothesised that OMV generated by *P. gingivalis* can carry virulence factors from the parent and also play a role in gingipain-mediated endothelial damage.

## 4.2   AIMS AND OBJECTIVES

The aim of this chapter was to study the gingipain content in *P. gingivalis*-derived OMV and bacterial secreted products and whether these factors can cause vascular damage through cell-to-cell attachments independently from the bacterial whole cell.

Objectives

- To isolate OMV and secreted proteins from *P. gingivalis.*
- To characterise isolated OMV and secreted proteins from wild-type W83 and the ΔK/R-ab-derived gingipain null mutant.
- To visualise OMV using electron microscopy
- To study the effects of OMV and secreted proteins on endothelial cell permeability using a dextran fluorescent assay.
- To study the effects of OMV and secreted proteins on cell adhesion molecule PECAM-1 abundance using flow cytometry.
- To assess the effects of OMV systemic infection *in vivo* using a zebrafish embryo systemic infection model.

## 4.3   MATERIALS AND METHODS

*P. gingivalis* whole cells, OMV and secreted proteins were isolated as described in section 2.9.1 and as illustrated in Figure 4.1.
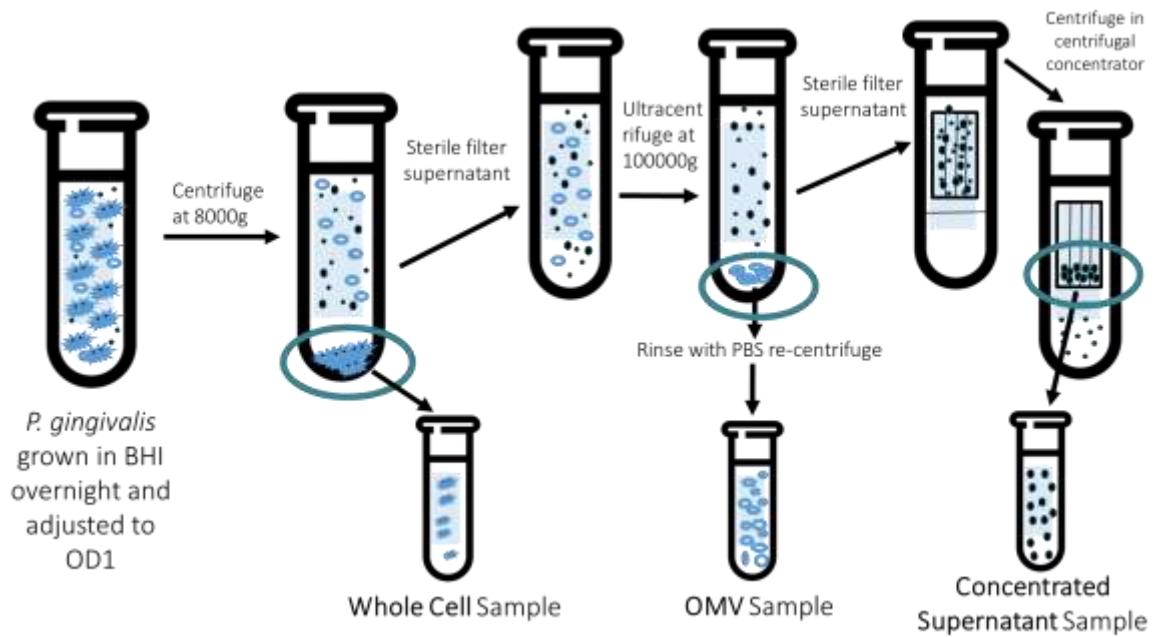
**Figure 4.1: Isolation of samples for whole cell, OMV and concentrated supernatant/secreted protein Sample:** Illustration shows the process of obtaining samples used for this chapter's experiments through centrifugation and size-exclusion filtration cycles. Sterile filter: 0.2μm. Centrifugal concentrator: 10K MW.

Other methods used in this chapter and their relevant Chapter 2 section are listed below:

- 2.3.1 Culture of microbial strains
- 2.3.2 Immortalised human microvascular endothelial cell line
- 2.9.2 Sample characterisation
- 2.9.3 Systemic infection in zebrafish larvae
- 2.9.4 *In vitro* effects
- 2.11 STATISTICS

## 4.4    RESULTS

### 4.4.1  Gingipain presence confirmed through characterisation of isolated OMV and secreted proteins

Prior to assessment of isolated OMV and secreted protein (Figure 4.1) effects on endothelial cells and *in vivo,* samples were characterised to examine the protein, nanoparticle content and gingipain activity.

Gradient SDS-PAGE gels followed by Coomassie staining identified similar protein band sizes and patterns in all W83 derived samples analysed (whole cell, OMV and concentrated supernatant) (Figure 4.2A) in the 10-20 kDa and 50-100 kDa regions. Protein bands for whole cell were more pronounced than for OMV and concentrated supernatant due to their increased abundance in this sample. In contrast, bands in whole cell ΔK/R-ab sample were more dispersed and did not show clear bands in the same regions as the W83 equivalent. In the ΔK/R-ab OMV samples showed a prominent band at the 30-35 kDa region and supernatant samples in the 20 kDa, 30 kDa and 110 kDa region.

This confirmed differences between the wild-type *P. gingivalis* and gingipain-null mutant in terms of protein content for whole cell, OMV and concentrated supernatant. BCA analysis (Figure 4.2B-D) showed no significant differences in the actual protein content between samples derived from whole cell, OMV and concentrated supernatant (B, C and D respectively) generated from wild-type and mutant *P. gingivalis* ($p > 0.1$ in all three groups).
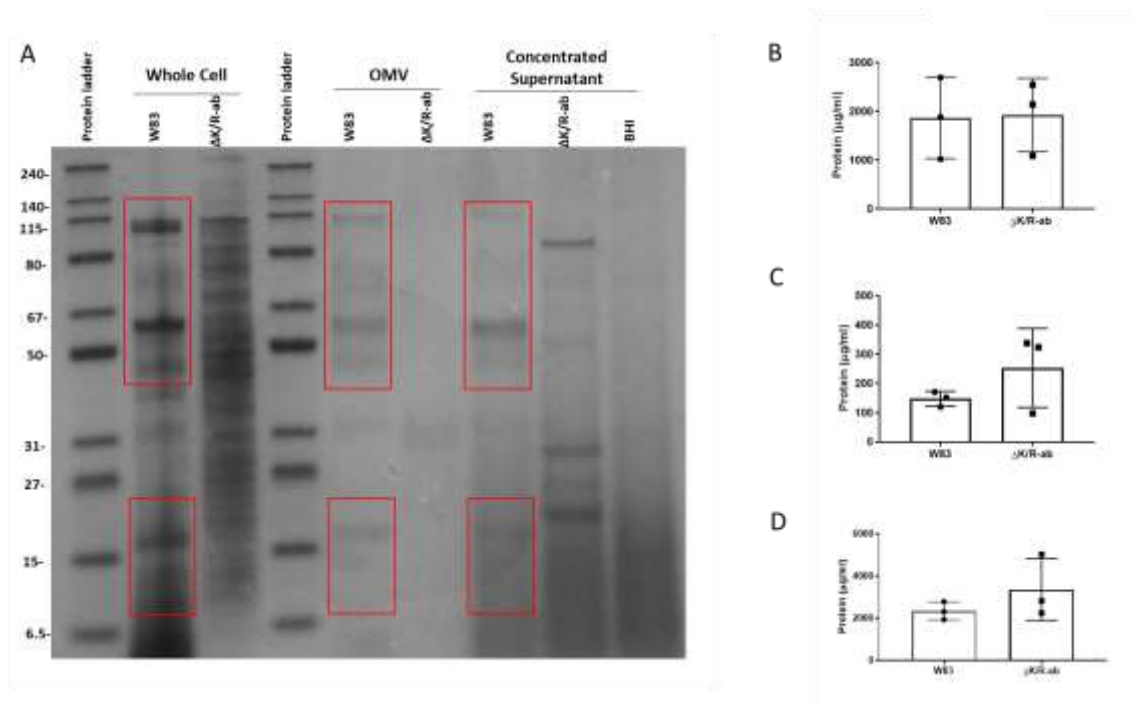


**Figure 4.2: Coomassie stain and total protein content.** Samples were diluted in PBS and together with a protein ladder (Prime Step®) were resolved via SDS-PAGE gels protein ladder were resolved by SDS-PAGE. (A) Coomassie staining was carried out and similar protein band patterns in all 3 sample groups (Whole Cell, OMV and Concentrated Protein) originating from W83 (highlighted in red) were observed, particularly in the 50 kDa and 100 kDa region (highlighted in the red boxes). These bands were not as pronounced in the gingipain null mutant samples. (B-D) A BCA assay determined total protein content in (B) Whole Cell, (C) OMV and (D) Concentrated Supernatant samples. A Mann-Whitney test determined no statistically significant differences between W83 and ΔK/R-ab derived samples total protein content ($p < 0.05$). Data are mean ± SD total protein concentration from 3 independent experiments.

HRgpA, RgpB and Lys (Kgp) gingipain proteins are claimed to be around 95 kDa, 50 kDa and 51 kDa respectively (Imamura 2003, Kuboniwa, Amano and Shizukuishi 1998), suggesting that differences observed in the band patterns in Coomassie staining are potentially attributed to gingipains, although a more specific technique such as immunoblotting was required to resolve this issue. Therefore, immunoblotting with anti-gingipain mAb 1B5 and Rb7 anti-gingipain antiserum was carried out to confirm gingipain presence along with CryoEM followed by immunogold labelling using mAb 1B5 to determine the location of gingipains on whole cells and OMV. A gingipain activity assay was also used to assess the gingipains activity in the generated samples.

Immunoblotting with the RgpA/B specific antisera Rb7 produced immunoreactive bands of 45 kDa for whole W83 cells and W83-derived OMV, whereas this band was absent from counterpart ΔK/R-ab samples (Figure 4.3). Similar immunoblot data was obtained when using the monoclonal antibody 1B5 that binds to the Rgp glycan epitope, which showed immunoreactive bands for Rgp and A-lipopolysaccharide of *P. gingivalis,* as well as Lys Kgp spanning between the 6.5 kDa to 51 kDa region and a band at the 95 kDa region(Figure 4.3). Observed banding patterns were similar to those previously described by other authors using other *P. gingivalis* strains (Aduse Opoku et al. 2006; Curtis et al. 1999).
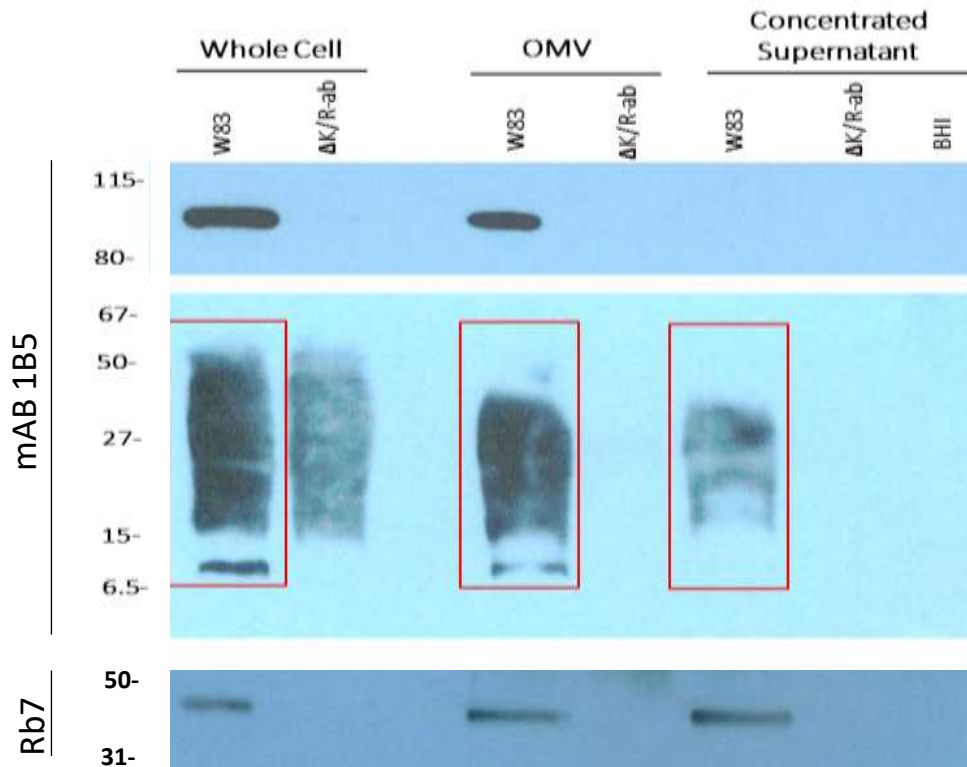
**Figure 4.3: mAB 1B5 and rB7 in W83 derived Whole Cell, OMV and Concentrated supernatant.** Representative immunoblot of W83 and ΔK/R-ab- whole bacteria, OMV and concentrated supernatant were separated on 4-12% NuPAGE® gels, transferred to nitrocellulose membranes and immunoblotted against mouse monoclonal antibody 1B5, an antibody that binds to the shared glycan epitope between Rgp and A-lipopolysaccharide of *P. gingivalis* (observed in the ΔK/R-ab whole cell lane and as a much weaker band in ΔK/R-ab OMV in the 10-55 kDa region at 3 minutes exposure). Following mAb 1B5 immunopositive bands were observed in 95 kDa region (10 minutes exposure time) in the whole cell and OMV samples. Immunopositive bands of 45 kDa were observed in the W83 whole-cell and OMV samples but not in the gingipain-null ΔK/R-ab equivalents when protein extracts were analysed by immunoblotting using the Rb7 anti-gingipain antiserum.

Presence of gingipains on the bacterial surface and periphery of purified W83-derived OMV was confirmed by Cryo-EM using mAb 1B5 immunogold labelling, whereas ΔK/R-ab OMV did not show any immunoreactivity (Figure 4.4). Cryo-EM did not reveal any morphological differences between whole cell and OMV from either strain (Figure 4.4).
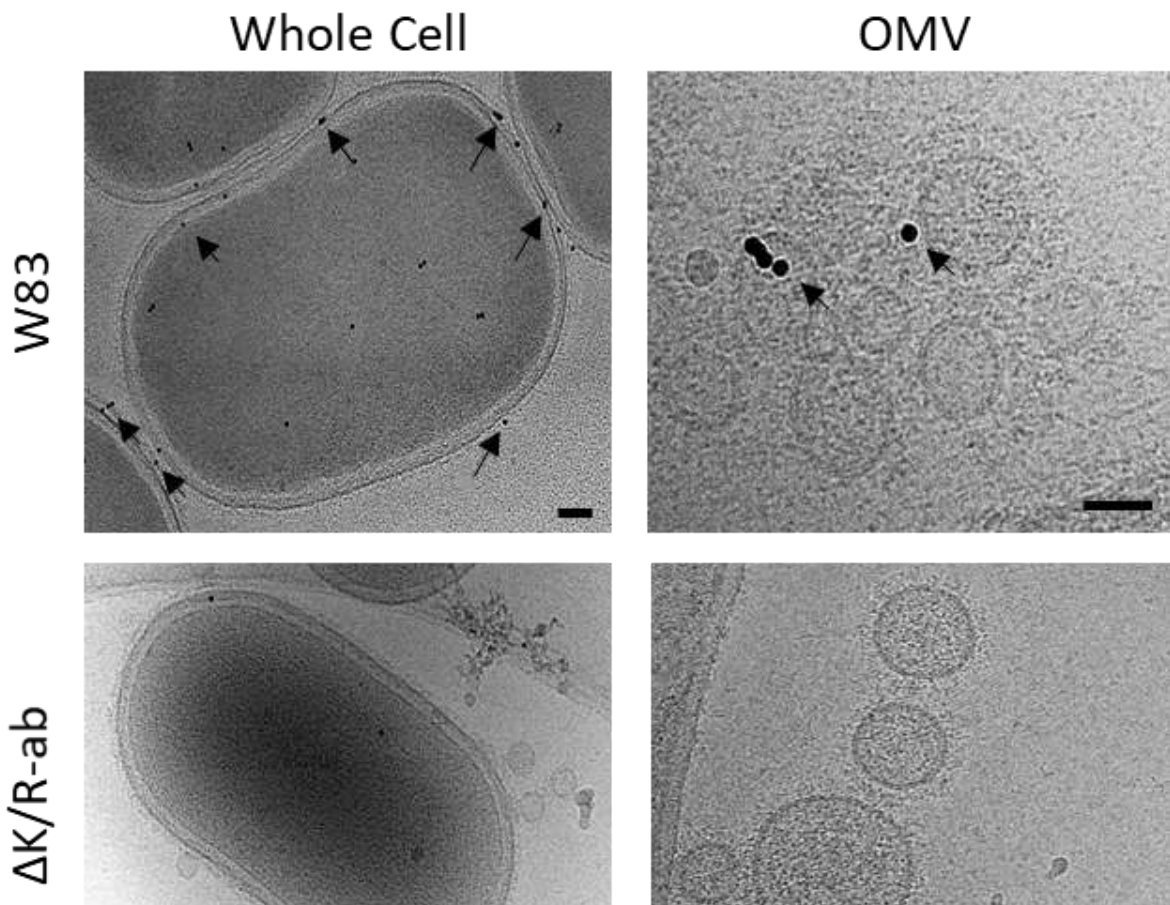
**Figure 4.4: maB 1B5 in W83 derived Whole Cell and OMV in Cryo-EM micrographs.** Representative cryo–electron microscopy (EM) micrographs showing mAb 1B5 immunogold-labelled W83 bacteria and OMV. The gingipain expression is mainly located to the cell wall in both W83 whole cells and OMV (black arrows) but is absent in ΔK/R-ab equivalents (scale bar: whole bacteria = 100 nm; OMV = 50 nm).

Finally, W83 whole cell, OMV and concentrated supernatant displayed the expected gingipain enzyme activity for both argine- (Figure 4.5A-C) and lysine- based (Figure 4.5D-F) substrate that was absent in the ΔK/R-ab strain (p<0.001; Figure 4.5A-F). Average fluorescence in the arginine assay from W83-derived samples (whole Cell, OMV and concentrated supernatant) was 6.383 ± 0.02 compared to 3.539 ± 0.21 in gingipain mutant-derived samples (Figure 4.5A-C). A similar pattern was observed in lysine assay data with an average fluorescence of 4.167 ± 0.189 in W83-derived samples and 3.91 ± 0.075 in ΔK/R-ab-derived samples with differences being less marked the concentrated supernatant sample (Figure 4.5D-F).
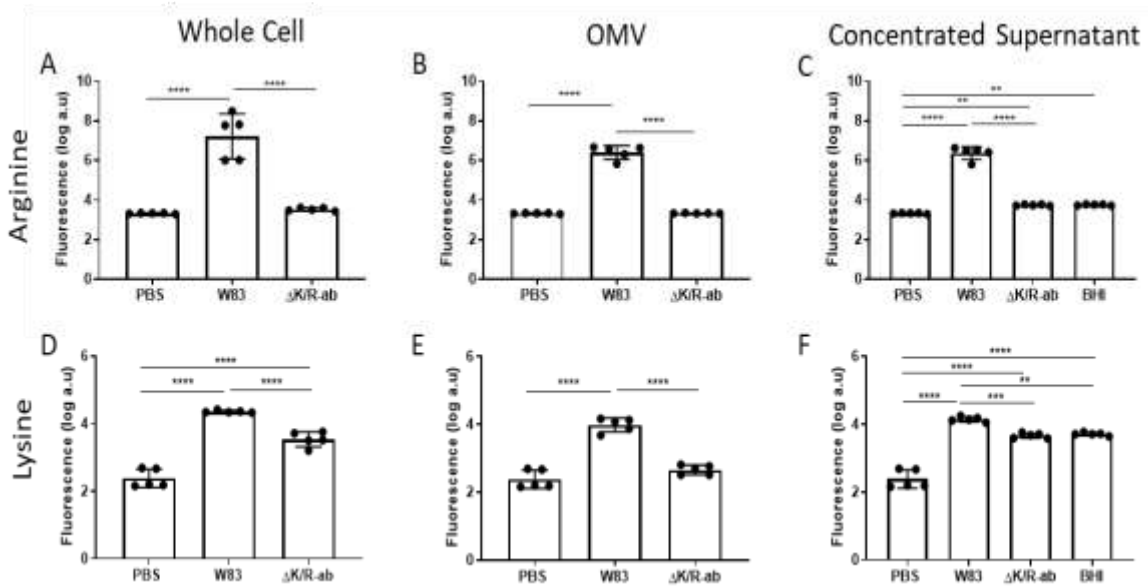
**Figure 4.5: Gingipains activity in W83 derived Whole Cell, OMV and Concentrated supernatant:** (A–F) Gingipain fluorometric enzyme activity assays showing the higher levels of activity of (A-C) arginine-specific (Arg) and (D-F) lysine-specific (Lys) protease in W83 whole cells, OMV and concentrated supernatant compared to ΔK/R-ab mutant equivalents. Data are mean ± SD of 5 independent experiments with each individual experiment performed in triplicate. Statistical significance was determined by 1-way analysis of variance, (**p < 0.01,***p < 0.001, ****p < 0.0001).

ZetaView nanoparticle-tracking analysis was carried out on whole cell-derived sterile filtered supernatant prior to ultracentrifugation (Figure 4.6A,D,G), OMV (Figure 4.6B,E,H) and concentrated supernatant samples (Figure 4.6C,F,I). Nanoparticle analysis identified that there were no statistically significant differences between W83 and ΔK/R-ab-derived sample nanoparticle concentrations in all sample groups (p > 0.05) (Figure 4.6A-C). While statistically significant differences in sample concentrations were present between *P. gingvalis*-derived (W83 and ΔK/R-ab) OMV samples and BHI OMV samples (p < 0.05) (Figure 4.6B). Significant differences in concentration were identified between W83 and sterile BHI OMV samples (p = 0.0057) and between ΔK/R-ab and BHI OMV samples (p = 0.0306) (Figure 4.6B). Differences in particle sizes were identified between *P. gingivalis* (W83 and ΔK/R-ab) derived samples and BHI control in both the supernatant (Figure 4.6 D,G) and OMV group (Figure 4.6E,H) (p <0.05). Overall, wild-type W83 OMV were 24% larger (p<0.05) than those from ΔK/R-ab (144 ± 23 nm).
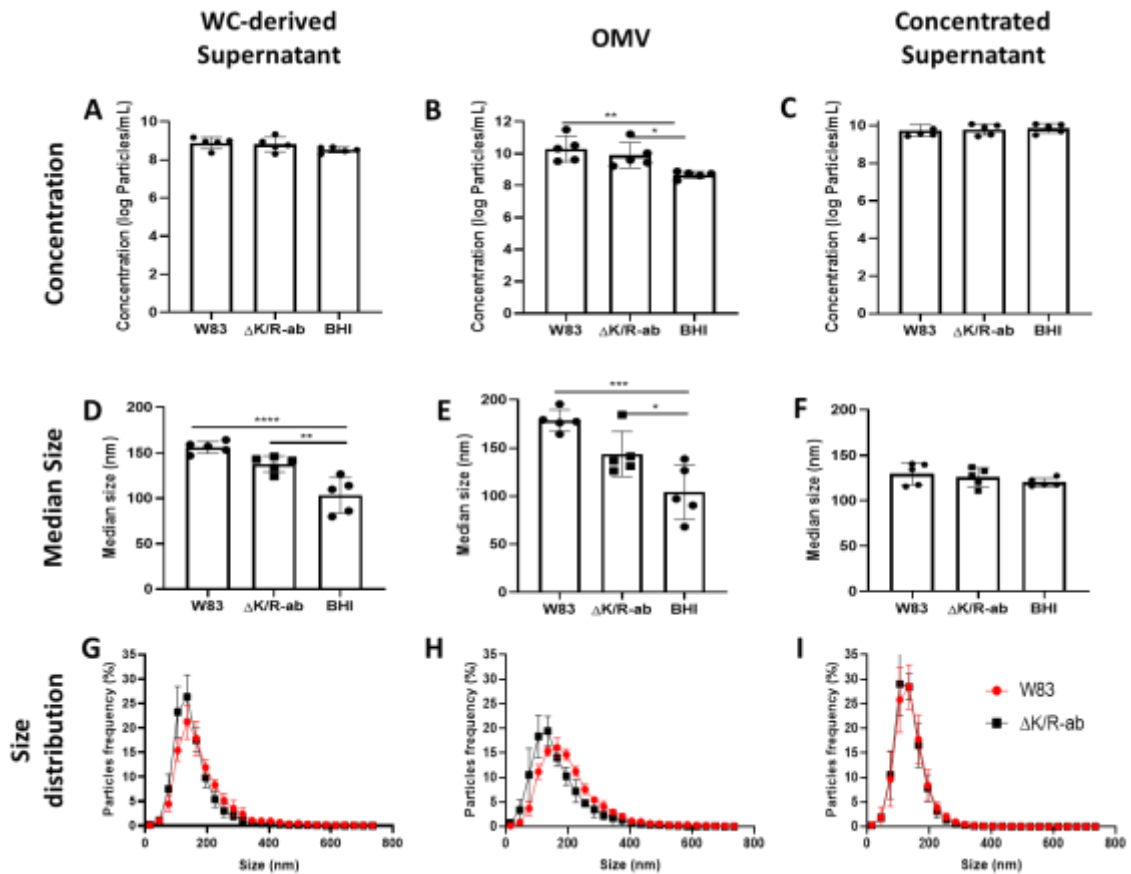
**Figure 4.6: ZetaView nanoparticle-tracking analysis of *P. gingivalis*-derived samples**. (A,D,G) Supernatant, (B,E,H) OMV and (C,F,I) concentrated supernatant from wild-type W83 and its isogenic gingipain-deficient mutant, ΔK/R-ab. .. (A-C) Histograms of number of particles released showing OMV released were similar for both W83 and ΔK/R-ab, but significantly different from the BHI control. (D-F) Quantification of median particle size analysis and (G-I) histograms of size distribution  for W83 and ΔK/R-ab-derived samples. (E) OMV nanoparticles derived from W83 were larger than those derived from the gingipain null-mutant. For ZetaView analysis, instrument calibration was performed using 100 nm polystyrene beads. Data in all panels are means ± SD of 5 independent experiments and statistical significance was determined using one-way ANOVA, *p < 0.05, **p < 0.01, ***p < 0.001.

In summary, characterisation confirmed that purified OMV were achieved through the sample preparation used, that gingipains were present in W83 derived-samples and not in the ΔK/R-ab-derived samples, and that total protein concentration and OMV concentration of W83 and ΔK/R-ab-derived-samples was comparable. Data collected were used for dosing calculations in the subsequent infection experiments to ensure equal protein and nanoparticle loading.

## 4.4.2 *P. gingivalis* OMV and concentrated supernatant increase endothelial cell permeability *in vitro* in a gingipain-dependent manner

Since increased vascular permeability has been linked to cardiovascular risk (Chistiakov et al. 2015), a fluorescent dextran-based *in vitro* permeability assay on confluent HMEC-1 microvascular endothelial cell monolayers was used to determine the influence of OMV-expressed gingipains, as well as secreted gingipains within the concentrated supernatant, on endothelial permeability. Confluent, untreated endothelial monolayers proved an effective barrier with little of the applied 70 kDa fluorescent dextran permeating the cell layer after 5 hours (Figure 4.7A). Contrastingly, the endothelium displayed significantly increased dextran permeability upon treatment with W83 whole cell (Figure 4.7B; $p < 0.01$), W83-derived OMV or W83-derived concentrated supernatant (Figure 4.7C and D; $p < 0.05$) when compared to counterpart ΔK/R-ab-treated or uninfected controls, suggesting that altered vascular permeability is gingipain-dependent. ΔK/R-ab-treated endothelial cells also displayed similar permeability ($p > 0.095$) to the untreated and BHI control in all of the three sample types (whole cell, OMV and concentrated supernatant). Notably, endothelium permeability was significantly higher ($p < 0.05$) in the presence of W83 whole cells (12.69% ± 9.016 dextran release) compared to OMV (6.06% ± 4.768 dextran release) and concentrated supernatant (6.56% ± 5.082 dextran release).
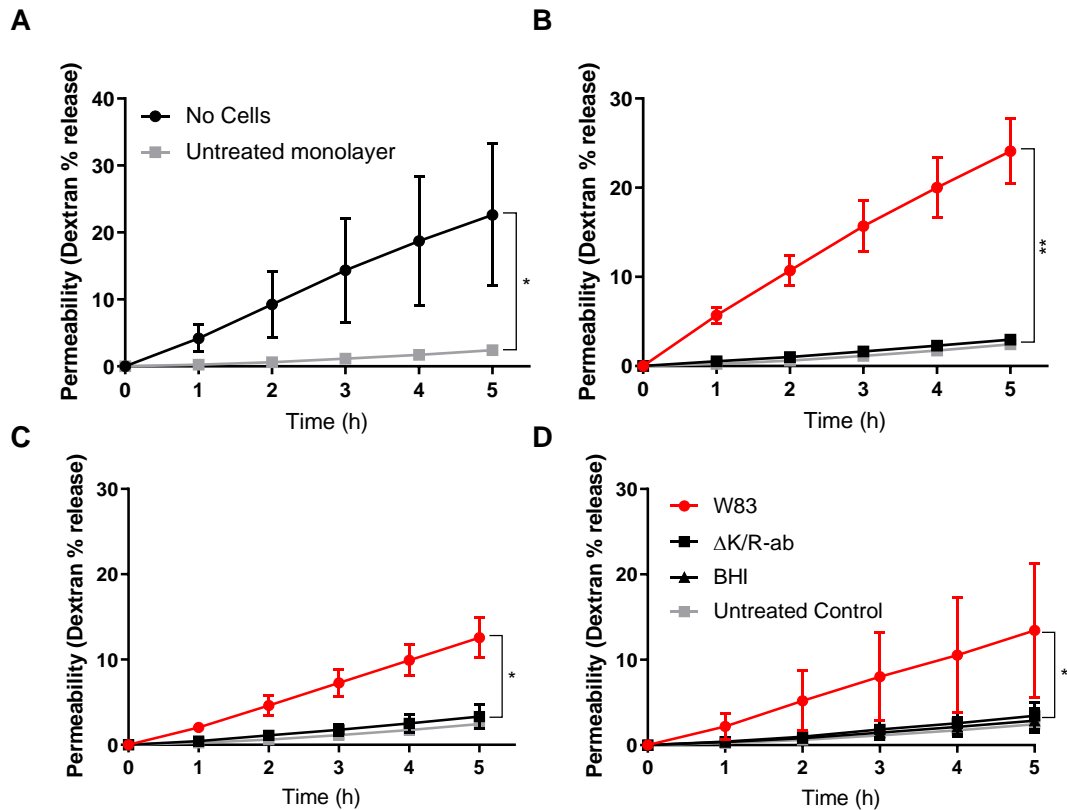
**Figure 4.7: Increase in permeability following *P. gingivalis* whole cell and OMV infection is gingipain dependent.** Cells were grown to monolayers on hanging fibronectin-coated inserts, exposed to control (non-infected media), W83 or ΔK/R-ab samples for 1.5 hours. High molecular (70 kDa) fluorescein-dextran passing through the monolayer was measured. (A) In the controls group percentage dextran release and therefore monolayer permeability was significantly higher in inserts without cells when compared to inserts with a healthy monolayer ($p = 0.0144$). This was mirrored by increased permeability following exposure to W83 samples when compared to ΔK/R-ab in both the (B) whole cell group ($p = 0.0056$), the (C) OMV group ($p = 0.0396$) and the (D) Concentrated Supernatant group ($p > 0.0105$). W83 infected equivalents were also significantly more permeable than the non-infected control ($p < 0.03$), while no significant differences were observed between ΔK/R-ab infected samples and the non-infected controls ($p > 0.95$) or the BHI treated control ($p > 0.9981$). Data are presented as means of 3 biological repeats ± SD and were analysed with unpaired t-test for A and One-way ANOVA for B, C and D.

### 4.4.3 *P. gingivalis* OMV and concentrated supernatant decrease PECAM-1 abundance *in vitro* in a gingipain dependent manner

Increased permeability following *P. gingivalis* infection of endothelial cells may be due to gingipain-mediated cleavage of cell adhesion molecules (Widziolek et al. 2016, Sheets et al. 2006). PECAM-1 cell adhesion molecule abundance was therefore analysed through flow cytometry of live gated HMEC-1 cells (Figure 4.8A) and quantified using the normalised median fluorescence index (nMFI) as previously described by Chan *et al.,* 2013 (Chan et al. 2013). PECAM-1 abundance significantly decreased following whole cell W83 infection (Figure 4.8D) (p = 0.0005), infection with W83-derived OMV (Figure 4.8F) (p < 0.0045), as well as incubation with W83-derived concentrated supernatant (Figure 4.8H) (p = 0.0041) when compared to infection with counterpart ΔK/R-ab-derived samples. No difference in PECAM-1 abundacne was observed when exposing endothelial cells to the concentrated BHI controls (Figure 4.8H) and to all of the ΔK/R-ab-derived samples in all 3 groups (p > 0.05). Mean nmFI of endothelial cells infected with W83-derived samples from all 3 groups (whole cell, OMV and concentrated supernatant) was nmFI 0.8330 ± 0.118 while those infected with ΔK/R-ab-derived samples resulted in an average nmFI 17.347 ± 0.216. This translates to on average 20 times less surface PECAM-1 abundance in cells infected with gingipain containing samples when compared to those infected with the gingipain-null derived samples.
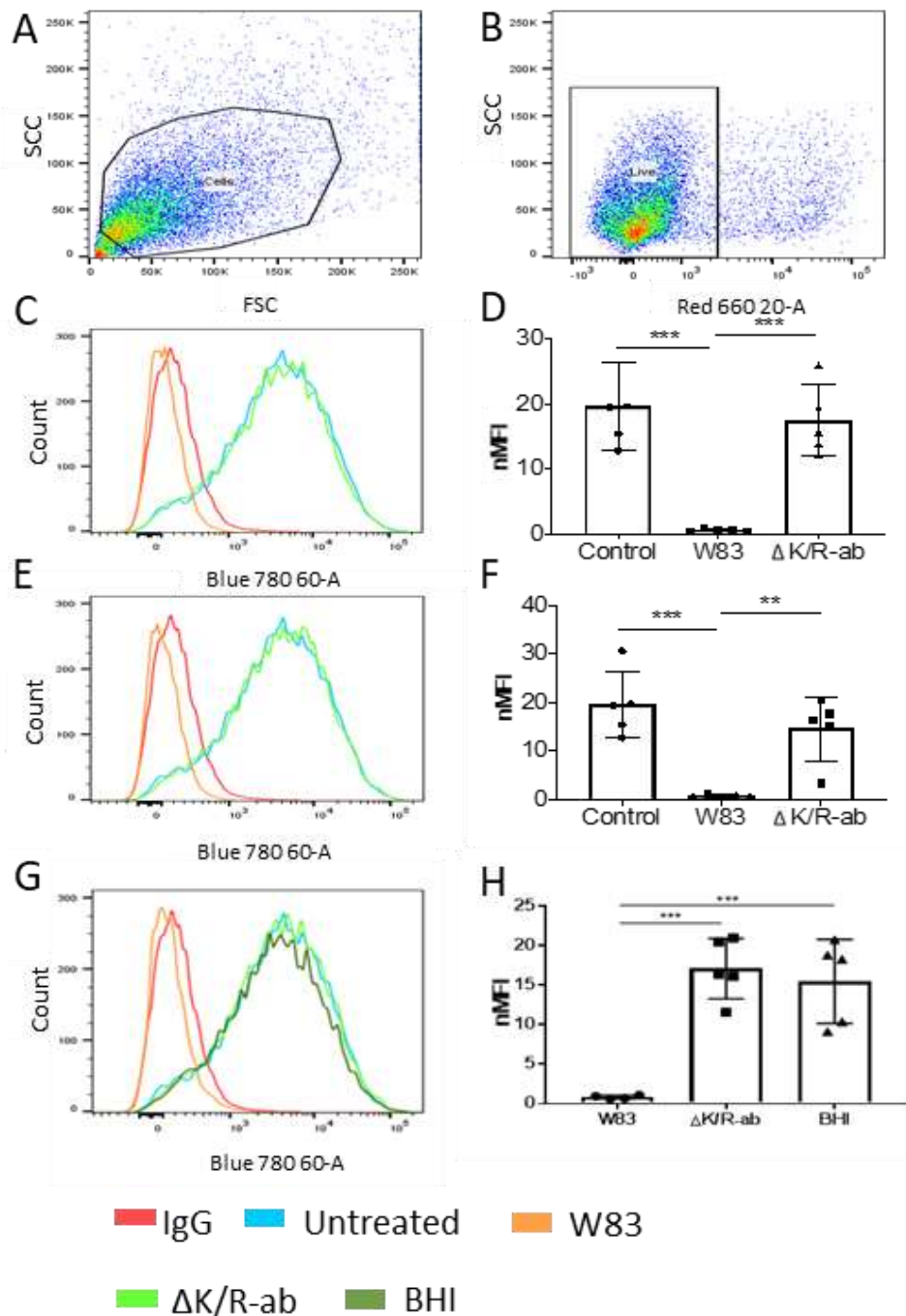
**Figure 4.8: PECAM-1 reduction following exposure to W83 whole cell, OMV and concentrated supernatant is gingipain mediated.** (A) Following 1.5 hours exposure to W83 or ΔK/R-ab Whole Cell or OMV HMEC-1 cells were gated using forward scatter (FSC) and side scatter (SSC) voltages. (B) TO-PRO-3® (1 mg/ml, Invitrogen) was used as a cell viability dye to exclude dead cells 10000 live cells were collected and threshold for positively fluorescent cells was set using isotype-matched controls. (C,E,G) Histograms highlight decreased PECAM-1 expression after exposure to W83 (orange) (C) whole cells, (E) OMV and (G) concentrated supernatant. This decrease was not observed following exposure to all ΔK/R-ab derived samples (light green) or concentrated BHI (dark green). (D,F,H) Calculation of nMFI confirmed differences in PECAM-1 expression with statistically significant differences between the W83 and ΔK/R-ab in the (D) whole cell, (F) OMV and (H) concentrated supernatant equivalents. ** and *** indicate statistical significance determined by a one-way ANOVA with a $p < 0.01$ and $p < 0.0001$ respectively.

In order to further assess the role of gingipain in OMV and concentrated supernatant reduction in PECAM-1 abundance, W83-derived samples were treated with 2 μM KYT-1 and KYT-36 specific gingipain inhibitors for 1 hour prior to infection (Figure 4.9). Pre-incubation with these inhibitors significantly inhibited the reduction of PECAM-1 cell surface abundance caused by W83 OMV (p =0.0215) and W83 concentrated supernatant (p < 0.0001). A similar trend was observed in the whole cell sample but 2 μM treatment did not sufficiently block whole cell gingipains activity at the concentrations used (Figure 4.9). These results further highlight the role of OMV and secreted protein (through concentrated supernatant) derived-gingipains in reduction of PECAM-1 abundance and potential role in vascular damage.
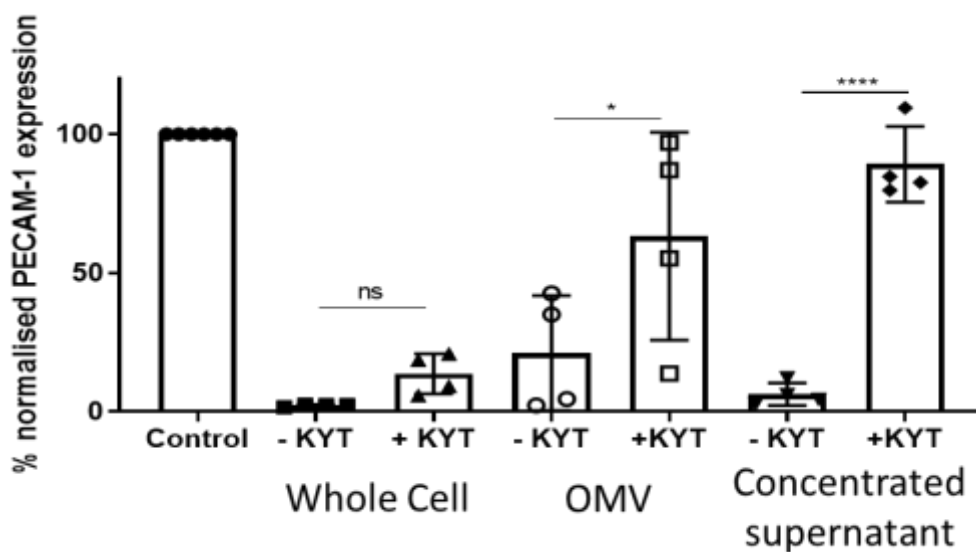


**Figure 4.9: Gingipain inhibitors reduce PECAM-1 reduction following W83 OMV and concentrated supernatant infection:** W83 OMV and concentrated supernatant treated with 2 μM kyt-1 and kyt-36 gingipain inhibitors (mixed) for 1 hour in anaerobic conditions prior to centrifugation resulted in significantly less PECAM-1 reduction in HMEC-1 cells when compared to cells infected with non-inhibited (- KYT) wild-type derived OMV. Although a similar trend was observed in the whole cell sample, KYT concentrations used did not yield significantly lower PECAM-1 reduction (p = 0.9531). Statistical significance was determined by a one-way ANOVA with  *p<0.05 and ***p < 0.001, respectively.

## 4.4.4 *P. gingivalis* OMV-associated gingipains are responsible for systemic symptoms in zebrafish *in vivo*

Previous studies have shown that zebrafish larvae display increased mortality (death) and morbidity (cardiac and yolk oedema) when systemically injected with *P. gingivalis* (Widziolek

et al. 2016). This systemic infection *in vivo* model was used to assess whether the observed presence of gingipain on the surface of OMV has the potential to contribute to systemic disease *in vivo*. Kaplan-Meier survival plot analysis showed that both whole cell W83 and W83-derived OMV caused significantly more zebrafish mortality than PBS-injected controls (p < 0.001; Figure 4.10). In contrast, morbidity in zebrafish larvae injected with ΔK/R-ab-derived OMV was not significantly different to controls (p= 0.55).
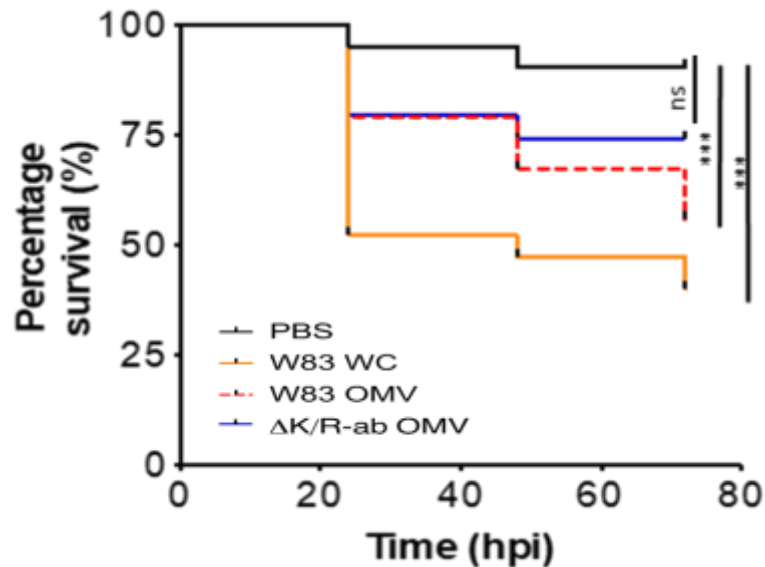


**Figure 4.10: Decreased percentage survival after systemic zebrafish infection with W83-derived whole cell and OMV.** Kaplan-Meier survival plots of zebrafish larvae infected with PBS control, *P. gingivalis* W83 whole cell (WC), *P. gingivalis* W83 OMV or ΔK/R-ab OMV. Comparisons between survival curves using the log rank test show differences between survival curves of PBS control injected and W83 whole cell injected or W83 OMV injected zebrafish embryos. While survival curves of zebrafish embyros injected with ΔK/Ra-b OMV were not statistically different to the PBS control. Ns indicates no significant difference (p > 0.05), while *** indicates a p < 0.001.

To interrogate the data further we stratified the fish into viable or diseased (non-viable + oedematous) groups. A significant increase in the number of diseased zebrafish treated with W83-derived OMV was observed when compared to ΔK/R-ab-derived OMV in a time-dependent manner (p<0.01, Figure 4.11A-C). W83 OMV-treated zebrafish larvae displayed marked cardiac oedema and enlarged yolk sac, whereas those injected with ΔK/R-ab-derived OMV or PBS-treated controls displayed mild or no oedema (Figure 4.11E), providing further evidence that gingipains present on the surface of OMV can cause systemic disease *in vivo*.

**Figure 4.11: Systemic infection in zebrafish.** (A-C) Percentage live, oedematous and dead zebrafish at (A) 24 (B) 48 and (C) 72 hpi showing that percentage of live zebrafish is lower after W83 OMV infection when compared to ΔK/R-ab OMV at all time points. $p < 0.05$ following Tukey multiple comparison test. *$p < 0.05$ and ** $p < 0.01$ (D) Micrographs showing morphology of zebrafish larvae infected with PBS control, W83 whole cells, W83 OMV or ΔK/R-ab OMV. W83 WC and OMV infected zebrafish show oedema observed around yolk and heart highlighted by black arrows. Scale bars represent 500 μm. All experiments were performed 3 times and in all experiments injections were carried out in 30 hours post fertilisation (hpf) zebrafish larvae using at least 39 zebrafish per group.

## 4.5   DISCUSSION

Like many Gram-negative bacteria, *P. gingivalis* produces abundant OMV (Xie 2015). Despite this being well known, there is limited data as to their effects in host-pathogen interactions. The data presented in this chapter show for the first time that *P. gingivalis* OMV markedly increase vascular permeability *in vitro* and potentiate vascular oedema and mortality *in vivo* in a gingipain-dependent manner, suggesting that they may act in concert with whole bacteria to impact cardiovascular disease risk.

126

Gingipains are key virulence factors of *P. gingivalis*. As well as functions in bacterial co-aggregation, biofilm formation and haem acquisition, they also cleave soluble and cell surface human proteins (Hočevar et al. 2018). RgpA/B and Kgp gingipains have been previously detected in *P. gingivalis*-derived OMV by mass spectrometry (Haurat et al. 2011). It was therefore reasoned that gingipain-expressing OMV might be key mediators of endothelial cell surface receptor degradation leading to increased vascular permeability. Suggesting its importance in the context of systemic disease as their small size and abundance is likely to allow OMV to penetrate host tissue micro-niches that may not readily accessible to *P. gingivalis* whole cells. To test this chapter's hypothesis, OMV and secreted proteins were generated from W83 wild-type and its isogenic gingipain-deficient counterpart, ΔK/R-ab and presence or absence of gingipains was confirmed. Gingipains on OMV was previously observed using W50 and other *P. gingivalis* strains in other studies (Naylor et al. 2017, Aduse-Opoku et al. 2006, Curtis et al. 1999). Immunogold labelling followed by cryo-EM additionally showed that gingipains were located to the OMV cell surface. Although no structural abnormalities were visibly observed by cryo-EM, nanoparticle-tracking analysis showed that W83-derived OMV were larger in size than their gingipain-deficient counterparts. It is plausible that this size difference is due to changes in the molecular structure within the cell wall owing to loss of gingipain-mediated cell wall processing.

Studies examining the role of *P. gingivalis* OMV and secretions on vascular biology are sparse. Bartruff *et al*., showed that *P. gingivalis* ATCC33277-derived OMV inhibited human umbilical vein endothelial cell (HUVEC) proliferation by up to 80% as well as capillary tubule formation in an OMV dose-dependent manner (Bartruff, Yukna and Layman 2005). These effects were inhibited by heat treatment but not by protease inhibitors, suggesting that these effects were protein but not protease-mediated, although no specific factor was identified (Bartruff et al. 2005). Using the same *P. gingivalis* strain, Jia *et al*., observed that OMV suppressed endothelial nitric oxide synthase (eNOS) transcript and protein expression in HUVEC via activation of the ERK1/2 and p38 MAPK signalling pathways in a Rho-associated protein kinase-dependent manner (Jia et al. 2015b). This study provides good evidence that OMV may regulate vascular oxidative injury, although the OMV factors driving this effect were not examined. *P gingivalis*-derived OMV have recently been shown to promote vascular smooth muscle cell differentiation and calcification by increasing the activity of runx-related transcription factor

2, a crucial driver of osteoblastic differentiation and mineralization of vascular smooth muscle cells (Yang et al. 2016).

This study provides further evidence that OMV and to a lesser extent non-OMV protein secretions can significantly perturb endothelial homeostasis. *In vitro,* W83-derived OMV and secreted factors not only cleaved PECAM-1 on endothelial cell monolayers but also increased endothelial cell permeability. Moreover, cleavage of PECAM-1 was significantly reduced when W83-derived OMV were either pre-incubated with the gingipain protease inhibitors KYT1 and KYT36 or infected with gingipain-deficient OMV. Not only do these data show that *P. gingivalis* OMV and secretions mediate vascular damage but also that this is via a gingipain-dependent mechanism, the first time that this has been documented for *P. gingivalis* OMV. Some of these *in vitro* observations were confirmed *in vivo* using a systemic zebrafish infection model. Although zebrafish larvae have been widely used to examine systemic host-pathogen interactions (Sullivan et al. 2017), only a few studies have examined the role of bacterial OMV in systemic disease and, to our knowledge, none have been performed using *P. gingivalis* OMV. OMV derived from W83 but not ΔK/R-ab caused significant oedema and mortality in zebrafish larvae, although the effects were less extreme than those observed with injection of whole cell W83. *In vitro* and *in vivo* data presented in this chapter further confirms that OMV have the potential to cause disease in the absence of the parent whole cell bacteria and augment current evidence that OMV are able to exert their effects beyond that of the periodontal pocket.

These data and from those in chapter 3 lead to the speculation that gingipains on OMV as well as whole bacteria cleave endothelial intercellular junction proteins such as PECAM-1, thereby loosening cell-to-cell contacts to permit increased endothelial cell permeability. This may have two consequences; to allow exudate from the circulation into tissues and progressing to tissue oedema, which we observed *in vivo*; and secondly to expose underlying connective tissue that may lead to platelet activation and subsequently foci for immune cell activation on the endothelium. The latter would have dramatic implications for increased risk of systemic disease (Chistiakov, Orekhov and Bobryshev 2015). Moreover, the nanoscale size of OMV would allow proteolytic damage to occur at vascular sites inaccessible to whole bacteria. Although this hypothesis requires further evaluation, the data in this chapter provide a potential mechanism for the link between periodontal disease and cardiovascular disease. It

also provides clear evidence that the role of OMV in host-microbial pathogenesis may be as important as whole bacteria, a factor that needs to be taken into consideration in the on-going drive to decipher the oral health systemic connection.

## 4.6 SUMMARY

These novel data demonstrate that *P. gingivalis* OMV and secreted proteins may play a pivotal role in disrupting the vasculature, a process that may drive or markedly increase the risk of cardiovascular disease.

There is also now an appreciation that many bacterial-mediated diseases are polymicrobial in nature, with periodontitis being a case in point. In periodontitis it is considered that several organisms within the sub-gingival plaque drive pathogenesis rather than one organism in isolation.  It is therefore very likely that other oral bacteria contribute to systemic disease. Indeed in the oral context, studies have shown significant impacts on the functional behaviour of *P. gingivalis* when in the presence of other oral microbes such as *T. forsythia* or *F. nucleatum* (Chukkapalli et al. 2017a). Investigation of these effects will be described in the final results chapter.

# CHAPTER 5: *Fusobacterium nucleatum* and multispecies effects on endothelial permeability and PECAM-1

## 5.1 INTRODUCTION

Periodontitis is a polymicrobial disease and therefore it is unsurprising that several periodontal pathogens have been identified in the human vasculature including *P. gingivalis* (Gaetti-Jardim et al. 2009, Kozarov et al. 2005, Marcelino et al. 2010, Szulc et al. 2015, Mougeot et al. 2017b, Marín et al. 2016, Castillo et al. 2011); *F. nucleatum* (Marín et al. 2016, Marcelino et al. 2010, Lockhart et al. 2008) and *T. forsythia* (Castillo et al. 2011, Marcelino et al. 2010). However, studies examining the interaction of *P. gingivalis* with endothelial cells greatly outnumber those of other periodontal pathogens identified in vascular tissues (Reyes et al. 2013b). Therefore, there is a knowledge gap in periodontal polymicrobial interactions with the endothelium.

In Chapters 3 and 4, gingipain-dependent cleavage of PECAM-1 following *P. gingivalis* infection was shown, highlighting the effect of this keystone pathogen on the vasculature. However, changes in vascular integrity following *F. nucleatum* infection have been previously described in human umbilical vein endothelial cells that was attributed to bacterial FadA adherins (Fardini et al. 2010). A decrease in PECAM-1 abundance following *F. nucleatum* infection of endothelial cells was also reported by Mendes et al. (Mendes et al. 2016), while effects of *T. forsythia* on PECAM-1 or any other adhesion molecule have as yet not been reported. Moreover, the polymicrobial effects of *P. gingivalis*, *F. nucleatum* and *T. forsythia* on endothelial cell protein expression and permeability have yet to be investigated, even though periodontal pathogens, *P. gingivalis* in particular, are generally found associated with other periodontal pathogens and not as solitary organisms (Yao et al. 1996). Polymicrobial assessment of periodontal pathogen-vascular interactions and their pathogenicity on endothelial cells is relatively infrequent in the literature. Published data has shown that polymicrobial infection can alter the pathogenicity of periodontal pathogens. *F. nucleatum* has been shown to enhance the invasion of *P. gingivalis* into aortic endothelial cells *in vitro* (Saito et al. 2008a), while *in vivo* polymicrobial infection elicits a distinct inflammatory response and

increased aortic oxidative stress  (Chukkapalli et al. 2015c, Nahid et al. 2011, Rivera et al. 2013, Velsko et al. 2015).

## 5.2    AIMS AND OBJECTIVES

The aim of this chapter was to compare the effects of *F. nucleatum* and *T. forsythia* infection on endothelial cell PECAM-1 abundance and permeability with that of *P. gingivalis* as reported in Chapter 3 and 4. In addition, this chapter also aimed to investigate whether these effects are altered in polymicrobial infections and following polymicrobial interactions.

**Objectives**

- To assess the effects of single species infections of *P. gingivalis, F. nucleatum* and *T. forsythia* (MOI 100) on endothelial permeability and PECAM-1 cell surface abundance
- To investigate potential differences in endothelial pathogenicity between *F. nucleatum* strains *in vitro*
- To visualise *F. nucleatum* systemic dissemination and study pathogenicity *in vivo*
- To assess permeability and PECAM-1 expression following mixed culture infection
- To study the role of *P. gingivalis* gingipains in mixed culture infection
- To assess changes in pathogenicity after allowing mixed cultures to interact in aerobic conditions
- To visualise multispecies systemic dissemination *in vivo*

## 5.3    MATERIALS AND METHODS

Methods used in this chapter and their relevant Chapter 2 section are listed below:

- 2.3.1 Culture of microbial strains
- 2.3.2 Immortalised human microvascular endothelial cell line
- 2.10.1  *In vitro* single species infection
- 2.10.2  *In vivo F. nucleatum* systemic infection
- 2.10.2.1 Assessment of zebrafish larvae morbidity and mortality after systemic infection

- 2.10.2.2 Assessment of zebrafish larvae morbidity and mortality after systemic infection
- 2.10.3 *In vitro* multispecies infection
- 2.10.4 *In vivo* multispecies systemic infection
- 2.10.5 Role of multispecies adhesion on PECAM-1
- 2.11 STATISTICS

## 5.4 RESULTS

### 5.4.1 *Fusobacterium nucleatum* and *Porphyromonas gingivalis* at MOI 100 significantly decrease PECAM-1 abundance and increase endothelial permeability

The effects of *P. gingivalis* (wild-type and ΔK/R-ab) as well as *F. nucleatum* ssp *nucleatum*, *F. nucleatum* ssp *polymorphum* and *T. forsythia* on endothelial cell PACAM-1 abundance was measured by flow cytometry. Similar to previous results, PECAM-1 abundance was significantly (p < 0.05) decreased following infection with wild-type *P. gingivalis* W83 in an MOI-dependent manner (Figure 5.1A, whilst the *P. gingivalis* gingipain-deficient mutant (ΔK/R-ab) did not (Figure 5.1B). *F. nucleatum* ssp *nucleatum* and *F. nucleatum* ssp *polymorphum* both reduced PECAM-1 abundance compared to controls with significant reduction seen at MOI100 for both strains (Figure 5.1C&D, p < 0.05). In contrast, infection with *T. forsythia* did not alter PECAM-1 abundance at any MOI tested (Figure 5.1E).

Endothelial monolayer permeability in response to bacterial infection mirrored the data obtained for PECAM-1 abundance. A time-dependent Increase in endothelial permeability was observed for *P. gingivalis* W83 and both the *F. nucleatum* ssp to *P. gingivalis* ΔK/R-ab, *T. forsythia* or uninfected controls (Figure 5.2). At the 5-hour time point infection with either *F. nucleatum* ssp *nucleatum* or *polymorphum* resulted in a 4-fold increase (17.7±3.0%; p < 0.001 and 16.2±4.2%; p < 0.0001) in dextran release respectively compared to uninfected controls (4.0±1.8%). For *P. gingivalis* W83, dextran release was 3-fold increased (12.3±0.8%; p < 0.01)

(Figure 5.2). Infection with either *P. gingivalis* ΔK/R-ab or *T. forsythia* did not alter endothelial permeability (Figure 5.2).
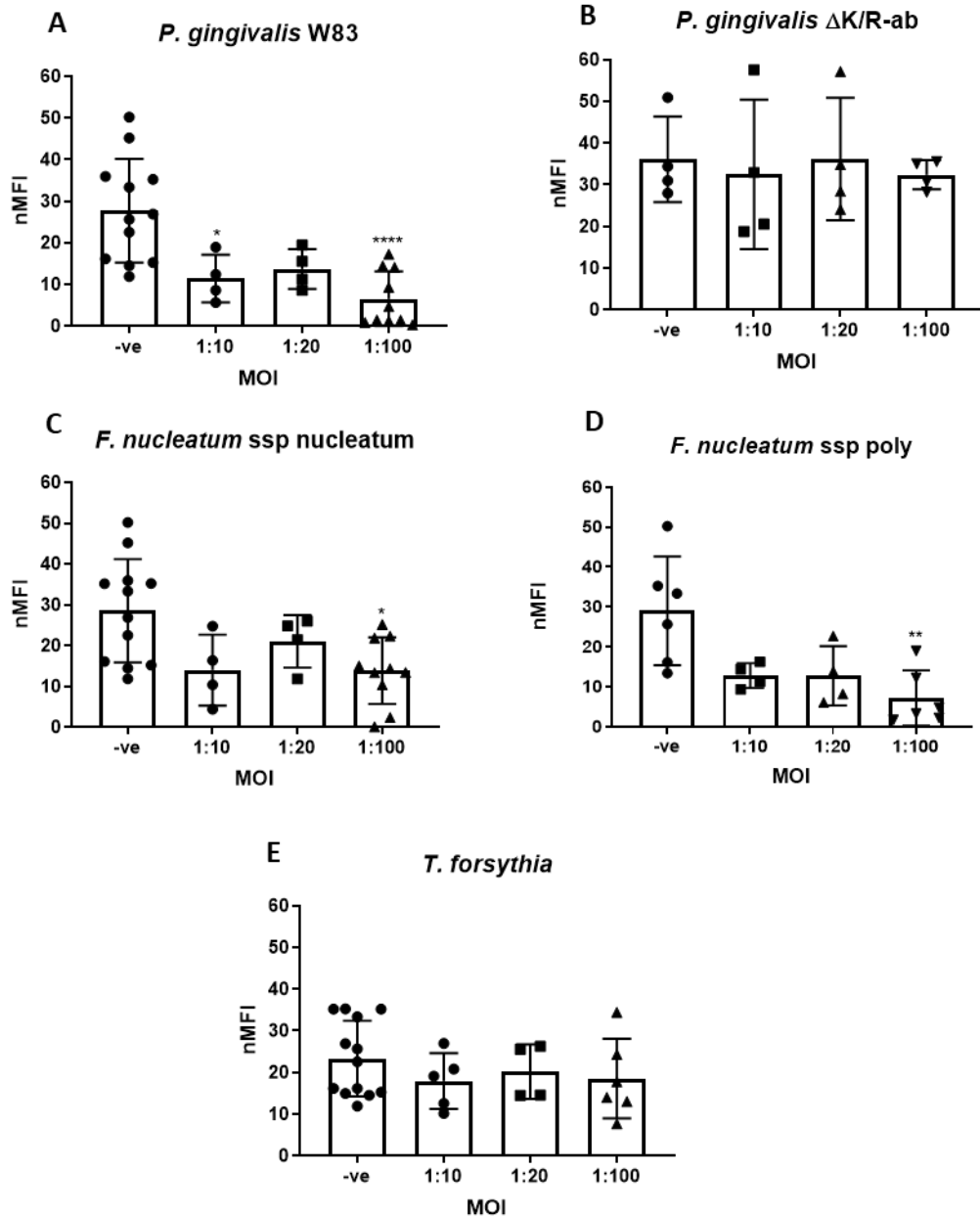


**Figure 5.1: Reduction in PECAM-1 abundance** after periodontal pathogen infection. HMEC-1 were infected with wild-type strain (A) *P. gingivalis* W83, (B) *P. gingivalis* gingipain-null mutant ΔK/R-ab, (C) *F. nucleatum* ssp *nucleatum* (D) *F. nucleatum* ssp *polymorphum* or (E) *T. forsythia* ATCC 43037 at Multiplicity of infection (MOI) 10, 20 and 100. Normalised median fluorescence intensity (nMFI) histograms of PECAM-1 following single species infection or uninfected control (enclosed shapes represent data for each individual experiment/n, carried out on different days using fresh aliquot of cells and fresh bacterial culture) show a significant decrease in PECAM-1 after (A) *P. gingivalis* W83 and (C,D) *F. nucleatum* infection at MOI100 ($p < 0.05$). Statistical differences were analysed by one-way ANOVA with Tukey's multiple comparison test. *$p < 0.05$, **$p < 0.01$, ****$p < 0.0001$.
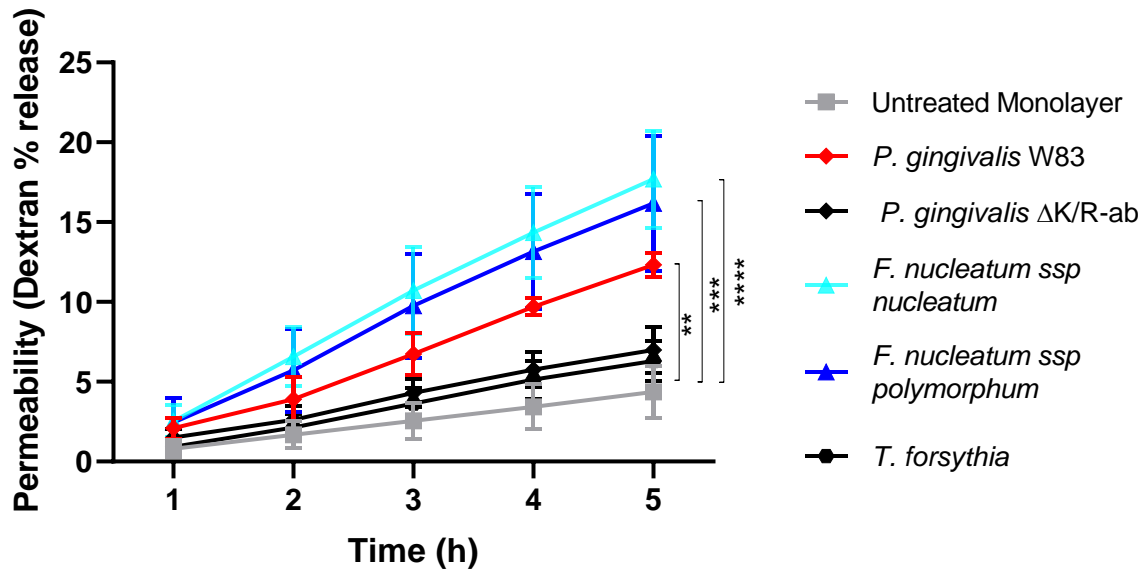
**Figure 5.2: Increased endothelial permeability following *P. gingivalis* W83 and *F. nucleatum* infection at MOI100.** Movement of fluorescently labelled 70 kDa dextran from the upper well to the lower well in a Transwell assay increased in a time-dependent manner when HMEC-1 endothelial monolayers were treated with *P. gingivalis* W83 (red), *F. nucleautum* ssp *nucleatum* (light blue) and *F. nucleatum* ssp *polymorphum* (dark blue) for 1.5 hours and dextran permeability across the endothelium measured for or up to after 5 hours. Uninfected controls (grey), *P. gingivalis* ΔK/R-ab-treated and *T. forsythia*-treated monolayers (black) did not result in significant changes in permeability ($p > 0.05$). Permeability data are presented as mean ± SD of 3 independent experiments. Statistical differences were analysed by one‐way ANOVA with Tukey's multiple comparison test. **$p < 0.01$, ***$p < 0.001$, ****$p < 0.0001$.

## 5.4.2 *Fusobacterium nucleatum* systemic injection increases zebrafish morbidity in a dose-dependent manner

As previously determined for *P. gingivalis, F. nucleatum* ssp *polymorphum was* injected systemically in to LWT zebrafish embryos and its effect on zebrafish embryo morbidity assessed. Ssp *polymorphum* was selected since it showed slightly increased pathogenicity in *in vitro* PECAM-1 abundance assays. Zebrafish embryo mortality was affected in a dose-dependent manner when analysed by Kaplan-Meier survival plots (Figure 5.3A). Injection with 2 X 10$^3$ CFU/mL *F. nucleatum* ssp *polymorphum* had significantly lower survival rates (66 ± 7 %; p = 0.027) when compared to PBS injected controls (87 ± 4 %) (Figure 5.3A). When zebrafish embryos were stratified into disease status, systemic injection with *F. nucleatum* ssp *polymorphum* at all concentrations tested resulted in a significant increase in the number of diseased (live + oedematous) zebrafish compared to PBS injected controls over a period of 72 hours ($p < 0.01$) (Figure 5.3B-D). Here, the numbers of zebrafish classified as diseased

increased in both a time- and dose-dependent manner. *F. nucleatum* ssp *polymorphum* injection resulted in marked cardiac and yolk oedema compared to PBS injected controls (Figure 5.3E).
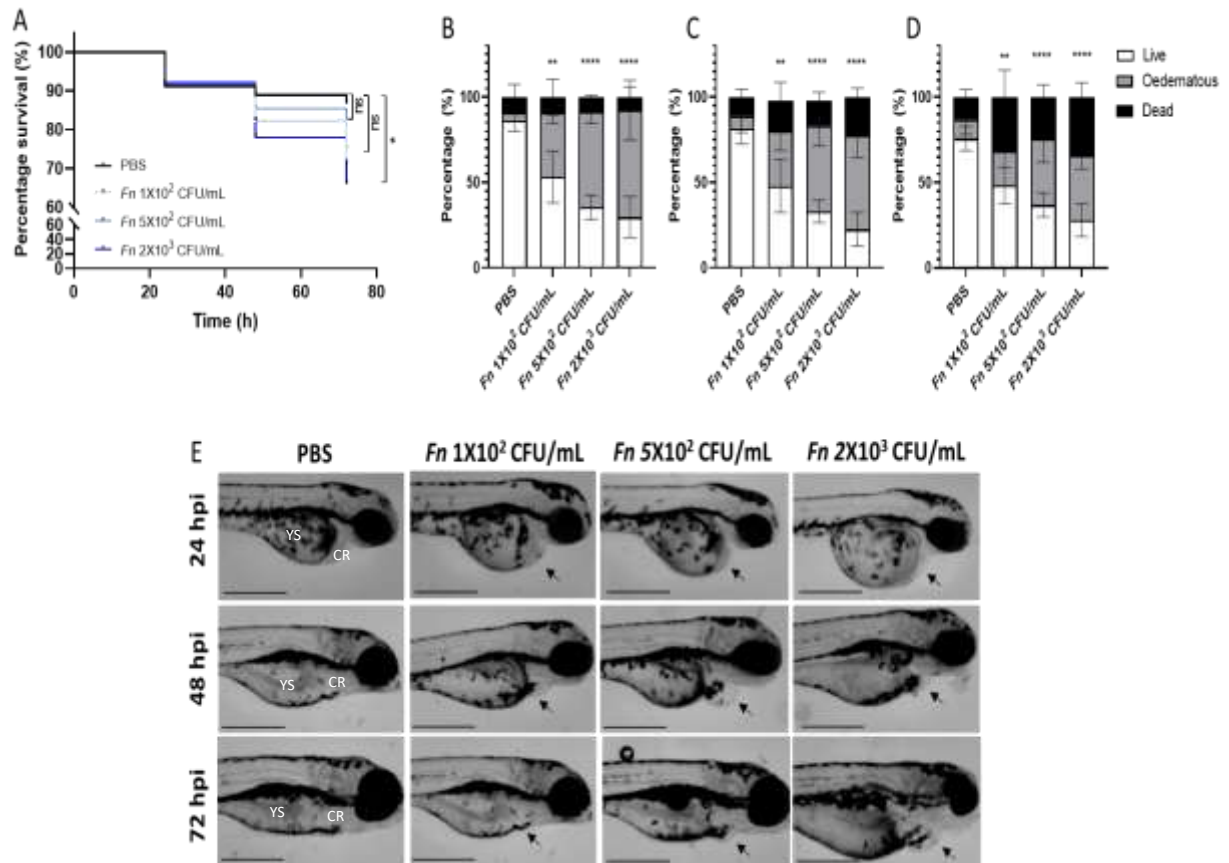


**Figure 5.3: *F. nucleatum* ssp *polymorphum* systemic injection in zebrafish embryo model increases morbidity.** (A) Kaplan-Meier survival plots of zebrafish larvae infected 30 hpf with phosphate-buffered saline (PBS) control or *F. nucleatum* (*Fn*) at $1 \times 10^2$, $5 \times 10^2$ or $2 \times 10^3$ CFU/mL. Comparison of survival curves using the log-rank test shows significant differences between $2 \times 10^3$ CFU/mL *Fn*–injected zebrafish compared to PBS controls at 72 hpi but no significant differences in survival at lower *F. nucleatum* concentrations. (B-D) Percentage healthy, oedematous and dead zebrafish larvae at (B) 24, (C) 48 and (D) 72 hpi showing that the percentage of diseased (oedematous + dead) zebrafish was significantly increased following systemic infection with *F. nucleatum* at all time points. Data are presented as mean ± SD of 4 independent experiments with a minimum of 9 embryos per group. (E) Representative micrographs showing the morphology of zebrafish larvae infected with PBS control, *Fn* $1 \times 10^2$ CFU/mL, *Fn* $5 \times 10^2$ CFU/ML or *Fn* $2 \times 10^3$ CFU/mL at 24, 48 and 72 hpi. *Fn*-infected zebrafish showed marked oedema around the yolk sac (YS) and cardiac region (CR) (black arrows). Scale bars = 500 μm. Statistical differences were analysed by one-way ANOVA with Tukey's multiple comparison test. *p < 0.05, **p < 0.01, ***p < 0.001, ****p < 0.0001.

The presence of intravascular *F. nucleatum* ssp *polymorphum* was confirmed following systemic injection of fluorescently-labelled bacteria into 72 hpf kdrl:mCherry transgenic zebrafish followed by confocal microscopy analysis 2 hpi. Injections were performed using an adaption of a previously used methodology to assess presence of *P. gingivalis* within the vasculature *in vivo* (Widziolek et al. 2016). Imaging at 2 hpi shows presence of *F. nucleatum*

ssp *polymorphum* in the cardiac and systemic vasculature by co-localisation with the endothelium (Figure 5.4A-D). This co-localisation is further highlighted by orthogonal views of the cardiac region in Figure 5.4 E-G.
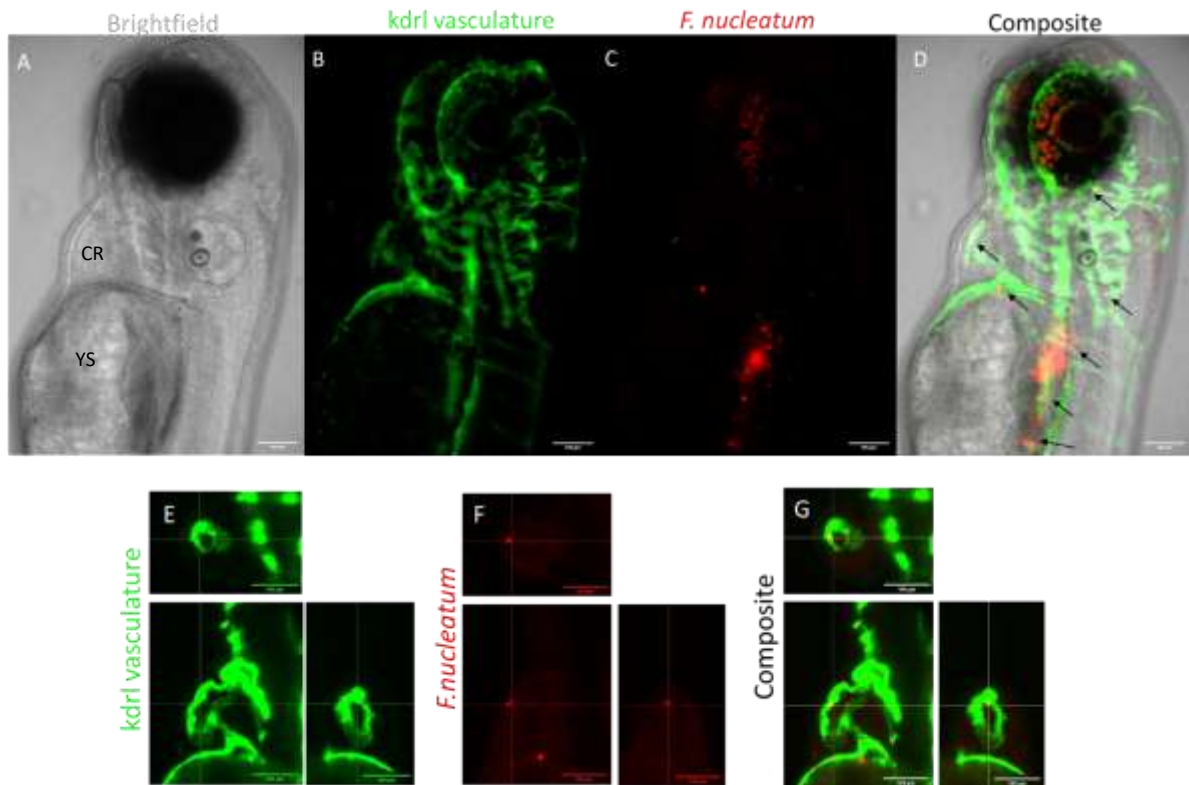


**Figure 5.4: *F. nucleatum* systemic dissemination in zebrafish embryo**. Representative images of Lightsheet (Zeiss) micrographs showing kdrl/vasculature (false coloured green) and *F. nucleatum* ssp *polymorphum* (false coloured red). $2X10^3$ CFU/mL (5(6)-FAM, SE) stained *F. nucleatum polymorphum* were systemically injected at 72 hpf in *kdrl:mcherry* zebrafish embryos and imaged 2 hpi. (A-D) Micrographs of embryo from head to the yolk region highlighting vascular infiltration of *F. nucleatum* (indicated by black arrows). Images A-D were generated using SUM Z-projection function on FIJI®. A-C show separate channels for (A) brightfield, (B) kdrl and (C) *F. nucleatum* respectively. While a composite image is shown in D. (E-G) Orthogonal views of cardiac region (E) vasculature, (F) *F. nucleatum* and (G) composite further highlight intravascular position of *F. nucleatum.* Scale bars: 100 μm. CR: Cardiac region. YS: Yolk sac.

### 5.4.3 *F. nucleatum* subspecies *polymorphum* decreases endothelial viability and PECAM-1 abundance in multispecies infection

For multispecies assessment planktonic *P. gingivalis* W83, *F. nucleatum* (subspecies nucleatum or polymorphum) and *T. forsythia* were used in triplicates at 1:1:1 ratios or pairs at 1:1 ratios at a total MOI of 100. No significant differences in HMEC-1 viability ($p > 0.05$) were observed in response to multispecies infection containing *F. nucleatum* subspecies *nucleatum* compared to control (Figure 5. 5A). In contrast, significant decreases in cell viability

were observed in response to infections that contained *F. nucleatum* subspecies *polymorphum* (p < 0.01) (5B) suggesting differences in the pathogenicity between the two subspecies.
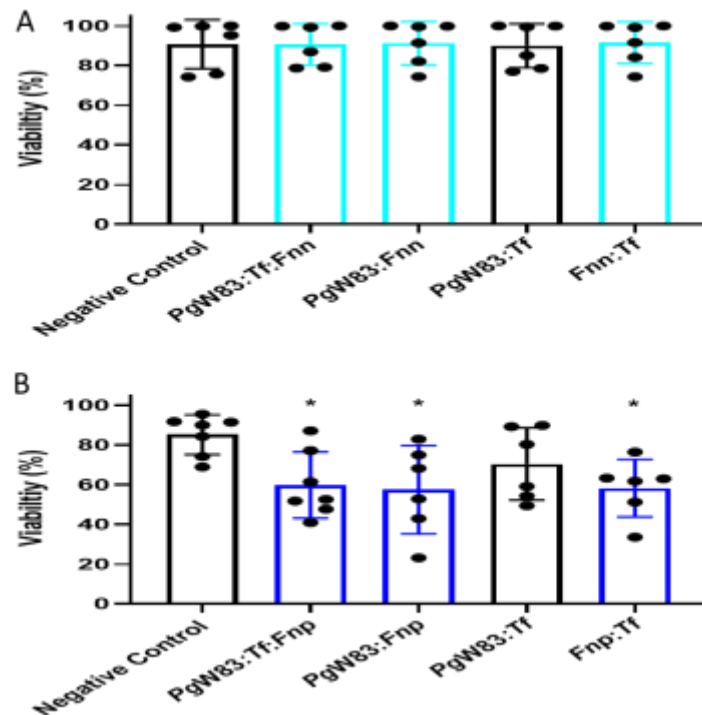


**Figure 5. 5: Viability of endothelial cells following multispecies infection.** HMEC-1 infected for 1.5 h with multispecies 1:1:1 mixes or 1:1 pairs of *P. gingivalis* (*Pg)* W83, (A) *F. nucleatum* ssp *nucleatum* (*Fnn*), (B) *F. nucleatum* ssp *polymorphum* (*Fnp*) or *T. forsythia* (*Tf* )ATCC 43037 at MOI100. Viability was determined by flow cytometry following To-pro-3 staining to identify the live cell portion. Endothelial cells infected with mixed bacteria containing (A) *Fnn* (light blue) did not result in significantly decreased viability when compared to the negative control. On the other hand those containing (B) *Fnp* (dark blue) resulted in significantly decreased viability. Enclosed circles represent data from each individual experiment. Statistical differences were analysed by one‐way ANOVA with Tukey's multiple comparison test. *p < 0.05

Although both *F. nucleatum* ssp *nucleatum* (Figure 5.6A) and *polymorphum* (Figure 5.6B) decreased PECAM-1 abundance when paired or in triplicate (ratio 1:1:1), this decrease was only statistically significant when the infection mixture contained *F. nucleatum* ssp polymorphum (p < 0.1). A statistically significant decrease in PECAM-1 abundance compared to uninfected control was also observed when this subspecies was paired with either *P. gingivalis* W83 (p < 0.05), *T. forsythia* (p < 0.001) or as part of a triplicate 1:1:1 multispecies infection (p < 0.05) (Figure 5.6B). Mixed infection using planktonic *P. gingivalis* W83 and *T.*

*forsythia* pairs (1:1 ratio, total MOI100) significantly decreased PECAM-1 cell surface abundance (p < 0.05; Figure 5.6).
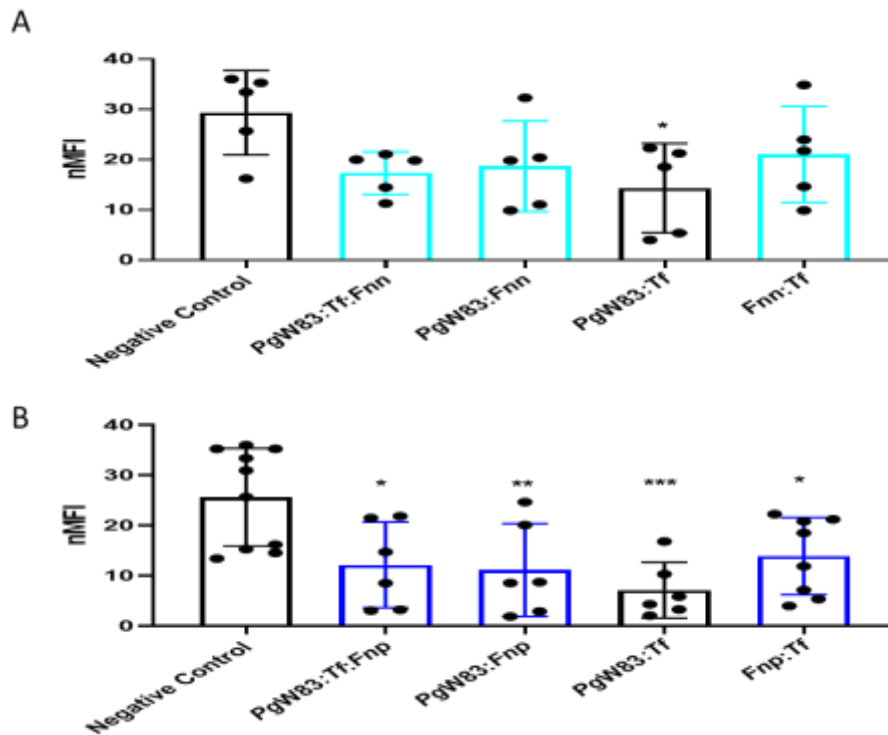


**Figure 5.6**: **PECAM-1 abundance following multispecies infections.** (A-B) HMEC-1 were infected with *P. gingivalis* (*Pg)* W83, (A) *F. nucleatum* ssp *nucleatum* (*Fnn*), (B) *F. nucleatum* ssp *polymorphum* (*Fnp*) or *T. forsythia* (*Tf*) multispecies mixed in 1:1 pairs or 1:1:1 triplicates at MOI100. Normalised median fluorescence intensity (nMFI) histograms of PECAM-1 determined by flow cytometry following live-cell selection show a significant decrease compared to the negative control after all single and multispecies 1.5 hour infections containing (B) *Fnp* (dark blue) but not in infections containing (A) *Fnn* (light blue). Enclosed circles represent data from each individual experiment. Statistical differences were analysed by one‐way ANOVA with Tukey's multiple comparison test. *p < 0.05, **p < 0.01, ***p < 0.001, ****p < 0.0001.

## 5.4.4 PECAM-1 and permeability changes are independent of gingipains in mixed culture infections

Since *P. gingivalis* gingipain played a significant role in PECAM-1 reduction in single species infections its potential role in multispecies infections was investigated. The ability of *P. gingivalis* to cleave PECAM-1 in a gingipain-dependent manner in multispecies infections was assessed when *P. gingivalis* (W83 in red or ΔK/R-ab) was mixed with *F. nucleatum* ssp *polymorphum.* Flow cytometry analysis showed a significant decrease (p < 0.05) in PECAM-1 cell surface abundance in all mixed species infections containing *F. nucleatum* ssp *polymorphum,* even in the absence of gingipains (ΔK/R-ab) (Figure 5.7A). In addition, both

triplicate (Figure 5.7B) and pair mixed species infections increased HMEC-1 permeability independent of the presence of *P. gingivalis* gingipain (Figure 5.7C). Interestingly even though *P. gingivalis* and *T. forsythia* pairs were shown to decrease PECAM-1 abundance this pair did not significantly increase endothelial permeability (Figure 5.7C). *F. nucleatum* ssp *polymorphum* was also found to decrease HMEC-1 viability when mixed with ΔK/R-ab (p < 0.001) (data not shown).
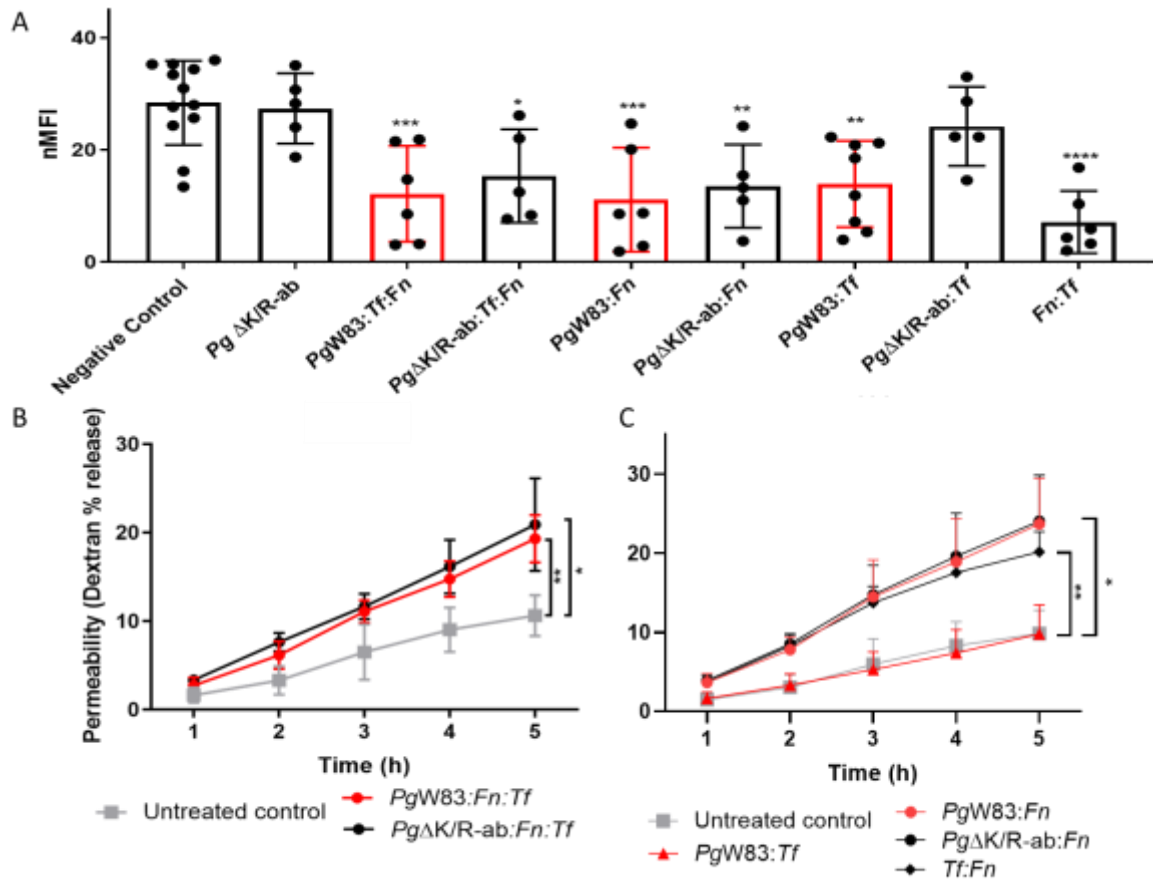


**Figure 5.7: PECAM-1 abundance and permeability of HMEC-1 is independent of gingipain in multispecies infections.** (A) PECAM-1 cell surface abundance decreased on viable HMEC-1 treated with both *P. gingivalis* (*Pg*) W83 (red) and *P. gingivalis* (*Pg*) ΔK/R-ab (black) pairs and triplicate multispecies mixes containing *F. nucleatum* (*Fn*) ssp *polymorphum*. Data are presented as mean ± SD normalized median fluorescence index (nMFI) with enclosed circles representing independent experiments. (B) A significant increase in permeability of HMEC-1 was observed after treatment with triplicates containing *P. gingivalis* W83 (*Pg*W83:*Fn*:*Tf*, red) and *P. gingivalis* gingipain null mutant (*Pg*ΔK/R-ab:*Fn*:*Tf*, black). (C) Similarly, permeability determined by dextran assay resulted in significantly increased permeability after infection with all pairs containing *F. nucleatum*, independent from gingipain/*Pg*W83 (red) presence. (B,C) Permeability data are presented as mean ± SD of 4 independent experiments. Statistical significance was determined by a 1-way analysis of variance with Tukey's post hoc multiple comparisons test. *p < 0.05, **p < 0.01, ***p < 0.001, ****p< 0.0001.

## 5.4.5 Altered pathogenic effects on PECAM-1 abundance after *in vitro* multispecies interactions

*F. nucleatum species* facilitates adhesive interactions between itself and other microorganisms to form bacterial aggregates that may affect virulence (Brennan and Garrett 2019). Multispecies bacteria (*P. gingivalis* W83/ΔK/R-ab, *F. nucleatum species and/*or *T. f*orsythia) were therefore incubated for 1 hour in anaerobic conditions to allow bacteria to aggregate. Infection of endothelial cells with aggregates was then compared to those using planktonic grown bacteria. Scanning electron micrographs confirmed the presence of bacteria with different morphologies that one could tentatively assign to different species within the bacterial aggregate (Figure 5.8A-D). Viable HMEC-1 showed no difference in PECAM-1 cell surface abundance after infection with both mixed species planktonic infection compared to mixed species aggregates when *F. nucleatum* subspecies *nucleatum* was used (p > 0.42) when compared to the negative control. In contrast, a significant decrease in PECAM-1 abundance was observed when *P. gingivalis* (W83 and ΔK/R-ab)*, T. f*orsythia and *F. nucleatum* subspecies *polymorphum* were allowed to interact prior to infection (*Pg*W83*:Tf:Fn* or *Pg*K*:Tf:Fn*; p < 0.05) when compared to the uninfected control. Although no statistically significant differences in PECAM-1 abundance were identified between planktonic and 1 hour adhered mixes, these results anyway highlight how potential periodontal pathogen interactions could result in altered vascular pathogenicity.
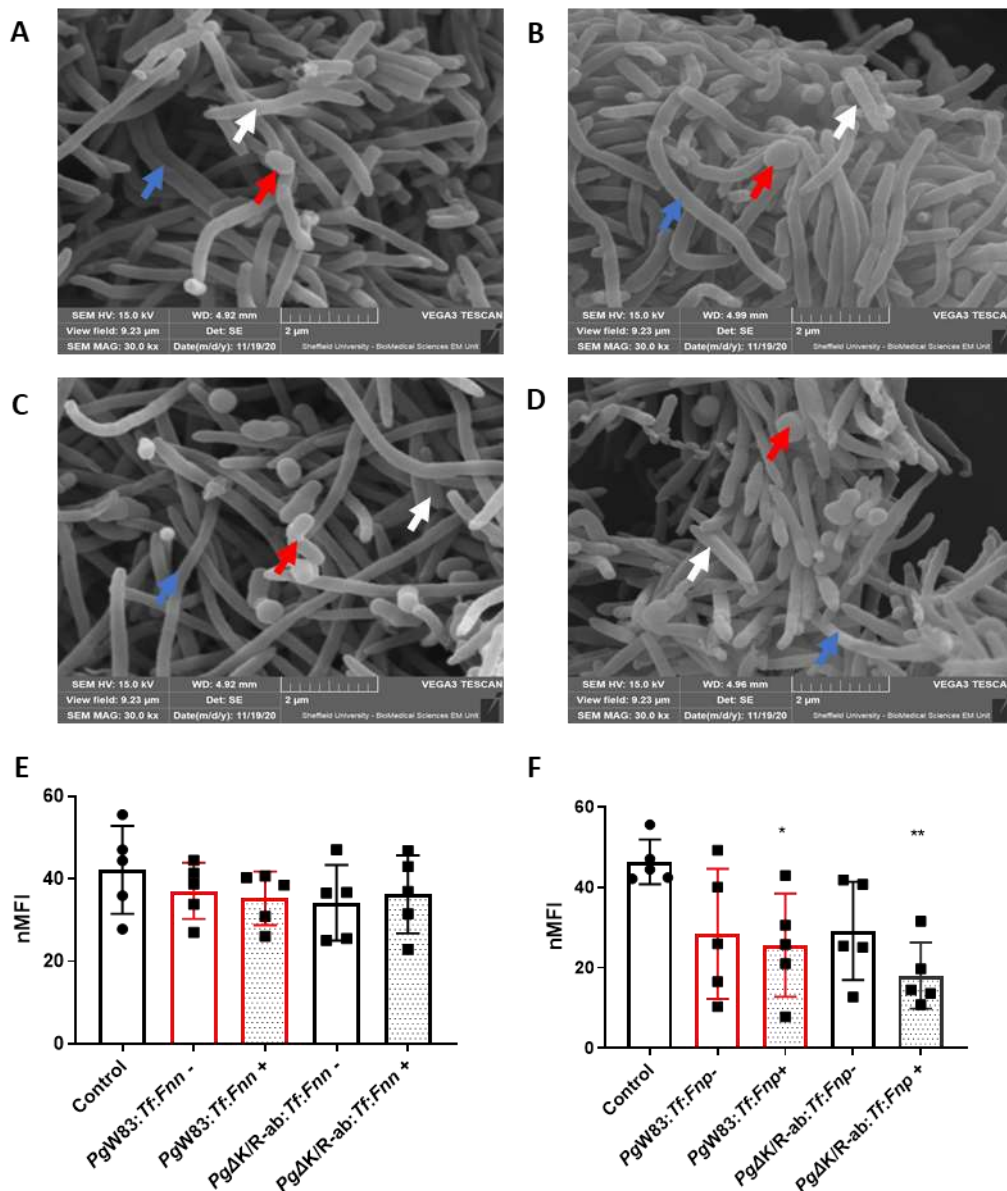
**Figure 5.8:** *In vitro* **multispecies interactions**. *P. gingivalis* (*Pg)* W83/ΔK/R-ab, *F. nucleatum* ssp *nucleatum/polymorphum* (*Fnn*/*Fnp*) *and T. forsythia* (*Tf)* at MOI 33.3 each were prepared and either allowed to interact in triplicates or left in separate sterile eppendorfs for 1 hour in anaerobic conditions. After which cultures were centrifuged and used for triplicate infections of HMEC-1 at total MOI100 for 1 hour. (A-D) Representative electron micrographs showing cultures of (A) *Pg*W83:*Fnn*:*Tf*, (B) *Pg*W83:*Fn*p:*Tf,* (C) *Pg*ΔK/R-ab:*Fnn*:*Tf* and (D) *Pg*ΔK/R-ab:*Fn*p:*Tf* after 1 hour anaerobic interactions. (A-D) Micrographs show presence of multiple morphologies suggesting multiple species, highlighted by arrows of different colours, red, blue and white. (E&F) nMFI histograms show no significant differences in viable PECAM-1 abundance in all triplicates containing (E) *F. nucleatum* ssp *nucleatum* (*Fnn*)*.* (F) On the other hand multispecies triplicates containing *F. nucleatum* ssp *polymorphum* (*Fnp*) allowed to adhere for 1 hour in anaerobic conditions containing *Pg*W83 (red dotted histogram, *Pg*W83:*Tf*:*Fnp* +) or *Pg*ΔK/R-ab (black dotted histogram, *Pg*ΔK/R-ab:*Tf*:*Fnp* +) resulted in significantly decreased PECAM-1 of viable HMEC-1 cells infected for 1.5 h when compared to the uninfected control. n = 5. Statistical differences were analysed by one‑way ANOVA with Tukey's multiple comparison test. *p < 0.05, **p < 0.01.

## 5.4.6 Multispecies periodontal pathogen systemic infection *in vivo*

The *in vitro* data has highlighted the importance of examining multispecies pathogen interactions when assessing how periodontal pathogens interact with the vasculature. Nonetheless, to date, data on multispecies behaviour and vascular interaction *in vivo* is lacking. Therefore, fluorescently labelled *P. gingivalis* W83, *F. nucleatum* ssp *polymorphum* and *T. forsythia* mixed planktonic cultures were systemically injected in Nacre zebrafish embryos to assess their behaviour real-time *in vivo* (Figure 5.9A-H). All three periodontal pathogens disseminated systemically at 2 hpi and representative micrographs show that while some bacteria disseminate around the vasculature as single species, others are in close proximity to other periodontal pathogen species, suggesting aggregate formation within the vessels occurs *in vivo* or that there is co-localised infection at the endothelial surface (Figure 5.9).
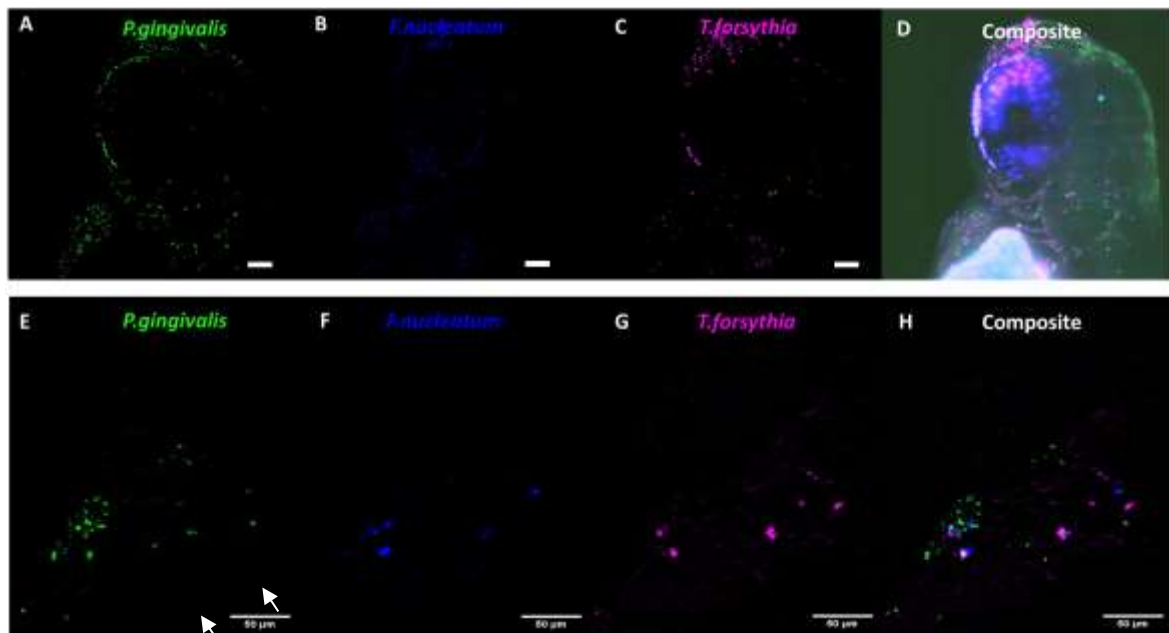


**Figure 5.9: Multispecies dissemination of periodontal pathogens *in vivo*.** (A-H) Maximum intensity projections generated 2 hpi of Nacre zebrafish embryo. 48 hpf zebrafish embryos were injected with a multispecies culture of 5(6)-FAM, SE -stained *P. gingivalis* W83 (green), Cell Tracker® CMPTX-stained *F. nucleatum* ssp *polymorphum* (false coloured blue) and Cell Tracker® Deep Red-stained *T. forsythia* (false coloured magenta) in the duct of Cauvier at 2X10$^3$ total CFU/mL. (A-D) Fluorescence micrographs show systemic dissemination of all 3 species in (A) composite and as separate channels with a background reduction of 50 corresponding to (B) *P. gingivalis*, (C) *F. nucleatum* polymorphum and (D) *T. forsythia*. (E-H) Maximum intensity projections with 50 background reduction micrographs at higher magnification in cardiac region of zebrafish embryo. (E) In the composite micrograph white arrows highlight colocalization of different species. (F-H) Separate channel micrographs further illustrate distribution of (F) *P. gingvalis,* (G) *F. nucleatum* ssp *polymorphum* and (H) *T. forsythia.*

## 5.5    DISCUSSION

Chronic periodontitis leads to entry of bacteria and/or their virulence factors into the bloodstream.  This can cause vascular damage partly through host inflammatory response mechanisms that may potentiate atheromatous lesion formation, maturation and exacerbation (Tonetti et al. 2013, Reyes et al. 2013b, Schenkein et al. 2020). Numerous oral microorganisms or their RNA/DNA have been identified in atherosclerotic plaques (Chiu 1999, Schenkein et al. 2020, Serra e Silva Filho et al. 2014). Most studies have concentrated on examining *P. gingivalis,* a keystone pathogen of periodontal disease (Hajishengallis et al. 2012) because it is the most abundant species found in coronary and femoral arteries (Mougeot et al. 2017b) and increases morbidity and mortality of zebrafish embryos in a gingipain-dependent manner after systemic injection (Widziolek et al. 2016). *P. gingivalis* produces the virulence factor gingipains; proteases that are capable of cleaving host proteins to sequester nutrients for growth (Hočevar et al. 2018). However, these proteins also mediate cell surface protein and extracellular matrix degradation, leading to loss of cellular and tissue integrity (Tada et al. 2003, Yun et al. 2005, Ruggiero et al. 2013). *F. nucleatum* and *T. forsythia* are known periodontal pathogens that can invade host cells and have also been identified in the vasculature (Reyes et al. 2013b), but their interaction with the endothelium is seldom studied. Moreover, periodontitis is a polymicrobial disease, yet infection experiments using more than one bacterial species are rarely performed.

The single species infection data for *P. gingivalis* provided in this chapter mirrors other studies and the data in Chapters 3 and 4, suggesting a gingipain-dependent reduction of PECAM-1 and concurrent increased endothelial permeability (Widziolek et al. 2016). Single species infection with *F. nucleatum* in particular subspecies *polymorphum*, resulted in similar endothelial damage to that observed by *P. gingivalis* W83. Like *P. gingivalis, F. nucleatum* is capable of living in hostile environments populated by immune cells (de Andrade, Almeida-da-Silva and Coutinho-Silva 2019) and although *F. nucleatum* does not produce gingipains, it produces several virulence factors including serine proteases such as fusolin that may cleave host cell proteins (Doron et al. 2014, Bachrach et al. 2004). Reduced cell surface PECAM-1 abundance, enhanced pro-inflammatory changes and suppressed endothelial cell proliferation have been reported following *F. nucleatum* ssp *nucleatum* infection of HUVEC (Mendes et al. 2016) suggesting that this bacterium may require longer infection times to decrease PEACAM-1

abundance. Since infections in this research were carried out at MOI 100 after a minimum of 4 hour and maximum of 24 hour infections (Mendes et al. 2016). *F. nucleatum* ssp *polymorphum* systemic infection resulted in a dose-dependent increase in zebrafish embryo mortality with increased cardiac and yolk oedema in zebrafish embryos at a CFU/mL lower than previously reported for W83 *P. gingivalis* in Chapter 4 (Farrugia, Stafford and Murdoch 2020a, Widziolek et al. 2016), suggesting increased virulence *in vivo*.    Infection with *T. forsythia* resulted in no changes in PECAM-1 abundance or endothelial cell permeability *in vitro*. In mice, *T. forsythia* increased expression inflammatory modulators but did not increase atherosclerotic lesion size (Chukkapalli et al. 2015b), suggesting that this periodontal bacterium has a limited role in cardiovascular disease.

Lack of polymicrobial research in the area and animal studies highlighting differing pathogenic effects from single species infection, led to further investigation on whether endothelial PECAM-1 and permeability are also affected when challenged with multi-species infections. *P. gingivalis* is generally found associated with other organisms such as *T. forsythia* and *T. denticola* (Yao et al. 1996) while *F. nucleatum* infections tend to involve multiple species (Jung, Jun and Choi 2017, Han 2015). *F. nucleatum* is known for its ability to produce outer membrane proteins including RadD arginine-inhibitable adhesins that are essential for interspecies adherence and multispecies biofilm formation (Kaplan et al. 2009). Investigation of their pathogenic affects when interacting with other species is therefore important. *F. nucleatum* was previously shown to enhance the invasion of *P. gingivalis* into gingival keratinocytes and aortic endothelial cells (Saito et al. 2008a). In contrast, another study showed that *P. gingivalis* suppressed invasion of *F. nucleatum* into gingival keratinocytes, with gingipain-mediated inactivation of the PI3K/AKT signalling pathway suggested as a contributing factor (Jung et al. 2017).

Data presented for polymicrobial infections in this chapter highlighted differences in the virulence between *F. nucleatum* ssp *nucleatum* and *polymorphum*. A significant decrease in PECAM-1 abundance and HMEC-1 viability were only identified in the presence of ssp *polymorphum* not ssp *nucleatum*, suggesting that these two subspecies may have different or varying amounts of virulence factors. Although proteases have been identified in both subspecies, the proteolytic band sizes varied between ssp (Doron et al. 2014) and this difference may be the contributing factor between how these species interact with the

endothelium, either as single species infections or when coupled with other periodontal organisms. For example, when *F. nucleatum* ssp *polymorphum* was used in mixed species infections this significantly increased or maintained virulence with *P. gingivalis* and *T. forsythia*, whereas *T. forsythia* was not virulent alone, highlighting the role of multispecies interactions. Synergistic effects between *P. gingivalis* and *F. nucleatum* have been previously documented *in vitro* as well as *in vivo*, mainly in the context of periodontal pathogenesis (Sharma et al. 2005, Settem et al. 2012, Honma, Ruscitto and Sharma 2018). Sharma et al. 2005 showed that coaggregations of these two microorganisms form stronger biofilms when compared to single species biofilms and this was partially attributed to *T. forsythia*'s BspA protein. Contrastingly this study also found that even though BspA is important for coaggregation, synergistic biofilms of *T. forythia* and *F. nucleatum* were independent of BspA (Sharma et al. 2005). *F. nucleatum* produces outer-membrane proteins including RadD (Kaplan et al. 2009), FadA (Han et al. 2005) and species-specific LPS (Martinho et al. 2016, Vinogradov et al. 2017b, Vinogradov et al. 2017a). Some of these factors are essential for interspecies adherence and multispecies biofilm formation (Kaplan et al. 2009) and RadD has also been shown to induce lymphocyte cell death (Kaplan et al. 2010, Kaplan et al. 2009). It is possible that the outer-membrane architecture of *F. nucleatum* might contribute to enhanced multispecies bacterial and vascular interactions, increasing vascular damage. Zebrafish embryo systemic infection showed that the multispecies interactions, which were observed *in vitro* also occurred in the vasculature *in vivo*, further validating the need for further research on effects of multispecies periodontal pathogen interactions on the vasculature.

PECAM-1 reduction and increased permeability in HMEC-1 following polymicrobial infection is not entirely gingipain-dependent since these changes were also observed in polymicrobial infections using the gingipain-null mutant in combination with *F. nucleatum* ssp *polymorphum*. Similar gingipain-independent observations were previously shown in polymicrobial culture growth, where it was observed that gingipain was not necessary for multispecies biofilm formation (Bao et al. 2014). But to date there are no studies showing the effects of gingipains on PECAM-1 in polymicrobial infections. Since changes appear to be mediated by *F. nucleatum* ssp *polymorphum*, this microorganism's virulence factors might play a greater role than the gingipains. *P. gingivalis* has been claimed to guide *F. nucleatum* spp *nucleatum* to a paracellular pathway (Jung et al. 2017) potentially suggesting  a potential reason why mixed infections of *P. gingivalis* and *F. nucleatum* showed no synergistic effects.

It is possible that *F. nucleatum* RadD (Kaplan et al. 2009) alter *P. gingivalis* gingipains, in turn reducing its virulence or that the proteases secreted by one of these bacteria may degrade virulence factors of the other or visa versa. Emerging research also shows that the LPS structure varies between different *F. nucleatum* spp and that this might also contribute to varying virulence (Vinogradov et al. 2017b, Cairns et al. 2020, Vinogradov, St Michael and Cox 2018a, Vinogradov et al. 2017c, Vinogradov, St Michael and Cox 2018b).

It is clear that the interplay between periodontal pathogens even in this simple model of polymicrobial is complex, given that periodontal plaque contains tens of different species of bacteria, unravelling these host-pathogen interactions will be challenging.

## 5.6    SUMMARY

These novel data demonstrate that *F. nucleatum*, similar to *P. gingivalis,* may play a pivotal role in disrupting the vasculature. In these data *F. nucleatum* ssp *polymorphum* was also shown to be virulent in polymicrobial infections and more so, after allowing cultures to aggregate in an anaerobic environment. Highlighting not only the importance of subspecies investigation and polymicrobial research, but also the consideration of interspecies interactions when assessing periodontal pathogen effects on the vasculature. To our knowledge this data also shows the first documented multispecies periodontal pathogen systemic injection in a zebrafish embryo model, with potential for development for the study multispecies interactions *in vivo* real-time investigation.

# CHAPTER 6: DISCUSSION AND FUTURE PROSPECTS

## 6.1  SUMMARY OF MAJOR FINDINGS

Although several studies have shown an association between periodontitis and cardiovascular disease, the biological mechanisms that may link these two conditions are still highly debated (Herrera et al. 2020, Schenkein et al. 2020). Chapter 3 of this thesis identified a mechanism by which gingipains, potent protease virulence factors of *P. gingivalis* (Hočevar et al. 2018), directly contribute to vascular damage by affecting the cell surface abundance of adhesion molecules PECAM-1 and VE-cadherin both *in vitro* and *in vivo*. The *in vivo* zebrafish embryo infection model allowed for real-time imaging and analysis of interactions between *P. gingivalis* W83 and its non-gingipain producing mutant with vascular PECAM-1 and VE-cadherin.

Chapter 4 examined the ability of *P. gingivalis* to produce OMV, another known virulence factor of this periodontal pathogen (Xie 2015). The data presented in this chapter not only confirmed previous studies reporting the presence of gingipains on *P. gingivalis* OMV (Naylor et al. 2017, Aduse-Opoku et al. 2006, Curtis et al. 1999), but also showed that these vesicles can also independently increase endothelium permeability, decrease PECAM-1 abundance and increase morbidity and mortality in zebrafish embryos in a gingipain-dependent manner. These data underscore the potential widespread effects of gingipains on the systemic vasculature through OMV dissemination.

Periodontitis is a polymicrobial disease therefore Chapter 5 aimed to assess whether other commonly identified periodontal pathogens (*F. nucleatum* and *T. forsythia*) could also affect endothelial cells when infected alone or in combination. These resulting data showed that *F. nucleatum* mediated effects similar to that of *P. gingivalis in vitro,* whereas infection with *T. forsythia* did not. *In vivo F. nucleatum* infection resulted in morbidity at lower concentrations than previously reported with *P. gingivalis* (Widziolek et al. 2016), suggesting the potential overlooked importance of this organisms role in the perio-vascular link. This was highlighted in the multispecies infection data, which showed that *F. nucleatum* could also reduce PECAM-

1 cell surface abundance, emphasising the importance and need for additional investigations on multispecies periodontal pathogen vascular interactions.

## 6.2   FUTURE WORK AND LIMITATIONS

### 6.2.1  *P. gingivalis* gingipains effects on cell adhesion molecules

The pathogenic role of *P. gingivalis* gingipains has been a topic of interest in the literature due to its wide range of pathogenic effects. These proteases have not only been attributed towards *P. gingivalis'* role in the shift from gingivitis to periodontitis in the oral cavity (Hajishengallis et al. 2012), but have several other disease states (Yun et al. 2005, Dominy et al. 2019). The data in this thesis also point to the important role of gingipains in CVD. Gingipain inhibitors have been proposed as potential treatments for periodontitis (Olsen and Potempa 2014). Given the findings of this thesis there is potential feasibility of using gingipain inhibitors as treatment strategies for systemic diseases associated with periodontitis. It would be of interest to assess whether inhibition of lysine or arginine gingipains, or both could reverse *P. gingivalis*-mediated cell adhesion molecule abundance or prevent endothelium permeability *in vivo* after single species infections as well as multispecies infections. Some gingipain mutants are also known to have altered fimbriae maturation (Shoji et al. 2004, Lee et al. 2018) and therefore further research is warranted here as this may have implications for protease inhibitor therapies.

PECAM-1 is not only expressed on endothelial cells, it is also found on the surfaces of neutrophils, monocytes, some T cell subsets and on platelets (Muller 1995). During this study the effects of periodontal pathogen infection on cells other than of endothelial origin was not examined and to our knowledge there is no published data on gingipain-mediated damage to leukocyte and platelet-bound PECAM-1 and whether this proteolytic mechanism could also be a contributor towards periodontal pathogen-mediated systemic effects to the vasculature. If gingipains do also affect leukocyte and platelet-bound PECAM-1 it could be speculated that this mechanism might play a more widespread role, especially since gingipains can also be disseminated systemically via OMV, independently from *P. gingivalis* whole cell infection. Studies suggest that decreased PECAM-1 abundance results in decreased angiogenesis and increased foreign body inflammation (Solowiej et al. 2003) which might provide another

pathway for propagation of cardiovascular effects. PECAM-1 plays multiple roles in inflammation and vascular biology and its complex functions continue to be studied (Woodfin, Voisin and Nourshargh 2007). Therefore, studying oral pathogen mediated PECAM-1 damage in a complex model (3D or *in* vivo) rather than single monolayers would be more beneficial to truly grasp extent of this mechanism.

## 6.2.2 Role of OMV in pathogenesis following systemic dissemination

While this work provided previously unreported insight on how *P. gingivalis* OMV can independently exert pathogenic effects on the vasculature, further research is required in this niche area. Determining the amount of OMV required to exert their vascular effects on larger animal models would provide a better perspective on how many OMV are required systemically to trigger or potentiate atherosclerotic events. This will not only be valuable to study the feasibility of the proposed mechanism, but also since *P. gingivalis* OMV have been proposed as a possible candidate for mucosal immunogen and adjuvant for a periodontitis vaccine, where *P. gingivalis* OMV may have unforeseen adverse effects (Nakao et al. 2016). In a 2005 study it was reported that sera from patients with generalised aggressive periodontitis (i.e. Stage 3 or 4, Grade C periodontitis) had elevated levels of gingipain-specific IgG (Gibson et al. 2005). It would also be of interest to assess whether presence of virulence factors such as gingipain or OMV in patient sera can be correlated with increased cardiovascular risk. Correlation between *P. gingivalis* gingipain specific IgG and cardiovascular risk or severity would suggest a potential new way of screening for cardiovascular risk.

In this study the role of gingipains in OMV and its role in vascular damage was the focus of the study. Although this provided novel knowledge to an emerging field it is important to note that several other virulence factors are transported on *P. gingivalis* OMV and that other Gram-negative periodontal pathogens are known to produce OMV (Cecil et al. 2016). Looking in the virulence potential of OMV generated from different *P. gingivalis* strains and different periodontal pathogens such as *F. nucleatum*, as well as differences in OMV virulence when generated in multispecies interactions might provide more clinically relevant insight on this virulence factor's role. Most research in the area focuses on *P. gingivalis* OMV and their role in periodontal disease, with very little data on the role of a wide range of periodontal pathogen OMV virulence factors and their potential role in the perio-systemic link.

With the advent of ever-growing microscopy techniques such as high resolution wide-field microscopy (Kner et al. 2010) it might be possible to track OMV in a zebrafish embryo *in vivo* model and assess how OMV are transported in the vasculature which will provide insight on how truly wide-spread their effects are *in vivo* and whether they preferentially accumulate in distinct areas.

## 6.2.3 Multispecies periodontal pathogen interaction with the vasculature

A recent study has shown that *P. gingivalis* can also compromise endothelial integrity through induction of endothelial mesenchymal transformation and endothelial apoptosis. *Pg*-induced effects on TLR-NF-κB signalling were reversed through the use of a TLR antagonist or NF-κB signalling inhibitor (Tovar-Lopez et al. 2019). Given that this thesis' data showed decreased viability after *F. nucleatum* single (spp *nucleatum* and *polymorphum*) and multispecies infections (spp *polymorphum*), it would be interesting to look into the possibility of *F. nucleatum*'s effects on TLR-NF-κB signalling pathway and whether such antagonists could also reverse intercellular damage *in vitro* and *in vivo.* Such an investigation would highlight potential treatment approaches that target mechanisms against multiple periodontal pathogens, which is more likely to be the clinical scenario and therefore more translatable.

Even in the limited mixed species experiments presented in this thesis, differences in pathogenicity were observed when different subspecies were used (2 *F. nucleatum* ssps used), as well as differences in the significance of virulence factors between single species and multispecies infections. This highlighted the importance of studying the differences in virulence factors between *F. nucleatum* ssps and more importantly multispecies interactions with the vasculature, an area that is seldom researched. Studying multispecies periodontal pathogen behaviour *in vitro* as well as *in vivo* models will provide further clues towards a better understanding on how periodontal pathogens from the periodontal pocket travel to the vasculature, elicit effects further away from the original site and which interactions might be playing a part in mediating endothelial damage. Further research on bacterial DNA in the human vasculature could shed light on the limited knowledge currently available.  This can be done by integrating the use of current genome sequencing advances, such as Oxford Nanopore, which  are making genomic investigations more accessible and reliable than ever before (van Heyningen 2019).

A recent review published stated that there was still a lack of evidence that periodontal bacteria obtained from human atheromas can cause atherosclerosis in animal models (Herrera et al. 2020). This could be due to periodontal pathogens being extremely fastidious and can therefore lose their pathogenicity during the transfer from atheroma to reuse in animal models or else it could also be due to the disruption of potential multispecies interactions during the process. It therefore would be of interest to further develop the zebrafish larvae model proposed in the final results chapter of this thesis to visualise and quantify interaction/colocalization of different periodontal pathogens in an *in vivo* environment. Such an investigation would provide much needed insight on the behaviour of different periodontal pathogens once they are systemically disseminated and therefore provide direction as to where to focus *in vitro* multispecies investigations *in vivo*.

## 6.2.4 Models used to study role of periodontal pathogens in the oral systemic link

Two main research models have been used throughout this work: endothelial monolayers for *in vitro* assessments and zebrafish larvae for *in vivo* assessments.

While the simplistic endothelial monolayer allows for focused investigation of possible mechanistic contributors towards endothelial damage, the model lacks complexity that is synonymous with this area. An important missing feature from this model is the lack of flow. Blood flow is known to contribute to physical stress to the endothelium, which in turn plays a significant role in maintaining vascular integrity and homeostasis (Tovar-Lopez et al. 2019). Flow has also been shown to affect *Staphylococcus aureus* adhesion to the vessel wall (Claes et al. 2015), but to date to our knowledge there are no studies assessing whether different flow rates can also alter periodontal pathogen vascular attachment or pathogenicity. Current efforts to implement the 3Rs (replacement, reduction and refinement) are resulting in advances in various technologies which can deliver faster, more reproducible and more cost-effective results (MacArthur Clark 2018). One such area is the implementation of microfluidic models which are used to assess flow changes or disruptions to the endothelium (Tovar-Lopez et al. 2019) for assessment of periodontal pathogen vascular interactions. Preliminary studies

using an *in vitro* flow system were performed in this study but were dropped due to time constraints. Development of such models would provide better *in vitro* insight of true mechanisms in a more clinically relevant environment.

While zebrafish embryo models provide a platform for assessment of real-time cellular effects of periodontal pathogens and are extremely beneficial for studying mechanisms, it would be beneficial to translate this work's findings to longer term models, models with excess lipids and into higher animal models, such as murine models which are more frequently used to study the link between periodontal disease and cardiovascular disease (Gibson et al. 2004, Xuan et al. 2017, Chukkapalli et al. 2015a, Chukkapalli et al. 2015c, Chukkapalli et al. 2014). This would therefore allow direct comparisons of our findings to previously documented methods found in the literature.

## 6.3    RESEARCH IMPACT AND INNOVATION

The findings resulting from this PhD have significantly contributed to current knowledge on the molecular mechanisms involved in periodontal pathogen (*P. gingivalis, F. nucleatum, T. forsythia)* single and multispecies vascular interactions. The findings have not only proposed a possible mechanism through which periodontal pathogens can damage the vasculature, but also contributed towards development of zebrafish embryo infection models to study this complex question in real-time, a feature lacking in other models currently used.

To date, the data in this thesis has resulted in the publication of two peer-reviewed original articles (appended to this document) in FEBS Journal and the Journal of Dental Research respectively (Farrugia et al. 2020a, Farrugia et al. 2020b). The former publication was followed by a commentary in the same journal written by Prof. George Hajishengallis, a world-leading expert in the field, dedicated to the findings of the paper (Hajishengallis 2020).  In addition, this work has been presented to various audiences and through oral and poster presentations at several conferences organised by key leaders in the field, including the British Society of Oral and Dental Research (BSODR) and the British Society of Periodontology and Implant Dentistry (BSP). This presentation resulted in the award of the Senior Colgate Research Prize and the Sir Wilfred Fish Research Prize by the BSODR and BSP respectively. The highlighted

achievements further emphasize the impact of the findings, as well as the need for further investigation into this complex biological process.

## 6.4    CONCLUSIONS

As the importance and complexity of the oral systemic link continues to unravel through scientific findings, dentistry as a profession, and periodontology in particular, are moving towards a more personalised approach in patient care. Dental speciality societies are collaborating more than ever with other scientific disciplines and research on what measures can be integrated in the dental practice to fast-track early detection and referral of systemic issues (Sanz et al. 2020, Montero et al. 2020, Yonel et al. 2020, Yonel and Sharma 2017). The more we understand the mechanisms through which such disease links exist the more we can strive towards developing treatments and interventions that will not only improve patients' oral health but also contribute to their overall wellbeing.

# REFERENCES

(2000) Parameter on plaque-induced gingivitis. American Academy of Periodontology. *J Periodontol,* 71**,** 851-2.

(2020) Perio & Cardio campaign highlights key messages. *Br Dent J,* 229**,** 408.

Aarabi, G., T. Zeller, H. Seedorf, D. R. Reissmann, G. Heydecke, A. S. Schaefer & U. Seedorf (2017) Genetic Susceptibility Contributing to Periodontal and Cardiovascular Disease. *J Dent Res,* 96**,** 610-617.

Aas, J. A., B. J. Paster, L. N. Stokes, I. Olsen & F. E. Dewhirst (2005) Defining the normal bacterial flora of the oral cavity. *J Clin Microbiol,* 43**,** 5721-32.

Abranches, J., L. Zeng, M. Belanger, P. H. Rodrigues, P. J. Simpson-Haidaris, D. Akin, W. A. Dunn, Jr., A. Progulske-Fox & R. A. Burne (2009) Invasion of human coronary artery endothelial cells by Streptococcus mutans OMZ175. *Oral Microbiology and Immunology,* 24**,** 141-145.

Abusrewil, S., J. L. Brown, C. D. Delaney, M. C. Butcher, R. Kean, D. Gamal, J. A. Scott, W. McLean & G. Ramage (2020) Filling the Void: An Optimized Polymicrobial Interkingdom Biofilm Model for Assessing Novel Antimicrobial Agents in Endodontic Infection. *Microorganisms,* 8.

Acharya, C., S. E. Sahingur & J. S. Bajaj (2017) Microbiota, cirrhosis, and the emerging oral-gut-liver axis. *Jci Insight,* 2.

Ades, E. W., F. J. Candal, R. A. Swerlick, V. G. George, S. Summers, D. C. Bosse & T. J. Lawley (1992) HMEC-1: establishment of an immortalized human microvascular endothelial cell line. *J Invest Dermatol,* 99**,** 683-90.

Aduse-Opoku, J., J. M. Slaney, A. Hashim, A. Gallagher, R. P. Gallagher, M. Rangarajan, K. Boutaga, M. L. Laine, A. J. Van Winkelhoff & M. A. Curtis (2006) Identification and characterization of the capsular polysaccharide (K-antigen) locus of Porphyromonas gingivalis. *Infect Immun,* 74**,** 449-60.

Aghajanian, A., E. S. Wittchen, M. J. Allingham, T. A. Garrett & K. Burridge (2008) Endothelial cell junctions and the regulation of vascular permeability and leukocyte transmigration. *J Thromb Haemost,* 6**,** 1453-60.

Aird, W. C. (2005) Spatial and temporal dynamics of the endothelium. *J Thromb Haemost,* 3**,** 1392-406.

--- (2006) Endothelial cell heterogeneity and atherosclerosis. *Curr Atheroscler Rep,* 8**,** 69-75.

--- (2012) Endothelial cell heterogeneity. *Cold Spring Harb Perspect Med,* 2**,** a006429.

Akinkugbe, A. A., C. L. Avery, A. S. Barritt, S. R. Cole, M. Lerch, J. Mayerle, S. Offenbacher, A. Petersmann, M. Nauck, H. Voelzke, G. D. Slade, G. Heiss, T. Kocher & B. Holtfreter (2017) Do Genetic Markers of Inflammation Modify the Relationship between Periodontitis and Nonalcoholic Fatty Liver Disease? Findings from the SHIP Study. *Journal of Dental Research,* 96**,** 1392-1399.

Ali, R. W., L. Martin, A. D. Haffajee & S. S. Socransky (1997) Detection of identical ribotypes of Porphyromonas gingivalis in patients residing in the United States, Sudan, Romania and Norway. *Oral Microbiol Immunol,* 12**,** 106-11.

Amar, S. & S. Leeman (2013) Periodontal innate immune mechanisms relevant to obesity. *Mol Oral Microbiol,* 28**,** 331-41.

Amar, S., S.-c. Wu & M. Madan (2009) Is Porphyromonas gingivalis Cell Invasion Required for Atherogenesis? Pharmacotherapeutic Implications. *Journal of Immunology,* 182**,** 1584-1592.

Anand, N., C. S C & M. N. Alam (2013) The malnutrition inflammation complex syndrome-the micsing factor in the perio-chronic kidney disease interlink. *Journal of clinical and diagnostic research : JCDR,* 7**,** 763-7.

Anbalagan, R., P. Srikanth, M. Mani, R. Barani, K. G. Seshadri & R. Janarthanan (2017) Next generation sequencing of oral microbiota in Type 2 diabetes mellitus prior to and after neem stick usage and correlation with serum monocyte chemoattractant-1. *Diabetes Research and Clinical Practice,* 130**,** 204-210.

Ando, K., S. Fukuhara, N. Izumi, H. Nakajima, H. Fukui, R. N. Kelsh & N. Mochizuki (2016) Clarification of mural cell coverage of vascular endothelial cells by live imaging of zebrafish. *Development,* 143**,** 1328-39.

Androsz-Kowalska, O., K. Jankowski, Z. Rymarczyk, J. Kowalski, P. Pruszczyk & R. Gorska (2013) Correlation between clinical parameters of periodontal disease and mean platelet volume in patients with coronary artery disease: a pilot study. *Kardiologia Polska,* 71**,** 600-605.

Ansbro, K., W. G. Wade & G. P. Stafford (2020) *Tannerella serpentiformis* sp. nov., isolated from the human mouth. *Int J Syst Evol Microbiol,* 70**,** 3749-3754.

Aoyama, N., J. I. Suzuki, N. Kobayashi, T. Hanatani, N. Ashigaki, A. Yoshida, Y. Shiheido, H. Sato, Y. Izumi & M. Isobe (2018) Increased Oral Porphyromonas gingivalis Prevalence in Cardiovascular Patients with Uncontrolled Diabetes Mellitus. *Int Heart J,* 59**,** 802-807.

Araújo, I. R., T. C. Ferrari, A. Teixeira-Carvalho, A. C. Campi-Azevedo, L. V. Rodrigues, M. H. Guimarães Júnior, T. L. Barros, C. L. Gelape, G. R. Sousa & M. C. Nunes (2015) Cytokine Signature in Infective Endocarditis. *PLoS One,* 10**,** e0133631.

Arendorf, T. M. & D. M. Walker (1979) Oral candidal populations in health and disease. *Br Dent J,* 147**,** 267-72.

Armingohar, Z., J. J. Jorgensen, A. K. Kristoffersen, E. Abesha-Belay & I. Olsen (2014) Bacteria and bacterial DNA in atherosclerotic plaque and aneurysmal wall biopsies from patients with and without periodontitis. *Journal of Oral Microbiology,* 6.

Armitage, G. C. (1999) Development of a classification system for periodontal diseases and conditions. *Ann Periodontol,* 4**,** 1-6.

Arvikar, S., H. Hasturk, K. Strle, D. Nguyen, M. B. Bolster, D. Collier, A. Kantarci & A. Steere (2017) The Oral Microbiome Is Altered in Patients with Rheumatoid Arthritis. *Arthritis & Rheumatology,* 69.

Assinger, A., E. Buchberger, M. Laky, A. Esfandeyari, C. Brostjan & I. Volf (2011) Periodontopathogens induce soluble P-selectin release by endothelial cells and platelets. *Thromb Res,* 127**,** e20-6.

Atarbashi-Moghadam, F., S. R. Havaei, S. A. Havaei, N. S. Hosseini, G. Behdadmehr & S. Atarbashi-Moghadam (2018) Periopathogens in atherosclerotic plaques of patients with both cardiovascular disease and chronic periodontitis. *ARYA Atheroscler,* 14**,** 53-57.

Ayala-Herrera, J. L., C. Abud-Mendoza, R. F. Gonzalez-Amaro, L. F. Espinosa-Cristobal & R. E. Martínez-Martínez (2018) Distribution of Porphyromonas gingivalis fimA genotypes in patients affected by rheumatoid arthritis and periodontitis. *Acta Odontol Scand***,** 1-5.

Baba, A., T. Kadowaki, T. Asao & K. Yamamoto (2002) Roles for Arg- and Lys-gingipains in the disruption of cytokine responses and loss of viability of human endothelial cells by Porphyromonas gingivalis infection. *Biological Chemistry,* 383**,** 1223-1230.

Bacci, G., P. Paganin, L. Lopez, C. Vanni, C. Dalmastri, C. Cantale, L. Daddiego, G. Perrotta, D. Dolce, P. Morelli, V. Tuccio, A. De Alessandri, E. V. Fiscarelli, G. Taccetti, V. Lucidi, A. Bevivino & A. Mengoni (2016) Pyrosequencing Unveils Cystic Fibrosis Lung Microbiome Differences Associated with a Severe Lung Function Decline. *PLoS One,* 11**,** e0156807.

Bachrach, G., G. Rosen, M. Bellalou, R. Naor & M. N. Sela (2004) Identification of a Fusobacterium nucleatum 65 kDa serine protease. *Oral Microbiol Immunol,* 19**,** 155-9.

Baek, K. J., S. Ji, Y. C. Kim & Y. Choi (2015) Association of the invasion ability of Porphyromonas gingivalis with the severity of periodontitis. *Virulence,* 6**,** 274-81.

Bahrani-Mougeot, F. K., B. J. Paster, S. Coleman, J. Ashar, S. Barbuto & P. B. Lockhart (2008) Diverse and novel oral bacterial species in blood following dental procedures. *J Clin Microbiol,* 46**,** 2129-32.

Bai, D., R. Nakao, A. Ito, H. Uematsu & H. Senpuku (2015) Immunoreactive antigens recognized in serum samples from mice intranasally immunized with Porphyromonas gingivalis outer membrane vesicles. *Pathog Dis,* 73.

Bao, K., G. N. Belibasakis, T. Thurnheer, J. Aduse-Opoku, M. A. Curtis & N. Bostanci (2014) Role of Porphyromonas gingivalis gingipains in multi-species biofilm formation. *BMC Microbiol,* 14**,** 258.

Barbosa, M., I. Prada-López, M. Álvarez, B. Amaral, C. D. de los Angeles & I. Tomás (2015) Post-tooth extraction bacteraemia: a randomized clinical trial on the efficacy of chlorhexidine prophylaxis. *PLoS One,* 10**,** e0124249.

Barquera, S., A. Pedroza-Tobías, C. Medina, L. Hernández-Barrera, K. Bibbins-Domingo, R. Lozano & A. E. Moran (2015) Global Overview of the Epidemiology of Atherosclerotic Cardiovascular Disease. *Arch Med Res,* 46**,** 328-38.

Bartruff, J. B., R. A. Yukna & D. L. Layman (2005) Outer membrane vesicles from Porphyromonas gingivalis affect the growth and function of cultured human gingival fibroblasts and umbilical vein endothelial cells. *J Periodontol,* 76**,** 972-9.

Beall, C. J., A. G. Campbell, A. L. Griffen, M. Podar & E. J. Leys (2018) Genomics of the Uncultivated, Periodontitis-Associated Bacterium. *mSystems,* 3.

Benedyk, M., P. M. Mydel, N. Delaleu, K. Płaza, K. Gawron, A. Milewska, K. Maresz, J. Koziel, K. Pyrc & J. Potempa (2016) Gingipains: Critical Factors in the Development of Aspiration Pneumonia Caused by Porphyromonas gingivalis. *J Innate Immun,* 8**,** 185-98.

Bordenstein, S. & K. Theis (2015) Host Biology in Light of the Microbiome: Ten Principles of Holobionts and Hologenomes. *Plos Biology,* 13.

Bostanci, N. 2017. *Pathogenesis of periodontal diseases : biological concepts for clinicians*. New York, NY: Springer Berlin Heidelberg.

Bostanci, N. & G. N. Belibasakis (2012) Porphyromonas gingivalis: an invasive and evasive opportunistic oral pathogen. *FEMS Microbiol Lett,* 333**,** 1-9.

Bowen, W. H., R. A. Burne, H. Wu & H. Koo (2018) Oral Biofilms: Pathogens, Matrix, and Polymicrobial Interactions in Microenvironments. *Trends Microbiol,* 26**,** 229-242.

Brecx, M. C., K. Schlegel, P. Gehr & N. P. Lang (1987) Comparison between histological and clinical parameters during human experimental gingivitis. *J Periodontal Res,* 22**,** 50-7.

Brennan, C. A. & W. S. Garrett (2019) Fusobacterium nucleatum - symbiont, opportunist and oncobacterium. *Nat Rev Microbiol,* 17**,** 156-166.

Brodala, N., E. P. Merricks, D. A. Bellinger, D. Damrongsri, S. Offenbacher, J. Beck, P. Madianos, D. Sotres, Y. L. Chang, G. Koch & T. C. Nichols (2005) Porphyromonas gingivalis bacteremia induces coronary and aortic atherosclerosis in normocholesterolemic and

hypercholesterolemic pigs. *Arteriosclerosis Thrombosis and Vascular Biology,* 25**,** 1446-1451.

Cairns, C. M., F. St Michael, P. Fleming, E. V. Vinogradov & A. D. Cox (2020) Structural analysis of the lipopolysaccharide O-antigen from. *Can J Microbiol,* 66**,** 529-534.

Campbell, L. A. & M. E. Rosenfeld (2015) Infection and Atherosclerosis Development. *Arch Med Res,* 46**,** 339-50.

Carinci, F., M. Martinelli, M. Contaldo, R. Santoro, F. Pezzetti, D. Lauritano, V. Candotto, D. Mucchi, A. Palmieri, A. Tagliabue & L. Tettamanti (2018) FOCUS ON PERIODONTAL DISEASE AND DEVELOPMENT OF ENDOCARDITIS. *Journal of Biological Regulators and Homeostatic Agents,* 32**,** 143-147.

Carrion, J., E. Scisci, B. Miles, G. J. Sabino, A. E. Zeituni, Y. Gu, A. Bear, C. A. Genco, D. L. Brown & C. W. Cutler (2012) Microbial Carriage State of Peripheral Blood Dendritic Cells (DCs) in Chronic Periodontitis Influences DC Differentiation, Atherogenic Potential. *Journal of Immunology,* 189**,** 3178-3187.

Castillo, D. M., M. C. Sánchez-Beltrán, J. E. Castellanos, I. Sanz, I. Mayorga-Fayad, M. Sanz & G. I. Lafaurie (2011) Detection of specific periodontal microorganisms from bacteraemia samples after periodontal therapy using molecular-based diagnostics. *J Clin Periodontol,* 38**,** 418-27.

Ceccarelli, F., G. Orrù, A. Pilloni, I. Bartosiewicz, C. Perricone, E. Martino, R. Lucchetti, S. Fais, M. Vomero, M. Olivieri, M. di Franco, R. Priori, V. Riccieri, R. Scrivo, Y. Shoenfeld, C. Alessandri, F. Conti, A. Polimeni & G. Valesini (2018) Porphyromonas gingivalis in the tongue biofilm is associated with the clinical outcome in rheumatoid arthritis patients. *Clin Exp Immunol*.

Cecil, J. D., N. M. O'Brien-Simpson, J. C. Lenzo, J. A. Holden, Y. Y. Chen, W. Singleton, K. T. Gause, Y. Yan, F. Caruso & E. C. Reynolds (2016) Differential Responses of Pattern Recognition Receptors to Outer Membrane Vesicles of Three Periodontal Pathogens. *PLoS One,* 11**,** e0151967.

Champagne, C., N. Yoshinari, J. A. Oetjen, E. L. Riche, J. D. Beck & S. Offenbacher (2009) Gender differences in systemic inflammation and atheroma formation following Porphyromonas gingivalis infection in heterozygous apolipoprotein E-deficient mice. *Journal of Periodontal Research,* 44**,** 569-577.

Chan, L. Y., E. K. Yim & A. B. Choo (2013) Normalized median fluorescence: an alternative flow cytometry analysis method for tracking human embryonic stem cell states during differentiation. *Tissue Eng Part C Methods,* 19**,** 156-65.

Chaparro, A., A. Sanz, A. Quintero, C. Inostroza, V. Ramirez, F. Carrion, F. Figueroa, R. Serra & S. E. Illanes (2013) Increased inflammatory biomarkers in early pregnancy is associated with the development of pre-eclampsia in patients with periodontitis: a case control study. *Journal of Periodontal Research,* 48**,** 302-307.

Chapple, I. L. C., B. L. Mealey, T. E. Van Dyke, P. M. Bartold, H. Dommisch, P. Eickholz, M. L. Geisinger, R. J. Genco, M. Glogauer, M. Goldstein, T. J. Griffin, P. Holmstrup, G. K. Johnson, Y. Kapila, N. P. Lang, J. Meyle, S. Murakami, J. Plemons, G. A. Romito, L. Shapira, D. N. Tatakis, W. Teughels, L. Trombelli, C. Walter, G. Wimmer, P. Xenoudi & H. Yoshie (2018) Periodontal health and gingival diseases and conditions on an intact and a reduced periodontium: Consensus report of workgroup 1 of the 2017 World Workshop on the Classification of Periodontal and Peri-Implant Diseases and Conditions. *J Periodontol,* 89 Suppl 1**,** S74-S84.

Chen, C., C. Hemme, J. Beleno, Z. J. Shi, D. Ning, Y. Qin, Q. Tu, M. Jorgensen, Z. He, L. Wu & J. Zhou (2018a) Oral microbiota of periodontal health and disease and their changes after nonsurgical periodontal therapy. *ISME J,* 12**,** 1210-1224.

Chen, T., W. H. Yu, J. Izard, O. V. Baranova, A. Lakshmanan & F. E. Dewhirst (2010) The Human Oral Microbiome Database: a web accessible resource for investigating oral microbe taxonomic and genomic information. *Database (Oxford),* 2010**,** baq013.

Chen, T. C., C. T. Lin, S. J. Chien, S. F. Chang & C. N. Chen (2018b) Regulation of calcification in human aortic smooth muscle cells infected with high-glucose-treated Porphyromonas gingivalis. *Journal of Cellular Physiology,* 233**,** 4759-4769.

Chen, Y. T., C. J. Shih, S. M. Ou, S. C. Hung, C. H. Lin, D. C. Tarng & T. G. K. D. T. R. Group (2015) Periodontal Disease and Risks of Kidney Function Decline and Mortality in Older People: A Community-Based Cohort Study. *Am J Kidney Dis,* 66**,** 223-30.

Chhibber-Goel, J., V. Singhal, D. Bhowmik, R. Vivek, N. Parakh, B. Bhargava & A. Sharma (2016) Linkages between oral commensal bacteria and atherosclerotic plaques in coronary artery disease patients. *Npj Biofilms and Microbiomes,* 2.

Chistiakov, D. A., A. N. Orekhov & Y. V. Bobryshev (2015) Endothelial Barrier and Its Abnormalities in Cardiovascular Disease. *Front Physiol,* 6**,** 365.

Chiu, B. (1999) Multiple infections in carotid atherosclerotic plaques. *American Heart Journal,* 138**,** S534-S536.

Cho, I. & M. Blaser (2012) APPLICATIONS OF NEXT-GENERATION SEQUENCING The human microbiome: at the interface of health and disease. *Nature Reviews Genetics,* 13**,** 260-270.

Choi, E. K., S. A. Park, W. M. Oh, H. C. Kang, H. K. Kuramitsu, B. G. Kim & I. C. Kang (2005) Mechanisms of Porphyromonas gingivalis-induced monocyte chemoattractant protein-1 expression in endothelial cells. *FEMS Immunol Med Microbiol,* 44**,** 51-8.

Chukkapalli, S. S., M. Easwaran, M. F. Rivera-Kweh, I. M. Velsko, S. Ambadapadi, J. Dai, H. Larjava, A. R. Lucas & L. Kesavalu (2017a) Sequential colonization of periodontal pathogens in induction of periodontal disease and atherosclerosis in LDLRnull mice. *Pathogens and Disease,* 75.

Chukkapalli, S. S., M. F. Rivera, I. M. Velsko, J. Y. Lee, H. Chen, D. Zheng, I. Bhattacharyya, P. R. Gangula, A. R. Lucas & L. Kesavalu (2014) Invasion of oral and aortic tissues by oral spirochete Treponema denticola in ApoE(-/-) mice causally links periodontal disease and atherosclerosis. *Infect Immun,* 82**,** 1959-67.

Chukkapalli, S. S., M. F. Rivera-Kweh, I. M. Velsko, H. Chen, D. Zheng, I. Bhattacharyya, P. R. Gangula, A. R. Lucas & L. Kesavalu (2015a) Chronic oral infection with major periodontal bacteria Tannerella forsythia modulates systemic atherosclerosis risk factors and inflammatory markers. *Pathog Dis,* 73.

--- (2015b) Chronic oral infection with major periodontal bacteria Tannerella forsythia modulates systemic atherosclerosis risk factors and inflammatory markers. *Pathogens and Disease,* 73.

Chukkapalli, S. S., I. M. Velsko, M. F. Rivera-Kweh, H. Larjava, A. R. Lucas & L. Kesavalu (2017b) Global TLR2 and 4 deficiency in mice impacts bone resorption, inflammatory markers and atherosclerosis to polymicrobial infection. *Molecular Oral Microbiology,* 32**,** 211-225.

Chukkapalli, S. S., I. M. Velsko, M. F. Rivera-Kweh, D. Zheng, A. R. Lucas & L. Kesavalu (2015c) Polymicrobial Oral Infection with Four Periodontal Bacteria Orchestrates a Distinct Inflammatory Response and Atherosclerosis in ApoE null Mice. *PLoS One,* 10**,** e0143291.

Claes, J., L. Liesenborghs, M. Lox, P. Verhamme, T. Vanassche & M. Peetermans (2015) In Vitro and In Vivo Model to Study Bacterial Adhesion to the Vessel Wall Under Flow Conditions. *Jove-Journal of Visualized Experiments*.

Cobb, C. M., P. J. Kelly, K. B. Williams, S. Babbar, M. Angolkar & R. J. Derman (2017) The oral microbiome and adverse pregnancy outcomes. *International Journal of Womens Health,* 9.

Cole, L. A. & P. R. Kramer. 2016. *Human physiology, biochemistry, and basic medicine*. Amsterdam ; Boston: Elsevier/AP, Academic Press is an imprint of Elsevier.

Corada, M., F. Liao, M. Lindgren, M. G. Lampugnani, F. Breviario, R. Frank, W. A. Muller, D. J. Hicklin, P. Bohlen & E. Dejana (2001) Monoclonal antibodies directed to different regions of vascular endothelial cadherin extracellular domain affect adhesion and clustering of the protein and modulate endothelial permeability. *Blood,* 97**,** 1679-84.

Corada, M., L. Zanetta, F. Orsenigo, F. Breviario, M. G. Lampugnani, S. Bernasconi, F. Liao, D. J. Hicklin, P. Bohlen & E. Dejana (2002) A monoclonal antibody to vascular endothelial-cadherin inhibits tumor angiogenesis without side effects on endothelial permeability. *Blood,* 100**,** 905-11.

Curtis, M. A., J. Aduse Opoku, M. Rangarajan, A. Gallagher, J. A. Sterne, C. R. Reid, H. E. Evans & B. Samuelsson (2002) Attenuation of the virulence of Porphyromonas gingivalis by using a specific synthetic Kgp protease inhibitor. *Infect Immun,* 70**,** 6968-75.

Curtis, M. A., A. Thickett, J. M. Slaney, M. Rangarajan, J. Aduse-Opoku, P. Shepherd, N. Paramonov & E. F. Hounsell (1999) Variable carbohydrate modifications to the catalytic chains of the RgpA and RgpB proteases of Porphyromonas gingivalis W50. *Infect Immun,* 67**,** 3816-23.

Darveau, R. P. (2010) Periodontitis: a polymicrobial disruption of host homeostasis. *Nat Rev Microbiol,* 8**,** 481-90.

Dashper, S. G., L. Brownfield, N. Slakeski, P. S. Zilm, A. H. Rogers & E. C. Reynolds (2001) Sodium ion-driven serine/threonine transport in Porphyromonas gingivalis. *J Bacteriol,* 183**,** 4142-8.

de Andrade, K. Q., C. L. C. Almeida-da-Silva & R. Coutinho-Silva (2019) Immunological Pathways Triggered by *Porphyromonas gingivalis* and *Fusobacterium nucleatum*: Therapeutic Possibilities? *Mediators Inflamm,* 2019**,** 7241312.

De Nardo, D. & E. Latz (2011) NLRP3 inflammasomes link inflammation and metabolic disease. *Trends Immunol,* 32**,** 373-9.

de Souza, A. F., A. L. Rocha, W. H. Castro, F. M. Ferreira, C. L. Gelape, D. V. Travassos & T. A. da Silva (2016) Dental care before cardiac valve surgery: Is it important to prevent infective endocarditis? *Int J Cardiol Heart Vasc,* 12**,** 57-62.

Dejana, E., F. Orsenigo & M. G. Lampugnani (2008) The role of adherens junctions and VE-cadherin in the control of vascular permeability. *J Cell Sci,* 121**,** 2115-22.

Denes, A., C. Drake, J. Stordy, J. Chamberlain, B. W. McColl, H. Gram, D. Crossman, S. Francis, S. M. Allan & N. J. Rothwell (2012) Interleukin-1 mediates neuroinflammatory changes associated with diet-induced atherosclerosis. *J Am Heart Assoc,* 1**,** e002006.

Deshpande, R. G., M. Khan & C. A. Genco (1998a) Invasion strategies of the oral pathogen Porphyromonas gingivalis: Implications for cardiovascular disease. *Invasion and Metastasis,* 18**,** 57-69.

Deshpande, R. G., M. B. Khan & C. A. Genco (1998b) Invasion of aortic and heart endothelial cells by Porphyromonas gingivalis. *Infection and Immunity,* 66**,** 5337-5343.

Dewhirst, F. E., T. Chen, J. Izard, B. J. Paster, A. C. Tanner, W. H. Yu, A. Lakshmanan & W. G. Wade (2010) The human oral microbiome. *J Bacteriol,* 192**,** 5002-17.

Dietrich, T., P. Sharma, C. Walter, P. Weston & J. Beck (2013) The epidemiological evidence behind the association between periodontitis and incident atherosclerotic cardiovascular disease. *J Periodontol,* 84**,** S70-84.

Ding, Y., J. Ren, H. Yu, W. Yu & Y. Zhou (2018), a periodontitis causing bacterium, induces memory impairment and age-dependent neuroinflammation in mice. *Immun Ageing,* 15**,** 6.

Dominy, S. S., C. Lynch, F. Ermini, M. Benedyk, A. Marczyk, A. Konradi, M. Nguyen, U. Haditsch, D. Raha, C. Griffin, L. J. Holsinger, S. Arastu-Kapur, S. Kaba, A. Lee, M. I. Ryder, B. Potempa, P. Mydel, A. Hellvard, K. Adamowicz, H. Hasturk, G. D. Walker, E. C. Reynolds, R. L. M. Faull, M. A. Curtis, M. Dragunow & J. Potempa (2019) in Alzheimer's disease brains: Evidence for disease causation and treatment with small-molecule inhibitors. *Sci Adv,* 5**,** eaau3333.

Dorn, B. R., J. N. Burks, K. N. Seifert & A. Progulske-Fox (2000) Invasion of endothelial and epithelial cells by strains of Porphyromonas gingivalis. *Fems Microbiology Letters,* 187**,** 139-144.

Dorn, B. R., W. A. Dunn & A. Progulske-Fox (1999) Invasion of human coronary artery cells by periodontal pathogens. *Infection and Immunity,* 67**,** 5792-5798.

Doron, L., S. Coppenhagen-Glazer, Y. Ibrahim, A. Eini, R. Naor, G. Rosen & G. Bachrach (2014) Identification and characterization of fusolisin, the Fusobacterium nucleatum autotransporter serine protease. *PLoS One,* 9**,** e111329.

Eberhard, J., N. Stumpp, A. Winkel, C. Schrimpf, T. Bisdas, P. Orzak, O. E. Teebken, A. Haverich & M. Stiesch (2017) Streptococcus mitis and Gemella haemolysans were simultaneously found in atherosclerotic and oral plaques of elderly without periodontitis-a pilot study. *Clinical Oral Investigations,* 21**,** 447-452.

Ebersole, J. L., D. Dawson, P. Emecen-Huja, R. Nagarajan, K. Howard, M. E. Grady, K. Thompson, R. Peyyala, A. Al-Attar, K. Lethbridge, S. Kirakodu & O. A. Gonzalez (2017) The periodontal war: microbes and immunity. *Periodontol 2000,* 75**,** 52-115.

Edberg, S. C. & A. Miskin (1980) Turbidimetric determination of blood aminoglycoside levels by growth curve analysis. *J Pharm Sci,* 69**,** 1442-3.

Edlund, A., T. M. Santiago-Rodriguez, T. K. Boehm & D. T. Pride (2015) Bacteriophage and their potential roles in the human oral cavity. *J Oral Microbiol,* 7**,** 27423.

Ekuni, D., T. Tomofuji, T. Sanbe, K. Irie, T. Azuma, T. Maruyama, N. Tamaki, J. Murakami, S. Kokeguchi & T. Yamamoto (2009) Periodontitis-induced lipid peroxidation in rat descending aorta is involved in the initiation of atherosclerosis. *J Periodontal Res,* 44**,** 434-42.

El Kholy, K., R. J. Genco & T. E. Van Dyke (2015) Oral infections and cardiovascular disease. *Trends in Endocrinology and Metabolism,* 26**,** 315-321.

Emery, D. C., D. K. Shoemark, T. E. Batstone, C. M. Waterfall, J. A. Coghill, T. L. Cerajewska, M. Davies, N. X. West & S. J. Allen (2017) 16S rRNA Next Generation Sequencing Analysis Shows Bacteria in Alzheimer's Post-Mortem Brain. *Frontiers in Aging Neuroscience,* 9.

Fan, X., A. V. Alekseyenko, J. Wu, B. A. Peters, E. J. Jacobs, S. M. Gapstur, M. P. Purdue, C. C. Abnet, R. Stolzenberg-Solomon, G. Miller, J. Ravel, R. B. Hayes & J. Ahn (2016) Human oral microbiome and prospective risk for pancreatic cancer: a population-based nested case-control study. *Gut*.

Fardini, Y., P. Chung, R. Dumm, N. Joshi & Y. W. Han (2010) Transmission of Diverse Oral Bacteria to Murine Placenta: Evidence for the Oral Microbiome as a Potential Source of Intrauterine Infection. *Infection and Immunity,* 78**,** 1789-1796.

Fardini, Y., X. Wang, S. Témoin, S. Nithianantham, D. Lee, M. Shoham & Y. W. Han (2011) Fusobacterium nucleatum adhesin FadA binds vascular endothelial cadherin and alters endothelial integrity. *Mol Microbiol,* 82**,** 1468-80.

Farrugia, C., G. P. Stafford & C. Murdoch (2020a) Outer Membrane Vesicles Increase Vascular Permeability. *J Dent Res***,** 22034520943187.

Farrugia, C., G. P. Stafford, J. Potempa, R. N. Wilkinson, Y. Chen, C. Murdoch & M. Widziolek (2020b) Mechanisms of vascular damage by systemic dissemination of the oral pathogen Porphyromonas gingivalis. *FEBS J.*

Fiehn, N. E., T. Larsen, N. Christiansen, P. Holmstrup & T. V. Schroeder (2005) Identification of periodontal pathogens in atherosclerotic vessels. *J Periodontol,* 76**,** 731-6.

Finegold, J. A., P. Asaria & D. P. Francis (2013) Mortality from ischaemic heart disease by country, region, and age: statistics from World Health Organisation and United Nations. *Int J Cardiol,* 168**,** 934-45.

Fisher, M. A. & G. W. Taylor (2009) A prediction model for chronic kidney disease includes periodontal disease. *J Periodontol,* 80**,** 16-23.

Fisher, M. A., G. W. Taylor, P. N. Papapanou, M. Rahman & S. M. Debanne (2008a) Clinical and serologic markers of periodontal infection and chronic kidney disease. *Journal of Periodontology,* 79**,** 1670-1678.

Fisher, M. A., G. W. Taylor, B. J. Shelton, K. A. Jamerson, M. Rahman, A. O. Ojo & A. R. Sehgal (2008b) Periodontal disease and other nontraditional risk factors for CKD. *American Journal of Kidney Diseases,* 51**,** 45-52.

Fitzpatrick, R. E., L. C. Wijeyewickrema & R. N. Pike (2009) The gingipains: scissors and glue of the periodontal pathogen, Porphyromonas gingivalis. *Future Microbiology,* 4**,** 471-487.

Fournier, P. E., F. Thuny, H. Richet, H. Lepidi, J. P. Casalta, J. P. Arzouni, M. Maurin, M. Célard, J. L. Mainardi, T. Caus, F. Collart, G. Habib & D. Raoult (2010) Comprehensive diagnostic strategy for blood culture-negative endocarditis: a prospective study of 819 new cases. *Clin Infect Dis,* 51**,** 131-40.

Freitas, C. O., I. S. Gomes-Filho, R. C. Naves, G. a. R. Nogueira Filho, S. S. Cruz, C. A. Santos, L. Dunningham, L. F. Miranda & M. D. Barbosa (2012) Influence of periodontal therapy on C-reactive protein level: a systematic review and meta-analysis. *J Appl Oral Sci,* 20**,** 1-8.

Freudenheim, J. L., R. J. Genco, M. J. LaMonte, A. E. Millen, K. M. Hovey, X. Mai, N. Nwizu, C. A. Andrews & J. Wactawski-Wende (2016a) Periodontal Disease and Breast Cancer: Prospective Cohort Study of Postmenopausal Women. *Cancer Epidemiology Biomarkers & Prevention,* 25**,** 43-50.

Freudenheim, J. L., A. E. Millen & J. Wactawski-Wende (2016b) Periodontal Disease and Breast Cancer-Response. *Cancer Epidemiol Biomarkers Prev,* 25**,** 862.

Frey, A. M., M. J. Satur, C. Phansopa, J. L. Parker, D. Bradshaw, J. Pratten & G. P. Stafford (2018) Evidence for a carbohydrate-binding module (CBM) of. *Biochem J,* 475**,** 1159-1176.

Friedewald, V. E., K. S. Kornman, J. D. Beck, R. Genco, A. Goldfine, P. Libby, S. Offenbacher, P. M. Ridker, T. E. Van Dyke, W. C. Roberts, A. J. o. Cardiology & J. o. Periodontology (2009) The American Journal of Cardiology and Journal of Periodontology Editors' Consensus: periodontitis and atherosclerotic cardiovascular disease. *Am J Cardiol,* 104**,** 59-68.

Furuta, N., K. Tsuda, H. Omori, T. Yoshimori, F. Yoshimura & A. Amano (2009) Porphyromonas gingivalis outer membrane vesicles enter human epithelial cells via an endocytic pathway and are sorted to lysosomal compartments. *Infect Immun,* 77**,** 4187-96.

G Caton, J., G. Armitage, T. Berglundh, I. L. C. Chapple, S. Jepsen, K. S Kornman, B. L Mealey, P. N. Papapanou, M. Sanz & M. S Tonetti (2018) A new classification scheme for periodontal and peri-implant diseases and conditions - Introduction and key changes from the 1999 classification. *J Periodontol,* 89 Suppl 1**,** S1-S8.

Gaetti-Jardim, E., S. L. Marcelino, A. C. R. Feitosa, G. A. Romito & M. J. Avila-Campos (2009) Quantitative detection of periodontopathic bacteria in atherosclerotic plaques from coronary arteries. *Journal of Medical Microbiology,* 58**,** 1568-1575.

Ganesh, P., R. Karthikeyan, A. Muthukumaraswamy & J. Anand (2017) A Potential Role of Periodontal Inflammation in Alzheimer's Disease: A Review. *Oral Health & Preventive Dentistry,* 15**,** 7-12.

Gao, S., S. Li, Z. Ma, S. Liang, T. Shan, M. Zhang, X. Zhu, P. Zhang, G. Liu, F. Zhou, X. Yuan, R. Jia, J. Potempa, D. A. Scott, R. J. Lamont, H. Wang & X. Feng (2016) Presence of Porphyromonas gingivalis in esophagus and its association with the clinicopathological characteristics and survival in patients with esophageal cancer. *Infect Agent Cancer,* 11**,** 3.

Genco, C. A. (1995) Regulation of hemin and iron transport in Porphyromonas gingivalis. *Adv Dent Res,* 9**,** 41-7.

Genco, C. A., B. M. Odusanya & G. Brown (1994) Binding and accumulation of hemin in Porphyromonas gingivalis are induced by hemin. *Infect Immun,* 62**,** 2885-92.

Ghannoum, M. A., R. J. Jurevic, P. K. Mukherjee, F. Cui, M. Sikaroodi, A. Naqvi & P. M. Gillevet (2010) Characterization of the oral fungal microbiome (mycobiome) in healthy individuals. *PLoS Pathog,* 6**,** e1000713.

Gharbia, S. E. & H. N. Shah (1992) Fusobacterium nucleatum subsp. fusiforme subsp. nov. and Fusobacterium nucleatum subsp. animalis subsp. nov. as additional subspecies within Fusobacterium nucleatum. *Int J Syst Bacteriol,* 42**,** 296-8.

Giacaman, R. A., A. C. Asrani, K. F. Ross & M. C. Herzberg (2009) Cleavage of protease-activated receptors on an immortalized oral epithelial cell line by Porphyromonas gingivalis gingipains. *Microbiology,* 155**,** 3238-46.

Gibson, F. C., C. Hong, H. H. Chou, H. Yumoto, J. Q. Chen, E. Lien, J. Wong & C. A. Genco (2004) Innate immune recognition of invasive bacteria accelerates atherosclerosis in apolipoprotein E-deficient mice. *Circulation,* 109**,** 2801-2806.

Gibson, F. C., J. Savelli, T. E. Van Dyke & C. A. Genco (2005) Gingipain-specific IgG in the sera of patients with periodontal disease is necessary for opsonophagocytosis of Porphyromonas gingivalis. *J Periodontol,* 76**,** 1629-36.

Gimbrone, M. A. & G. García-Cardeña (2016) Endothelial Cell Dysfunction and the Pathobiology of Atherosclerosis. *Circ Res,* 118**,** 620-36.

Goldman, H. M. 1953. *Periodontia: a study of the histology, physiology, and pathology of the periodontium and the treatment of its diseases*. St. Louis: Mosby.

Goldsmith, J. R. & C. Jobin (2012) Think small: zebrafish as a model system of human pathology. *J Biomed Biotechnol,* 2012**,** 817341.

Gomes, M. C. & S. Mostowy (2020) The Case for Modeling Human Infection in Zebrafish. *Trends Microbiol,* 28**,** 10-18.

Gomes-Filho, I. S., J. S. Passos & S. Seixas da Cruz (2010) Respiratory disease and the role of oral bacteria. *J Oral Microbiol,* 2.

Gomez, D., R. A. Baylis, B. G. Durgin, A. A. C. Newman, G. F. Alencar, S. Mahan, C. St Hilaire, W. Müller, A. Waisman, S. E. Francis, E. Pinteaux, G. J. Randolph, H. Gram & G. K. Owens (2018) Interleukin-1β has atheroprotective effects in advanced atherosclerotic lesions of mice. *Nat Med,* 24**,** 1418-1429.

Grenier, D. & D. Mayrand (1987) Functional characterization of extracellular vesicles produced by Bacteroides gingivalis. *Infect Immun,* 55**,** 111-7.

Gui, M. J., S. G. Dashper, N. Slakeski, Y. Y. Chen & E. C. Reynolds (2016) Spheres of influence: Porphyromonas gingivalis outer membrane vesicles. *Mol Oral Microbiol,* 31**,** 365-78.

Guo, S., J. Chen, F. Chen, Q. Zeng, W. L. Liu & G. Zhang (2020) Exosomes derived from *Fusobacterium nucleatum*-infected colorectal cancer cells facilitate tumour metastasis by selectively carrying miR-1246/92b-3p/27a-3p and CXCL16. *Gut*.

Gur, C., Y. Ibrahim, B. Isaacson, R. Yamin, J. Abed, M. Gamliel, J. Enk, Y. Bar-On, N. Stanietsky-Kaynan, S. Coppenhagen-Glazer, N. Shussman, G. Almogy, A. Cuapio, E. Hofer, D. Mevorach, A. Tabib, R. Ortenberg, G. Markel, K. Miklić, S. Jonjic, C. A. Brennan, W. S. Garrett, G. Bachrach & O. Mandelboim (2015) Binding of the Fap2 protein of Fusobacterium nucleatum to human inhibitory receptor TIGIT protects tumors from immune cell attack. *Immunity,* 42**,** 344-355.

Gustafsson, N., J. Ahlqvist, U. Näslund, K. Buhlin, A. Gustafsson, B. Kjellström, B. Klinge, L. Rydén & E. Levring Jäghagen (2020) Associations among Periodontitis, Calcified Carotid Artery Atheromas, and Risk of Myocardial Infarction. *J Dent Res,* 99**,** 60-68.

Gut, P., S. Reischauer, D. Y. R. Stainier & R. Arnaout (2017) LITTLE FISH, BIG DATA: ZEBRAFISH AS A MODEL FOR CARDIOVASCULAR AND METABOLIC DISEASE. *Physiol Rev,* 97**,** 889-938.

Górski, A. & B. Weber-Dabrowska (2005) The potential role of endogenous bacteriophages in controlling invading pathogens. *Cell Mol Life Sci,* 62**,** 511-9.

Górski, B., E. Nargiełło, G. Opolski, E. Ganowicz & R. Górska (2016) The Association Between Dental Status and Systemic Lipid Profile and Inflammatory Mediators in Patients After Myocardial Infarction. *Adv Clin Exp Med,* 25**,** 625-30.

Hajishengallis, G. (2020) Oral bacteria and leaky endothelial junctions in remote extraoral sites. *FEBS J.*

Hajishengallis, G., R. P. Darveau & M. A. Curtis (2012) The keystone-pathogen hypothesis. *Nat Rev Microbiol,* 10**,** 717-25.

Hajishengallis, G. & R. J. Lamont (2012) Beyond the red complex and into more complexity: the polymicrobial synergy and dysbiosis (PSD) model of periodontal disease etiology. *Mol Oral Microbiol,* 27**,** 409-19.

Han, Y. P. W. (2015) Fusobacterium nucleatum: a commensal-turned pathogen. *Current Opinion in Microbiology,* 23**,** 141-147.

Han, Y. W., A. Ikegami, C. Rajanna, H. I. Kawsar, Y. Zhou, M. Li, H. T. Sojar, R. J. Genco, H. K. Kuramitsu & C. X. Deng (2005) Identification and characterization of a novel adhesin unique to oral fusobacteria. *J Bacteriol,* 187**,** 5330-40.

Han, Y. W. & X. Wang (2013) Mobile Microbiome: Oral Bacteria in Extra-oral Infections and Inflammation. *Journal of Dental Research,* 92**,** 485-491.

Harding, A., S. Robinson, S. J. Crean & S. K. Singhrao (2017) Can Better Management of Periodontal Disease Delay the Onset and Progression of Alzheimer's Disease? *Journal of Alzheimers Disease,* 58**,** 337-348.

Harry, B. L., J. M. Sanders, R. E. Feaver, M. Lansey, T. L. Deem, A. Zarbock, A. C. Bruce, A. W. Pryor, B. D. Gelfand, B. R. Blackman, M. A. Schwartz & K. Ley (2008) Endothelial cell PECAM-1 promotes atherosclerotic lesions in areas of disturbed flow in ApoE-deficient mice. *Arterioscler Thromb Vasc Biol,* 28**,** 2003-8.

Haseloff, R. F., S. Dithmer, L. Winkler, H. Wolburg & I. E. Blasig (2015) Transmembrane proteins of the tight junctions at the blood-brain barrier: structural and functional aspects. *Semin Cell Dev Biol,* 38**,** 16-25.

Hashizume, T., T. Kurita-Ochiai & M. Yamamoto (2011) Porphyromonas gingivalis stimulates monocyte adhesion to human umbilical vein endothelial cells. *FEMS Immunol Med Microbiol,* 62**,** 57-65.

Hasturk, H., R. Abdallah, A. Kantarci, D. Nguyen, N. Giordano, J. Hamilton & T. E. Van Dyke (2015) Resolvin E1 (RvE1) Attenuates Atherosclerotic Plaque Formation in Diet and Inflammation-Induced Atherogenesis. *Arteriosclerosis Thrombosis and Vascular Biology,* 35**,** 1123-1133.

Haurat, M. F., J. Aduse-Opoku, M. Rangarajan, L. Dorobantu, M. R. Gray, M. A. Curtis & M. F. Feldman (2011) Selective sorting of cargo proteins into bacterial membrane vesicles. *J Biol Chem,* 286**,** 1269-76.

Hay, S., S. Jayaraman, T. Truelsen, R. Sorensen, A. Millear, G. Giussani & E. Beghi (2017) GBD 2015 Disease and Injury Incidence and Prevalence Collaborators. Global, regional, and national incidence, prevalence, and years lived with disability for 310 diseases and injuries, 1990-2015: a systematic analysis for the Global Burden of Disease Study 2015 (vol 388, pg 1545, 2016). *Lancet,* 389**,** E1-E1.

Helmlinger, G., R. V. Geiger, S. Schreck & R. M. Nerem (1991) Effects of pulsatile flow on cultured vascular endothelial cell morphology. *J Biomech Eng,* 113**,** 123-31.

Hendrickson, E. L., T. Wang, D. A. Beck, B. C. Dickinson, C. J. Wright, R. J Lamont & M. Hackett (2014) Proteomics of Fusobacterium nucleatum within a model developing oral microbial community. *Microbiologyopen,* 3**,** 729-51.

Herrera, D., A. Molina, K. Buhlin & B. Klinge (2020) Periodontal diseases and association with atherosclerotic disease. *Periodontol 2000,* 83**,** 66-89.

Ho, M. H., Z. M. Guo, J. Chunga, J. S. Goodwin & H. Xie (2016) Characterization of Innate Immune Responses of Human Endothelial Cells Induced by Porphyromonas gingivalis and Their Derived Outer Membrane Vesicles. *Front Cell Infect Microbiol,* 6**,** 139.

Hogg, K., J. Thomas, D. Ashford, J. Cartwright, R. Coldwell, D. J. Weston, J. Pillmoor, D. Surry & P. O'Toole (2015) Quantification of proteins by flow cytometry: Quantification of human hepatic transporter P-gp and OATP1B1 using flow cytometry and mass spectrometry. *Methods,* 82**,** 38-46.

Hojo, K., S. Nagaoka, S. Murata, N. Taketomo, T. Ohshima & N. Maeda (2007) Reduction of vitamin K concentration by salivary Bifidobacterium strains and their possible nutritional competition with Porphyromonas gingivalis. *J Appl Microbiol,* 103**,** 1969-74.

Holmstrup, P., J. Plemons & J. Meyle (2018) Non-plaque-induced gingival diseases. *J Periodontol,* 89 Suppl 1**,** S28-S45.

Holt, S. C. & J. L. Ebersole (2005) Porphyromonas gingivalis, Treponema denticola, and Tannerella forsythia: the "red complex", a prototype polybacterial pathogenic consortium in periodontitis. *Periodontol 2000,* 38**,** 72-122.

Honda, T., T. Oda, H. Yoshie & K. Yamazaki (2005) Effects of Porphyromonas gingivalis antigens and proinflammatory cytokines on human coronary artery endothelial cells. *Oral Microbiol Immunol,* 20**,** 82-8.

Honma, K., A. Ruscitto & A. Sharma (2018) β-Glucanase Activity of the Oral Bacterium Tannerella forsythia Contributes to the Growth of a Partner Species, Fusobacterium nucleatum, in Cobiofilms. *Appl Environ Microbiol,* 84.

Hordijk, P. L. (2006) Endothelial signalling events during leukocyte transmigration. *FEBS J,* 273**,** 4408-15.

Horliana, A. C., L. Chambrone, A. M. Foz, H. P. Artese, M. e. S. Rabelo, C. M. Pannuti & G. A. Romito (2014) Dissemination of periodontal pathogens in the bloodstream after periodontal procedures: a systematic review. *PLoS One,* 9**,** e98271.

Horz, H. P., N. Robertz, M. E. Vianna, K. Henne & G. Conrads (2015) Relationship between methanogenic archaea and subgingival microbial complexes in human periodontitis. *Anaerobe,* 35**,** 10-2.

How, K. Y., K. P. Song & K. G. Chan (2016a) Porphyromonas gingivalis: An Overview of Periodontopathic Pathogen below the Gum Line. *Front Microbiol,* 7**,** 53.

--- (2016b) Porphyromonas gingivalis: An Overview of Periodontopathic Pathogen below the Gum Line. *Frontiers in Microbiology,* 7.

Hočevar, K., J. Potempa & B. Turk (2018) Host cell-surface proteins as substrates of gingipains, the main proteases of Porphyromonas gingivalis. *Biol Chem*.

Huang, J., A. Roosaar, T. Axéll & W. Ye (2016) A prospective cohort study on poor oral hygiene and pancreatic cancer risk. *Int J Cancer,* 138**,** 340-7.

Huck, O., R. Elkaim, J. L. Davideau & H. Tenenbaum (2015) Porphyromonas gingivalis-impaired innate immune response via NLRP3 proteolysis in endothelial cells. *Innate Immun,* 21**,** 65-72.

Humphrey, L. L., R. Fu, D. I. Buckley, M. Freeman & M. Helfand (2008) Periodontal disease and coronary heart disease incidence: a systematic review and meta-analysis. *J Gen Intern Med,* 23**,** 2079-86.

Idrissi Janati, A., R. Durand, I. Karp, R. Voyer, J. F. Latulippe & E. Emami (2016) [Association between oral conditions and colorectal cancer: A literature review and synthesis]. *Rev Epidemiol Sante Publique,* 64**,** 113-9.

Ilievski, V., J. M. Kinchen, R. Prabhu, F. Rim, L. Leoni, T. G. Unterman & K. Watanabe (2016) Experimental Periodontitis Results in Prediabetes and Metabolic Alterations in Brain, Liver and Heart: Global Untargeted Metabolomic Analyses. *Journal of oral biology (Northborough, Mass.),* 3.

Imamura, T. (2003) The role of gingipains in the pathogenesis of periodontal disease. *J Periodontol,* 74**,** 111-8.

Imamura, T., J. Travis & J. Potempa (2003) The biphasic virulence activities of gingipains: activation and inactivation of host proteins. *Curr Protein Pept Sci,* 4**,** 443-50.

Jain, A., E. L. Batista, C. Serhan, G. L. Stahl & T. E. Van Dyke (2003) Role for periodontitis in the progression of lipid deposition in an animal model. *Infection and Immunity,* 71**,** 6012-6018.

Jandik, K. A., M. Belanger, S. L. Low, B. R. Dorn, M. C. K. Yang & A. Progulske-Fox (2008) Invasive differences among Porphyromonas gingivalis strains from healthy and diseased periodontal sites. *Journal of Periodontal Research,* 43**,** 524-530.

Jepsen, S., J. Blanco, W. Buchalla, J. C. Carvalho, T. Dietrich, C. Dörfer, K. A. Eaton, E. Figuero, J. E. Frencken, F. Graziani, S. M. Higham, T. Kocher, M. Maltz, A. Ortiz-Vigon, J. Schmoeckel, A. Sculean, L. M. Tenuta, M. H. van der Veen & V. Machiulskiene (2017) Prevention and control of dental caries and periodontal diseases at individual and population level: consensus report of group 3 of joint EFP/ORCA workshop on the boundaries between caries and periodontal diseases. *J Clin Periodontol,* 44 Suppl 18**,** S85-S93.

Jia, G., A. Zhi, P. F. H. Lai, G. Wang, Y. Xia, Z. Xiong, H. Zhang, N. Che & L. Ai (2018) The oral microbiota - a mechanistic role for systemic diseases. *Br Dent J,* 224**,** 447-455.

Jia, R., T. Hashizume-Takizawa, Y. Du, M. Yamamoto & T. Kurita-Ochiai (2015a) Aggregatibacter actinomycetemcomitans induces Th17 cells in atherosclerotic lesions. *Pathogens and Disease,* 73.

Jia, R., T. Kurita-Ochiai, S. Oguchi & M. Yamamoto (2013) Periodontal pathogen accelerates lipid peroxidation and atherosclerosis. *J Dent Res,* 92**,** 247-52.

Jia, Y., B. Guo, W. Yang, Q. Zhao, W. Jia & Y. Wu (2015b) Rho kinase mediates Porphyromonas gingivalis outer membrane vesicle-induced suppression of endothelial nitric oxide synthase through ERK1/2 and p38 MAPK. *Archives of Oral Biology,* 60**,** 488-495.

Jim, K. K., J. Engelen-Lee, A. M. van der Sar, W. Bitter, M. C. Brouwer, A. van der Ende, J. W. Veening, D. van de Beek & C. M. Vandenbroucke-Grauls (2016) Infection of zebrafish embryos with live fluorescent Streptococcus pneumoniae as a real-time pneumococcal meningitis model. *J Neuroinflammation,* 13**,** 188.

Jung, Y. J., H. K. Jun & B. K. Choi (2017) *Porphyromonas gingivalis* suppresses invasion of *Fusobacterium nucleatum* into gingival epithelial *cells*. *J Oral Microbiol,* 9**,** 1320193.

Kadowaki, T., R. Takii, A. Baba & K. Yamamoto (2003) Gingipains as the determinants of periodontopathogenicity. *Folia Pharmacologica Japonica,* 122**,** 37-44.

Kamer, A. R., A. P. Dasanayake, R. G. Craig, L. Glodzik-Sobanska, M. Bry & M. J. de Leon (2008) Alzheimer's disease and peripheral infections: The possible contribution from periodontal infections, model and hypothesis. *Journal of Alzheimers Disease,* 13**,** 437-449.

Kaplan, C. W., R. Lux, S. K. Haake & W. Shi (2009) The Fusobacterium nucleatum outer membrane protein RadD is an arginine-inhibitable adhesin required for inter-species adherence and the structured architecture of multispecies biofilm. *Mol Microbiol,* 71**,** 35-47.

Kaplan, C. W., X. Ma, A. Paranjpe, A. Jewett, R. Lux, S. Kinder-Haake & W. Shi (2010) Fusobacterium nucleatum outer membrane proteins Fap2 and RadD induce cell death in human lymphocytes. *Infect Immun,* 78**,** 4773-8.

Kariu, T., R. Nakao, T. Ikeda, K. Nakashima, J. Potempa & T. Imamura (2017) Inhibition of gingipains and Porphyromonas gingivalis growth and biofilm formation by prenyl flavonoids. *J Periodontal Res,* 52**,** 89-96.

Kerr, P., R. Tam & F. Plane. 2011. Endothelium. In *Mechanisms of Vascular Disease,* eds. R. Fitridge & M. Thompson, 1-12. University of Adelaide Press.

Khan, S. A., E. F. Kong, T. F. Meiller & M. A. Jabra-Rizk (2015) Periodontal Diseases: Bug Induced, Host Promoted. *PLoS Pathog,* 11**,** e1004952.

Khlgatian, M., H. Nassar, H. H. Chou, F. C. Gibson & C. A. Genco (2002) Fimbria-dependent activation of cell adhesion molecule expression in Porphyromonas gingivalis-infected endothelial cells. *Infect Immun,* 70**,** 257-67.

Kilian, M., I. L. Chapple, M. Hannig, P. D. Marsh, V. Meuric, A. M. Pedersen, M. S. Tonetti, W. G. Wade & E. Zaura (2016) The oral microbiome - an update for oral healthcare professionals. *Br Dent J,* 221**,** 657-666.

Kim, H. J., G. S. Cha, E. Y. Kwon, J. Y. Lee, J. Choi & J. Y. Joo (2018) accelerates atherosclerosis through oxidation of high-density lipoprotein. *J Periodontal Implant Sci,* 48**,** 60-68.

King, G. L. (2008) The role of inflammatory cytokines in diabetes and its complications. *J Periodontol,* 79**,** 1527-34.

Kner, P., J. W. Sedat, D. A. Agard & Z. Kam (2010) High-resolution wide-field microscopy with adaptive optics for spherical aberration correction and motionless focusing. *J Microsc,* 237**,** 136-47.

Kocgozlu, L., R. Elkaim, H. Tenenbaum & S. Werner (2009) Variable cell responses to P. gingivalis lipopolysaccharide. *J Dent Res,* 88**,** 741-5.

Koizumi, Y., T. Kurita-Ochiai, S. Oguchi & M. Yamamoto (2008) Nasal immunization with Porphyromonas gingivalis outer membrane protein decreases P-gingivalis-induced atherosclerosis and inflammation in spontaneously hyperlipidemic mice. *Infection and Immunity,* 76**,** 2958-2965.

Kolenbrander, P. E. (2000) Oral microbial communities: biofilms, interactions, and genetic systems. *Annu Rev Microbiol,* 54**,** 413-37.

Kolenbrander, P. E., R. N. Andersen, D. S. Blehert, P. G. Egland, J. S. Foster & R. J. Palmer (2002) Communication among oral bacteria. *Microbiol Mol Biol Rev,* 66**,** 486-505, table of contents.

Komatsu, T., K. Nagano, S. Sugiura, M. Hagiwara, N. Tanigawa, Y. Abiko, F. Yoshimura, Y. Furuichi & K. Matsushita (2012) E-selectin mediates Porphyromonas gingivalis adherence to human endothelial cells. *Infect Immun,* 80**,** 2570-6.

Kozarov, E. V., B. R. Dorn, C. E. Shelburne, W. A. Dunn & A. Progulske-Fox (2005) Human atherosclerotic plaque contains viable invasive Actinobacillus actinomycetemcomitans and Porphyromonas gingivalis. *Arterioscler Thromb Vasc Biol,* 25**,** e17-8.

Kramer, C. D., E. O. Weinberg, A. C. Gower, X. He, S. Mekasha, C. Slocum, L. M. Beaulieu, L. Wetzler, Y. Alekseyev, F. C. Gibson, III, J. E. Freedman, R. R. Ingalls & C. A. Genco (2014) Distinct gene signatures in aortic tissue from ApoE(-/-) mice exposed to pathogens or Western diet. *Bmc Genomics,* 15.

Kremer, B. H., B. G. Loos, U. van der Velden, A. J. van Winkelhoff, J. Craandijk, H. M. Bulthuis, J. Hutter, A. S. Varoufaki & T. J. van Steenbergen (2000) Peptostreptococcus micros smooth and rough genotypes in periodontitis and gingivitis. *J Periodontol,* 71**,** 209-18.

Kshirsagar, A. V., R. G. Craig, K. L. Moss, J. D. Beck, S. Offenbacher, P. Kotanko, P. J. Klemmer, M. Yoshino, N. W. Levin, J. K. Yip, K. Almas, E. M. Lupovici, L. A. Usvyat & R. J. Falk (2009) Periodontal disease adversely affects the survival of patients with end-stage renal disease. *Kidney International,* 75**,** 746-751.

Kshirsagar, A. V., S. Offenbacher, K. L. Moss, S. P. Barros & J. D. Beck (2007) Antibodies to periodontal organisms are associated with decreased kidney function - The dental atherosclerosis risk in communities study. *Blood Purification,* 25**,** 125-132.

Kuboniwa, M., A. Amano & S. Shizukuishi (1998) Hemoglobin-binding protein purified from Porphyromonas gingivalis is identical to lysine-specific cysteine proteinase (Lys-gingipain). *Biochem Biophys Res Commun,* 249**,** 38-43.

Kuboniwa, M., E. L. Hendrickson, Q. Xia, T. Wang, H. Xie, M. Hackett & R. J. Lamont (2009) Proteomics of Porphyromonas gingivalis within a model oral microbial community. *BMC Microbiol,* 9**,** 98.

Kulik, E. M., K. Lenkeit, S. Chenaux & J. Meyer (2008) Antimicrobial susceptibility of periodontopathogenic bacteria. *J Antimicrob Chemother,* 61**,** 1087-91.

Kulp, A. & M. J. Kuehn (2010) Biological functions and biogenesis of secreted bacterial outer membrane vesicles. *Annu Rev Microbiol,* 64**,** 163-84.

Kumar, N. V., T. Menon, P. Pathipati & K. M. Cherian (2013) 16S rRNA sequencing as a diagnostic tool in the identification of culture-negative endocarditis in surgically treated patients. *J Heart Valve Dis,* 22**,** 846-9.

Kumar, P. S., A. L. Griffen, J. A. Barton, B. J. Paster, M. L. Moeschberger & E. J. Leys (2003) New bacterial species associated with chronic periodontitis. *J Dent Res,* 82**,** 338-44.

Lagendijk, A. K., G. A. Gomez, S. Baek, D. Hesselson, W. E. Hughes, S. Paterson, D. E. Conway, H. G. Belting, M. Affolter, K. A. Smith, M. A. Schwartz, A. S. Yap & B. M. Hogan (2017) Live imaging molecular changes in junctional tension upon VE-cadherin in zebrafish. *Nat Commun,* 8**,** 1402.

Lagendijk, A. K., A. S. Yap & B. M. Hogan (2014) Endothelial cell-cell adhesion during zebrafish vascular development. *Cell Adh Migr,* 8**,** 136-45.

Lalla, E., I. B. Lamster, M. A. Hofmann, L. Bucciarelli, A. P. Jerud, S. Tucker, Y. Lu, P. N. Papapanou & A. M. Schmidt (2003) Oral infection with a periodontal pathogen

accelerates early atherosclerosis in apolipoprotein E-null mice. *Arteriosclerosis Thrombosis and Vascular Biology,* 23**,** 1405-1411.

Lamont, R. J., A. Chan, C. M. Belton, K. T. Izutsu, D. Vasel & A. Weinberg (1995) Porphyromonas gingivalis invasion of gingival epithelial cells. *Infect Immun,* 63**,** 3878-85.

Lamont, R. J. & H. F. Jenkinson (1998) Life below the gum line: Pathogenic mechanisms of Porphyromonas gingivalis. *Microbiology and Molecular Biology Reviews,* 62**,** 1244-+.

Lang, N. P., J. Lindhe & N. P. Lang. 2015. *Clinical periodontology and implant dentistry [electronic resource].* Chichester, West Sussex, UK: Chichester, West Sussex, UK : Wiley Blackwell, 2015.

Latz, E., T. S. Xiao & A. Stutz (2013) Activation and regulation of the inflammasomes. *Nat Rev Immunol,* 13**,** 397-411.

Lee, J. Y., D. P. Miller, L. Wu, C. R. Casella, Y. Hasegawa & R. J. Lamont (2018) Maturation of the Mfa1 Fimbriae in the Oral Pathogen. *Front Cell Infect Microbiol,* 8**,** 137.

Leys, E. J., S. R. Lyons, M. L. Moeschberger, R. W. Rumpf & A. L. Griffen (2002) Association of Bacteroides forsythus and a novel Bacteroides phylotype with periodontitis. *J Clin Microbiol,* 40**,** 821-5.

Li, L., E. Messas, E. L. Batista, R. A. Levine & S. Amar (2002) Porphyromonas gingivalis infection accelerates the progression of atherosclerosis in a heterozygous apolipoprotein E-deficient murine model. *Circulation,* 105**,** 861-867.

Li, P. L. (2015) Cardiovascular pathobiology of inflammasomes: inflammatory machinery and beyond. *Antioxid Redox Signal,* 22**,** 1079-83.

Lindskog Jonsson, A., F. F. Hållenius, R. Akrami, E. Johansson, P. Wester, C. Arnerlöv, F. Bäckhed & G. Bergström (2017) Bacterial profile in human atherosclerotic plaques. *Atherosclerosis,* 263**,** 177-183.

Livak, K. J. & T. D. Schmittgen (2001) Analysis of relative gene expression data using real-time quantitative PCR and the 2(-Delta Delta C(T)) Method. *Methods,* 25**,** 402-8.

Lockhart, P. B., M. T. Brennan, H. C. Sasser, P. C. Fox, B. J. Paster & F. K. Bahrani-Mougeot (2008) Bacteremia associated with toothbrushing and dental extraction. *Circulation,* 117**,** 3118-25.

Long, J., Q. Cai, M. Steinwandel, M. K. Hargreaves, S. R. Bordenstein, W. J. Blot, W. Zheng & X. O. Shu (2017) Association of oral microbiome with type 2 diabetes risk. *Journal of Periodontal Research,* 52**,** 636-643.

Loos, B. G. (2005) Systemic markers of inflammation in periodontitis. *J Periodontol,* 76**,** 2106-15.

--- (2006) Systemic effects of periodontitis. *Ann R Australas Coll Dent Surg,* 18**,** 27-9.

Loos, B. G., J. Craandijk, F. J. Hoek, P. M. Wertheim-van Dillen & U. van der Velden (2000) Elevation of systemic markers related to cardiovascular diseases in the peripheral blood of periodontitis patients. *J Periodontol,* 71**,** 1528-34.

Lourbakos, A., Y. P. Yuan, A. L. Jenkins, J. Travis, P. Andrade-Gordon, R. Santulli, J. Potempa & R. N. Pike (2001) Activation of protease-activated receptors by gingipains from Porphyromonas gingivalis leads to platelet aggregation: a new trait in microbial pathogenicity. *Blood,* 97**,** 3790-3797.

Lucas, A. R., R. K. Verma, E. Dai, L. Liu, H. Chen, S. Kesavalu, M. Rivera, I. Velsko, S. Ambadapadi, S. Chukkapalli & L. Kesavalu (2014) Myxomavirus anti-inflammatory chemokine binding protein reduces the increased plaque growth induced by chronic Porphyromonas gingivalis oral infection after balloon angioplasty aortic injury in mice. *PLoS One,* 9**,** e111353.

MacArthur Clark, J. (2018) The 3Rs in research: a contemporary approach to replacement, reduction and refinement. *Br J Nutr,* 120**,** S1-S7.

Macuch, P. J. & A. C. Tanner (2000) Campylobacter species in health, gingivitis, and periodontitis. *J Dent Res,* 79**,** 785-92.

Madan, M., B. Bishayi, M. Hoge, E. Messas & S. Amar (2007) Doxycycline affects diet- and bacteria-associated atherosclerosis in an ApoE heterozygote murine model: cytokine profiling implications. *Atherosclerosis,* 190**,** 62-72.

Mang-de la Rosa, M. R., L. Castellanos-Cosano, M. J. Romero-Perez & A. Cutando (2014) The bacteremia of dental origin and its implications in the appearance of bacterial endocarditis. *Med Oral Patol Oral Cir Bucal,* 19**,** e67-74.

Manoil, D., K. Al-Manei & G. N. Belibasakis (2020) A Systematic Review of the Root Canal Microbiota Associated with Apical Periodontitis: Lessons from Next-Generation Sequencing. *Proteomics Clin Appl,* 14**,** e1900060.

Mantri, C. K., C. H. Chen, X. Dong, J. S. Goodwin, S. Pratap, V. Paromov & H. Xie (2015) Fimbriae-mediated outer membrane vesicle production and invasion of Porphyromonas gingivalis. *Microbiologyopen,* 4**,** 53-65.

Mao, S., N. Maeno, S. Matayoshi, K. Yoshiie, T. Fujimura & H. Oda (2004) The induction of intercellular adhesion molecule-1 on human umbilical vein endothelial cells by a heat-stable component of Porphyromonas gingivalis. *Curr Microbiol,* 48**,** 108-12.

Marcelino, S. L., E. Gaetti-Jardim, V. Nakano, L. A. D. Canonico, F. D. Nunes, R. F. M. Lotufo, F. E. Pustiglioni, G. A. Romito & M. J. Avila-Campos (2010) Presence of periodontopathic bacteria in coronary arteries from patients with chronic periodontitis. *Anaerobe,* 16**,** 629-632.

Marsh, P. D. (1994) Microbial ecology of dental plaque and its significance in health and disease. *Adv Dent Res,* 8**,** 263-71.

Marsh, P. D., D. A. Head & D. A. Devine (2014) Prospects of oral disease control in the future - an opinion. *J Oral Microbiol,* 6**,** 26176.

Marsh, P. D. & E. Zaura (2017) Dental biofilm: ecological interactions in health and disease. *Journal of clinical periodontology,* 44 Suppl 18**,** S12-S22.

Martinho, F. C., F. R. Leite, L. M. Nóbrega, M. S. Endo, G. G. Nascimento, R. P. Darveau & B. P. Gomes (2016) Comparison of Fusobacterium nucleatum and Porphyromonas gingivalis Lipopolysaccharides Clinically Isolated from Root Canal Infection in the Induction of Pro-Inflammatory Cytokines Secretion. *Braz Dent J,* 27**,** 202-7.

Marín, M. J., E. Figuero, I. González, A. O'Connor, P. Diz, M. Álvarez, D. Herrera & M. Sanz (2016) Comparison of the detection of periodontal pathogens in bacteraemia after tooth brushing by culture and molecular techniques. *Med Oral Patol Oral Cir Bucal,* 21**,** e276-84.

Masi, S., F. D'Aiuto & J. Deanfield (2019) Cardiovascular prevention starts from your mouth. *Eur Heart J,* 40**,** 1146-1148.

Mayrand, D. & S. C. Holt (1988) Biology of asaccharolytic black-pigmented Bacteroides species. *Microbiol Rev,* 52**,** 134-52.

Mendes, R. T., D. Nguyen, D. Stephens, F. Pamuk, D. Fernandes, T. E. Van Dyke & A. Kantarci (2016) Endothelial Cell Response to Fusobacterium nucleatum. *Infect Immun,* 84**,** 2141-2148.

Merchant, A. T., G. J. Nahhas, R. P. Wadwa, J. J. Zhang, Y. F. Tang, L. R. Johnson, D. M. Maahs, F. Bishop, R. Teles & E. H. Morrato (2016) Periodontal Microorganisms and Cardiovascular Risk Markers in Youth With Type 1 Diabetes and Without Diabetes. *Journal of Periodontology,* 87**,** 376-384.

Mesia, R., F. Gholami, H. Huang, M. Clare-Salzler, I. Aukhil, S. M. Wallet & L. M. Shaddox (2016) Systemic inflammatory responses in patients with type 2 diabetes with chronic periodontitis. *BMJ Open Diabetes Res Care,* 4**,** e000260.

Michalowicz, B. S., M. Ronderos, R. Camara-Silva, A. Contreras & J. Slots (2000) Human herpesviruses and Porphyromonas gingivalis are associated with juvenile periodontitis. *J Periodontol,* 71**,** 981-8.

Mikuls, T. R., J. B. Payne, F. Yu, G. M. Thiele, R. J. Reynolds, G. W. Cannon, J. Markt, D. McGowan, G. S. Kerr, R. S. Redman, A. Reimold, G. Griffiths, M. Beatty, S. M. Gonzalez, D. A. Bergman, B. C. Hamilton, 3rd, A. R. Erickson, J. Sokolove, W. H. Robinson, C. Walker, F. Chandad & J. R. O'Dell (2014) Periodontitis and Porphyromonas gingivalis in patients with rheumatoid arthritis. *Arthritis Rheumatol,* 66**,** 1090-100.

Miyatani, F., N. Kuriyama, I. Watanabe, R. Nomura, K. Nakano, D. Matsui, E. Ozaki, T. Koyama, M. Nishigaki, T. Yamamoto, T. Mizuno, A. Tamura, K. Akazawa, A. Takada, K. Takeda, K. Yamada, M. Nakagawa, M. Ihara, N. Kanamura, R. P. Friedland & Y. Watanabe (2015) Relationship between Cnm-positive Streptococcus mutans and cerebral microbleeds in humans. *Oral Dis,* 21**,** 886-93.

Momen-Heravi, F., A. Babic, S. S. Tworoger, L. Zhang, K. Wu, S. A. Smith-Warner, S. Ogino, A. T. Chan, J. Meyerhardt, E. Giovannucci, C. Fuchs, E. Cho, D. S. Michaud, M. J. Stampfer, Y. H. Yu, D. Kim & X. Zhang (2017) Periodontal disease, tooth loss and colorectal cancer risk: Results from the Nurses' Health Study. *Int J Cancer,* 140**,** 646-652.

Montero, E., P. Matesanz, A. Nobili, J. Luis Herrera-Pombo, M. Sanz, A. Guerrero, A. Bujaldón, D. Herrera & S. R. N. o. D. Clinics (2020) Screening of undiagnosed hyperglycaemia in the dental setting: The DiabetRisk study. A field trial. *J Clin Periodontol*.

Mougeot, J. L. C., C. B. Stevens, B. J. Paster, M. T. Brennan, P. B. Lockhart & F. K. B. Mougeot (2017a) Porphyromonas gingivalis is the most abundant species detected in coronary and femoral arteries. *Journal of oral microbiology,* 9**,** 1281562-1281562.

--- (2017b) Porphyromonas gingivalis is the most abundant species detected in coronary and femoral arteries. *Journal of Oral Microbiology,* 9.

Muller, W. A. (1995) The role of PECAM-1 (CD31) in leukocyte emigration: studies in vitro and in vivo. *J Leukoc Biol,* 57**,** 523-8.

Murakami, S., B. L. Mealey, A. Mariotti & I. L. C. Chapple (2018) Dental plaque-induced gingival conditions. *J Periodontol,* 89 Suppl 1**,** S17-S27.

Mühlemann, H. R. & S. Son (1971) Gingival sulcus bleeding--a leading symptom in initial gingivitis. *Helv Odontol Acta,* 15**,** 107-13.

Nahid, M. A., M. Rivera, A. Lucas, E. K. L. Chan & L. Kesavalu (2011) Polymicrobial Infection with Periodontal Pathogens Specifically Enhances MicroRNA miR-146a in ApoE(-/-) Mice during Experimental Periodontal Disease. *Infection and Immunity,* 79**,** 1597-1605.

Nakagawa, I., A. Amano, M. Kuboniwa, T. Nakamura, S. Kawabata & S. Hamada (2002) Functional differences among FimA variants of Porphyromonas gingivalis and their effects on adhesion to and invasion of human epithelial cells. *Infect Immun,* 70**,** 277-85.

Nakao, R., H. Hasegawa, B. Dongying, M. Ohnishi & H. Senpuku (2016) Assessment of outer membrane vesicles of periodontopathic bacterium Porphyromonas gingivalis as possible mucosal immunogen. *Vaccine,* 34**,** 4626-4634.

Nakao, R., S. Takashiba, S. Kosono, M. Yoshida, H. Watanabe, M. Ohnishi & H. Senpuku (2014) Effect of Porphyromonas gingivalis outer membrane vesicles on gingipain-mediated detachment of cultured oral epithelial cells and immune responses. *Microbes Infect,* 16**,** 6-16.

Nakashima, Y., E. W. Raines, A. S. Plump, J. L. Breslow & R. Ross (1998) Upregulation of VCAM-1 and ICAM-1 at atherosclerosis-prone sites on the endothelium in the ApoE-deficient mouse. *Arterioscler Thromb Vasc Biol,* 18**,** 842-51.

Nassar, H., H. H. Chou, M. Khlgatian, F. C. Gibson, T. E. Van Dyke & C. A. Genco (2002) Role for fimbriae and lysine-specific cysteine proteinase gingipain K in expression of interleukin-8 and monocyte chemoattractant protein in Porphyromonas gingivalis-infected endothelial cells. *Infection and Immunity,* 70**,** 268-276.

Naylor, K. L., M. Widziolek, S. Hunt, M. Conolly, M. Hicks, P. Stafford, J. Potempa, C. Murdoch, C. W. Douglas & G. P. Stafford (2017) Role of OmpA2 surface regions of Porphyromonas gingivalis in host-pathogen interactions with oral epithelial cells. *Microbiologyopen,* 6.

Nazir, M. A. (2017) Prevalence of periodontal disease, its association with systemic diseases and prevention. *Int J Health Sci (Qassim),* 11**,** 72-80.

Noble, J. M., N. Scarmeas, R. S. Celenti, M. S. V. Elkind, C. B. Wright, N. Schupf & P. N. Papapanou (2014) Serum IgG Antibody Levels to Periodontal Microbiota Are Associated with Incident Alzheimer Disease. *Plos One,* 9.

Nosho, K., Y. Sukawa, Y. Adachi, M. Ito, K. Mitsuhashi, H. Kurihara, S. Kanno, I. Yamamoto, K. Ishigami, H. Igarashi, R. Maruyama, K. Imai, H. Yamamoto & Y. Shinomura (2016) Association of Fusobacterium nucleatum with immunity and molecular alterations in colorectal cancer. *World J Gastroenterol,* 22**,** 557-66.

O'Connor, S., C. Taylor, L. A. Campbell, S. Epstein & P. Libby (2001) Potential infectious etiologies of atherosclerosis: a multifactorial perspective. *Emerg Infect Dis,* 7**,** 780-8.

Offenbacher, S., P. N. Madianos, C. M. E. Champagne, J. H. Southerland, D. W. Paquette, R. C. Williams, G. Slade & J. D. Beck (1999) Periodontitis-atherosclerosis syndrome: an expanded model of pathogenesis. *Journal of Periodontal Research,* 34**,** 346-352.

Oliveira, F. A., C. P. Forte, P. G. Silva, C. B. Lopes, R. C. Montenegro, A. K. Santos, C. R. Sobrinho, M. R. Mota, F. B. Sousa & A. P. Alves (2015) Molecular Analysis of Oral Bacteria in Heart Valve of Patients With Cardiovascular Disease by Real-Time Polymerase Chain Reaction. *Medicine (Baltimore),* 94**,** e2067.

Olsen, I. & J. Potempa (2014) Strategies for the inhibition of gingipains for the potential treatment of periodontitis and associated systemic diseases. *J Oral Microbiol,* 6.

Olsen, I. & A. Progulske-Fox (2015) Invasion of Porphyromonas gingivalis strains into vascular cells and tissue. *Journal of Oral Microbiology,* 7.

Olsen, I., M. A. Taubman & S. K. Singhrao (2016) Porphyromonas gingivalis suppresses adaptive immunity in periodontitis, atherosclerosis, and Alzheimer's disease. *J Oral Microbiol,* 8**,** 33029.

Ozok, A. R., I. F. Persoon, S. M. Huse, B. J. Keijser, P. R. Wesselink, W. Crielaard & E. Zaura (2012) Ecology of the microbiome of the infected root canal system: a comparison between apical and coronal root segments. *Int Endod J,* 45**,** 530-41.

Page, R. C., P. Davies & A. C. Allison (1973) Effects of dental plaque on the production and release of lysosomal hydrolases by macrophages in culture. *Arch Oral Biol,* 18**,** 1481-95.

Papapanou, P. N., M. Sanz, N. Buduneli, T. Dietrich, M. Feres, D. H. Fine, T. F. Flemmig, R. Garcia, W. V. Giannobile, F. Graziani, H. Greenwell, D. Herrera, R. T. Kao, M. Kebschull, D. F. Kinane, K. L. Kirkwood, T. Kocher, K. S. Kornman, P. S. Kumar, B. G. Loos, E. Machtei, H. Meng, A. Mombelli, I. Needleman, S. Offenbacher, G. J. Seymour, R. Teles & M. S. Tonetti (2018) Periodontitis: Consensus report of workgroup 2 of the 2017 World Workshop on the Classification of Periodontal and Peri-Implant Diseases and Conditions. *J Periodontol,* 89 Suppl 1**,** S173-S182.

Passerini, A. G., D. C. Polacek, C. Shi, N. M. Francesco, E. Manduchi, G. R. Grant, W. F. Pritchard, S. Powell, G. Y. Chang, C. J. Stoeckert & P. F. Davies (2004) Coexisting proinflammatory and antioxidative endothelial transcription profiles in a disturbed flow region of the adult porcine aorta. *Proc Natl Acad Sci U S A,* 101**,** 2482-7.

Peng, C. H., Y. S. Yang, K. C. Chan, E. Kornelius, J. Y. Chiou & C. N. Huang (2017) Periodontal Treatment and the Risks of Cardiovascular Disease in Patients with Type 2 Diabetes: A Retrospective Cohort Study. *Intern Med,* 56**,** 1015-1021.

Pereira, P. A. B., V. T. E. Aho, L. Paulin, E. Pekkonen, P. Auvinen & F. Scheperjans (2017) Oral and nasal microbiota in Parkinson's disease. *Parkinsonism & Related Disorders,* 38**,** 61-67.

Persoon, I. F., M. J. Buijs, A. R. Özok, W. Crielaard, B. P. Krom, E. Zaura & B. W. Brandt (2017) The mycobiome of root canal infections is correlated to the bacteriome. *Clin Oral Investig,* 21**,** 1871-1881.

Persoon, I. F. & A. R. Özok (2017) Definitions and Epidemiology of Endodontic Infections. *Curr Oral Health Rep,* 4**,** 278-285.

Pinnock, A., C. Murdoch, K. Moharamzadeh, S. Whawell & C. W. Douglas (2014) Characterisation and optimisation of organotypic oral mucosal models to study Porphyromonas gingivalis invasion. *Microbes Infect,* 16**,** 310-9.

Pitts, N., D. Zero, P. Marsh, K. Ekstrand, J. Weintraub, F. Ramos-Gomez, J. Tagami, S. Twetman, G. Tsakos & A. Ismail (2017) Dental caries. *Nature Reviews Disease Primers,* 3**,** 1-16.

Potempa, J., A. Sroka, T. Imamura & J. Travis (2003) Gingipains, the major cysteine proteinases and virulence factors of Porphyromonas gingivalis: structure, function and assembly of multidomain protein complexes. *Curr Protein Pept Sci,* 4**,** 397-407.

Potempa, M., J. Potempa, M. Okroj, K. Popadiak, S. Eick, K. A. Nguyen, K. Riesbeck & A. M. Blom (2008) Binding of complement inhibitor C4b-binding protein contributes to serum resistance of Porphyromonas gingivalis. *J Immunol,* 181**,** 5537-44.

Power, M., D. Tilman, J. Estes, B. Menge, W. Bond, L. Mills, G. Daily, J. Castilla, J. Lubchenco & R. Paine (1996) Challenges in the quest for keystones. *Bioscience,* 46**,** 609-620.

Pradeep, A. R., R. Kathariya, P. A. Raju, R. S. Rani, A. Sharma & N. M. Raghavendra (2012) Risk factors for chronic kidney diseases may include periodontal diseases, as estimated by the correlations of plasma pentraxin-3 levels: a case-control study. *International Urology and Nephrology,* 44**,** 829-839.

Pride, D. T., J. Salzman, M. Haynes, F. Rohwer, C. Davis-Long, R. A. White, P. Loomer, G. C. Armitage & D. A. Relman (2012) Evidence of a robust resident bacteriophage population revealed through analysis of the human salivary virome. *ISME J,* 6**,** 915-26.

Pritchard, A. B., S. Crean, I. Olsen & S. K. Singhrao (2017) Periodontitis, Microbiomes and their Role in Alzheimer's Disease. *Frontiers in Aging Neuroscience,* 9.

Privratsky, J. R. & P. J. Newman (2014) PECAM-1: regulator of endothelial junctional integrity. *Cell Tissue Res,* 355**,** 607-19.

Rahman, A. & F. Fazal (2009) Hug tightly and say goodbye: role of endothelial ICAM-1 in leukocyte transmigration. *Antioxid Redox Signal,* 11**,** 823-39.

Ramseier, C. A., A. Anerud, M. Dulac, M. Lulic, M. P. Cullinan, G. J. Seymour, M. J. Faddy, W. Bürgin, M. Schätzle & N. P. Lang (2017) Natural history of periodontitis: Disease progression and tooth loss over 40 years. *J Clin Periodontol,* 44**,** 1182-1191.

Rapala-Kozik, M., G. Bras, B. Chruscicka, J. Karkowska-Kuleta, A. Sroka, H. Herwald, K. A. Nguyen, S. Eick, J. Potempa & A. Kozik (2011) Adsorption of components of the plasma kinin-forming system on the surface of Porphyromonas gingivalis involves gingipains as the major docking platforms. *Infect Immun,* 79**,** 797-805.

Read, M. A., M. Z. Whitley, S. Gupta, J. W. Pierce, J. Best, R. J. Davis & T. Collins (1997) Tumor necrosis factor alpha-induced E-selectin expression is activated by the nuclear factor-kappaB and c-JUN N-terminal kinase/p38 mitogen-activated protein kinase pathways. *J Biol Chem,* 272**,** 2753-61.

Reich, E. & K. A. Hiller (1993) Reasons for tooth extraction in the western states of Germany. *Community Dent Oral Epidemiol,* 21**,** 379-83.

Reyes, L., D. Herrera, E. Kozarov, S. Roldan & A. Progulske-Fox (2013a) Periodontal bacterial invasion and infection: contribution to atherosclerotic pathology. *Journal of Clinical Periodontology,* 40**,** S30-S50.

--- (2013b) Periodontal bacterial invasion and infection: contribution to atherosclerotic pathology (Reprinted from Journal of Clinical Periodontology, vol 40, pg S30-S50, 2013). *Journal of Periodontology,* 84**,** S30-S50.

Ribatti, D., B. Nico, A. Vacca, L. Roncali & F. Dammacco (2002) Endothelial cell heterogeneity and organ specificity. *J Hematother Stem Cell Res,* 11**,** 81-90.

Rivera, M. F., J. Y. Lee, M. Aneja, V. Goswami, L. Liu, I. M. Velsko, S. S. Chukkapalli, I. Bhattacharyya, H. Chen, A. R. Lucas & L. N. Kesavalu (2013) Polymicrobial infection with major periodontal pathogens induced periodontal disease and aortic atherosclerosis in hyperlipidemic ApoE(null) mice. *PLoS One,* 8**,** e57178.

Rodrigues, P. H., L. Reyes, A. S. Chadda, M. Bélanger, S. M. Wallet, D. Akin, W. Dunn & A. Progulske-Fox (2012) Porphyromonas gingivalis strain specific interactions with human coronary artery endothelial cells: a comparative study. *PLoS One,* 7**,** e52606.

Romero-Lastra, P., M. C. Sánchez, H. Ribeiro-Vidal, A. Llama-Palacios, E. Figuero, D. Herrera & M. Sanz (2017) Comparative gene expression analysis of Porphyromonas gingivalis ATCC 33277 in planktonic and biofilms states. *PLoS One,* 12**,** e0174669.

Rosen, S. D. & C. R. Bertozzi (1994) The selectins and their ligands. *Curr Opin Cell Biol,* 6**,** 663-73.

Rosenfeld, M. E. & L. A. Campbell (2011) Pathogens and atherosclerosis: update on the potential contribution of multiple infectious organisms to the pathogenesis of atherosclerosis. *Thromb Haemost,* 106**,** 858-67.

Ruggiero, S., R. Cosgarea, J. Potempa, B. Potempa, S. Eick & M. Chiquet (2013) Cleavage of extracellular matrix in periodontitis: gingipains differentially affect cell adhesion activities of fibronectin and tenascin-C. *Biochim Biophys Acta,* 1832**,** 517-26.

Ruokonen, H., K. Nylund, J. Furuholm, J. H. Meurman, T. Sorsa, K. Kotaniemi, F. Ortiz & A. M. Heikkinen (2017) Oral Health and Mortality in Patients With Chronic Kidney Disease. *J Periodontol,* 88**,** 26-33.

Ruospo, M., S. C. Palmer, G. Wong, J. C. Craig, M. Petruzzi, M. De Benedittis, P. Ford, D. W. Johnson, M. Tonelli, P. Natale, V. Saglimbene, F. Pellegrini, E. Celia, R. Gelfman, M. R. Leal, M. Torok, P. Stroumza, A. Bednarek-Skublewska, J. Dulawa, L. Frantzen, D. Del Castillo, S. Schon, A. G. Bernat, J. Hegbrant, C. Wollheim, L. Gargano, C. P. Bots, G. F. Strippoli & O. Investigators (2017) Periodontitis and early mortality among adults treated with hemodialysis: a multinational propensity-matched cohort study. *BMC Nephrol,* 18**,** 166.

Saito, A., S. Inagaki, R. Kimizuka, K. Okuda, Y. Hosaka, T. Nakagawa & K. Ishihara (2008a) Fusobacterium nucleatum enhances invasion of human gingival epithelial and aortic endothelial cells by Porphyromonas gingivalis. *Fems Immunology and Medical Microbiology,* 54**,** 349-355.

--- (2008b) Fusobacterium nucleatum enhances invasion of human gingival epithelial and aortic endothelial cells by Porphyromonas gingivalis. *FEMS Immunol Med Microbiol,* 54**,** 349-55.

Sanz, M., D. Beighton, M. Curtis, J. Cury, I. Dige, H. Dommisch, R. Ellwood, R. Giacaman, D. Herrera, M. Herzberg, E. Kononen, P. Marsh, J. Meyle, A. Mira, A. Molina, A. Mombelli, M. Quirynen, E. Reynolds, L. Shapira & E. Zaura (2017) Role of microbial biofilms in the maintenance of oral health and in the development of dental caries and periodontal diseases. Consensus report of group 1 of the Joint EFP/ORCA workshop on the boundaries between caries and periodontal disease. *Journal of Clinical Periodontology,* 44**,** S5-S11.

Sanz, M., A. Marco Del Castillo, S. Jepsen, J. R. Gonzalez-Juanatey, F. D'Aiuto, P. Bouchard, I. Chapple, T. Dietrich, I. Gotsman, F. Graziani, D. Herrera, B. Loos, P. Madianos, J. B. Michel, P. Perel, B. Pieske, L. Shapira, M. Shechter, M. Tonetti, C. Vlachopoulos & G. Wimmer (2020) Periodontitis and cardiovascular diseases: Consensus report. *J Clin Periodontol,* 47**,** 268-288.

Saremi, A., R. G. Nelson, M. Tulloch-Reid, R. L. Hanson, M. L. Sievers, G. W. Taylor, M. Shlossman, P. H. Bennett, R. Genco & W. C. Knowler (2005) Periodontal disease and mortality in type 2 diabetes. *Diabetes Care,* 28**,** 27-32.

Scannapieco, F. A. (2006) Pneumonia in nonambulatory patients - The role of oral bacteria and oral hygiene. *Journal of the American Dental Association,* 137**,** 21S-25S.

Schenkein, H. A. & B. G. Loos (2013) Inflammatory mechanisms linking periodontal diseases to cardiovascular diseases. *Journal of Clinical Periodontology,* 40**,** S51-S69.

Schenkein, H. A., P. N. Papapanou, R. Genco & M. Sanz (2020) Mechanisms underlying the association between periodontitis and atherosclerotic disease. *Periodontol 2000,* 83**,** 90-106.

Schätzle, M., H. Löe, W. Bürgin, A. Anerud, H. Boysen & N. P. Lang (2003) Clinical course of chronic periodontitis. I. Role of gingivitis. *J Clin Periodontol,* 30**,** 887-901.

Segal, L. N., J. C. Clemente, J. C. Tsay, S. B. Koralov, B. C. Keller, B. G. Wu, Y. Li, N. Shen, E. Ghedin, A. Morris, P. Diaz, L. Huang, W. R. Wikoff, C. Ubeda, A. Artacho, W. N. Rom, D. H. Sterman, R. G. Collman, M. J. Blaser & M. D. Weiden (2016) Enrichment of the lung microbiome with oral taxa is associated with lung inflammation of a Th17 phenotype. *Nat Microbiol,* 1**,** 16031.

Serra e Silva Filho, W., R. C. V. Casarin, E. L. Nicolela Junior, H. M. Passos, A. W. Sallum & R. B. Goncalves (2014) Microbial Diversity Similarities in Periodontal Pockets and Atheromatous Plaques of Cardiovascular Disease Patients. *Plos One,* 9.

Settem, R. P., A. T. El-Hassan, K. Honma, G. P. Stafford & A. Sharma (2012) Fusobacterium nucleatum and Tannerella forsythia induce synergistic alveolar bone loss in a mouse periodontitis model. *Infect Immun,* 80**,** 2436-43.

Sharma, A., S. Inagaki, W. Sigurdson & H. K. Kuramitsu (2005) Synergy between Tannerella forsythia and Fusobacterium nucleatum in biofilm formation. *Oral Microbiol Immunol,* 20**,** 39-42.

Sheets, S. M., J. Potempa, J. Travis, C. A. Casiano & H. M. Fletcher (2005) Gingipains from Porphyromonas gingivalis W83 induce cell adhesion molecule cleavage and apoptosis in endothelial cells. *Infect Immun,* 73**,** 1543-52.

Sheets, S. M., J. Potempa, J. Travis, H. M. Fletcher & C. A. Casiano (2006) Gingipains from Porphyromonas gingivalis W83 synergistically disrupt endothelial cell adhesion and can induce caspase-independent apoptosis. *Infect Immun,* 74**,** 5667-78.

Shi, T., M. Min, C. Sun, Y. Zhang, M. Liang & Y. Sun (2018) Periodontal disease and susceptibility to breast cancer: A meta-analysis of observational studies. *J Clin Periodontol*.

Shin, J. M., T. Luo, K. H. Lee, D. Guerreiro, T. M. Botero, N. J. McDonald & A. H. Rickard (2018) Deciphering Endodontic Microbial Communities by Next-generation Sequencing. *J Endod,* 44**,** 1080-1087.

Shoji, M., M. Naito, H. Yukitake, K. Sato, E. Sakai, N. Ohara & K. Nakayama (2004) The major structural components of two cell surface filaments of Porphyromonas gingivalis are matured through lipoprotein precursors. *Mol Microbiol,* 52**,** 1513-25.

Shokeen, B., M. D. B. Dinis, F. Haghighi, N. C. Tran & R. Lux (2021) Omics and interspecies interaction. *Periodontol 2000,* 85**,** 101-111.

Siqueira, J. & I. Rocas (2009) The Microbiota of Acute Apical Abscesses. *Journal of Dental Research,* 88**,** 61-65.

Siqueira, J. & I. Roccas (2008) Clinical Implications and Microbiology of Bacterial Persistence after Treatment Procedures. *Journal of Endodontics,* 34**,** 1291-1301.

Siqueira, J. F. & I. N. Rôças (2007) Bacterial pathogenesis and mediators in apical periodontitis. *Braz Dent J,* 18**,** 267-80.

Socransky, S. S. & A. D. Haffajee (1992) The bacterial etiology of destructive periodontal disease: current concepts. *J Periodontol,* 63**,** 322-31.

Socransky, S. S., A. D. Haffajee, M. A. Cugini, C. Smith & R. L. Kent (1998) Microbial complexes in subgingival plaque. *J Clin Periodontol,* 25**,** 134-44.

Solowiej, A., P. Biswas, D. Graesser & J. A. Madri (2003) Lack of platelet endothelial cell adhesion molecule-1 attenuates foreign body inflammation because of decreased angiogenesis. *Am J Pathol,* 162**,** 953-62.

Stafford, P., J. Higham, A. Pinnock, C. Murdoch, C. W. Douglas, G. P. Stafford & D. W. Lambert (2013) Gingipain-dependent degradation of mammalian target of rapamycin pathway proteins by the periodontal pathogen Porphyromonas gingivalis during invasion. *Mol Oral Microbiol,* 28**,** 366-78.

Stary, H. C. (2000) Natural history and histological classification of atherosclerotic lesions: an update. *Arterioscler Thromb Vasc Biol,* 20**,** 1177-8.

Stathopoulou, P. G., M. R. Benakanakere, J. C. Galicia & D. F. Kinane (2009) The host cytokine response to Porphyromonas gingivalis is modified by gingipains. *Oral Microbiol Immunol,* 24**,** 11-7.

Sullivan, C. & C. H. Kim (2008) Zebrafish as a model for infectious disease and immune function. *Fish Shellfish Immunol,* 25**,** 341-50.

Sullivan, C., M. A. Matty, D. Jurczyszak, K. A. Gabor, P. J. Millard, D. M. Tobin & C. H. Kim (2017) Infectious disease models in zebrafish. *Methods Cell Biol,* 138**,** 101-136.

Szafranski, S. P., Z.-L. Deng, J. Tomasch, M. Jarek, S. Bhuju, M. Rohde, H. Sztajer & I. Wagner-Doebler (2017) Quorum sensing of Streptococcus mutans is activated by Aggregatibacter actinomycetemcomitans and by the periodontal microbiome. *Bmc Genomics,* 18.

Szulc, M., W. Kustrzycki, D. Janczak, D. Michalowska, D. Baczynska & M. Radwan-Oczko (2015) Presence of Periodontopathic Bacteria DNA in Atheromatous Plaques from Coronary and Carotid Arteries. *Biomed Research International*.

Tada, H., S. Sugawara, E. Nemoto, T. Imamura, J. Potempa, J. Travis, H. Shimauchi & H. Takada (2003) Proteolysis of ICAM-1 on human oral epithelial cells by gingipains. *J Dent Res,* 82**,** 796-801.

Takahashi, Y., M. Davey, H. Yumoto, F. C. Gibson & C. A. Genco (2006) Fimbria-dependent activation of pro-inflammatory molecules in Porphyromonas gingivalis infected human aortic endothelial cells. *Cellular Microbiology,* 8**,** 738-757.

Takii, R., T. Kadowaki, T. Tsukuba & K. Yamamoto (2018) Inhibition of gingipains prevents Porphyromonas gingivalis-induced preterm birth and fetal death in pregnant mice. *Eur J Pharmacol,* 824**,** 48-56.

Tapiero, H., G. Mathe, P. Couvreur & K. D. Tew (2002) Dossier: Free amino acids in human health and pathologies - I. Arginine. *Biomedicine & Pharmacotherapy,* 56**,** 439-445.

Tashiro, K., T. Shimokama, S. Haraoka, O. Tokunaga & T. Watanabe (1994) Endothelial cell heterogeneity in experimentally-induced rabbit atherosclerosis. Demonstration of multinucleated giant endothelial cells by scanning electron microscopy and cell culture. *Virchows Arch,* 425**,** 521-9.

Terpenning, M. S., G. W. Taylor, D. E. Lopatin, C. K. Kerr, B. L. Dominguez & W. J. Loesche (2001) Aspiration pneumonia: Dental and oral risk factors in an older veteran population. *Journal of the American Geriatrics Society,* 49**,** 557-563.

Theilade, E., W. H. Wright, S. B. Jensen & H. Löe (1966) Experimental gingivitis in man. II. A longitudinal clinical and bacteriological investigation. *J Periodontal Res,* 1**,** 1-13.

To, S. S., P. M. Newman, V. J. Hyland, B. G. Robinson & L. Schrieber (1996) Regulation of adhesion molecule expression by human synovial microvascular endothelial cells in vitro. *Arthritis Rheum,* 39**,** 467-77.

Tomás, I., P. Diz, A. Tobías, C. Scully & N. Donos (2012) Periodontal health status and bacteraemia from daily oral activities: systematic review/meta-analysis. *J Clin Periodontol,* 39**,** 213-28.

Tonetti, M. S., T. E. Van Dyke & w. g. o. t. j. E. A. workshop (2013) Periodontitis and atherosclerotic cardiovascular disease: consensus report of the Joint EFP/AAP Workshop on Periodontitis and Systemic Diseases. *J Periodontol,* 84**,** S24-9.

Totten, K., W. Dunn & A. Progulske-Fox (2006) Effects of Porphyromonas gingivalis gingipains on junctional proteins and cell death of human endothelial cells. *Abstracts of the General Meeting of the American Society for Microbiology,* 106**,** 73-73.

Tovar-Lopez, F., P. Thurgood, C. Gilliam, N. Nguyen, E. Pirogova, K. Khoshmanesh & S. Baratchi (2019) A Microfluidic System for Studying the Effects of Disturbed Flow on Endothelial Cells. *Front Bioeng Biotechnol,* 7**,** 81.

Trombelli, L., R. Farina, C. O. Silva & D. N. Tatakis (2018) Plaque-induced gingivitis: Case definition and diagnostic considerations. *J Periodontol,* 89 Suppl 1**,** S46-S73.

Tucker, W. (1932) The possible relation of aciduric and acidogenic micro organisms to dental caries. *Journal of Infectious Diseases,* 51**,** 444-459.

Tuomainen, A. M., M. Jauhiainen, P. T. Kovanen, J. Metso, S. Paju & P. J. Pussinen (2008) Aggregatibacter actinomycetemcomitans induces MMP-9 expression and proatherogenic lipoprotein profile in apoE-deficient mice. *Microbial Pathogenesis,* 44**,** 111-117.

van Heyningen, V. (2019) Genome sequencing-the dawn of a game-changing era. *Heredity (Edinb),* 123**,** 58-66.

Vandamme, T. F. (2014) Use of rodents as models of human diseases. *J Pharm Bioallied Sci,* 6**,** 2-9.

--- (2015) Rodent models for human diseases. *Eur J Pharmacol,* 759**,** 84-9.

Veith, P. D., C. Luong, K. H. Tan, S. G. Dashper & E. C. Reynolds (2018) Outer Membrane Vesicle Proteome of Porphyromonas gingivalis Is Differentially Modulated Relative to the Outer Membrane in Response to Heme Availability. *J Proteome Res,* 17**,** 2377-2389.

Velsko, I. M., S. S. Chukkapalli, M. F. Rivera, J.-Y. Lee, H. Chen, D. Zheng, I. Bhattacharyya, P. R. Gangula, A. R. Lucas & L. Kesavalu (2014) Active Invasion of Oral and Aortic Tissues by Porphyromonas gingivalis in Mice Causally Links Periodontitis and Atherosclerosis. *Plos One,* 9.

Velsko, I. M., S. S. Chukkapalli, M. F. Rivera-Kweh, D. Zheng, I. Aukhil, A. R. Lucas, H. Larjava & L. Kesavalu (2015) Periodontal pathogens invade gingiva and aortic adventitia and elicit inflammasome activation in αvβ6 integrin-deficient mice. *Infect Immun,* 83**,** 4582-93.

Vieira Colombo, A. P., C. B. Magalhães, F. A. Hartenbach, R. Martins do Souto & C. Maciel da Silva-Boghossian (2016) Periodontal-disease-associated biofilm: A reservoir for pathogens of medical importance. *Microb Pathog,* 94**,** 27-34.

Vinogradov, E., F. St Michael & A. D. Cox (2017a) Structure of the LPS O-chain from Fusobacterium nucleatum strain 12230. *Carbohydr Res,* 448**,** 115-117.

--- (2017b) The structure of the LPS O-chain of Fusobacterium nucleatum strain 25586 containing two novel monosaccharides, 2-acetamido-2,6-dideoxy-l-altrose and a 5-acetimidoylamino-3,5,9-trideoxy-gluco-non-2-ulosonic acid. *Carbohydr Res,* 440-441**,** 10-15.

--- (2018a) Structure of the LPS O-chain from Fusobacterium nucleatum strain ATCC 23726 containing a novel 5,7-diamino-3,5,7,9-tetradeoxy-l-gluco-non-2-ulosonic acid presumably having the d-glycero-l-gluco configuration. *Carbohydr Res,* 468**,** 69-72.

--- (2018b) Structure of the LPS O-chain from Fusobacterium nucleatum strain MJR 7757 B. *Carbohydr Res,* 463**,** 37-39.

Vinogradov, E., F. St Michael, K. Homma, A. Sharma & A. D. Cox (2017c) Structure of the LPS O-chain from Fusobacterium nucleatum strain 10953, containing sialic acid. *Carbohydr Res,* 440-441**,** 38-42.

Wade, W., H. Thompson, A. Rybalka & S. Vartoukian (2016) Uncultured Members of the Oral Microbiome. *Journal of the California Dental Association,* 44**,** 447-56.

Wade, W. G. (2013) The oral microbiome in health and disease. *Pharmacol Res,* 69**,** 137-43.

Walter, C., J. Zahlten, B. Schmeck, C. Schaudinn, S. Hippenstiel, E. Frisch, A. C. Hocke, N. Pischon, H. K. Kuramitsu, J. P. Bernimoulin, N. Suttorp & M. Krüll (2004) Porphyromonas gingivalis strain-dependent activation of human endothelial cells. *Infect Immun,* 72**,** 5910-8.

Wan, M., J. R. Liu, D. Wu, X. P. Chi & X. Y. Ouyang (2015) E-selectin expression induced by Porphyromonas gingivalis in human endothelial cells via nucleotide-binding oligomerization domain-like receptors and Toll-like receptors. *Molecular Oral Microbiology,* 30**,** 399-410.

Wang, Y. & J. S. Alexander (2011) Analysis of endothelial barrier function in vitro. *Methods Mol Biol,* 763**,** 253-64.

Watts, A., E. M. Crimmins & M. Gatz (2008) Inflammation as a potential mediator for the association between periodontal disease and Alzheimer's disease. *Neuropsychiatr Dis Treat,* 4**,** 865-76.

Wayakanon, K., M. H. Thornhill, C. W. Douglas, A. L. Lewis, N. J. Warren, A. Pinnock, S. P. Armes, G. Battaglia & C. Murdoch (2013) Polymersome-mediated intracellular delivery of antibiotics to treat Porphyromonas gingivalis-infected oral epithelial cells. *FASEB J,* 27**,** 4455-65.

Werdan, K., S. Dietz, B. Löffler, S. Niemann, H. Bushnaq, R. E. Silber, G. Peters & U. Müller-Werdan (2014) Mechanisms of infective endocarditis: pathogen-host interaction and risk states. *Nat Rev Cardiol,* 11**,** 35-50.

Widziolek, M., T. K. Prajsnar, S. Tazzyman, G. P. Stafford, J. Potempa & C. Murdoch (2016) Zebrafish as a new model to study effects of periodontal pathogens on cardiovascular diseases. *Sci Rep,* 6**,** 36023.

Wiggenhauser, L. M. & J. Kroll (2018) Vascular damage in obesity and diabetes: Highlighting links between endothelial dysfunction and metabolic disease in zebrafish and man. *Curr Vasc Pharmacol*.

Wilson, W., K. A. Taubert, M. Gewitz, P. B. Lockhart, L. M. Baddour, M. Levison, A. Bolger, C. H. Cabell, M. Takahashi, R. S. Baltimore, J. W. Newburger, B. L. Strom, L. Y. Tani, M. Gerber, R. O. Bonow, T. Pallasch, S. T. Shulman, A. H. Rowley, J. C. Burns, P. Ferrier, T. Gardner, D. Goff & D. T. Durack (2007) Prevention of infective endocarditis: Guidelines from the American heart association. *Journal of the American Dental Association,* 138**,** 739-760.

Wittchen, E. S. (2009) Endothelial signaling in paracellular and transcellular leukocyte transmigration. *Front Biosci (Landmark Ed),* 14**,** 2522-45.

Woodfin, A., M. B. Voisin & S. Nourshargh (2007) PECAM-1: a multi-functional molecule in inflammation and vascular biology. *Arterioscler Thromb Vasc Biol,* 27**,** 2514-23.

Wu, J., B. A. Peters, C. Dominianni, Y. Zhang, Z. Pei, L. Yang, Y. Ma, M. P. Purdue, E. J. Jacobs, S. M. Gapstur, H. Li, A. V. Alekseyenko, R. B. Hayes & J. Ahn (2016) Cigarette smoking and the oral microbiome in a large study of American adults. *ISME J,* 10**,** 2435-46.

Wu, Z. & H. Nakanishi (2014) Connection Between Periodontitis and Alzheimer's Disease: Possible Roles of Microglia and Leptomeningeal Cells. *Journal of Pharmacological Sciences,* 126**,** 8-13.

Wunsch, C. M. & J. P. Lewis (2015) Porphyromonas gingivalis as a Model Organism for Assessing Interaction of Anaerobic Bacteria with Host Cells. *J Vis Exp,* e53408.

Wyble, C. W., K. L. Hynes, J. Kuchibhotla, B. C. Marcus, D. Hallahan & B. L. Gewertz (1997) TNF-alpha and IL-1 upregulate membrane-bound and soluble E-selectin through a common pathway. *J Surg Res,* 73**,** 107-12.

Xie, H. (2015) Biogenesis and function of Porphyromonas gingivalis outer membrane vesicles. *Future Microbiol,* 10**,** 1517-27.

Xu, W., Y. Pan, Q. Xu, Y. Wu, J. Pan, J. Hou, L. Lin, X. Tang, C. Li, J. Liu & D. Zhang (2018) Porphyromonas gingivalis ATCC 33277 promotes intercellular adhesion molecule-1 expression in endothelial cells and monocyte-endothelial cell adhesion through macrophage migration inhibitory factor. *BMC Microbiol,* 18**,** 16.

Xuan, Y., Q. Shi, G.-J. Liu, Q.-X. Luan & Y. Cai (2017) Porphyromonas gingivalis Infection Accelerates Atherosclerosis Mediated by Oxidative Stress and Inflammatory Responses in ApoE-/- Mice. *Clinical Laboratory,* 63**,** 1627-1637.

Yamaguchi, Y., T. Kurita-Ochiai, R. Kobayashi, T. Suzuki & T. Ando (2015) Activation of the NLRP3 inflammasome in Porphyromonas gingivalis-accelerated atherosclerosis. *Pathogens and Disease,* 73.

Yamatake, K., M. Maeda, T. Kadowaki, R. Takii, T. Tsukuba, T. Ueno, E. Kominami, S. Yokota & K. Yamamoto (2007) Role for gingipains in Porphyromonas gingivalis traffic to phagolysosomes and survival in human aortic endothelial cells. *Infect Immun,* 75**,** 2090-100.

Yang, S. F., H. D. Huang, W. L. Fan, Y. J. Jong, M. K. Chen, C. N. Huang, C. Y. Chuang, Y. L. Kuo, W. H. Chung & S. C. Su (2018) Compositional and functional variations of oral microbiota associated with the mutational changes in oral cancer. *Oral Oncol,* 77**,** 1-8.

Yang, W. W., B. Guo, W. Y. Jia & Y. Jia (2016) Porphyromonas gingivalis-derived outer membrane vesicles promote calcification of vascular smooth muscle cells through ERK1/2-RUNX2. *Febs Open Bio,* 6**,** 1310-1319.

Yao, E. S., R. J. Lamont, S. P. Leu & A. Weinberg (1996) Interbacterial binding among strains of pathogenic and commensal oral bacterial species. *Oral Microbiol Immunol,* 11**,** 35-41.

Yonel, Z., E. Cerullo, A. T. Kröger & L. J. Gray (2020) Use of dental practices for the identification of adults with undiagnosed type 2 diabetes mellitus or non-diabetic hyperglycaemia: a systematic review. *Diabet Med,* 37**,** 1443-1453.

Yonel, Z. & P. Sharma (2017) The Role of the Dental Team in the Prevention of Systemic Disease: the Importance of Considering Oral Health As Part of Overall Health. *Prim Dent J,* 6**,** 24-27.

Yun, P. L., A. A. Decarlo, C. C. Chapple & N. Hunter (2005) Functional implication of the hydrolysis of platelet endothelial cell adhesion molecule 1 (CD31) by gingipains of Porphyromonas gingivalis for the pathology of periodontal disease. *Infect Immun,* 73**,** 1386-98.

Yun, P. L., A. A. Decarlo & N. Hunter (2006) Gingipains of Porphyromonas gingivalis modulate leukocyte adhesion molecule expression induced in human endothelial cells by ligation of CD99. *Infect Immun,* 74**,** 1661-72.

Zhang, F. X., C. J. Kirschning, R. Mancinelli, X. P. Xu, Y. Jin, E. Faure, A. Mantovani, M. Rothe, M. Muzio & M. Arditi (1999) Bacterial lipopolysaccharide activates nuclear factor-kappaB through interleukin-1 signaling mediators in cultured human dermal endothelial cells and mononuclear phagocytes. *J Biol Chem,* 274**,** 7611-4.

Zhang, R. & J. Ge (2017) Proteinase-Activated Receptor-2 Modulates Ve-Cadherin Expression to Affect Human Vascular Endothelial Barrier Function. *J Cell Biochem,* 118**,** 4587-4593.

Zhang, Y. H., X. Wang, H. X. Li, C. Ni, Z. B. Du & F. H. Yan (2018) Human oral microbiota and its modulation for oral health. *Biomedicine & Pharmacotherapy,* 99**,** 883-893.

Zhang, Y. M., L. J. Zhong, P. Liang, H. Liu, L. T. Mu & S. K. Ai (2008) Relationship between microorganisms in coronary atheromatous plaques and periodontal pathogenic bacteria. *Chin Med J (Engl),* 121**,** 1595-7.

Zhao, H., M. Chu, Z. Huang, X. Yang, S. Ran, B. Hu, C. Zhang & J. Liang (2017) Variations in oral microbiota associated with oral cancer. *Sci Rep,* 7**,** 11773.

Zhou, X., J. Xu & W. Shi (2017) Human oral microbiome: progress, challenge and opportunity. *Weishengwu Xuebao,* 57**,** 806-821.

# Mechanisms of vascular damage by systemic dissemination of the oral pathogen *Porphyromonas gingivalis*

Cher Farrugia[1] (iD), Graham P. Stafford[1], Jan Potempa[3,5], Robert N. Wilkinson[2], Yan Chen[4], Craig Murdoch[1] (iD) and Magdalena Widziolek[1,3,6]

1 School of Clinical Dentistry, University of Sheffield, UK
2 School of Life Sciences, Medical School, University of Nottingham, UK
3 Department of Microbiology, Faculty of Biochemistry, Biophysics and Biotechnology, Jagiellonian University, Kraków, Poland
4 Department of Infection, Immunity and Cardiovascular Disease, Medical School, University of Sheffield, UK
5 Department of Oral Immunity and Infectious Diseases, University of Louisville School of Dentistry, KY, USA
6 Department of Evolutionary Immunology, Institute of Zoology and Biomedical Research, Faculty of Biology, Jagiellonian University, Kraków, Poland

Several studies have shown a clear association between periodontal disease and increased risk of cardiovascular disease. *Porphyromonas gingivalis* (*Pg*), a key oral pathogen, and its cell surface-expressed gingipains, induce oedema in a zebrafish larvae infection model although the mechanism of these vascular effects is unknown. Here, we aimed to determine whether *Pg*-induced vascular damage is mediated by gingipains. *In vitro*, human endothelial cells from different vascular beds were invaded by wild-type (W83) but not gingipain-deficient (ΔK/R-ab) *Pg*. W83 infection resulted in increased endothelial permeability as well as decreased cell surface abundance of endothelial adhesion molecules PECAM-1 and VE-cadherin compared to infection with ΔK/R-ab. In agreement, when transgenic zebrafish larvae expressing fluorescently labelled PECAM-1 or VE-cadherin were systemically infected with W83 or ΔK/R-ab, a significant reduction in adhesion molecule fluorescence was observed specifically in endothelium proximal to W83 bacteria through a gingipain-dependent mechanism. Furthermore, this was associated with increased vascular permeability *in vivo* when assessed by dextran leakage microangiography. These data are the first to show that *Pg* directly mediates vascular damage *in vivo* by degrading PECAM-1 and VE-cadherin. Our data provide a molecular mechanism by which *Pg* might contribute to cardiovascular disease.

## Introduction

The effect of oral health on systemic disease is currently a highly debated topic with increasing evidence indicating that blood-borne oral microbes significantly contribute to conditions such as cardiovascular disease (CVD) [1,2], rheumatoid arthritis [3], diabetes [4] and Alzheimer's disease [5]. The association between periodontitis and cardiovascular disease has been studied for the last three decades and is now generally accepted in the field [6].

Periodontitis is a chronic multifactorial inflammatory disease caused by the dysbiosis of indigenous

**Abbreviations**

CVD, cardiovascular disease; HCAEC, human primary coronary artery endothelial cells; HDMEC, human dermal microvascular endothelial cells; HMEC, human microvascular endothelial cells; ICAM, intercellular adhesion molecule; PECAM, platelet endothelial cell adhesion molecule; *Pg*, *Porphyromonas gingivalis*; VE, vascular endothelial.

microorganisms and characterised by the destruction of tooth-supporting structures leading to tooth loss [7,8]. *Porphyromonas gingivalis* (*Pg*), an oral anaerobic microbe, is considered the keystone pathogen that promotes the development of severe periodontitis by favouring oral microbial dysbiosis and dysregulation of the host immune response [9]. *Pg* resides in dental plaque and produces several virulence factors that enable this microbe to colonise the host, evade the immune system and contribute to disease progression and tissue destruction [9,10]. The predominant virulence factors appear to be gingipains, cysteine proteases with significant proteolytic activity [11].

The presence of oral bacteria has been detected in peripheral blood following tooth extractions and even regular oral hygiene procedures such as tooth brushing, giving rise to a transient bacteraemia in healthy individuals [12]. However, the likelihood of bacterial entry to the circulation is greatly increased in patients with chronic gingivitis or periodontitis where bacterial-mediated loss of gingival epithelial integrity facilitates bleeding, allowing pathogenic oral bacteria facile movement from the periodontal pocket into the bloodstream [13–15]. Indeed, oral microbiome profiling performed on patients with atherosclerotic CVD undergoing bypass surgery revealed that *Pg* was the most abundant species found in nondiseased vascular tissue [16]. Furthermore, *Pg* DNA was detected in cardiac valves of patients with CVD and deep periodontal pockets [17].

*Pg* is able to bind to and invade endothelial cells cultured *in vitro* [18,19]. This microbial–host interaction mediates increased gene expression of several chemokines (e.g. CXCL8, CCL2), adhesion molecules (CD54, CD62E, PECAM-1) and inflammatory factors by endothelial cells via various mechanisms [20–22]. Paradoxically, in an attempt by the pathogen to subvert the host immune response, the proteins of these pro-inflammatory genes are degraded by *Pg*-derived gingipains [20,23,24]. Adhesion molecules localised at the cellular junctions of adjacent endothelial cells selectively regulate vascular permeability [25]. Dysregulated adhesion molecule expression may initiate vascular pathology due to abnormally elevated vascular permeability leading to oedema, chronic inflammatory and vascular damage [26]. We recently showed that *Pg* can cause vascular damage in an *in vivo* zebrafish larvae model of systemic infection in a gingipain-dependent manner [27], suggesting that these bacterial proteases may be important factors in the development of CVD. Here, we hypothesised that gingipain-dependent cleavage of endothelial cell junction adhesion molecules is important in mediating the vascular damage. By

infecting transgenic zebrafish models that have fluorescent labelling of endothelial cell junctions with a wild-type and isogenic gingipain-null *Pg* mutant, we identify that gingipains dramatically alter adhesion molecule cell surface abundance leading to increased vascular permeability *in vitro* and *in vivo*. These data significantly enhance the growing evidence for the role of oral bacteria in CVD and indicate a potential mechanism by which oral bacteria can contribute to cardiovascular disease.

## Results

### *P. gingivalis* invades human endothelial cells and localises to the perinuclear region through a gingipain-dependent mechanism

We initially confirmed *Pg* invasion of endothelial cells using an antibiotic protection assay. All wild-type laboratory strains examined (ATCC33277, W83, W50) invaded HDMEC at significantly greater levels than the clinical isolate (A245Br) ($P \leq 0.05$, Fig. 1A). Wild-type W83 was not only capable of invading various types of endothelial cells including HDMEC ($0.072\% \pm 0.032$; Fig. 1A,B), HMEC-1 ($0.48\% \pm 0.2$; Fig. 1C) and HCAEC ($0.21\% \pm 0.1$; Fig. 1D), but was also shown to be significantly more invasive than the gingipain-deficient ΔK/R-ab mutant ($P < 0.001$) that displayed on average an 85% reduction in endothelial cell invasion for the three cell types tested (Fig. 1B–D). Multichromatic confocal microscopy revealed that intracellular dwelling *Pg* were predominantly localised to the perinuclear regions, where they were colocalised within wheat germ agglutinin-positive membranes, suggesting residence within membrane-bound intracellular vesicles following internalisation, as previously shown in other model systems (Fig. 1E).

### Endothelial cell permeability increases following *Pg* infection and is gingipain-dependent

We previously demonstrated that zebrafish systemically infected with *Pg* displayed significant oedema [27], suggesting that this bacterium may influence vascular permeability. To explore this possibility, we examined HDMEC monolayer permeability following *Pg* infection *in vitro*. Microscopically, *Pg*-infected HDMEC were found to lose cell–cell attachments compared with uninfected controls (Fig. 2A). Using a high molecular weight fluorescent dextran permeability assay, we observed a time-dependent increase in the levels of fluorescence passing through the endothelial monolayer and this was significantly increased in *Pg*-
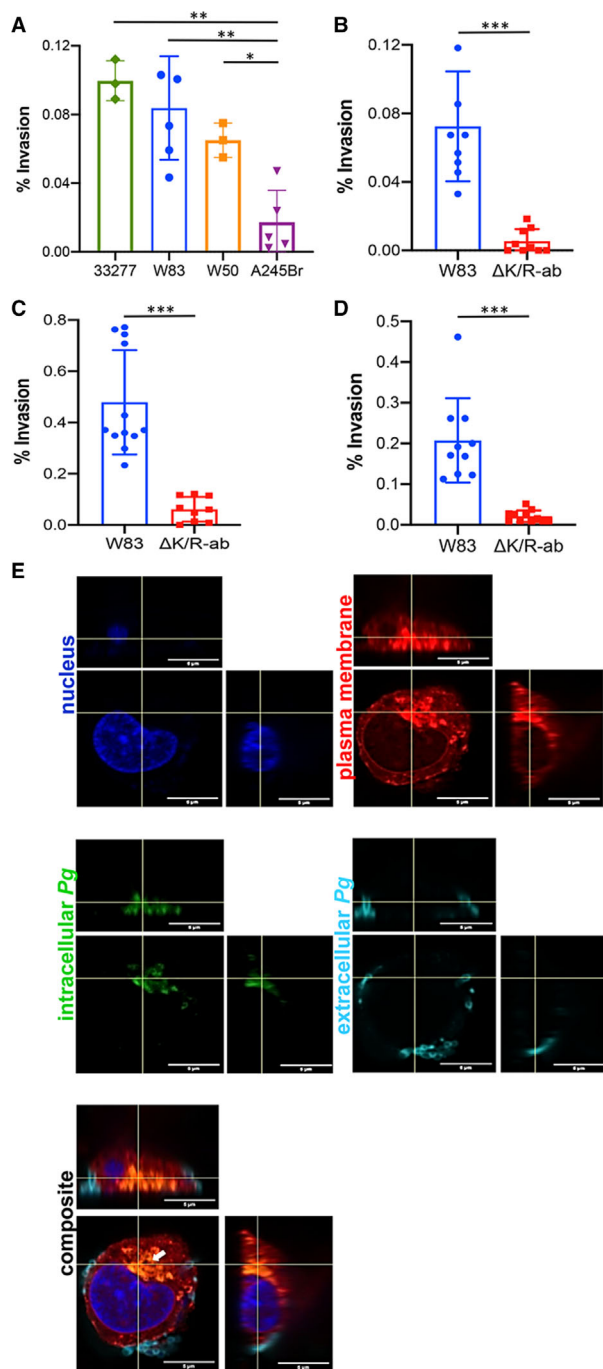
**Fig. 1.** Strain and gingipain-dependent invasion of *Pg* into human endothelial cells. HDMEC were infected with wild-type strain *Pg* ATCC33277, W83, W50 or A245Br (A) or wild-type *Pg* W83 and ΔK/R-ab (B) at a MOI 100 for 90 min. HMEC-1 (C) and HCAEC (D) were infected with wild-type *Pg* W83 or ΔK/R-ab mutant also at a MOI 100 for 90 min. Bacterial cell invasion was determined by antibiotic protection assay and expressed as a percentage of primary bacterial inoculum recovered. Graphs show means ± SD ($n$ = at least 3 individual experiments with each individual experiment performed in triplicate technical repeats; shown as filled circles). Data were analysed using one-way ANOVA with Tukey's post hoc comparison test (Fig. 1A) or Student's *t*-test (Fig 1B-D), $*P < 0.05$, $**P < 0.01$, $***P < 0.001$. Representative maximum intensity Z projection images of HMEC-1 with intracellular (green) and extracellular (cyan) *Pg* W83. Cell nucleus (blue) and plasma membrane (red). Composite image shows intracellular dwelling *Pg* as orange (green and red colocalisation, white arrow), and extracellular (cyan) bacteria bound to the cell surface (E). All images show *x*-axis, *y*-axis and *z*-axis planes, and scale bars in images are all 5 μm.

were infected with the gingipain-deficient mutant ΔK/R-ab compared with wild-type controls (Fig. 2D). Collectively, these data implicate gingipains as the primary permeabilising factor following *Pg* infection.

## *Pg* infection decreases endothelial cell surface adhesion molecule abundance but not gene expression *in vitro*

The endothelial cell surface adhesion proteins PECAM-1 (CD31) and VE-cadherin (CD144) are crucial for maintaining cell–cell junction integrity and preserving a restrictive endothelial permeability barrier [25,29]. Gingipains have been shown to mediate the proteolytic degradation of several human proteins [20,30]; therefore, we examined whether these proteases were responsible for cleavage of PECAM-1 and VE-cadherin. Flow cytometric analysis revealed that cell surface abundance of PECAM-1 on both HMEC-1 and HDMEC was almost completely abolished upon W83 infection compared with uninfected controls when analysed by both flow cytometry ($P < 0.05$; Fig. 3A,C) and immunofluorescence microscopy (Fig. 3E). In contrast, endothelial cells infected with the gingipain-null mutant, ΔK/R-ab, showed no loss of PECAM-1, displaying levels similar to uninfected controls (Fig. 3A,C). Cell surface abundance of VE-cadherin on both HMEC-1 and HDMEC was reduced by sixfold upon infection with W83 ($P \leq 0.05$; Fig. 3B,D). In contrast, cells infected with ΔK/R-ab displayed VE-cadherin levels similar to those of uninfected controls (Fig. 3B,D). Loss of VE-cadherin was observed predominantly at the cell–cell junctions by confocal microscopy, sites where this protein

treated compared with untreated HDMEC at all time points examined for up to 5 h (Fig. 2B). Moreover, this increase in endothelium permeability was significantly reduced ($P < 0.001$) compared with untreated control levels or when *Pg* W83 was pre-incubated with KYT, a specific inhibitor of gingipain activity (Fig. 2C) [28]. Similarly, endothelial permeability was also significantly reduced ($P < 0.001$) when monolayers
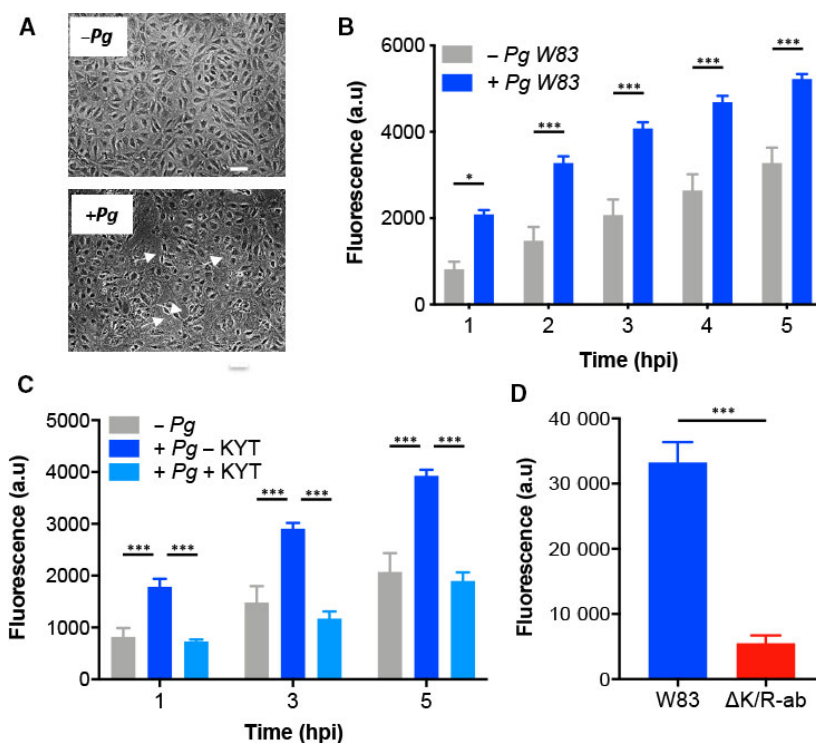
**Fig. 2.** *Pg* W83 increases permeability of endothelial cell monolayers in a gingipain-dependent manner. HDMEC (A–C) or HMEC-1 (D) cells were grown to confluent monolayers on fibronectin-coated inserts, infected with *Pg* at a MOI 1000 for 1.5 h, followed by the measurement of high molecular weight (70 kDa) fluorescein dextran passing through the monolayer barrier. Morphology of HDMEC monolayer in the absence (−*Pg*) or presence (+*Pg*) of W83 (A); white arrows indicate areas of cell attachment loss (scale bar in A = 20 μm). *In vitro* permeability assay of HDMEC in the absence (−*Pg*) or presence (+*Pg*) of W83 (B) and upon treatment with KYT inhibitors prior to HDMEC *Pg* infection (C). *In vitro* permeability assay of HMEC-1 infected with W83 or ΔK/R-ab (D). Data in B&C are presented as means ± SD and were analysed by one-way ANOVA followed by Tukey's post hoc comparison test. *$P < 0.05$, ***$P < 0.001$. Data in D are presented as means ± SD and were analysed by Student's t-test. ***$P < 0.001$; for all experiments, $n = 3$ individual experiments with each individual experiment performed in triplicate technical repeats.

preferentially accumulates (Fig. 3F). Loss of PECAM-1 adhesion molecule cell surface expression was MOI-dependent (Fig. 4A) and not due to differences in endothelial cell death upon infection as cell viability was similar to controls following infection with either W83 or ΔK/R-ab (Fig. 4B–E). In addition, reduced abundance of the endothelial cell surface adhesion molecule, E-selectin (CD62E), a protein that plays a role in leucocyte adhesion rather than vascular permeability, was also observed (Fig. 5). The levels of cell surface E-selectin were increased on HDMEC at 4 and 8 h following treatment with TNFα, whereas immortalised HMEC-1 cells did not display E-selectin at any time point examined irrespective of cytokine treatment (Fig. 5A–D). *Pg* was able to invade both HDMEC and HMEC-1 at similar levels in the absence or presence of pro-inflammatory stimulation (Fig. 5E,F). In 8-h TNFα-treated HDMEC, infection with *Pg* significantly ($P < 0.001$) reduced E-selectin cell surface abundance by fivefold compared with uninfected controls (Fig. 5G,H).

An alternative explanation for the loss of endothelial cell surface adhesion molecule expression is that the bacterial infection may reduce gene expression. To test for this possibility, we checked for differences in endothelial mRNA expression by qRT–PCR following incubation with wild-type W83 and mutant ΔK/R-ab *Pg*. Incubation with either of these strains did not significantly alter gene expression of *VE-cadherin*, *PECAM-1* or other tested cytokines (*CXCL8, CCL2, ICAM-1*) in HMEC-1 and HDMEC cultures when compared to the treatment with the potent pro-inflammatory cytokine, TNFα (Fig. 6A,B).

### *P. gingivalis* reduces endothelial cell surface adhesion molecule abundance in an *in vivo* zebrafish infection model

We next used our established *Pg* zebrafish infection model [27] to determine whether the observed changes in adhesion molecule cell surface abundance seen *in*
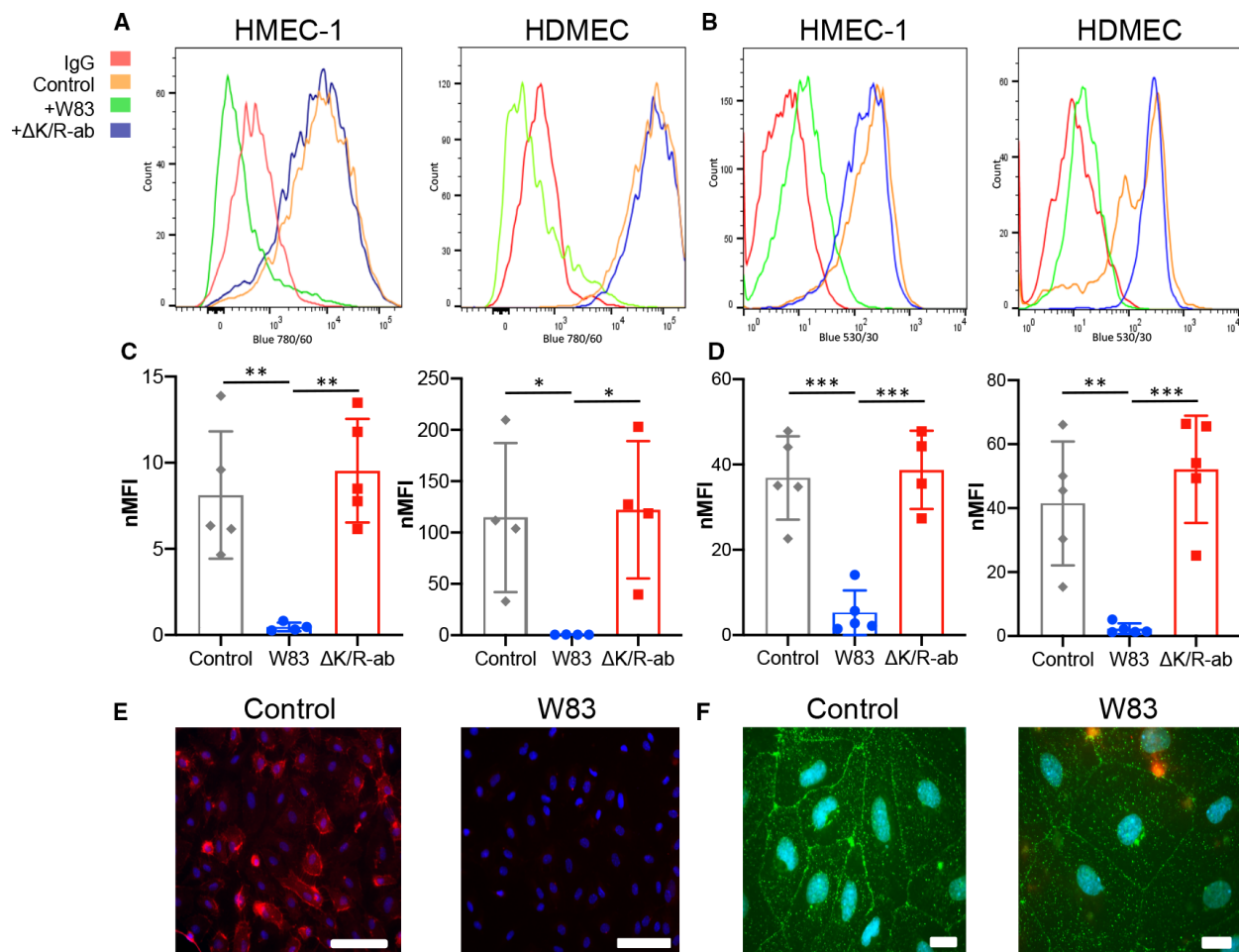
**Fig. 3.** Degradation of endothelial cell surface-expressed junctional adhesion molecules *in vitro*. Representative flow cytometry histograms of cell surface expression of PECAM-1 (A) and VE-cadherin (B) on HMEC-1 and HDMEC following infection with *Pg* W83 (green) or ΔK/R-ab mutant (blue); IgG control (red); and uninfected control (orange). Normalised median fluorescence intensity (nMFI) histograms of PECAM-1 (C) and VE-cadherin (D) on HMEC-1 and HDMEC following infection with *Pg* W83, ΔK/R-ab or uninfected control (enclosed circles represent data from each individual experiment, $n = 4$). Statistical differences were analysed by one-way ANOVA with Tukey's multiple comparison test *$P < 0.05$, **$P < 0.01$, ***$P < 0.001$. Micrograph images show immunofluorescent detection of cell surface expression of PECAM-1 (red, E) and VE-cadherin (green, F) in control or *Pg*-treated HDMEC ($n = 3$). Nuclei were counterstained blue with DAPI. Scale bars in E & F = 100 μm.

*vitro* were replicated *in vivo*. Transgenic zebrafish with endothelial cell-specific PECAM-1-EGFP expression *tg (fli1a:PECAM1-EGFP)sh524* were inoculated systemically with either red-labelled wild-type W83 or ΔK/R-ab *Pg*. Reporter fluorescence was quantified where the endothelium and *Pg* colocalised in the intersegmental vessels and the caudal vein adjacent to the yolk sac, anatomical sites that are free from any natural pigmentation to avoid problems with background fluorescence and where individual vessels were easily distinguished. In PBS-injected zebrafish, PCAM-1 expression was observed on the endothelial cell surface of the intersegmental vessels as well as the caudal

artery and vein (Fig. 7A,D). Both W83 and ΔK/R-ab gingipain-null bacteria could be visualised within the vessels at these sites (Fig. 7B,E and C,F), binding to and in some instances having traversed the vascular barrier into surrounding tissue (Fig. 7Gii). Importantly, in W83-infected zebrafish, colocalisation of *Pg* at the endothelial surface was associated with a marked reduction in endothelial PECAM-1 fluorescence at these sites (Fig. 7Gi,Gii). Consistent with our *in vitro* experiments, we observed that loss of PECAM-1-EGFP fluorescence was gingipain-dependent since infection with the gingipain-null mutant, ΔK/R-ab, was not associated with loss of PECAM-1-
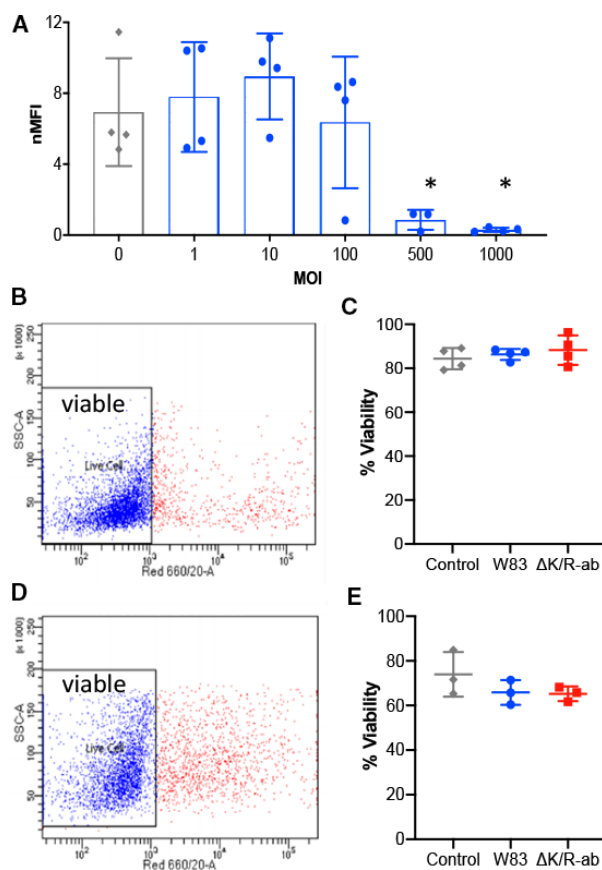
**Fig. 4.** *Pg*-mediated decrease in PECAM-1 cell surface abundance is MOI-dependent on viable endothelial cells. (A) PECAM-1 cell surface abundance on HMEC-1 cells as determined by flow cytometric analysis following infection with increasing MOI of *Pg*; uninfected cells were used as controls (enclosed circles represent data from each individual experiment). Data are displayed as normalised median fluorescence intensity (nMFI), and statistical differences were analysed by one-way ANOVA with Tukey's multiple comparison test; *$P < 0.05$, **$P < 0.01$ compared with MOI 0, 1, 10. HMEC-1 (B&C) and HDMEC (C&D) viability postinfection as assessed by a live/dead TO-PRO-3 exclusion flow cytometric assay. The level of per cent viable cells (TO-PRO-3-negative, blue dots) in the cell population was measured for W83 and ΔK/R-ab-treated cells. One-way ANOVA with Tukey's multiple comparison test showed no statistically significant differences in cell survival between groups following infection.

EGFP fluorescence (Fig. 7Gi). Indeed, fluorescence intensity analysis showed that PECAM-1 fluorescence was significantly reduced in the presence of W83 compared with ΔK/R-ab on both the intersegmental vessels in the tail (Fig. 7H, $P < 0.001$) and caudal vein (Fig. 7I, $P < 0.01$). We next employed fluorescently tagged VE-cadherin-TS transgenic zebrafish larvae and quantified transgene fluorescence following PBS, W83 or ΔK/R-ab infection (Fig. 8A–F). Similar to the effect
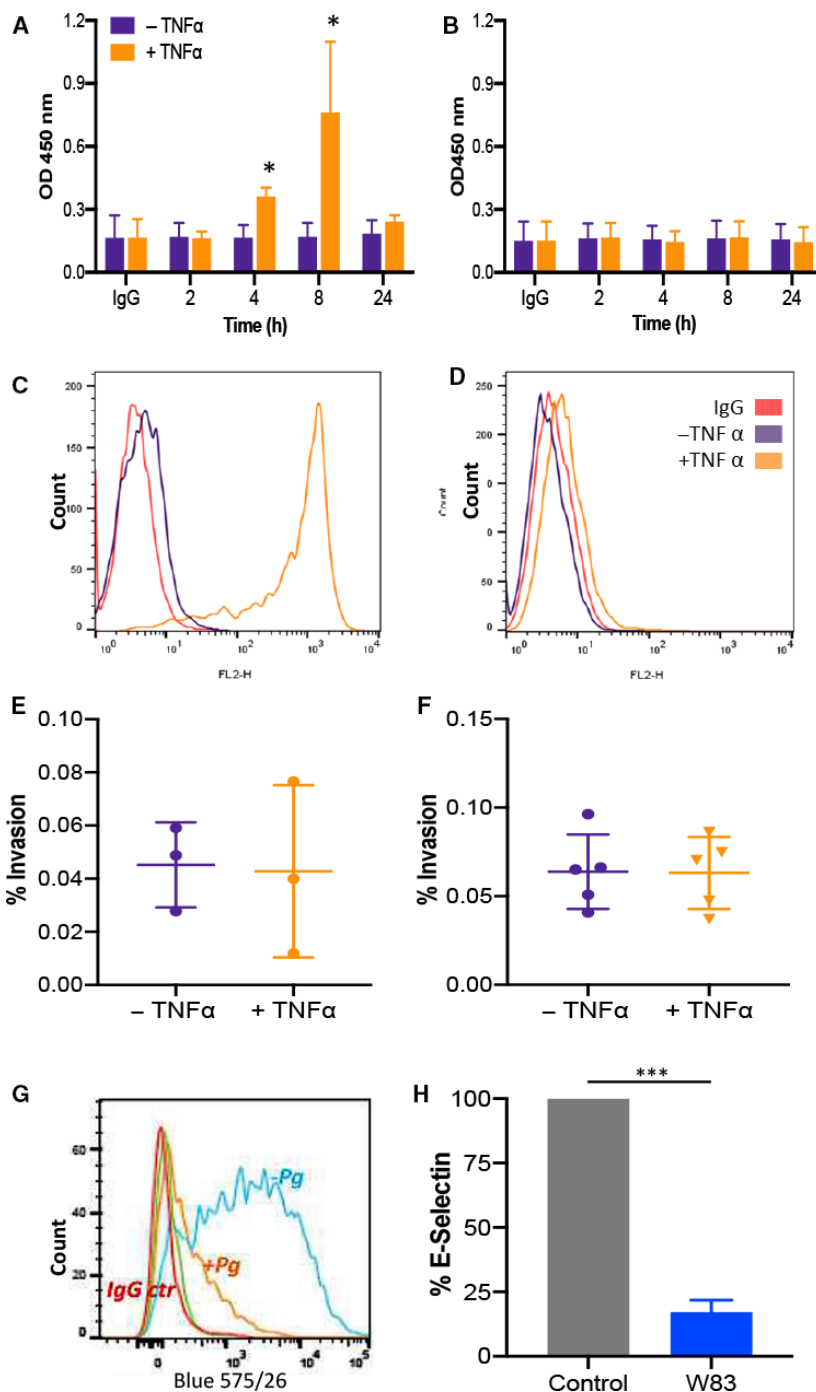
on PECAM1-EGFP, when colocalised with the vasculature (Fig. 8B,Gi), wild-type *Pg* significantly reduced the fluorescence intensity of the VE-cadherin-TS reporter on both intersegmental (Fig. 8H, $P < 0.01$) and caudal vein (Fig. 8I, $P < 0.05$) vessels when compared to ΔK/R-ab mutants, suggesting reduced fluorescence of this reporter fusion protein was also gingipain-dependent.

### *Pg* infection increases vascular permeability *in vivo*

We next tested whether *Pg* infection could also lead to increased vascular permeability in an *in vivo* setting. Here, we used transgenic zebrafish expressing a cyan fluorescent protein, mTurquiose2, in endothelial cells (*tg(fli1a:mTQ2)sh321*), to fluorescently label the vasculature and injected these with either fluorescein-labelled *Pg* or PBS as control followed by further injection with tetramethylrhodamine (a red fluorescent) dextran at 24 hpi. In PBS-injected larvae, the fluorescent dextran strictly localised to the lumen of the aortic arches, opercular artery, hypobranchial artery and other vessels in the vascular network, indicating that the high molecular weight dextran was not able to pass across the vascular barrier (Fig. 9A,D). Following infection, *Pg* was observed both within blood vessels, their surrounding tissues and in particular around the oedematous heart (Fig. 9B,E). In these infected larvae, diffuse fluorescent dextran staining was observed throughout tissues, extending far beyond the confines of the aortic arches suggesting widespread dextran leakage from vessels (Fig. 9C,F). Furthermore, dextran fluorescence was observed in the oedematous pericardiac region suggesting widespread vessel leakage in this area (Fig. 9C,F). These data, along with our *in vitro* studies, provide compelling evidence that *Pg* is able to mediate vascular damage leading to loss of endothelial integrity and increased vascular permeability.

## Discussion

Increasing evidence suggests that periodontal disease is associated with CVD and that this is influenced, in part, by bacteria that enter the circulation via diseased tissues in the oral cavity [1,6]. Further supporting evidence comes from *in vitro* studies showing that oral microbes, in particular *Pg*, can invade endothelial cells, but more compellingly from human studies where the DNA of several oral bacteria, including *Pg*, has been found in nondiseased vascular tissue from patients undergoing bypass surgery [16] as well as in atherosclerotic plaques [31–33]. However, the molecular

**Fig. 5.** *Pg W83* infection decreases E-selectin abundance on HDMEC *in vitro*. Cell surface abundance of E-selectin increased in a time-dependent manner on HDMEC (A) upon treatment with TNFα (10 ng·mL$^{-1}$) when analysed by cell-based ELISA. Expression increased at 4 h, displayed maximal expression after 8 h ($P < 0.05$, Mann–Whitney *U*-test, $n = 3$) with levels returning to baseline by 24 h. HMEC-1 cells did not express E-selectin at any time point examined (B). These data were confirmed by flow cytometric analysis where E-selectin abundance was increased on HDMEC after 8 h TNFα stimulation (C) but was not present on HMEC-1 with levels being similar to unstimulated controls (D). Whisker plots showing that stimulation of HDMEC (E) or HMEC-1 (F) with 10 ng·mL$^{-1}$ TNFα for 8 h did not result in increased invasion of *Pg* W83 compared with unstimulated control cells (enclosed squares and circles denote number of experiments performed, and data are mean ± SD). Representative flow cytometry histogram of cell surface expression of E-selectin (G) on 8 h TNFα-stimulated HDMEC following infection with *Pg* W83 (orange), IgG control (red) and uninfected control (blue). E-selectin normalised median fluorescence intensity (nMFI) histograms of *Pg* W83-infected and *Pg* W83-uninfected controls. Statistical differences in E, F and H were analysed by Mann–Whitney U-test of $n = 3$ independent experiments, ***$P < 0.001$.

mechanism driving this association is, as yet, unknown, with several divided theories proposed on how this relationship develops. Therefore, in this study we used both *in vitro* and *in vivo* approaches to decipher the mechanisms at play with particular emphasis on the role of gingipains, potent proteases known to play a key role in *Pg*-mediated disease processes [34].

Our initial *in vitro* studies using monolayers of endothelial cells from various vascular beds showed that *Pg* (strains ATCC33277, W83, W50, A245Br) were invasive but at low levels (~ 0.1%), which is in agreement with previous findings from other groups [18,19,35,36]. Collectively, these data show that endothelial cells are less susceptible to invasion than
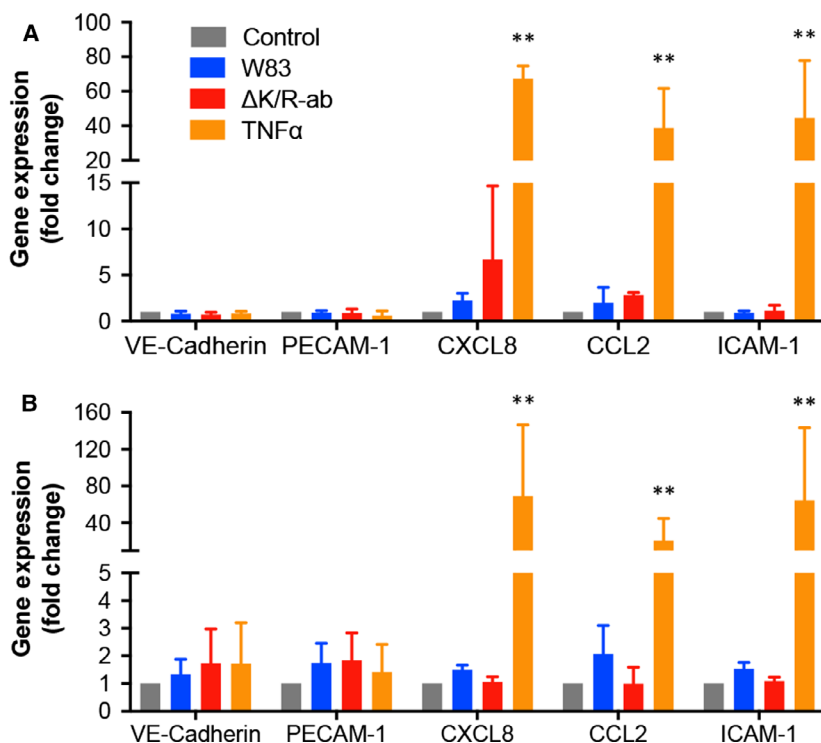
**Fig. 6.** Infection of endothelial cells with *Pg* W83 or ΔK/R-ab does not alter mRNA expression of pro-inflammatory genes. HMEC-1 (A) and HDMEC (B) cells were infected with either W83 or ΔK/R-ab (MOI 100) for 4 h, unstimulated or TNFα-stimulated (25 ng·mL$^{-1}$) cells were used as controls. Bars represent means ± SD of relative fold change expression of VE-cadherin, PECAM-1, CXCL8, CCL2 and ICAM-1. Data were analysed by Kruskal–Wallis with Dunn's multiple comparison test; **$P \leq 0.01$, $n = 3$ individual biological experiments each performed in triplicate technical repeats.

oral epithelial keratinocytes that can display from 2% to 10% cell invasion depending on the strain examined [37,38]. Moreover, the gingipain-null mutant ΔK/R-ab failed to invade endothelial cells, suggesting that bacterial gingipains are crucial for this process. Confocal microscopy analysis confirmed the presence of intracellular dwelling *Pg* enclosed within membrane-bound vesicles at perinuclear sites in endothelial cells, similar to that documented for gingival epithelial cells, most likely as a result of endocytosis [19,39,40]. Internalisation has several beneficial outcomes for the bacterium including protection from the host immune response, resistance to antibiotic therapy (many cannot pass the plasma membrane) and increased survival [39]. When infected with wild-type *Pg*, HDMEC within confluent monolayers became detached and the endothelium displayed significant loss of permeability *in vitro* that was prevented by inhibition of gingipain enzyme activity or upon infection with ΔK/R-ab, the gingipain-null strain. Similar observations were reported by Sheets *et al.* [24] who noted that bovine coronary artery endothelial cells and HDMEC exhibited loss of adhesion to tissue culture plastic upon culture with *Pg*-derived culture extracts. These data clearly point to proteolytic degradation of cell surface molecules as the likely mechanism for loss of cell–cell contacts and adhesion. Indeed, our flow cytometric and confocal microscopy analysis revealed gingipain-dependent

cleavage of PECAM-1, VE-cadherin and E-selectin (CD62E) on human endothelial cells when cultured as monolayers *in vitro*.

E-selectin is an adhesion molecule associated with tethering of leucocytes to the endothelium during inflammation. It was previously shown that *Pg* adhesion to human umbilical vein endothelial cells (HUVEC) that are derived from large blood vessels is mediated by E-selectin [24,41]. In contrast, our data indicate that *Pg* adhere and invade both E-selectin-deficient HMEC-1 and E-selectin-expressing HDMEC at similar levels, suggesting that E-selectin is not essential for invasion into microvascular endothelial cells. Gingipain-dependent degradation of other leucocyte adhesion molecules (ICAM-1/CD54, VACM-1/CD106) has also been observed [30], suggesting that *Pg* is able to modulate leucocyte recruitment at the endothelium surface. PECAM-1 and VE-cadherin act to form intercellular junctions that are crucial for maintaining a continuous endothelium and so loss of these cell–cell contacts will inevitably lead to loss of tissue integrity, increased permeability and endothelial dysfunction. In this study, loss of PECAM-1 and VE-cadherin cell surface abundance was identified in response to whole bacteria, whereas previous studies have used recombinant gingipains to show cleavage of endothelial cell surface proteins including N-cadherin and integrin β1 as well as VE-cadherin [24]. Gene expression analysis

**Fig. 7.** PECAM-1 expression in an *in vivo* zebrafish embryo systemic infection model. Representative images of spinning disc confocal micrographs showing PECAM-1 expression (green) in the tail region (A–C) and yolk region (D–F) of zebrafish embryos at 24 hpi. Embryos were injected with PBS control (A&D), wild-type W83 *Pg* (red, B&E) or ΔK/R-ab mutant (red, C, F) *n* = 15. Decreased fluorescence in W83 expression was observed in infected segmental vessels, while loss of definition in W83-infected vessels is clearer than in caudal vein and artery. Loss of PECAM-1 expression is exemplified in high-magnification images of the caudal vein showing PBS controls (Gi, top), W83-infected (Gi, middle) and ΔK/R-ab-infected (Gi, lower) embryos and in the intersegmental vessels which show a marked loss of PECAM-1 fluorescence (green) when colocalised with red-labelled W83 (Gii, circled areas). W83 can also be observed in the tissues having traversed the vasculature (Gii, white arrows). Image analysis showed significantly decreased normalised median fluorescence values and therefore PECAM-1 expression in both the tail (H) and caudal vein (I) between zebrafish embryo infected with W83 and ΔK/R-ab *Pg* (**P < 0.01, ***P < 0.001, Student's *t*-test; data are means ± SD of 3 pooled independent biological experiments (*n* = 3) with 5 technical repeats per experiment). CA, caudal artery; CV, caudal vein; DLAV, dorsal longitudinal anastomotic vessel; Se, intersegmental vessels; Y, yolk sac. Scale bar A–G = 40 μm.
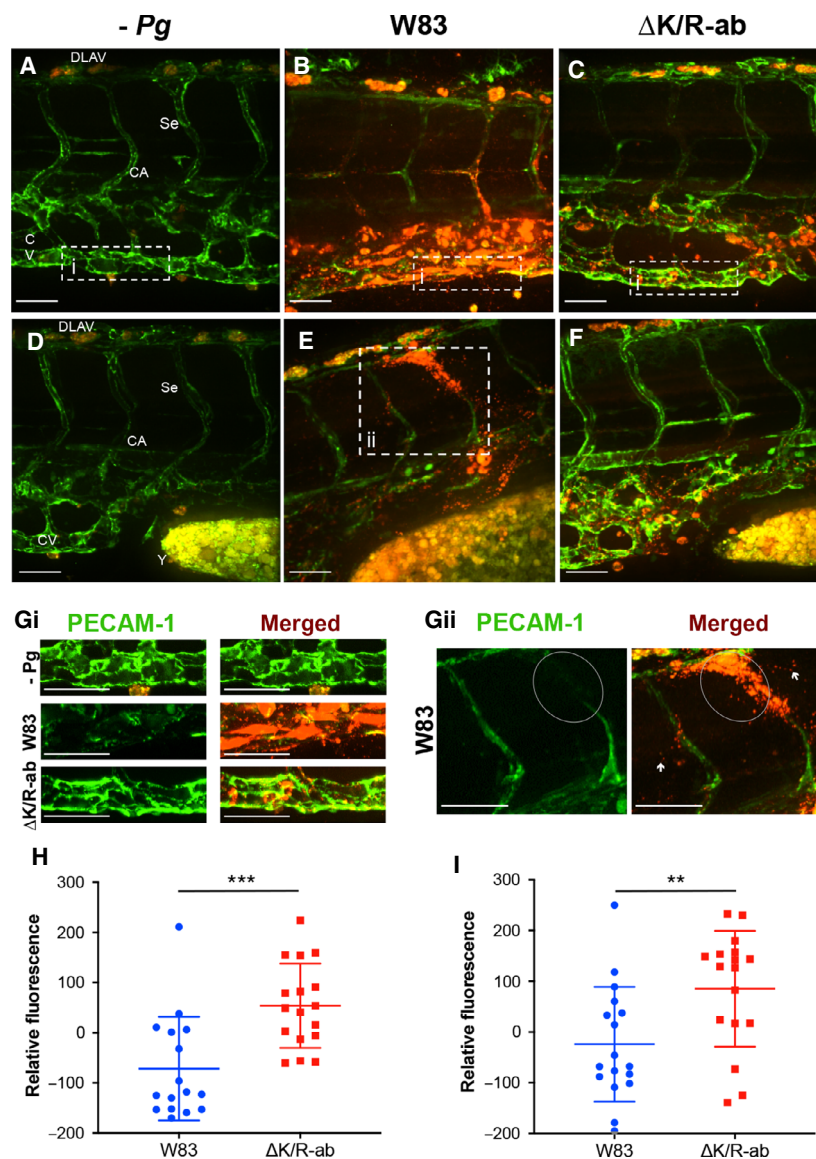
showed no change in expression levels of PECAM-1 or VE-cadherin as well as other inflammatory cytokines (CCL2, CXCL8 and ICAM-1) in response to infection with either wild-type W83 or ΔK/R-ab *Pg*, confirming that loss of cell surface protein was due to protein cleavage and not altered gene transcription. Interestingly, our gene expression data are in contrast to those reported by others who have observed increased gene expression for CCL2 (formally MCP-1) by HUVEC in response to *Pg* strain 381 [42] and ICAM-1 by E.A.hy926 cells (an endothelial/epithelial hybrid cell line) or HUVEC upon infection with *Pg* strain ATCC33277 or W83, respectively [43,44], which may be due to bacterial strain differences or to use of cell

lines or endothelial cells derived from large compared with microvascular vessels.

*In vitro* generated data using monolayer endothelium provide valuable information, but these experiments lack conditions such as flow, shear stress and presence of other cells that are important when examining systemic infection. We therefore set about confirming the *in vitro* data using our zebrafish *Pg* infection model [27]. Zebrafish have been extensively used for host–pathogen interactions as well as for cardiovascular studies [45] and have several advantages over murine models such as transparency and availability of fluorescently tagged proteins that allow for real-time analysis of cell–cell interactions. Moreover,
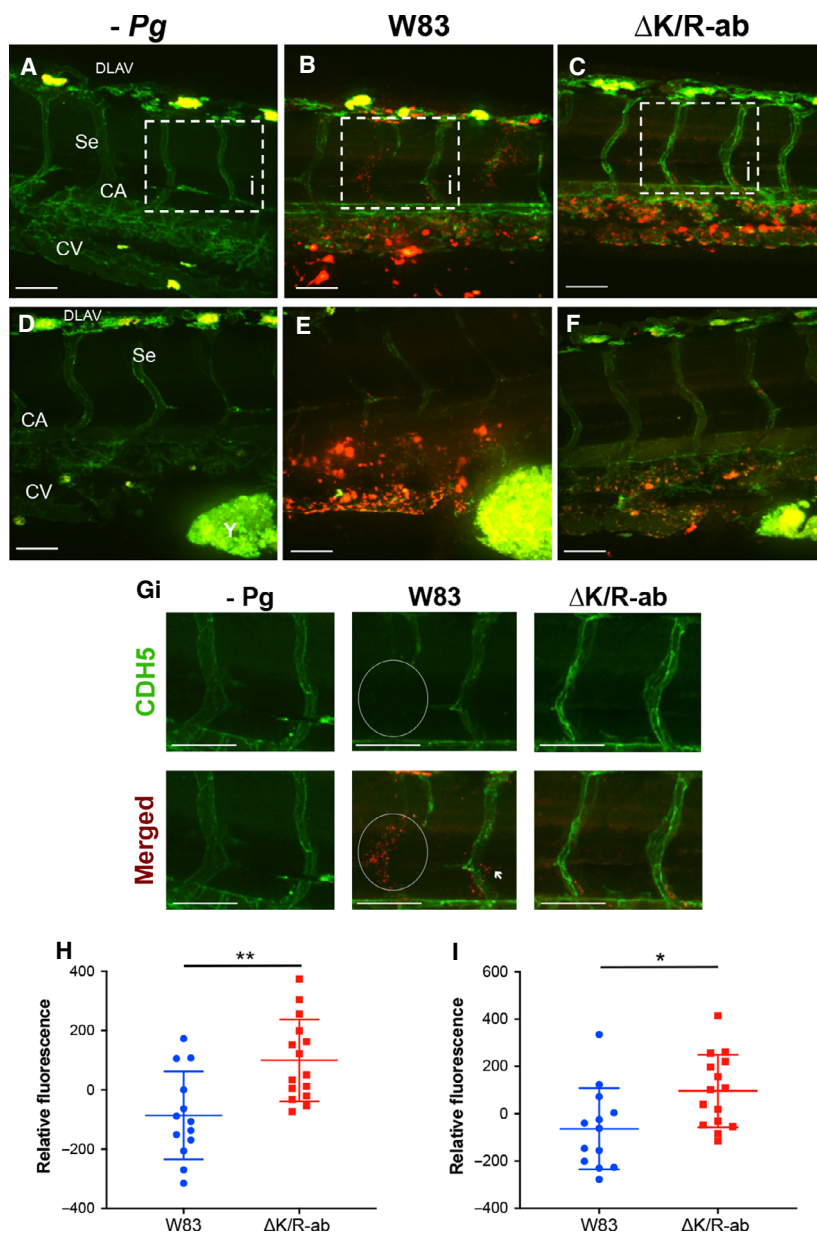
**Fig. 8.** VE-cadherin (CDH5) expression in an *in vivo* zebrafish embryo systemic infection model. Representative images of spinning disc confocal micrographs showing VE-cadherin expression (green) in the tail region (A–C) and yolk region (D–F) of zebrafish embryos at 24 hpi. Embryos were injected with PBS control (A, D), wild-type W83 *Pg* (red, B, E) or ΔK/R-ab mutant (red, C, F) $n = 12$. Decreased VE-cadherin fluorescence when colocalised with W83 was observed in infected segmental vessels and caudal vein. The loss of VE-cadherin expression is exemplified in high-magnification images from A, B and C showing PBS controls (Gi, left), W83-infected (Gi, middle) and ΔK/R-ab-infected (Gi, right) intersegmental vessels. Image analysis showed significantly decreased normalised median fluorescence values and therefore VE-cadherin expression in both the tail (G) and caudal vein (H) between zebrafish embryo infected with W83 and ΔK/R-ab mutant *Pg* (*$P < 0.05$, **$P < 0.01$, Student's *t*-test, and data are means $\pm$ SD of 3 pooled independent biological experiments ($n = 3$) with 4 technical repeats per experiment). CA, caudal artery; CV, caudal vein; DLAV, dorsal longitudinal anastomotic vessel; Se, intersegmental vessels; Y, yolk sac. Scale bar A-G = 40 μm.

the close homology between numerous zebrafish and human innate immune and cardiovascular-associated molecules means that this *in vivo* model system is also ideally placed to examine pathogen-mediated host responses that may impact on CVD risk. We previously showed that zebrafish present with oedema upon infection with wild-type but not the ΔK/R-ab gingipain-null mutant [27] and given our *in vitro* data on gingipain-dependent endothelial cell adhesion molecule degradation we hypothesised that gingipains would be responsible for cleavage of these molecules *in vivo* leading to vascular permeability. Using genetically engineered zebrafish whereby PECAM-1 or VE-cadherin

was fluorescently labelled, we observed, for the first time, *in vivo Pg*-mediated loss of fluorescence upon infection with wild-type (W83) but not with the gingipain-null mutant strain, indicating gingipain-dependent degradation of these molecules. Loss of PECAM-1 and VE-cadherin on the endothelium was most evident when colocalised with W83 *Pg* and was apparent in several vascular regions of the zebrafish indicating that infection is widespread and that *Pg* adhesion and gingipain-mediated protein degradation are not confined to specific vascular beds. Even more important was that loss of adhesion molecule abundance was associated with increased vascular permeability as
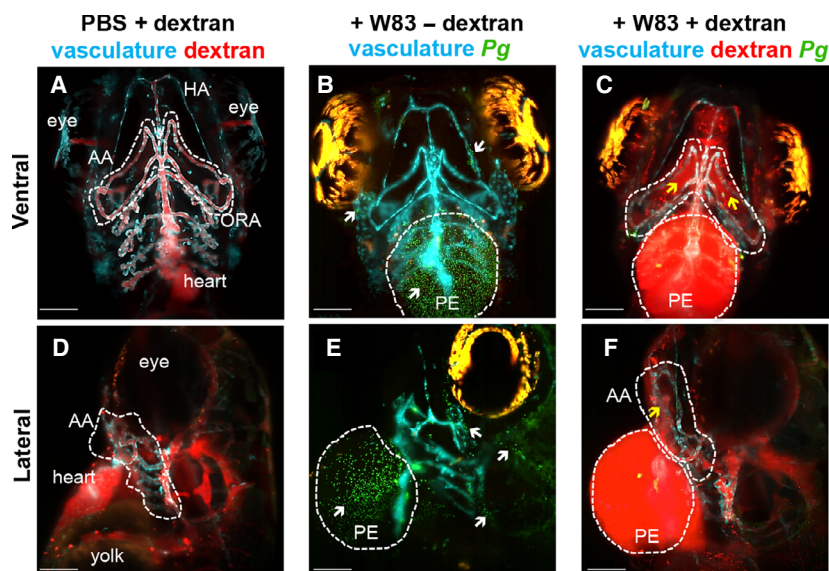
**Fig. 9.** *Pg* W83 infection increases vascular permeability in zebrafish embryos. Representative maximum intensity Z projection microangiography of PBS-injected (A, D) or fluorescein-stained wild-type W83 *Pg*-infected (green, B, C, E, F) zebrafish embryos with cyan-labelled vasculature before (B, E) and after red fluorescent dextran injection (A, C). Upper panels show ventral view and lower panels lateral view. White arrows in panels B&E indicate W83 within blood vessels, tissues and oedematous heart. Dashed lines in A, C, D and F outline the aortic arches (AA) and opercular artery (ORA) vascular regions. Yellow arrows in C and F point to regions demonstrating dextran leakage from the vasculature into the tissues. Data are representative of $n = 3$ independent biological experiments. HA, hypobranchial artery; PE, pericardial oedema. Scale bar = 100 μm.

determined by dextran vascular leakage, signifying loss of endothelium integrity and vascular damage, both implicated in the pathogenesis of cardiovascular disease [46].

Several *in vivo* studies using murine experimental models, in particular the hyperlipidaemic ApoE(null) mice, have shown that *Pg* infection directly influences atherosclerotic lesion formation or development [47,48] and several mechanisms have been suggested. However, visualising bacterial–host interactions at a cellular and even protein level are not possible in these models. To our knowledge, this is the first time that the effects of systemic *Pg* infection at the cellular level, *in vivo*, have been reported and our data clearly point to a role for *Pg* in mediating vascular damage. At present, it is unknown whether *Pg* acts as an initiating event, where it could be speculated that *Pg*-mediated endothelial cell damage leads to the exposure of the underlying vascular connective tissue leading to localised platelet activation and leucocyte recruitment. However, it could also be speculated that *Pg* acts to exacerbate the disease process by negatively modulating the immune response. Clearly, further studies are warranted to decipher the precise role of *Pg* in CVD.

As with most *in vivo* experimental infection models, animals (mice or zebrafish) are systemically inoculated

with high numbers of bacteria, much more than would be observed in humans, and it could be argued that these studies are therefore not completely physiologically relevant. However, it should be noted that many cardiovascular diseases are long-term, chronic conditions where the disease manifests over long periods with repeat exposure to transient levels of one if not several aetiological agents. Replicating this experimentally *in vivo* is extremely challenging and would require repeat low-dose inoculation or a long time frame, giving raise to ethical concerns over animal distress as well as experimental cost. Current, *in vivo* infection strategies aim to provide key information that collectively points to significant risk factors within the full knowledge of their limitations. In this regard, zebrafish provide clear benefits as an *in vivo* model to examine systemic host–pathogen interactions, and our data significantly add to others in implicating *Pg* in vascular pathogenicity. There is now an appreciation that many bacterial-mediated diseases are polymicrobial in nature, with periodontitis being a case in point where it is considered that several organisms within the subgingival plaque drive pathogenesis rather than one organism in isolation. It is therefore likely that other oral bacteria contribute to systemic disease. Indeed, in the oral context, studies have shown significant impacts on

the functional behaviour of *Pg* when in the presence of other oral microbes such as *Tannerella forsythia* or *Fusobacterium nucleatum* [49] and it will be important to determine whether other microbes affect disease progression. Nevertheless, this study provides crucial evidence for the role of *Pg*, and gingipains in particular, in affecting endothelial function, reaffirming the likely role or oral microbes in influencing systemic disease outcomes.

## Materials and methods

### *P. gingivalis* strains and culture

Wild-type strains W50, ATCC33277 and W83, as well as clinical strain A245Br, were maintained on Fastidious Anaerobe (FA) agar plates (NeoGen, Ayr, UK) supplemented with 5% v/v oxalated horse blood (Oxoid, Basingstoke, UK). Isogenic gingipain-deficient mutant $kgp\Delta598$-1732::Tc$^R$ $rgpA$-::Cm$^R$ $rgpB\Delta410$-507::Em$^R$ ($\Delta K/$R-ab) was grown on blood FA plates supplemented with 1 $\mu g \cdot mL^{-1}$ tetracycline and 5 $\mu g \cdot mL^{-1}$ erythromycin. Liquid cultures were maintained in either Schaedler (BTL Ltd., èódź, Poland) or brain–heart infusion broth (Oxoid) supplemented with 0.5 % yeast extract, 250 $\mu g \cdot mL^{-1}$ cysteine, 1 $mg \cdot mL^{-1}$ haemin and 1 $mg \cdot mL^{-1}$ vitamin K (Oxoid). Both liquid and agar cultures were incubated at 37 °C in an anaerobic chamber with an atmosphere of 80% $N_2$, 10% $CO_2$ and 10% $H_2$. For use in experiments, strains were grown as liquid cultures anaerobically overnight, adjusted to an optical density ($OD_{600}$) equal to 0.1 and cultured until late log phase. Bacteria were then harvested by centrifugation at 8000 $g$ for 3 min, washed with PBS and resuspended at the required density. For zebrafish experiments, bacteria were resuspended in PBS at $5 \times 10^9$ $CFU \cdot mL^{-1}$ for microinjection.

### Endothelial cell culture

Human primary coronary artery endothelial cells (HCAEC, purchased from the American Tissue Culture Collection) and human primary microvascular endothelial cells (HDMEC, purchased from PromoCell, Heidelberg, Germany) were maintained in MV medium containing MV supplement medium (PromoCell®), while immortalised human dermal microvascular endothelial cells (HMEC-1 provided by F.J. Candal, Centers for Disease Control and Prevention, Atlanta, GA) were grown in MCDB131 (Fisher Scientific, Loughborough, UK) supplemented with 10 $ng \cdot mL^{-1}$ epidermal growth factor (Sigma-Aldrich, Poole, UK), 1 $\mu g \cdot mL^{-1}$ hydrocortisone (Sigma), 10% v/v fetal calf serum (Thermo Fisher Scientific, Loughborough, UK) and 2 mM L-glutamine (Sigma-Aldrich). All cells were cultured at 37 °C, 5% $CO_2$ in a humidified atmosphere.

### Animals

Zebrafish maintenance and experimental work were carried out in accordance with UK Home Office regulations and UK Animals (Scientific Procedures) Act 1986 and EU directive 2010/63/EU under Project Licence P1A4A7A5E using zebrafish embryos under 5 days postfertilisation (dpf). Nacre wild-type, VE-cadherin transgenic *tg(cdh5$^{ubs8-/}$ $^-$;cdh5TS)*, PECAM-1 transgenic *tg(fli1a:PECAM1-EGFP)sh524* and *tg(fli1a:mTurquoise2)sh321* embryos were maintained in E3 medium at 30 °C according to standard protocols. Anaesthesia of zebrafish larvae was achieved by adding 0.16 $mg \cdot mL^{-1}$ tricaine (Sigma-Aldrich) to E3 medium, while addition of 0.3 $mg \cdot mL^{-1}$ tricaine was used for euthanasia.

### Generation of zebrafish transgenic lines

*Tg(fli1a:PECAM1-EGFP)sh524* was generated via injection of pTol2-fli1a-pecam1-EGFP according to standard protocols. *Tg(fli1a:mTurquoise2)sh321* was generated by PCR amplifying the coding sequence of *mTurquoise2* from pmTQ21-C1, a kind gift of Joachim Goedhart (University of Amsterdam), using the following primers 5′-ggccggatc-catggtgagcaagggcgag-3, 5′-ggccctcgagttacttgtacagctcgtc′-3′ and cloning into the BamHI/XhoI sites of pME-MCS2 [50] to generate pME-mTurquoise2. The pFli1a:mTurquoise2-SV40pA construct was generated using the Tol2kit via standard methods and the following components: *fli1a* enhancer/promoter, pDestTol2-pA2, pME-mTurquoise2 and p3E-SV40pA, and injected into embryos alongside *Tol2* mRNA at 25 $pg \cdot nL^{-1}$.

### Endothelial cell invasion quantification and visualisation

Antibiotic protection endothelial cell invasion assays were performed as described in Naylor *et al.* [51], with modification. HCAEC, HDMEC or HMEC-1 cells were seeded at $2 \times 10^5$ cells per well in a 24-well plate and cultured to confluence. Cell monolayers were washed with PBS and blocked for 1 h with 2% bovine serum albumin (BSA; Sigma-Aldrich) in cell culture medium. Endothelial cells were infected with *Pg* strains (ATCC33277, W83, W50 or A245Br) at a multiplicity of infection (MOI) of 100 in cell culture medium and incubated for 90 min at 37 °C, 5% $CO_2$. Serial dilutions were carried out to determine viable counts through colony-forming units (CFUs). Nonadhered bacteria were removed with PBS and the cell-adherent bacteria killed by incubation with 200 $\mu g \cdot mL^{-1}$ metronidazole (Sigma-Aldrich) for 1 h at 37 °C, 5 % $CO_2$. Cells were then washed with PBS, lysed with $dH_2O$, scraped, serially diluted on FA plates and incubated anaerobically for 3 days. CFUs were enumerated to determine the total

number of invading bacteria, expressed as a percentage of the viable count of the initial inoculum.

To visualise *Pg* invasion, HMEC-1 cells were grown overnight on 4-well glass-bottom culture chambers (Sarstedt AG, Nümbrecht, Germany). *Pg* W83 was fluorescently labelled by re-suspension in 0.4 μg·mL$^{-1}$ 5-(and-6-carboxyfluorescein, succinimidyl ester (5(6)-FAM, SE) (excitation 494 nm, emission 518 nm) (Thermo Fisher Scientific) in PBS for 15 min with shaking at 4 °C. FAM-labelled *Pg* were further biotinylated by diluted in 0.3 mg·mL$^{-1}$ 6-((biotinoyl)amino)hexanoic acid, succinimidyl ester (Thermo Fisher Scientific) in PBS and incubated for 30 min and then resuspended in nonsupplemented MCDB medium. FAM-biotinylated *Pg* were used for invasion (MOI 1000) into HMEC-1 cells for 1 h at 37 °C, 5% $CO_2$. HMEC-1 cells were fixed with 4% paraformaldehyde (Sigma-Aldrich) for 20 min, washed and blocked with 10% v/v FCS in PBS for 5 min. Alexa Fluor 647®-conjugated streptavidin (excitation 650 nm, emission 655 nm) (Thermo Fisher Scientific) 5 μg·mL$^{-1}$ in PBS containing 10% v/v FCS was incubated with the cells for 45 min at 37 °C, 5% $CO_2$. After washing, nuclei were counterstained with 7.5 μg·mL$^{-1}$ Hoechst® (excitation 350 nm, emission 461 nm) (Thermo Fisher Scientific) for 10 min, rinsed and the endothelial plasma membrane stained with 5 μg·mL$^{-1}$ wheat germ agglutinin (WGA) (excitation 555 nm, emission 565 nm) (Thermo Fisher Scientific) for 10 min at 37 °C. Chamber slides were analysed using a Zeiss LSM 880 inverted Axio Imager and AiryScan confocal microscope. Images were processed using AiryScan® processing (Zeiss, Oberkochen, Germany), and composite and orthogonal views were created using FIJI® software (National Institute of Health, Bethesda, MD, USA).

## Endothelial cell permeability

Endothelial monolayer permeability was measured using a Transwell assay system. Millicell® cell culture inserts (Merck Millipore, Watford, UK) were fibronectin-coated (10 μg·mL$^{-1}$) prior to seeding with HDMEC that were cultured until confluent. *Pg* W83 were treated with KYT-1 or KYT-36 (2 μM; Peptides International, Louisville, KY, USA) to inhibit gingipain activity as previously described [28]. HDMEC were infected in the absence or presence of *Pg* W83 (with or without inhibitors) at a MOI of 1000 for 1.5 h at 37 °C in nonsupplemented MV medium. Bacteria were removed, inserts transferred to a new 12-well plate with 500 μL supplemented MV medium and 450 μL of MV supplemented medium added to the apical compartment of the insert together with 70 kDa fluorescent-labelled dextran, a molecular weight that does not readily pass through a confluent endothelial monolayer (Thermo Fisher Scientific; final concentration of 65 μg·mL$^{-1}$). Dextran leakage through the cell monolayer from apical compartment of the insert to the bottom well was monitored for up to 5 h by measuring the fluorescence intensity (excitation 494 nm,

emission 521 nm; Tecan Ltd, Männedorf, Switzerland) of 250 μL medium aspirated from the bottom well; 250 μL of fresh medium was added to the bottom well for further readings. Inserts without cells were used as control wells.

## *In vitro* PECAM-1 and VE-cadherin cell adhesion protein expression

*In vitro* cell adhesion protein expression was analysed using flow cytometry and immunofluorescence microscopy. For flow cytometric analysis, HMEC-1 and HDMEC were seeded at $4 \times 10^5$ cells per well, cultured until confluent, rinsed and infected with MOI 1000 W83 or ΔK/R-ab *Pg* in nonsupplemented medium for 1 h. Addition of medium only was used as a control. Cells were washed, removed using 0.02% EDTA (Sigma-Aldrich) for 20 min, centrifuged and resuspended in 100 μL FACS buffer (0.1 % BSA and 0.1 % sodium azide in PBS). For PECAM-1 (CD31) expression, 0.06 μg per test of PE-Cyanine7-conjugated anti-human PECAM-1 (Clone MW59; Thermo Fisher Scientific) or its matching conjugated IgG control (IgG2254 Isotype Control; Thermo Fisher Scientific) was added and cells incubated for 45 min on ice. For VE-cadherin (CD144), 0.25 μg per reaction anti-human VE-cadherin antibody (Clone 123413, R&D Systems, Minneapolis, MN, USA) or IgG isotype control (Clone 11711, R&D Systems) was incubated for 45 min on ice, supernatant was removed and Alexa Fluor® 488 goat anti-mouse antiserum (Abcam, Cambridge, UK) diluted at 1 : 100 in FACS buffer was added for 30 min on ice. Cells were washed and resuspended in 300 μL FACS buffer, and single-colour sample analysis was carried out using a LSR II flow cytometer (BD Biosciences, San Jose, CA, USA) for PE-CAM1 and FACSCalibur flow cytometer (BD Biosciences) for VE-cadherin analysis. The cell viability dye, TO-PRO-3® (1 mg·mL$^{-1}$, Thermo Fisher Scientific), was added to each sample before analysis. Cell populations were gated using forward scatter (FSC) and side scatter (SSC) voltages and TO-PRO-3-positive cells excluded from the analysed population. Five thousand viable cells were collected for HDMEC analysis, while 10 000 live cells were collected for HMEC-1 analysis. Threshold for positively fluorescent cells was set using isotype-matched controls, and data were analysed using FlowJo software (BD Biosciences). The normalised median fluorescence index (nMFI) was calculated by dividing the median fluorescence intensity of the positive samples by that of the IgG controls.

For immunofluorescence microscopy, fibronectin-coated (10 μg·mL$^{-1}$) glass coverslips were seeded with $5 \times 10^4$ endothelial cells. *Pg* was stained with 5 μM Red CMTPX CellTracker® (Thermo Fisher Scientific) and diluted to an MOI 1000 in nonsupplemented cell culture medium to infect primary and immortalised endothelial cells. Cells were washed with PBS, fixed in 3.7% formalin for 10 min at room temperature, washed again and blocked for 1 h

with blocking buffer (2% BSA, 5% goat serum v/v in PBS). For VE-cadherin staining, the cells were incubated overnight at 4 °C with 3 μg·mL$^{-1}$ mouse anti-human VE-cadherin (Clone # 123413, R&D Systems) in blocking buffer, or with mouse IgG1 isotype control (Clone P3.6.2.8.1, R&D Systems) at the same concentration. Following incubation, slides were washed with PBS and incubated with 1 μg·mL$^{-1}$ Alexa Fluor 488 goat anti-mouse IgG (H + L) secondary antibody for 1 h. Cells were rinsed again, mounted in ProLong™ Diamond Antifade Mountant containing 4',6-diaminidine-2'-phylindole dihydrochloride (DAPI) (Thermo Fisher Scientific) and imaged using a Zeiss Axiovert 200M inverted fluorescence microscope with an integrated high-resolution digital camera (AxioCam MRm; Zeiss) with AxioVision 4.6 software (Zeiss). For PECAM-1 staining, cells were blocked with 2.5% BSA in PBS for 40 min and fixed in 2% paraformaldehyde for 20 min at room temperature. Cells were then washed in PBS and stained with PE-Cy7 conjugated anti-human PECAM-1 antibody (Clone WM59, BD Biosciences) for 40 min at room temperature. Nuclei were stained for 5 min with 5 μg·mL$^{-1}$ DAPI (Sigma-Aldrich), washed, mounted ProLong Diamond Antifade Mountant (Thermo Fisher Scientific) and left to set overnight. Images were captured using a Nikon A1 confocal microscope.

### In vitro gene expression analysis

Quantitative reverse transcription polymerase chain reaction (qRT–PCR) was used to analyse mRNA expression of endothelial immune molecules. HMEC-1 and HDMEC were seeded at $4 \times 10^5$ cells per well and cultured until confluent. Cells were either infected with *P. gingivalis* W83 or ΔK/R-ab mutant at a MOI 100 for 4 h, and unstimulated or TNFα-stimulated (25 ng·mL$^{-1}$) cells were used as controls. Total RNA extraction was carried out using ISO-LATE II RNA Mini Kit (Bioline, Meridian Bioscience Inc., Cincinnati, OH, USA) according to the manufacturer's instructions and RNA measured by NanoDrop (Thermo Fisher Scientific). High-Capacity cDNA Reverse Transcription Kit (Thermo Fisher Scientific) was used to produce cDNA and qPCR performed using Qiagen Rotor-Gene (Qiagen, Hilden, Germany). Reactions consisted of 5 μL of TaqMan® qPCR BioProbe Blue Master Mix (PCR Biosystems, London, UK), 3.5 μL RNase-free water, 0.5 μL human β-2-microglobulin (B2M) as an endogenous reference control (VIC/MGB Probe, Thermo Fisher Scientific), 0.5 μL target primer and 0.5 μL cDNA. Target primers used were PECAM-1 (Hs01065279_m1), VE-cadherin (Hs00901465_m1), CXCL8 (Hs00174103_m1), CCL2 (Hs00234140_m1) and ICAM-1 (Hs0014932_m1) (Thermo Fisher Scientific). All samples were run in triplicate; control samples excluded cDNA. The threshold cycle (Ct) for each test gene was normalised against their respective reference

controls. Fold change in expression relative to unstimulated cells was calculated with $\Delta C_t$ values of the sample and reference gene using the formula $2^{-\Delta\Delta C_t}$.

### In vivo PECAM-1 and VE-cadherin cell adhesion protein expression

*Tg(fli1a:PECAM1-EGFP)sh524* and *Tg(cdh5ubs8-/-;cdh5TS)* transgenic zebrafish were outcrossed with nacre zebrafish. Embryos were dechorionated and green fluorescent protein (GFP)-positive embryos selected at 1 dpf using a fluorescent dissecting microscope (Zeiss Axio Zoom.V16 fitted with an HXP 200C Illuminator and a Zeiss Axiocam 503 monocamera). Zebrafish embryos at 30 hpf were anaesthetised using tricaine (0.02% (w/v) 3-amino benzoic acid ester tricaine/MS-322 (Sigma-Aldrich), positioned in a solution of 3% (w/v) methylcellulose (Sigma-Aldrich) in E3 medium and 2 nL ($5 \times 10^4$ CFU) of 5 μM Red CMPTX (CellTracker™, Thermo Fisher Scientific) stained W83 or ΔK/R-ab *Pg* were injected systemically using a microcapillary needle (Scientific Laboratory Supplies) via direct microinjection into the Duct of Cuvier (the common cardinal vein); PBS was used as control. Live imaging of anaesthetised fish (5 zebrafish embryos per group) was carried out 24 h postinfection (hpi) using a spinning disc confocal microscope (PerkinElmer UltraVIEW VoX, PerkinElmer Inc., Waltham, MA, USA) running on an inverted Olympus IX81 motorised microscope. 488-nm and 561-nm lasers were used to visualise fluorescent PECAM-1 or CDH5/VE-cadherin (green) and *Pg* bacteria (red) in zebrafish embryos. Micrographs were captured in two areas of the tail, adjacent to the cloaca (closer to the yolk) and 4 vessels further away from the cloaca (closer to the tip of the tail) using Volocity® software (Quorum Technologies Inc., Puslinch, Ontario, Canada). Quantification of relative GFP fluorescence intensity (pixel value) was performed by batch processing of maximum intensity z projection of micrographs of whole images in the yolk and tail region using an adjusted script on FIJI® Macros plug-in.

### In vivo vascular permeability

Zebrafish *Tg(fli1a:mTurquoise2)sh321* embryos were infected at 2 dpf with FAM-labelled *Pg* W83, ΔK/R-ab or PBS as a control, into the common cardinal vein. Embryos with a functional circulation at 24 hpi were anaesthetised and injected into the posterior cardinal vein (PCV) with 2 nL of 1 mg·mL$^{-1}$ tetramethylrhodamine dextran ($2 \times 10^6$ kDa, Thermo Fisher Scientific). Microangiogram images were acquired within an hour postdextran injection. Real-time changes in vascular integrity were measured in response to *Pg* W83 infection using light sheet microscopy (Z1, Zeiss) with lasers 445-24, 488-30 and 561-20 with LSB 445/514/640.

## Statistical analysis

All data presented are from at least 3 independent experiments (unless specified). Results are expressed as the mean $\pm$ standard deviation (SD) except for flow cytometry data where the nMFI (normalised median fluorescence index) was used. Normality was determined using Kolmogorov–Smirnov analysis. The differences between two groups were assessed using either Student's *t*-test or Mann–Whitney *U*-test, while the differences between group data were assessed using one-way ANOVA followed by either Tukey's or Dunn's post hoc multiple comparison test depending on the nature of the data (parametric or non-parametric). All tests were carried out using GraphPad Prism v8.2 (GraphPad, San Diego, CA, USA), and statistical significance was assumed at $P < 0.05$.

## Acknowledgements

## Conflict of interest

The authors declare no conflict of interest.

## Author contributions

CM, GPS, JP, RNW and MW conceived, designed the research and planned experiments. CF, YC and MW performed the experiments. CF, MW, GPS and CM analysed the data, conducted statistical analysis and interpreted the results. CF, MW and CM wrote the manuscript draft, and further editing was performed by GPS, CM, JP and RNW.

## References

1 Tonetti MS & Van Dyke TE (2013) Periodontitis and atherosclerotic cardiovascular disease: consensus report of the Joint EFP/AAP Workshop on Periodontitis and Systemic Diseases. *J Periodontol* **84**, S24–S29.

2 Fiehn NE, Larsen T, Christiansen N, Holmstrup P & Schroeder TV (2005) Identification of periodontal pathogens in atherosclerotic vessels. *J Periodontol* **76**, 731–736.

3 Mikuls TR, Payne JB, Yu F, Thiele GM, Reynolds RJ, Cannon GW, Markt J, McGowan D, Kerr GS, Redman RS *et al.* (2014) Periodontitis and *Porphyromonas gingivalis* in patients with rheumatoid arthritis. *Arthritis Rheumatol* **66**, 1090–1100.

4 Saremi A, Nelson RG, Tulloch-Reid M, Hanson RL, Sievers ML, Taylor G, Shlossman M, Bennett PH, Genco R & Knowler WC (2005) Periodontal disease and mortality in type 2 diabetes. *Diabetes Care* **28**, 27–32.

5 Olsen I, Taubman MA & Singhrao SK (2016) *Porphyromonas gingivalis* suppresses adaptive immunity in periodontitis, atherosclerosis, and Alzheimer's disease. *J Oral Microbiol* **8**, 33029.

6 Friedewald VE, Kornmam KS, Beck JD, Genco R, Goldfine A, Libby P, Offenbacher S, Ridker PM, Van Dyke TE & Roberts WC (2009) The American Journal of Cardiology and Journal of Periodontology editors' consensus: periodontitis and atherosclerotic cardiovascular disease. *Am J Cardiol* **104**, 59–68.

7 Darveau RP (2010) Periodontitis: a polymicrobial disruption of host homeostasis. *Nat Rev Microbiol* **8**, 481–490.

8 Lamont RJ, Koo H & Hajishengallis G (2018) The oral microbiota: dynamic communities and host interactions. *Nat Rev Microbiol* **16**, 745–759.

9 Hajishengallis G, Darveau RP & Curtis MA (2012) The keystone-pathogen hypothesis. *Nat Rev Microbiol* **10**, 717–725.

10 How KY, Song KP & Chan KG (2016) *Porphyromonas gingivalis*: an overview of periodontopathic pathogen below the gum line. *Front Microbiol* **7**, 53.

11 Potempa J, Sroka A, Imamura T & Travis J (2003) Gingipains, the major cysteine proteinases and virulence factors of *Porphyromonas gingivalis*: structure, function and assembly of multidomain protein complexes. *Curr Protein Pept Sci* **4**, 397–407.

12 Bahrani-Mougeot FK, Paster BJ, Coleman S, Ashar J, Barbuto S & Lockhart PB (2008) Diverse and novel oral bacterial species in blood following dental procedures. *J Clin Microbiol* **46**, 2129–2132.

13 Schenkein HA & Loos BG (2013) Inflammatory mechanisms linking periodontal diseases to cardiovascular diseases. *J Clin Periodontol* **40**, S51–S69.

14 Loos BG (2005) Systemic markers of inflammation in periodontitis. *J Periodontol* **76**, 2106–2115.

15 Castillo DM, Sánchez-Beltrán MC, Castellanos JE, Sanz I, Mayorga-Fayad I, Sanz M & Lafaurie GI (2011) Detection of specific periodontal microorganisms from bacteraemia samples after periodontal therapy using molecular-based diagnostics. *J Clin Periodontol* **38**, 418–27.

16 Mougeot JLC, Stevens CB, Paster BJ, Brennan MT, Lockhart PB & Mougeot FKB (2017) *Porphyromonas gingivalis* is the most abundant species detected in coronary and femoral arteries. *J Oral Microbiol* **9**, 1281562.

17 Oliveira FA, Forte CP, Silva PG, Lopes CB, Montenegro RC, Santos AK, Sobrinho CR, Mota MR, Sousa FB & Alves AP (2015) Molecular analysis of oral bacteria in heart valve of patients with cardiovascular disease by real-time polymerase chain reaction. *Medicine* **94**, e2067.

18 Dorn BR, Dunn WA & Progulske-Fox A (1999) Invasion of human coronary artery cells by periodontal pathogens. *Infect Immun* **67**, 5792–5798.

19 Deshpande RG, Khan MB & Genco CA (1998) Invasion of aortic and heart endothelial cells by *Porphyromonas gingivalis*. *Infect Immun* **66**, 5337–5343.

20 Nassar H, Chou HH, Khlgatian M, Gibson FC, Van Dyke TE & Genco CA (2002) Role for fimbriae and lysine-specific cysteine proteinase gingipain K in expression of interleukin-8 and monocyte chemoattractant protein in *Porphyromonas gingivalis*-infected endothelial cells. *Infect Immun* **70**, 268–276.

21 Takahashi Y, Davey M, Yumoto H, Gibson FC & Genco CA (2006) Fimbria-dependent activation of pro-inflammatory molecules in *Porphyromonas gingivalis*-infected human aortic endothelial cells. *Cell Microbiol* **8**, 738–757.

22 Walter C, Zahlten J, Schmeck B, Schaudinn C, Hippenstiel S, Frisch E, Hocke AC, Pischon N, Kuramitsu HK, Bernimoulin JP *et al.* (2004) *Porphyromonas gingivalis* strain-dependent activation of human endothelial cells. *Infect Immun* **72**, 5910–5918.

23 Yun PL, Decarlo AA, Chapple CC & Hunter N (2005) Functional implication of the hydrolysis of platelet endothelial cell adhesion molecule 1 (CD31) by gingipains of *Porphyromonas gingivalis* for the pathology of periodontal disease. *Infect Immun* **73**, 1386–1398.

24 Sheets SM, Potempa J, Travis J, Casiano CA & Fletcher HM (2005) Gingipains from *Porphyromonas gingivalis* W83 induce cell adhesion molecule cleavage and apoptosis in endothelial cells. *Infect Immun* **73**, 1543–1552.

25 Dejana E, Orsenigo F & Lampugnani MG (2008) The role of adherens junctions and VE-cadherin in the control of vascular permeability. *J Cell Sci* **121**, 2115–2122.

26 Aghajanian A, Wittchen ES, Allingham MJ, Garrett TA & Burridge K (2008) Endothelial cell junctions and the regulation of vascular permeability and leukocyte transmigration. *J Thromb Haemost* **6**, 1453–1460.

27 Widziolek M, Prajsnar TK, Tazzyman S, Stafford GP, Potempa J & Murdoch C (2016) Zebrafish as a new model to study effects of periodontal pathogens on cardiovascular diseases. *Sci Rep* **6**, 36023.

28 Kadowaki T, Baba A, Abe N, Takii R, Hashimoto M, Tsukuba T, Okazaki S, Suda Y, Asao T & Yamamoto K (2004) Suppression of pathogenicity of *Porphyromonas gingivalis* by newly developed gingipain inhibitors. *Mol Pharmacol* **66**, 1599–1606.

29 Privratsky JR & Newman PJ (2014) PECAM-1: regulator of endothelial junctional integrity. *Cell Tissue Res* **355**, 607–619.

30 Yun PL, Decarlo AA & Hunter N (2006) Gingipains of *Porphyromonas gingivalis* modulate leukocyte adhesion molecule expression induced in human endothelial cells by ligation of CD99. *Infect Immun* **74**, 1661–1672.

31 Kozarov EV, Dorn BR, Shelburne CE, Dunn WA & Progulske-Fox A (2005) Human atherosclerotic plaque contains viable invasive *Actinobacillus actinomycetemcomitans* and *Porphyromonas gingivalis*. *Arterioscler Thromb Vasc Biol* **25**, e17–e18.

32 Gaetti-Jardim E, Marcelino SL, Feitosa ACR, Romito GA & Avila-Campos MJ (2009) Quantitative detection of periodontopathic bacteria in atherosclerotic plaques from coronary arteries. *J Med Microbiol* **58**, 1568–1575.

33 Szulc M, Kustrzycki W, Janczak D, Michalowska D, Baczynska D & Radwan-Oczko M (2015) Presence of periodontopathic bacteria DNA in atheromatous plaques from coronary and carotid arteries. *Biomed Res Int* **2015**, 825397.

34 Fitzpatrick RE, Wijeyewickrema LC & Pike RN (2009) The gingipains: scissors and glue of the periodontal pathogen, *Porphyromonas gingivalis*. *Future Microbiol* **4**, 471–487.

35 Rodrigues PH, Reyes L, Chadda AS, Bélanger M, Wallet SM, Akin D, Dunn W & Progulske-Fox A (2012) *Porphyromonas gingivalis* strain specific interactions with human coronary artery endothelial cells: a comparative study. *PLoS One* **7**, e52606.

36 Olsen I & Progulske-Fox A (2015) Invasion of *Porphyromonas gingivalis* strains into vascular cells and tissue. *J Oral Microbiol* **7**, 28788.

37 Lamont RJ, Chan A, Belton CM, Izutsu KT, Vasel D & Weinberg A (1995) *Porphyromonas gingivalis* invasion of gingival epithelial cells. *Infect Immun* **63**, 3878–3885.

38 Pinnock A, Murdoch C, Moharamzadeh K, Whawell S & Douglas CW (2014) Characterisation and optimisation of organotypic oral mucosal models to

study *Porphyromonas gingivalis* invasion. *Microbes Infect* **16**, 310–319.

39 Yamatake K, Maeda M, Kadowaki T, Takii R, Tsukuba T, Ueno T, Kominami E, Yokota S & Yamamoto K (2007) Role for gingipains in *Porphyromonas gingivalis* traffic to phagolysosomes and survival in human aortic endothelial cells. *Infect Immun* **75**, 2090–2100.

40 Deshpande RG, Khan M & Genco CA (1998) Invasion strategies of the oral pathogen *Porphyromonas gingivalis*: Implications for cardiovascular disease. *Invasion Metastasis* **18**, 57–69.

41 Komatsu T, Nagano K, Sugiura S, Hagiwara M, Tanigawa N, Abiko Y, Yoshimura F, Furuichi Y & Matsushita K (2012) E-selectin mediates *Porphyromonas gingivalis* adherence to human endothelial cells. *Infect Immun* **80**, 2570–2576.

42 Choi EK, Park SA, Oh WM, Kang HC, Kuramitsu HK, Kim BG & Kang IC (2005) Mechanisms of *Porphyromonas gingivalis*-induced monocyte chemoattractant protein-1 expression in endothelial cells. *FEMS Immunol Med Microbiol* **44**, 51–58.

43 Mao S, Maeno N, Matayoshi S, Yoshiie K, Fujimura T & Oda H (2004) The induction of intercellular adhesion molecule-1 on human umbilical vein endothelial cells by a heat-stable component of *Porphyromonas gingivalis*. *Curr Microbiol* **48**, 108–112.

44 Xu W, Pan Y, Xu Q, Wu Y, Pan J, Hou J, Lin L, Tang X, Li C, Liu J & *et al.* (2018) *Porphyromonas gingivalis* ATCC 33277 promotes intercellular adhesion molecule-1 expression in endothelial cells and monocyte-endothelial cell adhesion through macrophage migration inhibitory factor. *BMC Microbiol* **18**, 16.

45 Gut P, Reischauer S, Stainier DYR & Arnaout R (2017) Little fish, big data: zebrafish as a model for cardiovascular and metabolic disease. *Physiol Rev* **97**, 889–938.

46 Chistiakov DA, Orekhov AN & Bobryshev YV (2015) Endothelial barrier and its abnormalities in cardiovascular disease. *Front Physiol* **6**, 365.

47 Koizumi Y, Kurita-Ochiai T, Oguchi S & Yamamoto M (2008) Nasal immunization with *Porphyromonas gingivalis* outer membrane protein decreases *P. gingivalis*-induced atherosclerosis and inflammation in spontaneously hyperlipidemic mice. *Infect Immun* **76**, 2958–2965.

48 Velsko IM, Chukkapalli SS, Rivera MF, Lee J-Y, Chen H, Zheng D, Bhattacharyya I, Gangula PR, Lucas AR & Kesavalu L (2014) Active invasion of oral and aortic tissues by *Porphyromonas gingivalis* in mice causally links periodontitis and atherosclerosis. *PLoS One* **9**, e97811.

49 Chukkapalli SS, Easwaran M, Rivera-Kweh MF, Velsko IM, Ambadapadi S, Dai J, Larjava H, Lucas AR & Kesavalu L (2017) Sequential colonization of periodontal pathogens in induction of periodontal disease and atherosclerosis in LDLRnull mice. *Pathogen Dis* **75**, ftx003.

50 Savage AM, Kurusamy S, Chen Y, Jiang Z, Chhabria K, MacDonald RB, Kim HR, Wilson HL, van Eeden FJM, Armesilla AL *et al.* (2019) Tmem33 is essential for VEGF-mediated endothelial calcium oscillations and angiogenesis. *Nat Commun* **10**, 732.

51 Naylor KL, Widziolek M, Hunt S, Conolly M, Hicks M, Stafford P, Potempa J, Murdoch C, Douglas CWI & Stafford GP (2017) Role of OmpA2 surface regions of *Porphyromonas gingivalis* in host-pathogen interactions with oral epithelial cells. *Microbiologyopen* **6**, e00401.

**Research Reports: Biological**

# *Porphyromonas gingivalis* Outer Membrane Vesicles Increase Vascular Permeability

**C. Farrugia[1] , G.P. Stafford[1], and C. Murdoch[1]**

## Abstract

Periodontitis is increasingly associated with increased risk of cardiovascular and other systemic diseases. The Gram-negative anaerobe, *Porphyromonas gingivalis*, is a key periodontal pathogen, and several lines of evidence link the presence of this bacterium in the circulation with vascular disease. The outer membrane vesicles (OMVs) produced by *P. gingivalis* have been shown to play a role in periodontitis, although, to date, little is known about their interaction with the vasculature; therefore, this study assessed the effects of *P. gingivalis* OMVs on the endothelium. OMVs were isolated from wild-type strain W83 and the gingipain-deficient strain ΔK/R-ab. Immunoblotting along with cryo-EM showed gingipain expression in W83 but not ΔK/R-ab-derived OMVs, where gingipains were localized to the cell wall surface. Confluent endothelial cell monolayers infected with either W83 or W83-derived OMV displayed significantly increased dextran permeability over those infected with ΔK/R-ab or its OMV. Moreover, W83-derived OMVs induced significantly more vascular disease in a zebrafish larvae systemic infection model over 72 h compared to those injected with gingipain-deficient OMVs or controls. In line with these data, human microvascular endothelial cells (HMEC-1) displayed an OMV-associated, gingipain-dependent decrease in cell surface levels of the intercellular adhesion molecule PECAM-1 (CD31) when examined by flow cytometry. These data show, for the first time, that OMVs from *P. gingivalis* mediate increased vascular permeability, leading to a diseased phenotype both in vitro and in vivo. Moreover, these data strongly implicate gingipains present on the OMV surface in mediating these vascular events, most likely via a mechanism that involves proteolytic cleavage of endothelial cell-cell adhesins such as PECAM-1. These data provide important evidence for the role of bacterial-derived OMVs in mediating systemic disease.

**Keywords:** endothelial cells, periodontal disease, cardiovascular disease, infection, zebrafish, vascular disease

## Introduction

The association between periodontal disease and cardiovascular disease is well established. (Friedewald et al. 2009; Sanz et al. 2020). Periodontal disease has been found to increase the risk of both cardiovascular disease and coronary heart disease (Chhibber-Goel et al. 2016; Masi et al. 2019; Gustafsson et al. 2020). Nonetheless, the biological mechanisms through which this occurs are still unknown. Increasing evidence suggests that in cases of extreme gingivitis or periodontitis, the anaerobic periodontal pathogen, *Porphyromonas gingivalis*, can enter the bloodstream through inflamed and ulcerated periodontal tissue, an area coined the *porte d'entrée* (Loos 2005; Castillo et al. 2011). Here, loss of tissue integrity and increased bleeding facilitate movement of bacteria from the periodontal pocket into the bloodstream (Loos 2005; Schenkein and Loos 2013), with *P. gingivalis* repetitively detected in diseased vascular tissue (Kozarov et al. 2005; Gaetti-Jardim et al. 2009; Marcelino et al. 2010; Szulc et al. 2015), as well as disease-free femoral and coronary arteries (Mougeot et al. 2017).

*P. gingivalis* harbors several virulence factors that have been attributed to causing its pathogenic effects both locally and systemically. This includes gingipains, lysine, and arginine-specific cysteine proteases that cause virulence by their ability to cleave host proteins (Hočevar et al. 2018), not only avoiding immune response by degradation of cytokines and proinflammatory molecules (Nassar et al. 2002) but also mediating cell surface protein and extracellular matrix disruption, facilitating the loss of cellular and tissue integrity (Tada et al. 2003; Yun et al. 2005; Ruggiero et al. 2013). We recently showed that *P. gingivalis* dramatically increases the morbidity and mortality of zebrafish in a gingipain-dependent manner when injected systemically (Widziolek et al. 2016), suggesting that these proteases may play a key role in mediating vascular damage.

Like most Gram-negative organisms, *P. gingivalis* produces outer membrane vesicles (OMVs) that appear to retain many of the virulence factors of the parent cell, including lipopolysaccharide (LPS) (Haurat et al. 2011), fimbrae (Mantri et al. 2015), and gingipains (Haurat et al. 2011; Nakao et al. 2014). OMV-derived virulence factors have been shown to drive oral epithelial cell responses (Nakao et al. 2014; Cecil et al. 2016)

[1]School of Clinical Dentistry, University of Sheffield, Sheffield, UK

A supplemental appendix to this article is available online.

**Corresponding Author:**
C. Murdoch, Integrated Bioscience, School of Clinical Dentistry, University of Sheffield, Claremont Crescent, Sheffield, S10 2TA, UK.
Email: c.murdoch@sheffield.ac.uk

and influence the differentiation and calcification of smooth muscle cells in vitro (Yang et al. 2016), suggesting that OMVs may affect cells of the vasculature. Interestingly, the presence of *P. gingivalis*–derived OMVs has been detected in the peripheral blood and cerebrospinal fluid in animal models with severe bacterial infections (Bai et al. 2015; Jia et al. 2015), indicating that OMVs may be widespread within the circulation and access areas of tissue not accessible to whole bacteria. However, the effects of OMVs on endothelial cells remain to be determined and require further research. Using an in vitro and in vivo approach, we show for the first time that *P. gingivalis*–derived OMVs significantly affect endothelial permeability in a gingipain-dependent manner, a process that may be mediated by cleavage of cell-to-cell adhesion molecules. These novel data demonstrate that *P. gingivalis* OMVs may play a pivotal role in disrupting the vasculature, a process that may drive or markedly increase the risk of cardiovascular disease.

## Materials and Methods

### Bacterial Culture and OMV Preparation

Wild-type *P. gingivalis* strain W83 and its isogenic gingipain-deficient mutant ΔK/R-ab ($kgp\Delta598$-$1732$::$Tc^R$ $rgpA$-::$Cm^R$ $rgpB\Delta410$-$507$::$Em^R$; provided by Prof. Jan Potempa, Jagiellonian University, Kraków, Poland) were maintained on Fastidious Anaerobe agar (NeoGen) supplemented with 5% v/v oxalated horse blood and 1 μg/mL tetracycline. Bacteria were inoculated into brain-heart infusion broth (Oxoid) containing 5 mg/mL yeast extract, 250 μg/mL L-cysteine, 1 mg/mL hemin, and 1 mg/mL vitamin K and incubated anaerobically (37°C, 80% $N_2$, 10% $CO_2$, and 10% $H_2$). For OMV isolation, freshly grown bacterial cultures ($OD_{600} = 1$, equivalent to $9 \times 10^9$ colony-forming units [CFUs]) were centrifuged (8,000 g, 4°C, 5 min) and the pellet collected. The supernatant was filtered (0.2 μm) and further centrifuged for 1 h at 100,000 g, 4°C. The resulting OMV pellet was washed once with phosphate-buffered saline (PBS), ultracentrifuged again, resuspended in PBS, and characterized using nanoparticle-tracking analysis (ZetaView).

### Immunoblot Analysis

Protein concentrations of bacterial cell pellets and OMV were measured by a bicinchoninic acid (BCA) protein assay. Samples (10 μg protein) were run on 4% to 12% NuPAGE gels, transferred to nitrocellulose membranes, and then blocked with 5% w/v milk protein in Tris-buffered saline (TBS). Following washing with TBS–Tween-20 (0.1%), membranes were incubated with either rabbit Rb7 antiserum (Aduse-Opoku et al. 2006) or mouse monoclonal antibody 1B5 (Curtis et al. 1999) (gifts from Professor Mike Curtis, King's College London, London, UK). Immunoreactive bands were visualized using horseradish peroxidase–conjugated IgG antibody followed by ECL substrate (Thermo Scientific).

### Immunogold Cryo–Electron Microscopy

Immunogold cryo–electron microscopy (EM) was performed as described by Chen et al. (2011) with modifications. Briefly, exponential phase-grown W83 and ΔK/R-ab were adjusted to $OD_{600} = 1$, pelleted by centrifugation (10 min, 6,000 g at 10°C), washed, and resuspended in PBS. Cell suspensions were blocked with 3% bovine serum albumin (BSA) at 4°C, then incubated with MAb 1B5 (1/100 dilution) in 1% BSA for 1 h. After washing, cells were incubated with 12 nm gold-conjugated goat anti-mouse antibody (Abcam; 1/20 dilution) for 1 h and then washed with PBS. For cryo-EM, a 5-μL sample was applied onto a Quantifoil R3.5/1 holey carbon film mounted on a 300-mesh copper grid (Quantifoil MicroTools GmbH), rendered hydrophilic by glow discharge in a reduced atmosphere of air for 30 s. The grid was then frozen in liquid ethane and imaged under cryogenic temperatures using a Tecnai Artica (FEI Co.) at 200 kV, equipped with a Falcon 3 Camera (Gatan). Micrographs were recorded under low-dose conditions with underfocus values of 4 to 10 μm.

### Gingipain Activity

Arg- and Lys-gingipain proteinase activity was determined using a fluorescence-based substrate activity assay as described previously (Naylor et al. 2017). For Arg-proteinase activity, 100 μL PBS containing 1 mM L-cysteine and 200 μM αN-benzoyl-L-arginine-7-amido-4-methylcourmarin was added to 50 μL ($4.5 \times 10^8$ CFUs) of each sample. Lys-proteinase activity was quantified using 100 μL PBS containing 1 mM L-cysteine, 10 μM D-ab-Leu-Lys-7-amido-4-methylcourmain, and 50 μL of sample. After a 10-min incubation, the reaction was terminated by the addition of 200 μM or 500 μM N-α-tosyl-L-phenylalanine chloromethyl ketone for Arg and Lys activity, respectively. In both assays, released 7-amido-4-methylcourmarin was measured spectrophotometrically at a 365-nm excitation and a 460-nm emission.

### Cell Culture, Infection, and Flow Cytometry

Immortalized human microvascular endothelial cells (HMEC-1) (Ades et al. 1992) were grown in MCDB131 supplemented with 10 ng/mL epidermal growth factor, 1 μg/mL hydrocortisone, 10% fetal calf serum, and 2 mM L-glutamine. For flow cytometry, confluent HMEC-1 cultured in 6-well plates were infected with W83, ΔK/R-ab (multiplicity of infection [MOI] of 100), or OMVs ($2.8 \times 10^{10}$ particles/mL) derived from these bacteria for 1.5 h at 37°C in serum-free medium. For inhibition of gingipain activity, OMVs were pretreated with 2 μM KYT-1 and KYT-36 for 30 min in anaerobic conditions prior to isolation. Medium alone was used as control. Following infection, HMEC-1 were washed, removed from plates using 0.02% ethylenediaminetetraacetic acid for 20 min, and resuspended in 100 μL FACS buffer (0.1% BSA, 0.1% sodium azide in PBS). Phycoerythrin-Cyanine7-conjugated anti-human CD31 (clone MW59) or isotype-conjugated IgG control was added for

45 min on ice. Cells were washed and resuspended in FACS buffer and analyzed using a LSRII flow cytometer (BD Biosciences). FlowJo software (TreeStar) was used to calculate the normalized median fluorescence index (nMFI).

## Fluorescent Dextran Permeability Assay

A fluorescent dextran permeability assay was performed as previously described (Wang and Alexander 2011). Fibronectin-coated (10 µg/mL) 0.4-µm pore, hanging cell culture inserts (Millicell) were seeded with HMEC-1 until confluent and then incubated with W83 or ΔK/R-ab whole cells (MOI 100) or OMVs ($2.8 \times 10^{10}$ particles/mL) derived from these bacteria for 1.5 h at 37°C in serum-free medium. Inserts without cells or HMEC-1 alone were used as controls. Solutions were removed, inserts were transferred to a new plate containing 500 µL supplemented MCDB131, and 450 µL supplemented MCDB131 containing 65 µg/mL 70 kDa fluorescent dextran (Molecular Probes) was added to the insert. Dextran leakage through the cell monolayer to the bottom well was monitored hourly for a 5-h period by aspirating 250 µL medium from the bottom well and measuring dextran fluorescence at a 494-nm excitation and 521-nm emission. The aspirated volume was replaced with supplemented MCDB131 for further readings.

## Systemic Injection into Zebrafish Larvae

Zebrafish maintenance and experimental work was performed in accordance with UK Home Office regulations and the UK Animals (Scientific Procedures) Act of 1986 and under project license P1A4A7A5E using larvae under 5 d postfertilization (dpf). London wild-type inbred zebrafish larvae were maintained in E3 medium at 29°C according to standard protocols. The 30-h postfertilization (hpf), Tricaine-anesthetized, dechorionated zebrafish larvae were injected with PBS, $5 \times 10^4$ CFU W83, or OMVs ($1.15 \times 10^5$ particles) derived from W83 or ΔK/R-ab via direct systemic inoculation into the common cardinal vein (Widziolek et al. 2016). Zebrafish viability was assessed by examining the presence of a heartbeat and blood flow within the circulation. Live imaging was performed using a stereomicroscope (WILD) equipped with a camera.

## Statistical Analysis

Data are presented as mean ± standard deviation (SD) from at least 3 independent experiments carried out in triplicate except for flow cytometry data where nMFI was used. Differences between 2 groups were assessed using either Student's *t* test or Mann-Whitney *U* test, while differences between group data were assessed using 1-way analysis of variance (ANOVA) followed by Tukey's post hoc multiple comparison test for parametric or nonparametric data, respectively, following a normality test. Survival data were evaluated using the Kaplan-Meier method, and comparisons between individual curves were made using the log-rank test. Statistical analysis was performed using GraphPad Prism v8.4.0 (GraphPad Software), and statistical significance was assumed at $P < 0.05$.

# Results

## Characterization of Wild-Type W83 and ΔK/R-ab-Derived OMVs

Our aim was to investigate whether *P. gingivalis* OMVs and their associated gingipains might mediate endothelial damage. We first characterized OMVs from wild-type W83 and its isogenic gingipain-negative (ΔK/R-ab) strain. Nanoparticle analysis showed that numbers of OMVs produced from these 2 strains were comparable (Appendix Fig. 1A). Overall, wild-type W83 OMVs were 24% larger in size ($P < 0.05$, Appendix Fig. 1B, C) than those from ΔK/R-ab (144 ± 23 nm). As expected, immunoblotting with the RgpA/B-specific antisera Rb7 produced immunoreactive bands of 45 kDa for whole W83 cells and W83-derived OMVs, whereas this band was absent from counterpart ΔK/R-ab samples (Fig. 1A). Similar immunoblot data were obtained when using the monoclonal antibody 1B5 that binds to a shared glycan epitope between Rgp and the minority A-LPS of *P. gingivalis* (Appendix Fig. 2). Furthermore, the presence of gingipains on the bacterial surface and periphery of purified W83-derived OMVs was confirmed by cryo-EM using 1B5 monoclonal antibody immunogold labeling, whereas ΔK/R-ab OMV did not show any immunoreactivity (Fig. 1B). Cryo-EM did not reveal any morphological differences between whole cells and OMVs from either strain (Fig. 1B). Finally, W83 whole cells and OMVs displayed the expected gingipain enzyme activity for both lysine- and arginine-based substrate that was absent in the ΔK/R-ab strain ($P < 0.001$; Fig. 1C–F).

## Gingipains Mediate Increased Endothelium Permeability In Vitro

Since increased vascular permeability has been linked to cardiovascular risk (Chistiakov et al. 2015), we performed a fluorescent dextran-based in vitro permeability assay on confluent HMEC-1 monolayers to determine the influence of OMV-expressed gingipains on endothelial permeability. Confluent, untreated endothelial monolayers proved an effective barrier with little of the applied 70-kDa fluorescent dextran permeating the cell layer after 5 h (Fig. 2A). In contrast, the endothelium displayed significantly increased dextran permeability upon treatment with whole-cell W83 (Fig. 2B; $P < 0.01$) or W83-derived OMVs (Fig. 2C; $P < 0.05$) compared to counterpart ΔK/R-ab-treated or noninfected controls, suggesting that altered vascular permeability is gingipain dependent. Notably, endothelium permeability was significantly higher ($P < 0.05$) in the presence of W83 whole cells (4.8% dextran/h) compared to OMVs (2.5% dextran/h).

## OMV-Associated Gingipains Are Responsible for Systemic Symptoms in a Zebrafish Larvae Infection Model

We have previously shown that zebrafish larvae display increased mortality (death) and morbidity (cardiac and yolk
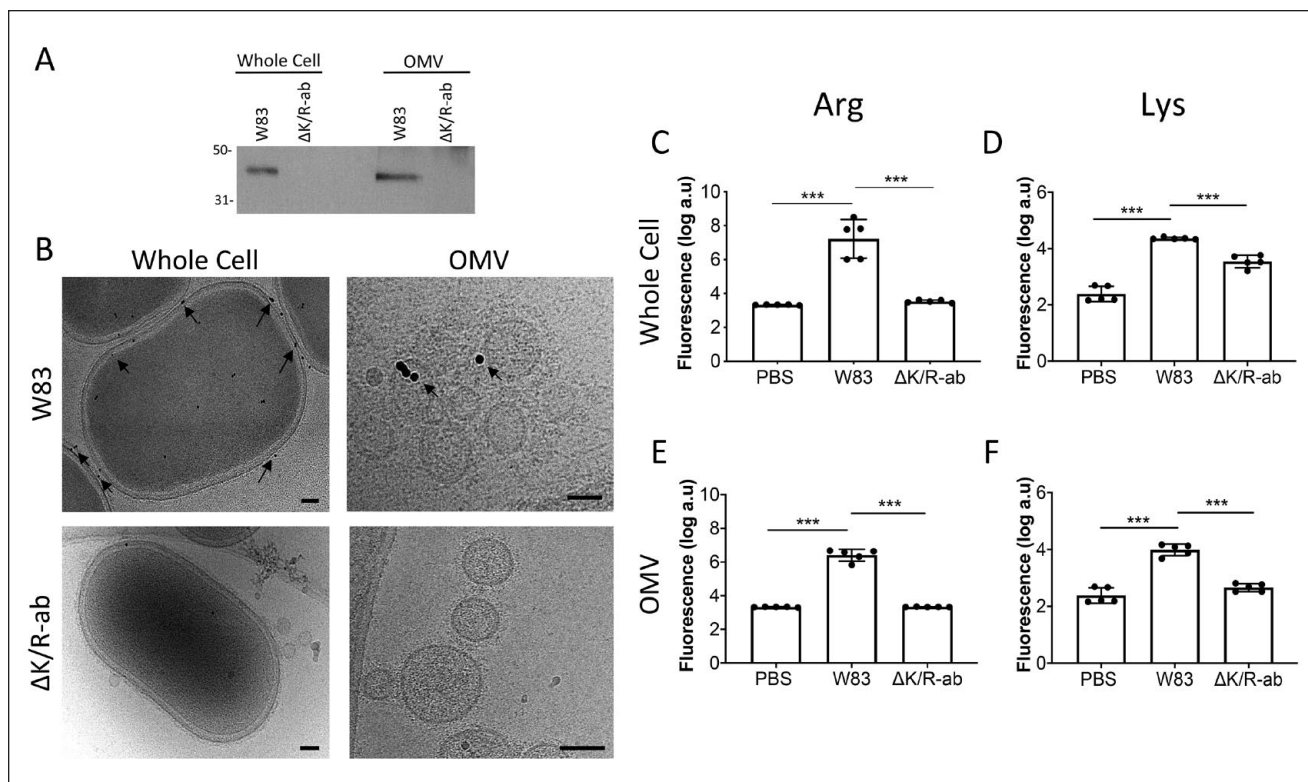
**Figure 1.** Presence and activity of wild-type and ΔK/R-ab *Porphyromonas gingivalis* gingipains on whole bacteria and outer membrane vesicles (OMVs). (**A**) Immunopositive bands of 45 kDa were observed in the W83 whole-cell and OMV samples but not in the gingipain-null ΔK/R-ab equivalents when protein extracts were analyzed by immunoblotting using the Rb7 antigingipain antiserum. (**B**) Cryo–electron microscopy (EM) micrographs showing mAb 1B5 immunogold-labeled W83 bacteria and OMV. The gingipain expression is mainly located to the cell wall in both W83 whole cells and OMVs (black arrows) but is absent in ΔK/R-ab equivalents (scale bar: whole bacteria = 100 nm; OMV = 50 nm). (**C–F**) Gingipain fluorometric enzyme activity assays showing the higher levels of activity of arginine-specific (Arg, C, E) and lysine-specific (Lys, D, F) protease in W83 whole cells and OMVs compared to ΔK/R-ab mutant equivalents. In C–F, data are mean ± SD of 5 independent experiments with each individual experiment performed in triplicate. Statistical significance was determined by 1-way analysis of variance, ***$P < 0.001$.

edema) when systemically injected with *P. gingivalis* (Widziolek et al. 2016). The presence of gingipain on the surface of OMV suggests that these may contribute to systemic disease. Kaplan-Meier survival plot analysis showed that both whole-cell W83 and W83-derived OMVs caused significantly more zebrafish mortality than PBS-injected controls ($P < 0.001$; Fig. 3A). In contrast, morbidity in zebrafish larvae injected with ΔK/R-ab-derived OMVs was not significantly different from controls. To interrogate the OMV data further, we stratified the fish into viable or diseased (nonviable + edematous) groups. A significant increase in the number of diseased zebrafish treated with W83-derived OMVs was observed when compared to ΔK/R-ab-derived OMVs in a time-dependent manner (Fig. 3B–D). W83 OMV-treated zebrafish larvae displayed marked cardiac edema and enlarged yolk sack, whereas those injected with ΔK/R-ab-derived OMV or PBS-treated controls displayed mild or no edema (Fig. 4E), providing further evidence that gingipains present on the surface of OMVs can cause systemic disease in vivo.

## OMV-Expressing Gingipains Cleave Endothelial Cell Adhesion Molecules

PECAM-1 is a major endothelial adhesion molecule responsible for maintaining vascular integrity at cell-cell junctions, with its loss leading to increased vascular leakage (Privratsky and Newman 2014). Previous studies have shown that gingipains can cleave recombinant PECAM-1 (Yun et al. 2005; Sheets et al. 2006; Widziolek et al. 2016). We therefore examined if OMV-associated gingipains could cleave intercellular PECAM-1. Treatment of HMEC-1 monolayers with W83 or W83 OMVs did not alter endothelial viability (Fig. 4A, B). In contrast, PECAM-1 cell surface abundance was significantly ($P < 0.001$) decreased following infection with whole-cell W83 (Fig. 4C, D) and W83-derived OMVs (Fig. 4E, F) compared to both untreated controls and the ΔK/R-ab equivalents. To confirm these findings, W83-derived OMVs were pretreated with the gingipain-specific protease inhibitors KYT1 and KYT36 before incubation with HMEC-1 monolayers.
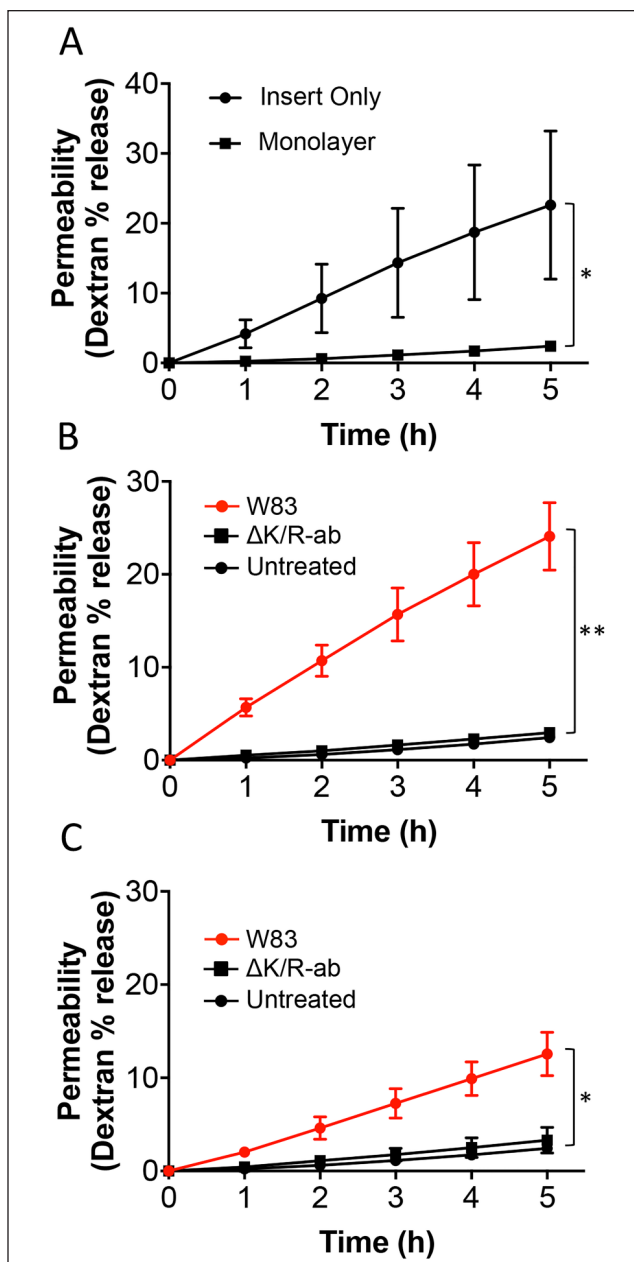
**Figure 2.** Increased endothelium permeability in vitro following treatment with *Porphyromonas gingivalis* whole cells and outer membrane vesicles (OMVs) is gingipain dependent. (**A**) Movement of fluorescently labeled 70 kDa dextran from the upper well to the lower well in a Transwell assay increased in a time-dependent manner in the absence of human microvascular endothelial cells (HMEC-1; insert only), whereas this movement was almost abolished when a confluent endothelium was cultured on the insert surface (monolayer). Endothelial monolayers were treated with (**B**) whole bacteria or (**C**) OMVs from either W83 or ΔK/R-ab for 1.5 h, and then dextran permeability across the endothelium was measured for up to 5 h; phosphate-buffered saline (PBS)–treated endothelium was used as controls. Increased endothelial permeability was significantly increased in a time-dependent manner following exposure to W83 when compared to ΔK/R-ab equivalents and untreated controls for both whole bacteria and OMVs. No significant differences were observed between ΔK/R-ab-treated and uninfected controls. Data are presented as mean ± SD of 3 independent experiments and were analyzed by 1-way analysis of variance followed by Tukey's post hoc multiple comparisons test. *$P < 0.05$. **$P < 0.01$.

Here, inhibition of gingipain activity significantly ($P < 0.05$) prevented OMV-mediated cleavage of PECAM-1 (Fig. 5), indicating that loss of cell surface PECAM-1 by W83 OMV is gingipain mediated.

## Discussion

Periodontal disease is one of the most common diseases worldwide and a major public health issue (Tonetti et al. 2017). It is frequently associated with several systemic conditions, leading to the notion of the now commonly phrased "oral health systemic connection" (Tonetti et al. 2013). Like many bacteria, *P. gingivalis* produces abundant OMVs (Xie 2015), although there are limited data as to their effects in host-pathogen interactions. Here, we show for the first time that *P. gingivalis* OMVs dramatically increase vascular permeability in vitro and potentiate vascular edema and mortality in vivo in a gingipain-dependent manner, suggesting that they may act in concert with whole bacteria to affect cardiovascular disease risk.

Gingipains are key virulence factors of *P. gingivalis*. As well as functions in bacterial coaggregation, biofilm formation, and heme acquisition, they also cleave soluble and cell surface human proteins (Hočevar et al. 2018). Since both RgpA/B and Kgp gingipains have been previously detected in *P. gingivalis*–derived OMVs by mass spectrometry (Haurat et al. 2011), we reasoned that gingipain-expressing OMVs might be a key mediator of endothelial cell surface receptor degradation, leading to increased vascular permeability. This may be important in the context of systemic disease as their small size and abundance are likely to allow OMVs to penetrate host tissue micro-niches that may not be readily accessible to *P. gingivalis* whole cells. To test our hypothesis, we generated OMVs from wild-type W83 and its isogenic gingipain-deficient counterpart, ΔK/R-ab, and confirmed presence or absence of gingipains on these strains/OMVs as previously observed using W50 and other *P. gingivalis* strains (Curtis et al. 1999; Aduse-Opoku et al. 2006; Naylor et al. 2017). Immunogold labeling followed by cryo-EM also showed that gingipains were located to the OMV cell surface. Although no structural abnormalities were visibly observed by cryo-EM, nanoparticle-tracking analysis showed that W83-derived OMV were larger in size than their gingipain-deficient counterparts. It is plausible that this size difference is due to changes in the molecular structure within the cell wall owing to loss of gingipain-mediated cell wall processing.

Very few studies have examined the role of *P. gingivalis* OMVs on vascular biology. Bartruff et al. (2005) showed that *P. gingivalis* ATCC33277-derived OMVs inhibited human umbilical vein endothelial cell (HUVEC) proliferation by up to 80% as well as capillary tubule formation in an OMV dose-dependent manner. These effects were inhibited by heat treatment but not by protease inhibitors, suggesting that these effects were protein but not protease mediated, although no specific factor was identified (Bartruff et al. 2005). Using the same *P. gingivalis* strain, Jia et al. (2015) observed that OMVs suppressed endothelial nitric oxide synthase (eNOS) transcript and protein expression in HUVECs via activation of the
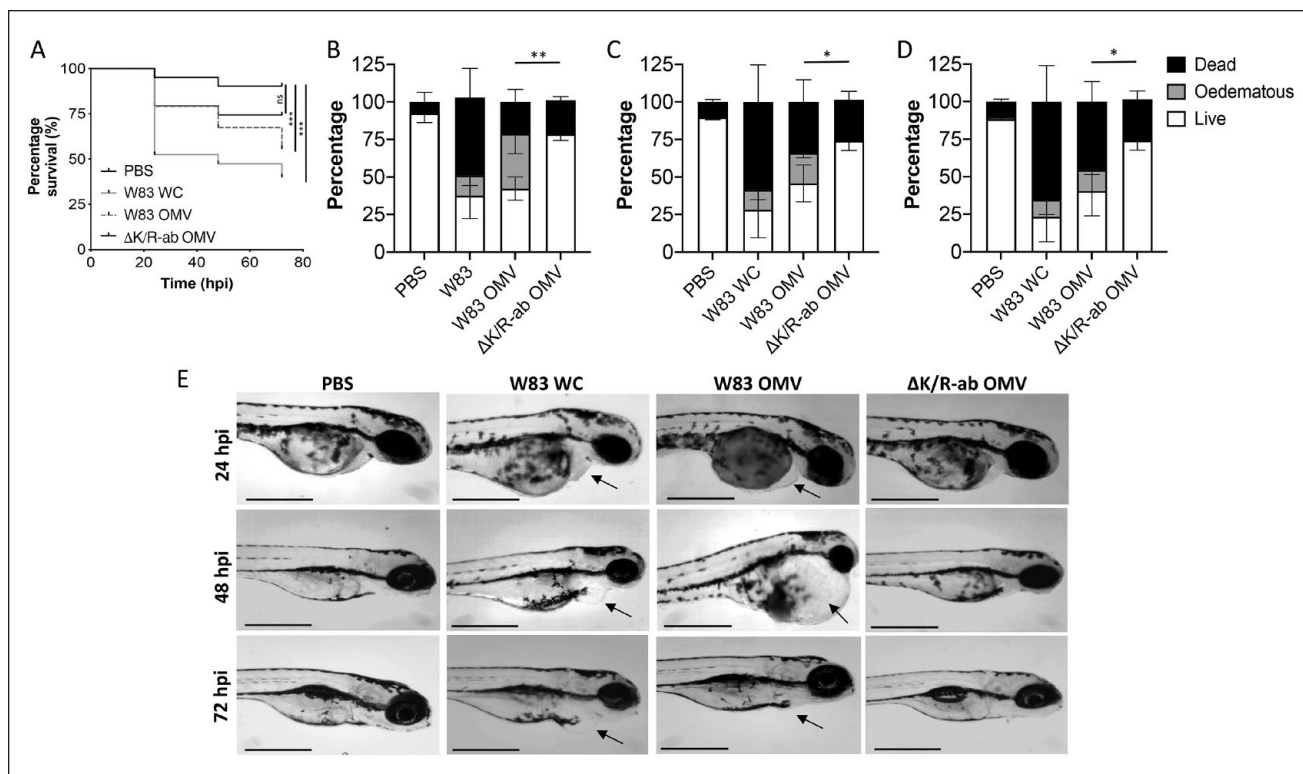
**Figure 3.** W83 outer membrane vesicles (OMVs) induce systemic disease in zebrafish larvae in a gingipain-dependent manner. (**A**) Kaplan-Meier survival plots of zebrafish larvae infected 30-h postfertilization (hpf) with phosphate-buffered saline (PBS) control, *Porphyromonas gingivalis* (*Pg*) W83 whole cells (WCs), *Pg* W83 OMVs, or ΔK/R-ab OMVs. Comparison of survival curves using the log-rank test shows significant differences between W83 whole cell–injected and W83 OMV-injected zebrafish compared to PBS controls. Survival curves of zebrafish larvae injected with ΔK/Ra-b OMVs were not statistically different from the PBS control (ns = no significant difference, ***$P < 0.001$). (**B–D**) Percentage live, edematous, and dead zebrafish larvae at (B) 24, (C) 48, and (D) 72 hpi showing that the percentage of diseased (dead + edematous) zebrafish was significantly increased following systemic infection with W83 OMVs compared to ΔK/R-ab OMVs at all time points (*$P < 0.05$, **$P < 0.01$ by 1-way analysis of variance with Tukey's post hoc multiple comparisons test). (**E**) Representative micrographs showing the morphology of zebrafish larvae infected with PBS control, W83 whole cells (WCs), W83 OMVs, or ΔK/R-ab OMVs. W83 whole-cell and OMV-infected zebrafish showed marked edema around yolk sac and heart (black arrows). Scale bars = 500 μm. Data in A–D are mean ± SD pooled from 3 independent experiments with at least 39 zebrafish total per group.

ERK1/2 and p38 MAPK signaling pathways in a Rho-associated protein kinase-dependent manner. This study provides good evidence that OMVs may regulate vascular oxidative injury, although the OMV factors driving this effect were not examined. *P. gingivalis*–derived OMVs have recently been shown to promote vascular smooth muscle cell differentiation and calcification by increasing the activity of runt-related transcription factor 2 that is crucial in driving osteoblastic differentiation and mineralization of vascular smooth muscle cells (Yang et al. 2016).

Our study provides further evidence that OMVs can significantly perturb endothelial homeostasis. In vitro, W83-derived OMVs not only cleaved PECAM-1 on endothelial cell (HMEC-1) monolayers but also increased their permeability. Moreover, cleavage of PECAM-1 was significantly reduced when W83-derived OMVs were either preincubated with the gingipain protease inhibitors KYT1 and KYT36 or infected with gingipain-deficient OMVs. Not only do these data show that *P. gingivalis* OMVs mediate vascular damage but also that this is via a gingipain-dependent mechanism, the first time that this

has been documented for *P. gingivalis* OMVs. We confirmed some of these in vitro observations in vivo using a systemic zebrafish infection model. Although zebrafish larvae have been used extensively to examine systemic host-pathogen interactions (Sullivan et al. 2017), only a few studies have examined the role of bacterial OMVs in systemic disease, and to our knowledge, none have been performed using *P. gingivalis* OMVs. OMVs derived from W83 but not ΔK/R-ab caused significant edema and mortality in zebrafish larvae, although the effects were less extreme than those observed with injection of whole-cell W83. These in vitro and in vivo data further confirm that OMVs have the potential to cause disease in the absence of whole-cell bacteria from which they are derived and augment current evidence that OMVs are able to exert their effects beyond that of the periodontal pocket.

Our data lead to the speculation that gingipains on OMVs as well as whole bacteria cleave endothelial intercellular junction proteins such as PECAM-1 and likely other adhesion molecules (VE-cadherin, CD99), thereby loosening cell-to-cell contacts to permit increased endothelial cell permeability. This
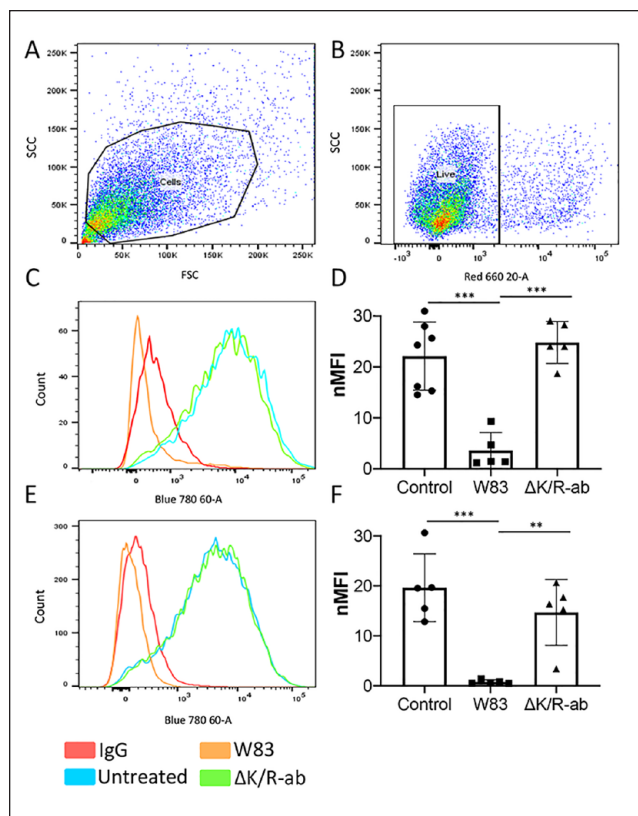
**Figure 4.** Loss of endothelial cell surface PECAM-1 by W83 whole bacteria and outer membrane vesicles (OMVs) is mediated by gingipains. Following a 1.5-h exposure to W83 or ΔK/R-ab whole bacteria or OMVs, human microvascular endothelial cells (HMEC-1) were removed from tissue culture plates and subjected to flow cytometric analysis for PECAM-1 cell surface abundance. Cells were gated using (**A**) side-scatter (SSC) and forward-scatter (FSC) voltages, then for (**B**) cell viability using TO-PRO-3 live/dead staining. Untreated cells were used as controls. Representative histograms and bar chart of 10,000 gated cells showing that PECAM-1 cell surface abundance is significantly decreased upon treatment with (**C, D**) W83 whole bacteria and (**E, F**) W83-derived OMVs compared to ΔK/R-ab-treated equivalents and untreated controls. PECAM-1 cell surface abundance was similar on HMEC-1 treated with ΔK/R-ab whole bacteria or ΔK/R-ab-derived OMVs to those observed on untreated controls. Data in D and F are presented as mean ± SD normalized median fluorescence index (nMFI) from 5 independent experiments with statistical significance determined by a 1-way analysis of variance with Tukey's post hoc multiple comparisons test. **$P < 0.01$. ***$P < 0.001$.



**Figure 5.** Inhibition of gingipain activity prevents ablation of PECAM-1 expression following W83 outer membrane vesicle (OMV) infection. W83 OMVs were treated with 2 μM KYT gingipain inhibitors for 1 h prior to human microvascular endothelial cell (HMEC-1) infection. HMEC-1 treated with W83 OMVs or untreated cells were used as controls. Flow cytometric analysis showed that the gingipain-specific inhibitor, KYT, prevented the loss of PECAM-1 cell surface abundance that was mediated by W83 OMVs. Data are mean ± SD normalized median fluorescence index (nMFI) from 4 independent experiments with statistical significance determined by a 1-way analysis of variance with Tukey's post hoc multiple comparisons test. *$P < 0.05$. ***$P < 0.001$.

OMVs in host-microbial pathogenesis may be as important as whole bacteria, a factor that needs to be taken into consideration in the ongoing drive to decipher the oral health systemic connection.

## ORCID iDs

C. Farrugia (iD) https://orcid.org/0000-0003-1318-8885

C. Murdoch (iD) https://orcid.org/0000-0001-9724-122X

may have 2 consequences: first, to allow exudate from the circulation into tissues leading to tissue edema, which we observed in vivo, and, second, to expose underlying connective tissue that may lead to platelet activation and subsequently foci for immune cell activation on the endothelium that would have dramatic implications for increased risk of systemic disease (Chistiakov et al. 2015). Moreover, the nanoscale size of OMVs would allow proteolytic damage to occur at vascular sites not accessible to whole bacteria. Although this hypothesis requires further evaluation, our data provide a potential mechanism for the link between periodontal disease and cardiovascular disease. It also provides clear evidence that the role of
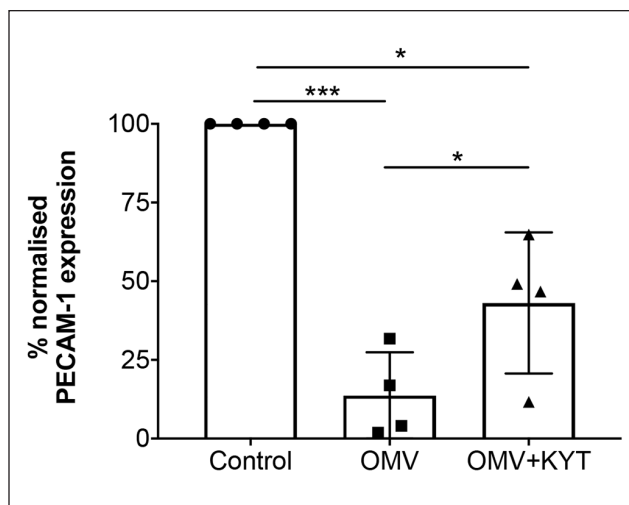
## References

Ades EW, Candal FJ, Swerlick RA, George VG, Summers S, Bosse DC, Lawley TJ. 1992. HMEC-1: establishment of an immortalized human microvascular endothelial cell line. J Invest Dermatol. 99(6):683–690.

Aduse-Opoku J, Slaney JM, Hashim A, Gallagher A, Gallagher RP, Rangarajan M, Boutaga K, Laine ML, Van Winkelhoff AJ, Curtis MA. 2006. Identification and characterization of the capsular polysaccharide (K-antigen) locus of porphyromonas gingivalis. Infect Immun. 74(1):449–460.

Bai D, Nakao R, Ito A, Uematsu H, Senpuku H. 2015. Immunoreactive antigens recognized in serum samples from mice intranasally immunized with *Porphyromonas gingivalis* outer membrane vesicles. Pathog Dis. 73(3):ftu006.

Bartruff JB, Yukna RA, Layman DL. 2005. Outer membrane vesicles from *Porphyromonas gingivalis* affect the growth and function of cultured human gingival fibroblasts and umbilical vein endothelial cells. J Periodontol. 76(6):972–979.

Castillo DM, Sánchez-Beltrán MC, Castellanos JE, Sanz I, Mayorga-Fayad I, Sanz M, Lafaurie GI. 2011. Detection of specific periodontal microorganisms from bacteraemia samples after periodontal therapy using molecular-based diagnostics. J Clin Periodontol. 38(5):418–427.

Cecil JD, O'Brien-Simpson NM, Lenzo JC, Holden JA, Chen YY, Singleton W, Gause KT, Yan Y, Caruso F, Reynolds EC. 2016. Differential responses of pattern recognition receptors to outer membrane vesicles of three periodontal pathogens. PLoS One. 11(4):e0151967.

Chen YY, Peng B, Yang Q, Glew MD, Veith PD, Cross KJ, Goldie KN, Chen D, O'Brien-Simpson N, Dashper SG, et al. 2011. The outer membrane protein LptO is essential for the O-deacylation of LPS and the co-ordinated secretion and attachment of A-LPS and CTD proteins in porphyromonas gingivalis. Mol Microbiol. 79(5):1380–1401.

Chhibber-Goel J, Singhal V, Bhowmik D, Vivek R, Parakh N, Bhargava B, Sharma A. 2016. Linkages between oral commensal bacteria and atherosclerotic plaques in coronary artery disease patients. NPJ Biofilms Microbiomes. 2:7.

Chistiakov DA, Orekhov AN, Bobryshev YV. 2015. Endothelial barrier and its abnormalities in cardiovascular disease. Front Physiol. 6:365.

Curtis MA, Thickett A, Slaney JM, Rangarajan M, Aduse-Opoku J, Shepherd P, Paramonov N, Hounsell EF. 1999. Variable carbohydrate modifications to the catalytic chains of the RgpA and RgpB proteases of *Porphyromonas gingivalis* W50. Infect Immun. 67(8):3816–3823.

Friedewald VE, Kornman KS, Beck JD, Genco R, Goldfine A, Libby P, Offenbacher S, Ridker PM, Van Dyke TE, Roberts WC, et al. 2009. The *American Journal of Cardiology* and *Journal of Periodontology* editors' consensus: periodontitis and atherosclerotic cardiovascular disease. Am J Cardiol. 104(1):59–68.

Gaetti-Jardim E, Marcelino SL, Feitosa ACR, Romito GA, Avila-Campos MJ. 2009. Quantitative detection of periodontopathic bacteria in atherosclerotic plaques from coronary arteries. J Med Microbiol. 58(12):1568–1575.

Gustafsson N, Ahlqvist J, Näslund U, Buhlin K, Gustafsson A, Kjellström B, Klinge B, Rydén L, Levring Jäghagen E. 2020. Associations among periodontitis, calcified carotid artery atheromas, and risk of myocardial infarction. J Dent Res. 99(1):60–68.

Haurat MF, Aduse-Opoku J, Rangarajan M, Dorobantu L, Gray MR, Curtis MA, Feldman MF. 2011. Selective sorting of cargo proteins into bacterial membrane vesicles. J Biol Chem. 286(2):1269–1276.

Hočevar K, Potempa J, Turk B. 2018. Host cell-surface proteins as substrates of gingipains, the main proteases of *Porphyromonas gingivalis*. Biol Chem. 399(12):1353–1361.

Jia Y, Guo B, Yang W, Zhao Q, Jia W, Wu Y. 2015. Rho kinase mediates *Porphyromonas gingivalis* outer membrane vesicle-induced suppression of endothelial nitric oxide synthase through ERK1/2 and p38 MAPK. Arch Oral Biol. 60(3):488–495.

Kozarov EV, Dorn BR, Shelburne CE, Dunn WA, Progulske-Fox A. 2005. Human atherosclerotic plaque contains viable invasive *Actinobacillus actinomycetemcomitans* and *Porphyromonas gingivalis*. Arterioscler Thromb Vasc Biol. 25(3):e17–e18.

Loos BG. 2005. Systemic markers of inflammation in periodontitis. J Periodontol. 76(11 Suppl):2106–2115.

Mantri CK, Chen CH, Dong X, Goodwin JS, Pratap S, Paromov V, Xie H. 2015. Fimbriae-mediated outer membrane vesicle production and invasion of *Porphyromonas gingivalis*. Microbiologyopen. 4(1):53–65.

Marcelino SL, Gaetti-Jardim E, Nakano V, Canonico LAD, Nunes FD, Lotufo RFM, Pustiglioni FE, Romito GA, Avila-Campos MJ. 2010. Presence of periodontopathic bacteria in coronary arteries from patients with chronic periodontitis. Anaerobe. 16(6):629–632.

Masi S, D'Aiuto F, Deanfield J. 2019. Cardiovascular prevention starts from your mouth. Eur Heart J. 40(14):1146–1148.

Mougeot JLC, Stevens CB, Paster BJ, Brennan MT, Lockhart PB, Mougeot FKB. 2017. *Porphyromonas gingivalis* is the most abundant species detected in coronary and femoral arteries. J Oral Microbiol. 9(1):1281562.

Nakao R, Takashiba S, Kosono S, Yoshida M, Watanabe H, Ohnishi M, Senpuku H. 2014. Effect of *Porphyromonas gingivalis* outer membrane vesicles on gingipain-mediated detachment of cultured oral epithelial cells and immune responses. Microbes Infect. 16(1):6–16.

Nassar H, Chou HH, Khlgatian M, Gibson FC, Van Dyke TE, Genco CA. 2002. Role for fimbriae and lysine-specific cysteine proteinase gingipain K in expression of interleukin-8 and monocyte chemoattractant protein in *Porphyromonas gingivalis*–infected endothelial cells. Infect Immun. 70(1):268–276.

Naylor KL, Widziolek M, Hunt S, Conolly M, Hicks M, Stafford P, Potempa J, Murdoch C, Douglas CW, Stafford GP. 2017. Role of OmpA2 surface regions of *Porphyromonas gingivalis* in host-pathogen interactions with oral epithelial cells. Microbiologyopen. 6(1):e00401.

Privratsky JR, Newman PJ. 2014. PECAM-1: regulator of endothelial junctional integrity. Cell Tissue Res. 355(3):607–619.

Ruggiero S, Cosgarea R, Potempa J, Potempa B, Eick S, Chiquet M. 2013. Cleavage of extracellular matrix in periodontitis: gingipains differentially affect cell adhesion activities of fibronectin and tenascin-c. Biochim Biophys Acta. 1832(4):517–526.

Sanz M, Marco Del Castillo A, Jepsen S, Gonzalez-Juanatey JR, D'Aiuto F, Bouchard P, Chapple I, Dietrich T, Gotsman I, Graziani F, et al. 2020. Periodontitis and cardiovascular diseases: consensus report. J Clin Periodontol. 47(3):268–288.

Schenkein HA, Loos BG. 2013. Inflammatory mechanisms linking periodontal diseases to cardiovascular diseases. J Clin Periodontol. 40(Suppl 14):S51–S69.

Sheets SM, Potempa J, Travis J, Fletcher HM, Casiano CA. 2006. Gingipains from *Porphyromonas gingivalis* W83 synergistically disrupt endothelial cell adhesion and can induce caspase-independent apoptosis. Infect Immun. 74(10):5667–5678.

Sullivan C, Matty MA, Jurczyszak D, Gabor KA, Millard PJ, Tobin DM, Kim CH. 2017. Infectious disease models in zebrafish. Methods Cell Biol. 138:101–136.

Szulc M, Kustrzycki W, Janczak D, Michalowska D, Baczynska D, Radwan-Oczko M. 2015. Presence of periodontopathic bacteria DNA in atheromatous plaques from coronary and carotid arteries. Biomed Res Int. 2015:825397.

Tada H, Sugawara S, Nemoto E, Imamura T, Potempa J, Travis J, Shimauchi H, Takada H. 2003. Proteolysis of ICAM-1 on human oral epithelial cells by gingipains. J Dent Res. 82(10):796–801.

Tonetti MS, Jepsen S, Jin L, Otomo-Corgel J. 2017. Impact of the global burden of periodontal diseases on health, nutrition and wellbeing of mankind: a call for global action. J Clin Periodontol. 44(5):456–462.

Tonetti MS, Van Dyke TE; Working Group 1 of the Joint EFP/AAP Workshop. 2013. Periodontitis and atherosclerotic cardiovascular disease: consensus report of the joint EFP/AAP workshop on periodontitis and systemic diseases. J Periodontol. 84(4 Suppl):S24–S29.

Wang Y, Alexander JS. 2011. Analysis of endothelial barrier function in vitro. Methods Mol Biol. 763:253–264.

Widziolek M, Prajsnar TK, Tazzyman S, Stafford GP, Potempa J, Murdoch C. 2016. Zebrafish as a new model to study effects of periodontal pathogens on cardiovascular diseases. Sci Rep. 6:36023.

Xie H. 2015. Biogenesis and function of *Porphyromonas gingivalis* outer membrane vesicles. Future Microbiol. 10(9):1517–1527.

Yang WW, Guo B, Jia WY, Jia Y. 2016. *Porphyromonas gingivalis*–derived outer membrane vesicles promote calcification of vascular smooth muscle cells through ERK1/2-RUNX2. FEBS Open Bio. 6(12):1310–1319.

Yun PL, Decarlo AA, Chapple CC, Hunter N. 2005. Functional implication of the hydrolysis of platelet endothelial cell adhesion molecule 1 (CD31) by gingipains of *Porphyromonas gingivalis* for the pathology of periodontal disease. Infect Immun. 73(3):1386–1398.